Molecular characterization of a sodium-dependent NADH-Ubiquinone Oxidoreductase from *Vibrio alginolyticus*

Karen Ai Ling Tan

Thesis presented for the degree of Doctor of Philosophy
University of Edinburgh, 1997.

Declaration.

I declare that this thesis was composed by myself and the research presented is my own except where otherwise stated.

Karen Tan

1997.

Acknowledgments.

I am grateful to Bruce Ward and David Leach for their advice and ideas regarding my project. Bruce's encouragement and contribution to my thesis has been invaluable. A special mention and thanks to Bruce and Andrew Coulson for the sequence analysis of NqrF. In addition, I would like to thank Pam Beattie, who also worked on the *Vibrio alginolyticus* Na^+-NQR project, for the countless times she has put herself out to assist me and for being a good friend. Not forgetting all members in I.C.M.B. who have guided me in one way or another, I would also like to express my gratefulness and appreciation to Jo Thomas, Jason Clark, Richard Thomas, Margaret Daniel for their advice and camaraderie. Last but not least, my thanks and love to my fiance Dominique Jacquel for the aid and patient support he has given me, despite the frustrations of printing the coloured diagrams in this thesis!

Contents

Chapter 4 Results and discussion
Expression of Nqr subunits

Chapter 5 Results and discussion
Protein purification

Figures

Chapter 1 Introduction

Chapter 2 Materials and methods

Chapter 3 Results and discussion
Cloning and sequencing the *nqr* operon

Chapter 4 Results and discussion
Expression of Nqr subunits

Tables

Chapter 1 Introduction

Chapter 2 Materials and methods

Chapter 3 Results and discussion
Cloning and sequencing the *nqr* operon

Abbreviations

A	absorbance or adenine
ADP	adenosine diphosphate
$AgNO_3$	silver nitrate
Ala	alanine
APS	ammonium persulphate
Arg	arginine
Asn	asparagine
Asp	aspartate
ATP	adenosine triphosphate
ATPase	adenosine triphosphatase
BSA	bovine serum albumin
C	cytosine
°C	degrees Celsius
$CaCl_2$	calcium chloride
CCCP	carbonyl cyanide *m*-chlorophenylhydrazone
$CdCl_2$	cadmium chloride
CHAPS	3-[(3-cholamidopropyl)dimethylammonio]-1-propanesulfonate
cm	centimetre
$CuSO_4$	copper sulphate
Cys	cysteine
DCCD	dicyclohexylcarbodiimide
DEAE	diethylaminoethyl
DMSO	dimethyl sulphoxide
DNA	deoxyribonucleic acid
DTT	dithiothreitol
EDTA	ethylenediaminetetraacetic acid

FAD	flavin adenine dinucleotide (oxidised form)
$FADH_2$	flavin adenine dinucleotide (reduced form)
FMN	flavin mononucleotide (oxidised form)
$FMNH_2$	flavin mononucleotide (reduced form)
G	guanine
g	grams or standard acceleration of gravity
Gln	glutamine
Glu	glutamate
Gly	glycine
h	hours
HA	hydroxyapatite
HCl	hydrochloric acid
HIC	hydrophobic interaction chromatography
His	histidine
H_2O	water
H_2O_2	hydrogen peroxide
HPLC	high performance liquid chromatography
HQNO	2-heptyl-4-hydroxyquinoline-N-oxide
Ile	isoleucine
IPTG	isopropyl-β-D-thiogalactoside
kb	kilobases
kDa	kilodaltons
kg	kilogram
KCl	potassium chloride
KCN	potassium cyanide
$K_3Fe(CN)_6$	potassium permanganate
K_2HPO_4	di-potassium hydrogen phosphate

KH_2PO_4	potassium dihydrogen phosphate
ℓ	litres
LDAO	lauryl-dimethylamine oxide
Leu	leucine
LSB	laurylsulphobetaine
Lys	lysine
M	molar
mA	milliamperes
Mega 10	decanoyl-N-methylglucamide
Met	methionine
$MgCl_2$	magnesium chloride
min	minutes
mg	milligrams
µg	micrograms
ml	millilitres
µl	microlitres
mM	millimolar
µM	micromolar
mm	millimetres
$MnCl_2$	manganese chloride
NaCl	sodium chloride
NAD^+	nicotinamide adenine dinucleotide (oxidised form)
NADH	nicotinamide adenine dinucleotide (reduced form)
$dNAD^+$	deamino nicotinamide adenine dinucleotide (oxidised form)
dNADH	deamino nicotinamide adenine dinucleotide (reduced form)
$NADP^+$	nicotinamide adenine dinucleotide phosphate (oxidised form)
NADPH	nicotinamide adenine dinucleotide phosphate (reduced form)

NaOH	sodium hydroxide
$NiSO_4$	nickel sulphate
nm	nanometres
dNTP	deoxynucleotide triphosphate
PAGE	polyacrylamide gel electrophoresis
$Pb(CH_3COO)_2$	lead acetate
PCR	polymerase chain reaction
PEG	polyethylene glycol
Phe	phenylalanine
P_i	inorganic orthophosphate
PMSF	phenylmethylsulphonylfluoride
PNP	p-nitrophenyl phosphate
PP_i	inorganic pyrophosphate
Pro	proline
PVDF	polyvinylidene difluoride
Q	ubiquinone
QH_2	ubiquinol
RNA	ribonucleic acid
RNAse	ribonuclease
mRNA	messenger ribonucleic acid
s	seconds
SDS	sodium dodecyl sulphate
Ser	serine
T	thymine
TAE	Tris-acetate with EDTA
TBE	Tris-borate with EDTA
TCA	trichloroacetic acid

TE	Tris-EDTA
TEMED	N,N,N',N',-tetramethylethylenediamine
Thr	threonine
Trp	tryptophan
Tris	tris (hydroxymethyl)-aminomethane
U	units
UV	ultraviolet
V	volts
V/cm	volts per centimetre
Val	valine
v/v	volume per volume
w/v	weight per volume
X-gal	5-bromo-4-chloro-3-indolyl-β-galactoside
$ZnCl_2$	Zinc chloride

Abstract

The sodium-dependent NADH-ubiquinone oxidoreductase (Na^+-NQR) was discovered first in the marine bacterium, *Vibrio alginolyticus*. It acts as a primary electrogenic pump for sodium translocation during aerobic respiration, generating a sodium motive force which drives ATP synthesis, solute transport and flagellar motion. Early biochemical studies indicated that Na^+-NQR was composed of 3 subunits: α, β and γ, with apparent M_r values of 52, 46 and 32 kDa. A proposed model suggested that the β subunit, a NADH dehydrogenase, accepts electrons from NADH and reduces menadione or quinone by a Na^+-independent one-electron transfer reaction to produce the semiquinone. The subsequent reduction of the semiquinone is dependent on Na^+ and is catalyzed by the α subunit.

Degenerate oligonucleotides designed from the *N*-terminal sequences obtained from partially purified α and γ subunits were used to isolate clones from an *Eco*RI library of wild-type *V. alginolyticus* DNA. Six genes which comprise the *nqr* operon, *nqr*A-*nqr*F, were sequenced and identified. Sequence analysis and database comparisons led to the conclusion that this enzyme complex is both structurally and evolutionarily distinct from the H^+-translocating NADH-ubiquinone oxidoreductase. Na^+-NQR comprises 3 hydrophilic subunits, NqrA, NqrC and NqrF and 3 highly hydrophobic membrane-spanning subunits, NqrB, NqrD and NqrE. The 3 hydrophilic subunits, NqrA, NqrC and NqrF correspond to the previously identified α, γ and β subunits respectively. Based on sequence comparisons, a [2Fe-2S] cluster region, a FAD binding site and an NADH binding domain were identified in NqrF, the proposed NADH dehydrogenase subunit. From hydropathy plots, NqrF also appeared to possess a hydrophobic *N*-terminal region.

Pulse-chase radiolabelling of various clones expressing *nqr*B-*nqr*F verified that the putative products of the *nqr* operon identified from sequencing, were indeed trancribed and translated *in vivo*. The *nqr*F gene was cloned into pET16-b and expressed

in *Escherichia coli*, BL21(DE3)p*LysS*, as a 46 kDa polypeptide. Silver-sensitive NADH dehydrogenase activity was located in the membrane fraction and this was attributed to NqrF as all other known types of NADH dehydrogenases are silver-insensitive.

NqrF was overexpressed in *E. coli*, and purified successively to homogeneity on columns of DEAE sepharose, hydroxyapaptite and Mimetic Blue-2 (affinity chromatography). A 67-fold increase in specific activity and 50% recovery of total activity was achieved. Purified NqrF was further characterized and analysed biochemically to determine its stability in various physiological conditions, buffers and detergents. In addition, its absorption spectrum, inhibitor specificities and substrate specificities were determined.

Chapter 1

Introduction

1.1 *Vibrio* sp.

Indigenous marine vibrios are flagellated Gram-negative microbes which colonize sea water, intestinal tracts and body surfaces of marine animals and some pathogenic strains constitute a health hazard. A notorious member of this genus, *Vibrio cholerae* is responsible for the water-transmitted disease, cholera, a major cause of mortality in some parts of the developing world. *V. parahaemolyticus* is a frequent cause of gastroenteritis, associated with the consumption of raw fish (Stanier *et al.*, 1987). It is also believed that *V. vulnificus,* implicated in wound infections, may occasionally cause fatal septicaemia (Pelczar *et al.*, 1986).

V. alginolyticus, the bacterium of interest in this project, was shown to be a causative agent of food poisoning from consuming shrimps and of wound infections and septicaemia recently (Ji *et al.*, 1989). High incidences of pathogenic *V. alginolyticus* were found in farmed tiger shrimps in Karnataka, India (Bhaskar and Setty, 1994), oysters and mussels in Sao Paolo, Brazil (Matte *et al.*, 1994a, Matte *et al.,* 1994b), which pose potential risks of food poisoning. In addition, *Vibrio alginolyticus* was found to be the cause of ear infections in patients who have been exposed to Danish coastal seawater (Hornstrup and Gahrnhansen, 1993).

For these bacteria which occupy a marine niche, Na^+ is essential for growth and it is more energetically favourable to utilize Na^+ rather than H^+ for creating an electrochemical force that drives many physiological and biochemical reactions.

1.2 Sodium metabolism

With their active metabolism and rapid growth, bacteria must possess efficient substrate uptake systems in their membranes that exchange matter between the environment and the bacterial interior (Dimroth, 1990). Many of these systems import substrates by active transport which requires an electrochemical cation gradient that is driven by H^+ pumps in most bacteria. But Na^+ gradients appear to be essential in marine halophilic bacteria like vibrios and certain alkalophilic and rumen bacteria that live in Na^+-rich habitats. This is because an alkaline or high salt environment represents a natural niche where it is difficult to employ a proton electrochemical gradient, $\Delta_{\mu}H+$, of the usual direction (the interior of the bacterium is more negative and alkaline than the exterior). Here pumping of protons from the cytoplasm results in generation of a membrane potential, $\Delta\psi$, which is counterbalanced by a pH gradient, ΔpH of the opposite direction. Consequently, the electrochemical proton motive force appears to be too low to support energy-coupled reactions in the cytoplasmic membrane (Krulwich, 1983). Following this line of reasoning, one can now extrapolate our understanding why the animal plasma membrane uses an ATPase rather than a redox chain to become energized and employs Na^+ as the coupling ion. The sodium motive force can only drive biochemical and physiological reactions in the cell if the Na^+ concentration outside the cell is greater than that inside. This applies to animal cells due to the high Na^+ levels in the blood and to microbes other than freshwater bacteria. The best characterised sodium cycles are elucidated from marine micro-organisms such as *V. alginolyticus* and *Propionigenium modestum*.

Na^+ gradients have 4 principal functions in:

- sodium ion solute cotransport systems
- sodium coupled energy conservation and energy transduction
- activation of special enzymes
- pH homeostasis mechanisms (Dimroth, 1987)

The Na^+ cycle comprises import and export systems. Import of Na^+ down a sodium electrochemical gradient is required to drive ATP synthesis, solute symport and flagellar movement. The export of Na^+ from the cytoplasm is accomplished by either a Na^+/ H^+ antiporter (secondary sodium pump) driven by an electrochemical H^+ gradient or primary sodium pumps driven by decarboxylation, ATP hydrolysis or NADH oxidation (refer to Figure 1.1).

Being marine organisms, vibrios have an absolute requirement for sodium salts and survive at alkaline pH, extruding Na^+ and H^+ by aerobic respiration (Tokuda and Unemoto,1981). The Na^+ motive force generated by the sodium-translocating NADH-ubiquinone oxidoreductase (Na^+-NQR) is used to drive ATP synthesis and flagellar motion by Na^+ intake (Dibrov *et al.*, 1986). Enzymes, such as oxaloacetate decarboxylase in *Klebsiella pneumoniae*, also need to generate a Na^+ motive force for catalytic activity.

Sodium cycle

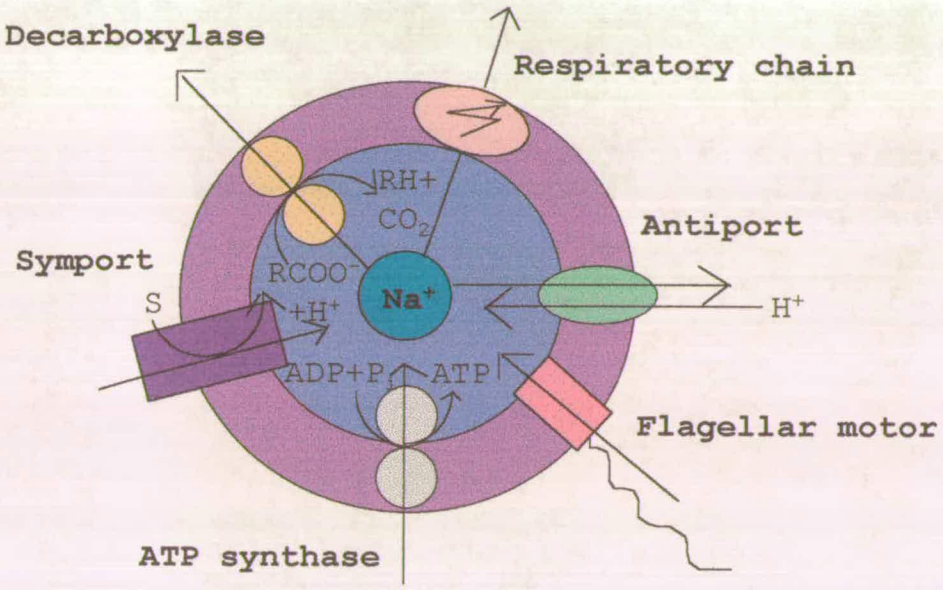

Fig. 1.1. Summary of systems performing energy coupling by sodium circulation in bacteria. Sodium transport decarboxylases and Na^+-coupled ATP synthase exist in anaerobic bacteria, a respiratory Na^+ pump occurs in marine organisms, Na^+-driven flagellar motors were found in marine and alkalophilic species, and Na^+/H^+ antiport and Na^+-symport systems are widely distributed (Dimroth, 1987).

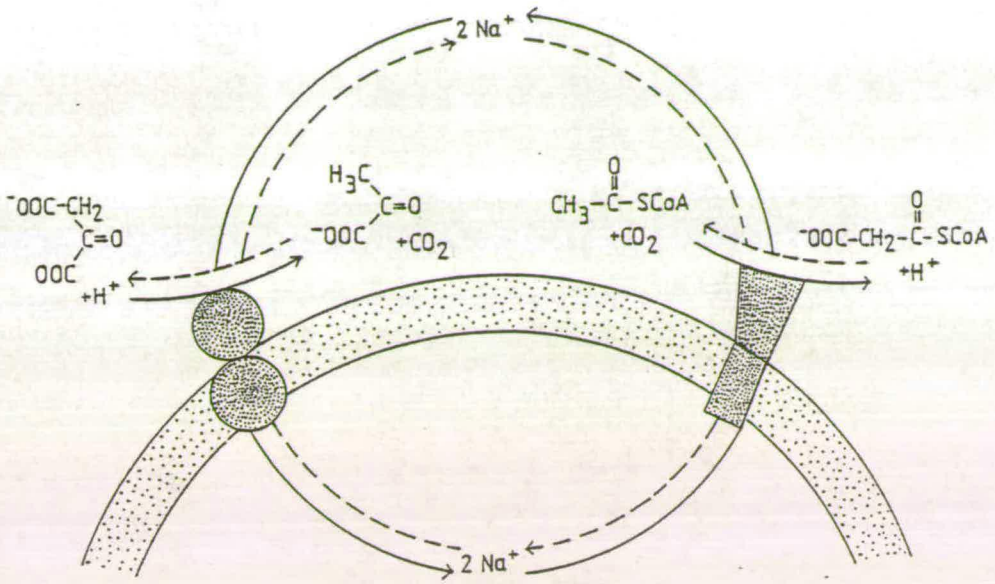

Fig. 1.2 Na^+ circuit mediating the transcarboxylation from oxaloacetate and acetyl-Co-A to pyruvate and malonyl-Co-A and vice versa (Dimroth, 1987).

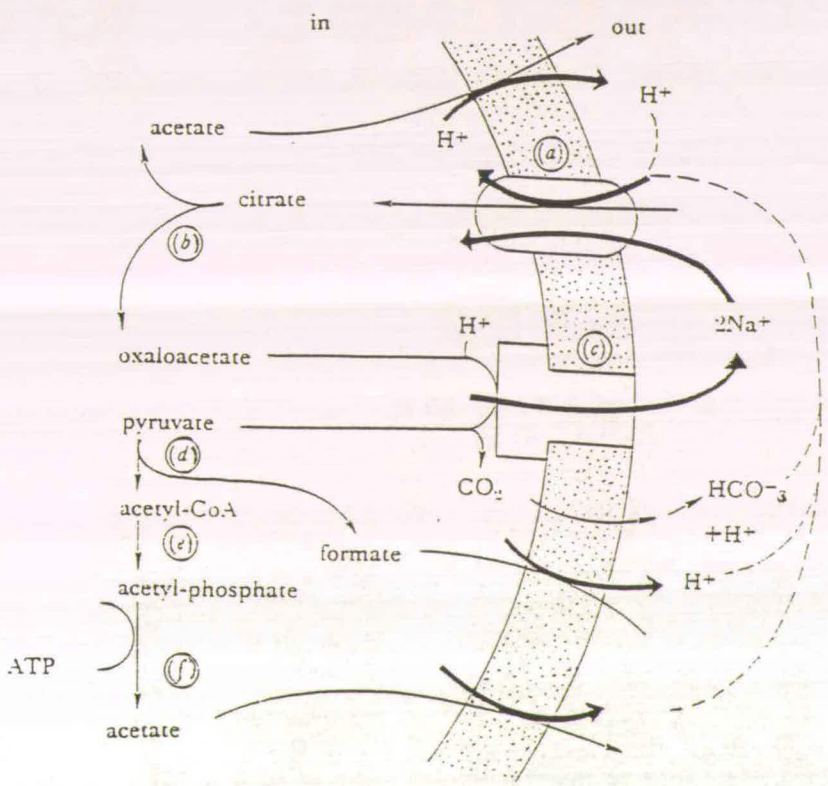

Fig. 1.3 The citrate fermentation pathway of *Klebsiella pneumoniae*. It demonstrates an Na^+ circuit as a possible coupling mechanism of citrate uptake and oxaloacetate decarboxylation, and a proton circuit as a possible coupling device between citrate uptake and end product extrusion. (a) Citrate uptake system; (b) citrate lyase; (c) oxaloacetate decarboxylase; (d) pyruvate formate lyase; (e) phosphotransacetylase; (f) acetate kinase (Dimroth, 1990).

The above mentioned enzymes were purified by chromatography on avidin-Sepharose, which binds biotinylated proteins strongly (Dimroth, 1982a). The sodium transport decarboxylases generally contain a peripheral membrane bound subunit with M_r 60,000 to 65,000 that catalyses the transfer of the carboxyl groups from the substrate to a prosthetic biotin group on the enzyme. They also possess a more firmly membrane bound subunit of M_r 30,000 to 35,000 that is Na^+ dependent and decarboxylates the carboxybiotin protein which is believed to be coupled to Na^+ translocation. Oxaloacetate decarboxylase and methylmalonyl-CoA decarboxylase contain an additional integral membrane protein of M_r 12,000 and 14,000 respectively, that are quite similar to each other. The proposed catalytic mechanism involved the carboxylation of the biotin prosthetic group by carboxyl transfer from the substrate, in the first step. Decarboxylation of the N-carboxybiotin enzyme intermediate would then regenerate the free biotin enzyme, accompanied by the export of Na^+ ions from the cell (Moss and Lane, 1971).

1.4 Sodium/ proton antiporters

Na^+/H^+ antiporters are carriers which translocate Na^+ and H^+ in opposite directions across a membrane (Fig. 1.1). These active transporters represent secondary Na^+ pumps and were first identified in *Streptococcus faecalis* (Krulwich, 1983). They function in the uptake of intracellular ions, control of osmolarity and pH homeostasis. A Na^+/H^+ antiporter can convert the proton motive force generated by the H^+ pump, to a Na^+ electrochemical gradient for Na^+ symport processes without the need for primary Na^+ pumps (Dimroth, 1987). Especially for halobacteria that perform most of their solute uptake as cotransport with Na^+, the generation of a Na^+ gradient is a critical event. Aerobic non-marine extreme alkalophiles possess requisite secondary Na^+/ H^+ antiporters as they do not have primary Na^+ pumps. Alkalophilic Na^+/H^+ antiporters can use Li^+ or Na^+, their activity has linear dependence upon the membrane potential and are inhibited by a high internal proton concentration (consistent with the role of the antiporter in acidifying the cell interior) (Krulwich and Guffanti, 1989).

In alkalophilic *Bacillus* sp., the Na^+/H^+ antiporter has been hypothesized to regulate cytoplasmic pH. The coupled exchange of Na^+ extrusion and H^+ uptake across the membrane is electrogenic, as the driving force for antiport activity was contributed by the membrane potential, $\Delta\psi$ with $H^+ > Na^+$. Hence, the combined activity of the respiratory chain, antiporters and solute transport systems coupled to Na^+ re-entry, allow alkalophiles to maintain a cytoplasmic pH that is several pH units more acidic than external pH values optimal for growth. Evidence for the involvement of Na^+/H^+ antiporters in pH homeostasis came from four sources. Firstly, nonalkalophilic mutant strains that can no longer grow well above pH 9.0 and have lost Na^+/H^+ antiporter activity were isolated (Koyama *et al.*, 1986; Krulwich, 1986; Krulwich and Guffanti, 1986). Another experiment with *Exiguobacterium aurantiacum* showed that in the absence of Na^+, the internal pH of the bacterium rapidly rose to equal the external pH but in the presence of Na^+, the pH inside the bacterial cell was maintained at a steady state level well below the pH of the

suspending medium (McLaggan *et al.*, 1984). Similar experiments with alkalophilic *Bacillus firmus* RAB demonstrated that the inclusion of protonophore CCCP impairs or abolishes the Na^+-dependent homeostasis (Krulwich *et al.*, 1984). Finally, supporting evidence of the role of Na^+/H^+ antiporter in pH homeostasis came from the finding that when *B. firmus* cells were plated at pH 10.5 on media with suboptimal concentrations of NaCl (3 mM), genetic variants were isolated and they exhibited growth at unusually low concentrations of added Na^+, growth at even higher pH values than usual (pH 11.5 or 12.0) and these are accompanied by increased Na^+/H^+ antiporter activity (Krulwich *et al.*, 1986).

It is also observed that alkalophiles keep a consistent level of antiporters in their membranes and regulate their activity by internal pH so that cells can adjust rapidly to acute changes in pH without a substantial growth lag (Krulwich and Guffanti, 1990). However, in neutrophiles like *Escherichia coli*, no single system provides pH homeostasis. Na^+/H^+ and K^+/H^+ antiporters may contribute to pH regulation such that loss of these antiporters interferes with pH regulation under stress, e.g. at high ionic strength, but neither sodium/proton nor potassium/proton exchange is solely responsible for the ability of *E. coli* to grow at high pH (Rosen, 1986). In the case of marine alkalophiles, Nakamura *et al.* (1992, 1994b) postulated that a Na^+/H^+ antiporter in *V. alginolyticus* is important in acidifying the cell interior in order to support cell growth at alkaline external pH under conditions where the activity of a K^+/H^+ antiporter is marginal. Usually, the K^+/ H^+ antiporter functions as a pH regulator over the pH range of 6.0 to 9.0.

There are two distinct Na^+/H^+ antiporters in *E. coli* that export Na^+ ions and are known as NhaA and NhaB. The *nhaA* mutants are sensitive to high salinity, alkaline pH and the toxicity of Li^+. Hydropathy plots of 41 kDa NhaA suggests that it possesses 11 membrane-spanning α helices (Taglicht *et al.*, 1991). On the other hand, NhaB is 47 kDa and hydropathy plots predict that it contains 12 transmembrane helices. Limited homology exists between NhaA and NhaB, but in one common region, a 43% identity was observed. NhaB also confers resistance to the toxic effects

of Li^+ and Na^+ (Pinner *et al.*, 1992). Results indicate that NhaB has a lower affinity for Li^+ ions but a higher activity for Na^+ ions compared with NhaA. The optimum activity of NhaA is higher than that of NhaB. All these suggest that NhaA-mediated Na^+/H^+ antiporter activity is important when concentrations of Na^+ and pH are high while in contrast NhaB is crucial in conditions whereby Na^+ concentrations and pH are low (Pinner *et al.*, 1992).

Recent studies show that the Na^+/H^+ antiporter gene *nhaA* from *V. alginolyticus* complemented an *E. coli* mutant strain, NM81, defective in an Na^+/H^+ antiporter (NhaA). This *nhaA* gene restored NM81 to grow in a medium containing 0.5 M NaCl at pH 7.5 and concomitantly led to an increase in Na^+/H^+ antiport activity (Nakamura *et al.*, 1994a). The *nhaA* nucleotide sequence from *V. alginolyticus* codes for a protein with a predicted 383 amino acids and molecular mass of 40.4 kDa. Its hydropathy plot indicated that it is a membrane protein with 11 membrane-spanning regions and its deduced amino acid sequence possessed 58% identity with the *E. coli* NhaA. *V. alginolyticus* NhaAv protein contains 3 aspartic residues, Asp-125, -155 and -156, conserved in *E. coli* NhaA, which were identified by site-directed mutagenesis to play a role in the activity of the antiporter (Nakamura *et al.*, 1995). Another gene from *V. alginolyticus, nhaB,* was recently identified by complementation studies in *E. coli* mutant TO114, defective in 3 Na^+/H^+ antiport genes (*nhaA, nhaB, chaA*). This *nhaB* gene from *V. alginolyticus* encodes a predicted 528 amino acid sequence and molecular mass of 57.2 kDa with 62% identity to the *E. coli nhaB* gene at DNA level and 67% identity with *E. coli* NhaB protein (Nakamura *et al.*, 1996).

1.5 Sodium dependent ATPases

The first Na^+-dependent ATPase was detected in the strict anaerobe, *Propionigenium modestum*. When this bacterium grows by fermentation of succinate, the only energy-yielding exergonic reaction involves the decarboxylation of methyl-malonyl-CoA (Fig. 1.4).

Membranes of *P. modestum* are punctuated with numerous of these Na^+-activated ATPases. These enzymes (F-ATPases) have typical highly conserved F_1F_0 structures found also in H^+-translocating ATPases (Fig. 1.5). The F_1 ATPase portion (Na^+ independent when dissociated from F_0 by incubating with EDTA at pH 8.0) has 5 different subunits, $\alpha,\beta,\gamma,\delta$ and ε that have molecular masses similar to the corresponding subunit found in *E. coli*, while the Na^+-binding F_0 moiety has 3 subunits a, b and c that correspond to the 3 F_0 subunits in *E. coli*. The integral membrane sector F_0 acts as a Na^+ channel in ATP synthesis and hydrolysis. The ATPase of *P. modestum* functions as a proton pump at low Na^+ concentrations, which then switches to pumping Na^+ if Na^+ levels elevate (Dimroth, 1990, Dimroth 1987). This ATPase is driven directly by a Na^+ gradient and is a primary sodium pump. A model was proposed by Boyer (1975) that cations may interact with the enzyme through coordination complexes and translocation would be completed by a conformational change which exposes the cation binding region to solute on the other side of the membrane and hence allows the conduction of both Na^+ and H^+ by the same route. Some sequence similarities are found at the C-terminus between the c subunits of the ATPases from *P. modestum* and from *V. alginolyticus*, another putative Na^+-translocating ATPase (Ludwig, 1990).

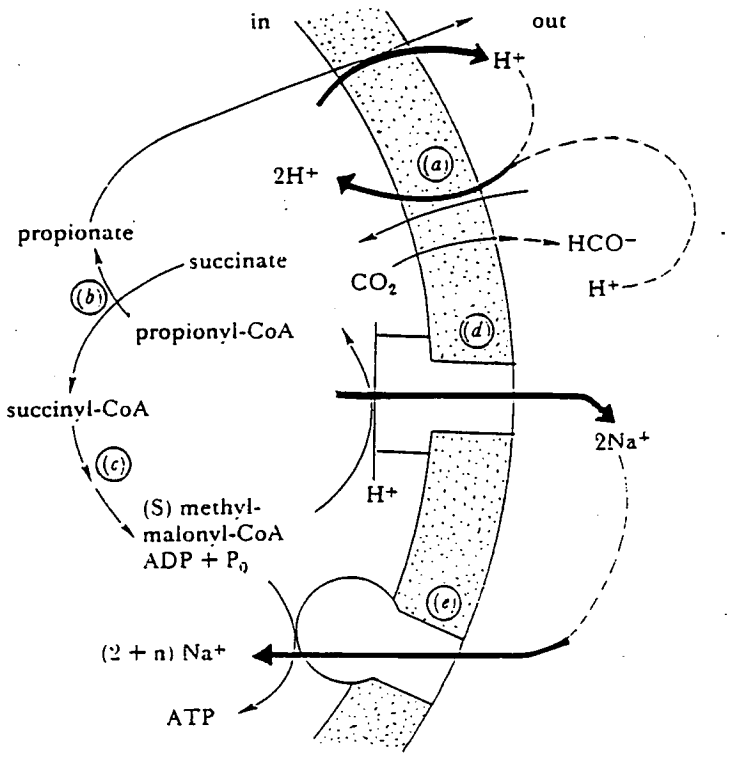

Fig. 1.4 Energy metabolism of *Propionigenium modestum* with a Na^+ cycle coupling the exergonic decarboxylation of *S*-methylmalonyl-CoA to endergonic ATP synthesis. A hypothetical proton circuit could couple succinate uptake with the extrusion of propionate and CO_2. (a) Succinate uptake system; (b) succinate propionyl-CoA:CoA transferase; (c) methylmalonyl-CoA mutase and methylmalony-CoA epimerase; (d) methylmalonyl-CoA decarboxylase; (e) ATPase (Dimroth, 1990).

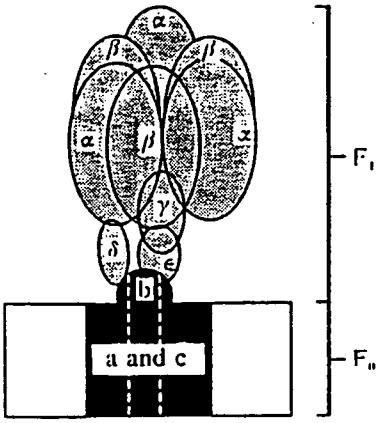

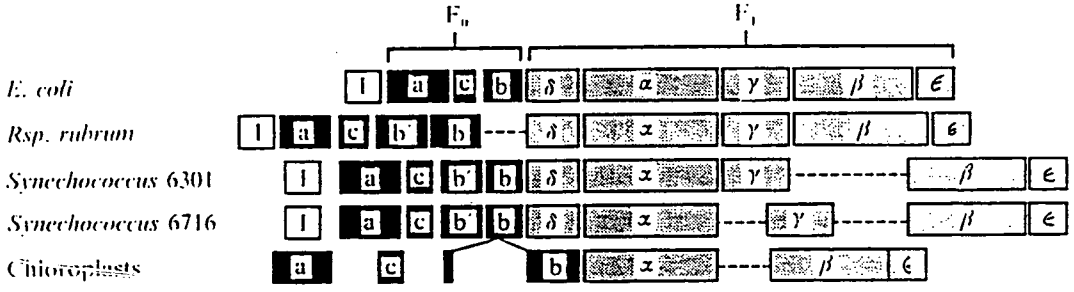

Fig. 1.5 Relationship between the structure of ATP synthase and the organization of genes for its subunits in bacteria and chloroplasts (Walker, 1992).

Skulachev and co-workers (1985 and 1987) reported their observation of Na^+-dependent ATP synthesis in *V. alginolyticus*. But controversy dominates the issue of whether *V. alginolyticus* possesses F-type ATPases that are driven by both Na^+ and H^+ motive forces, or independent H^+ F-ATPases and Na^+ V-ATPases. Krumholz *et al.* (1990) and Dmitriev *et al.* (1991, 1992) have characterized a H^+ F-ATPase in *V. alginolyticus* with structural similarity to the F-ATPase of *E. coli* and no Na^+ dependent activity. Initially, Capozza *et al.* (1991) detected only 1 type of ATPase in *V. alginolyticus* of the F-type but was driven by both H^+ and Na^+ motive forces. But this has now been disproved, as evidence in a recent Honours project in our lab (Clark, 1994) and by Solokov *et al.* (1988), point to the existence of a CCCP-resistant DCCD-sensitive Na^+ V-ATPase in addition to the H^+ F-ATPase previously discovered. This Na^+ V-ATPase is involved in oxidative phosphorylation along with the H^+ F-ATPase (Dibrov *et al.*, 1989).

V-type ATPases play key roles in the acidification of Golgi vesicles and lysozymes in mammalian cells, and vacuoles used for storage of amino acids, Ca^{2+}, carbohydrates, phosphates and hydrolases in yeast and fungi such as *Neurospora*. Its other functions include energizing accumulation of neurotransmitter amines by synaptic vesicles and chromaffin granules and energizing the acidification of urine and the reabsorption of bicarbonate by blood, which are essential for pH buffering (Harvey, 1992). These V-ATPases display several structural and functional similarities to the F-ATPases but differ in that they function exclusively as ATP-dependent proton/sodium pumps. Sequence homology exists only between the α and B, β and A subunits of the F-ATPases and V-ATPases respectively. The catalytic domain comprises of at least 4 subunits in the stoichiometry 3A:3B:1C:1E (Nelson, 1992) and unlike the F-ATPases, cannot function independently of the integral membrane ion translocating portion. This property is attributed to the co-existence of 6 membrane-spanning proteolipids fusing into each molecule of V-ATPase, in addition to the integral C and E subunits.

1.6 Sodium solute symport

If the extrusion of Na^+ is a pre-requisite for pH homeostasis, then Na^+-coupled solute porters provide a bioenergetically favourable means for Na^+ re-entry. Fermenting organisms preferentially utilize a Na^+ gradient instead of H^+ gradient to export large amounts of their metabolic products so as to conserve energy. These Na^+-dependent porters are numerous in halophilic and marine bacteria that inhabit sodium-rich environments, where the symporters are responsible for the transport of the great majority of metabolites (Lanyi, 1979), but these Na^+-dependent porters are apparently absent in freshwater bacteria (Skulachev, 1987).

In principle, cation dependence of solute porters can be caused by: (a) Na+ or other ions acting like an affector or cofactor, which induces a conformational change in the transport proteins, appropriate for transport, (b) participation of the ions in the translocation of metabolites across the membrane, with Na+ ions moving energetically downhill across the membrane to provide energy required for active transport, and (c) the influence of the ions on the driving force for transport, e.g. membrane potential, which will affect all energy-linked functions in the membrane (Lanyi, 1979).

K. pneumoniae possesses an anaerobic citrate transport system with a specific requirement for Na^+ or Li^+. Although there exists a great variety of citrate uptake systems in bacteria, Na^+-dependent citrate transport is rare, probably restricted to organisms such as *K. pneumoniae* which contain a decarboxylase Na^+ pump. The energetic requirements of the anaerobic citrate transport system of *K. pneumoniae* was studied using whole cells and vesicles and found to be dependent not only on Na^+, but also the two components of the proton motive force, the membrane potential and the pH gradient (Dimroth, 1987). Multiple citrate transport systems with different Na^+ and K^+ dependencies are found in *Salmonella typhimurium*. It was also observed that glutamate transport in *E. coli* is stimulated by Na^+, whereby Na^+ increased the affinity for the substrate (Dimroth, 1987). Both the citrate and glutamate transport systems have been proposed to symport sodium and protons with the solute

simultaneously. In addition, Kakinuma and Unemoto (1985) have demonstrated the presence of a sucrose Na^+-dependent symport system in *V. alginolyticus*.

In *E. coli*, the *melB* gene encodes for a 52 kDa melibiose carrier with unique coupling properties. This carrier system is able to use protons, sodium or lithium ions depending on the particular sugar to be transported and ionic environment (Niiya *et al.*, 1982). Sodium or lithium ions selectively increase the apparent affinity of the transporter for galactosides while protons inhibit. The primary amino acid sequences of melibiose and lactose transporters of *E. coli* have very little homology although they share several sugars as substrates, such as melibiose, *p*-nitrophenyl-α-D-galactoside and methyl-1-thio-β D-galactopyranoside). Pourcher and colleagues (1990) proposed a secondary structure model in which the melibiose carrier protein comprises 12 α-helical membrane spanning segments (Fig. 1.6). Based on von Heijne's (1986b) observations of other bacterial membrane proteins, the predicted cytoplasmic loops contain a high density of charged arginine and lysine residues. Histidine residues were postulated to be crucial in the carrier function of several lactose permeases. Hence, site-directed mutagenesis experiments proceeded, exchanging each of the seven histidine residues present in the putative melibiose transporter site, in turn for an arginine. Mutation of His 94 to Arg, drastically affected the transport of sugar analogue *p*-nitrophenyl-α-D-galactoside, identifying this residue as the essential residue for proper transport function (Pourcher *et al.*, 1990).

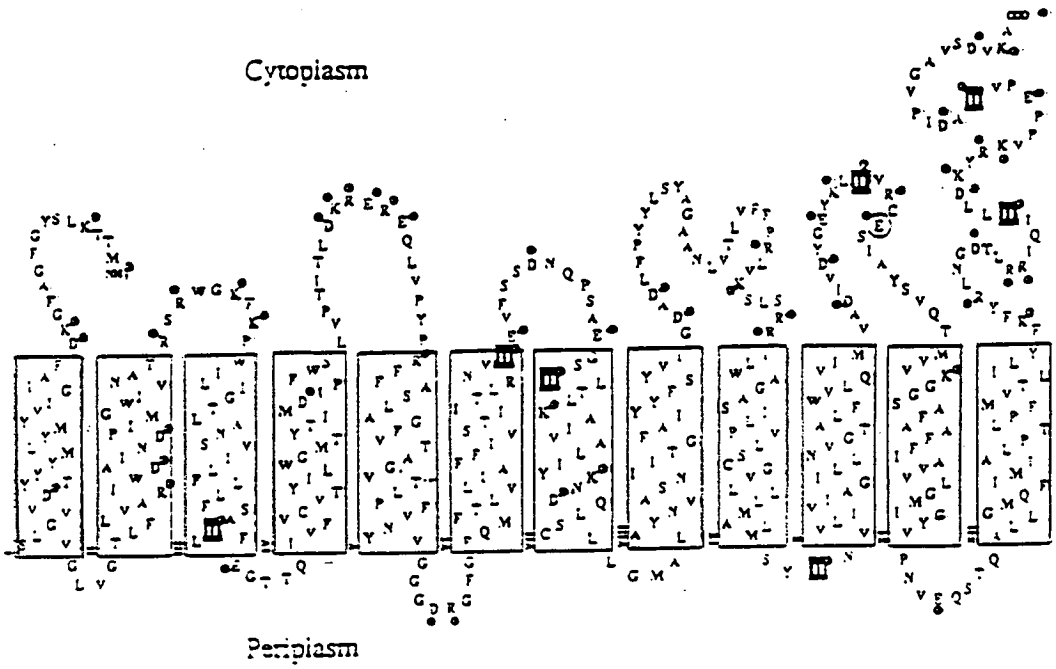

Fig 1.6. Secondary structural model of the melibiose permease of *E. coli*.

Alpha-helical transmembrane domains are shown in boxes; *N*- and *C*- termini are both located on the cytoplasmic surface of the membrane. Black squares indicate the location of the seven histidine residues which were mutated to identify any which are crucial to transporter function (Pourcher *et al.*, 1990).

Na^+-dependent transport systems for single amino acids exist in *Pseudomonas aeruginosa, Bacillus subtilis*, *V. costicola* and *V. alginolyticus* and have been observed by Tokuda, Sugasawa and Unemoto (1982), and Tokuda and Unemoto (1982) to contain Na^+ dependent amino acid symports, e.g. α-aminoisobutyric acid (AIB) (Unemoto, 1993). Evidence that Na^+-solute symporters provide a physiologically important route for Na^+ re-entry for pH homeostasis has come from studies whereby *B. firmus* RAB cells were shifted from a media at pH 8.5 to pH 10.5 in the presence or absence of the nonmetabolizable amino acid analogue AIB. The presence of AIB was discovered to greatly enhance the cells' abilities to maintain a constant internal pH despite a large increase in external pH (Krulwich *et al.*, 1984). Lee *et al.* (1979) succeeded in isolating the Na^+/proline symporter from *Mycobacterium phlei*, which is a 20 kDa single polypeptide. This purified symporter was reconstituted with phospholipids to form proteoliposomes which accumulated proline when driven by an artificially imposed membrane potential. This proline accumulation required Na^+, was sensitive to sulphydryl reagents and to protonophorous uncouplers which disrupt the membrane potential (Skulachev, 1987).

Mutants of *B. alcalophilus* and *B. firmus* unable to grow on alkaline pH, have been isolated whereby in addition to a defect in the Na^+/H^+ antiporter, the Na^+-coupling for several solutes was pleiotropically lost, and H^+ served instead as the coupling for these symport systems (Guffanti *et al.*, 1980, 1981; Krulwich *et al.*, 1979; Lewis *et al.*, 1982). A similar mutant of *E. coli* was also found to have defects in Na^+/H^+ antiport, Na^+/glutamate symport and Na^+/melibiose symport (Zilberstein *et al.*, 1982). The existence of mutants with a pleiotropic defect of several Na^+-coupled porters suggests that a common gene which codes for either a common Na^+-translocating subunit or more likely, have a regulatory function, is responsible for the function of these systems (Dimroth, 1987).

1.7 Sodium driven flagellar motors

Flagellated bacteria swim by rotating their flagella which act as semi-rigid helical propellers. Embedded in the cytoplasmic membrane at the base of each flagellum is a flagellar motor which powers the rotation of the flagellum. As the H^+ motive force is low in alkalophiles, motility is energized by the Na^+ electrochemical gradient (Dimroth, 1987; Krulwich and Guffanti, 1989) (Fig. 1.1).

There are two types of flagella (polar and lateral) in *V. alginolyticus.* Using mutants with only a polar flagellum or only lateral flagella, energy sources for the polar and lateral flagellar motors in *V. alginolyticus* were demonstrated to be Na^+ and H^+ motive forces respectively (Kawagishi *et al.*, 1995). This conforms to the results of Liu *et al.* who demonstrated that the *V. alginolyticus* polar flagellum is Na^+-driven. Using the same mutants with only 1 type of flagella, Atsumi and colleagues (1996) also demonstrated that the lateral flagella was required for swimming in viscous environments and the bacteria swam faster (from 20 μm/s to 40 μm/s) as viscosity increased from 1cP to 5cP. Lateral flagella are produced in media of high viscosity and the relevant viscosity sensor is the polar flagellum. It was proposed that marine vibrios sense a decrease in the rotation rate of the constitutively-synthesized polar flagellum when the bacterium encounters an increase in medium viscosity or a surface, as a trigger for lateral flagella induction (Kawagishi *et al.*, 1996). Moreover, it was hypothesized that the single polar flagellum propels the bacterium (swimming) in liquid, while the multiple peritrichous lateral flagella move the bacterium over surfaces (swarming) (McCarter, 1995). Again with the previous mutants, it was shown that mutants with only the polar flagellum respond chemotactically to attractant stimulus but did not respond to repellent stimulus. The reverse was true for mutants possessing only the lateral flagella (Homma *et al.*, 1996).

V. alginolyticus has been shown to possess a Na^+ or Li^+ driven polar flagellar motor (Liu *et al.*, 1990). The Na^+ gradient is probably generated by the respiratory Na^+ pump in *Vibrio alginolyticus*. Membrane potential and swimming speed of these bacteria approached maximal values as Na^+ and Li^+ concentrations were increased,

but an invariant Na^+ electrochemical gradient was maintained over a wide range of Na^+ concentrations. Hence this indicates a tight coupling between ion transfers and force generation. The torque of flagellar rotation was also stably generated at various Na^+ influxes through the motor (Muramoto *et al.*, 1995a). Muramoto and co-workers (1995b) also found that the rotation rate increased with increasing external concentration of NaCl, and reached 1000 r.p.s. at 30 mM NaCl. The force-generating unit of the motor (MotY) has an intracellular Na^+-binding site, at which the intracellular Na^+ concentration controls the rate of Na^+ influx for motor rotation (Yoshida *et al.*, 1990).

The flagellar motor (MotY) couples sodium influx to force generation for driving rotation of the helical flagellar filament. The *motY* gene in *V. alginolyticus* was sequenced and it encodes a 293 amino acid sequence which has a C-terminal domain similar to C-terminal regions of many peptidoglycan-interacting proteins, e.g. *E. coli* MotB and OmpA, suggesting that MotY may interact with peptidoglycan for anchoring the motor. Expression of this gene under the *lac* promotor-repressor system, increased the swimming fraction of *V. alginolyticus* after induction with IPTG. These results verify that *V. alginolyticus* MotY is the force-generating unit and its high identity to *V. parahaemolyticus* MotY and its ability to complement a *motY* mutation in *V. parahaemolyticus*, confirm this notion (Okunishi *et al.*, 1996).

1.8 Aerobic respiratory chains

The principal function of aerobic respiratory chains is the electrogenic translocation of protons (or other ions such as Na^+) across bacterial plasma membranes, mitochondrial inner membranes or chloroplast thylakoid membranes, generating a proton (or sodium) motive force which drives ATP synthesis, secondary active solute transport, protein secretion and cell motility. Peter Mitchell proposed that this proton translocation was tightly coupled to electron transport in his chemiosmotic theory (Mitchell, 1966). He postulated that in the energy metabolism of prokaryotes, an electrochemical gradient of protons is built at the expense of light or chemical energy by one of the proton pumps present in the bacterial membrane, e.g. respiratory chains, H^+-translocating adenosine triphosphatases (ATPases), photosynthetic reaction centres or bacteriorhodopsin (Dimroth 1987). This transmembrane proton electrochemical gradient ($\Delta\mu_{H^+}$) is composed of two essential components: a concentration difference of protons across the membrane, or simply a pH gradient (ΔpH) and a difference in electric potential between the two aqueous phases separated by the membrane, the membrane potential ($\Delta\psi$).

Proton motive force $\Delta_\mu H^+ = \Delta\psi + 2.3RT/F \log (H^+ \text{ in})/(H^+ \text{ out})$

where $\Delta pH = 2.3RT/F \log (H^+ \text{ in})/(H^+ \text{ out})$

Energy transducing membranes possess two distinct types of proton pumps. A primary pump, in the case of mitochondria or respiring bacteria, generates a proton gradient using energy liberated from the 'downhill' transfer of electrons from substrates such as NADH to final acceptors such as O_2 (Fig. 1.7). Other primary pumps in photosynthetic bacteria exploit energy made available from the absorption of quanta of visible light to create a gradient of protons, while in chloroplasts, in addition to accomplishing the former, also drive electrons 'uphill' from water to acceptors such as $NADP^+$.

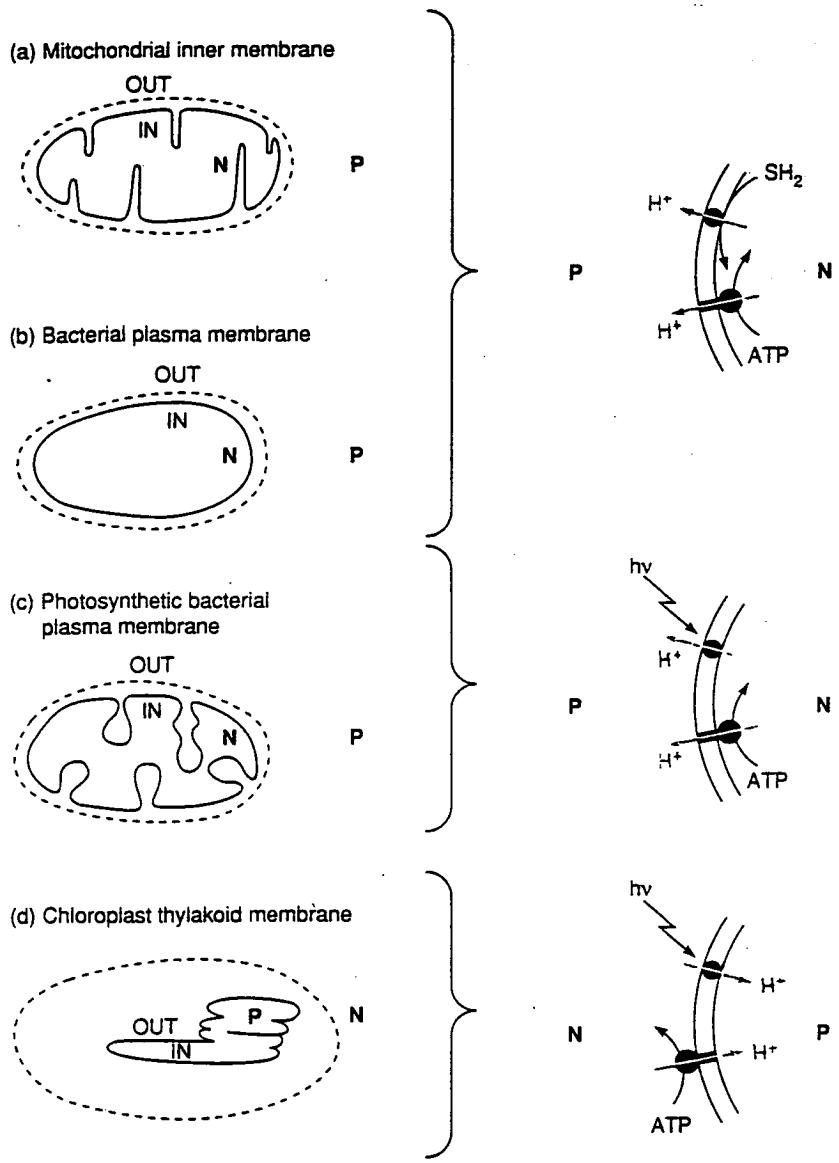

Fig. 1.7. Energy-transducing membranes contain pairs of proton pumps with the same orientation (Nicholls and Ferguson, 1992).

In contrast, the highly-conserved secondary pump normally produces a proton gradient in the same direction across the membrane as the primary pump when operating in isolation but in the presence of a primary pump, the high gradient of protons generated by a primary pump forces the secondary pump to reverse its direction of proton movement (Nicholls and Ferguson, 1992).

During aerobic respiration in mitochondria and bacteria, electrons obtained from the oxidation of substrates by the different dehydrogenases, are transferred to highly hydrophobic and mobile quinones, which are in turn oxidised by a series of membrane-bound cytochrome complexes. These cytochromes finally transfer the electrons to a terminal electron acceptor, oxygen.

The electron carriers in the respiratory assembly of the inner mitochondrial membrane are flavins, iron-sulphur complexes, quinones, haem groups of cytochromes and copper ions. Electrons from NADH are first transferred to the FMN prosthetic group of NADH-ubiquinone oxidoreductase (complex I), the first of three complexes (Fig. 1.8 and Fig. 1.9). Next, electrons are passed through the iron-sulphur clusters of the complex before emerging in the quinol, QH_2, the reduced form of ubiquinone (Q). This mobile carrier is oxidised by cytochrome reductase, a complex composed of cytochromes *b* and c_1 and an iron-sulphur centre. The second complex reduces cytochrome *c*, a water-soluble mobile peripheral membrane carrier of electrons, which then transfers electrons to cytochrome oxidase. This third complex comprises of cytochromes *a* and a_3 and two copper ions. A haem iron and copper ion in this oxidase deliver electrons to the ultimate acceptor, O_2 to form H_2O (Stryer, 1988, pg 446). Rare exceptions to this pathway include *Saccharomyces cerevisiae*, which contains a lactate b_2 oxidoreductase which transfers electrons directly from L-lactate to cytochrome *c* (De Vries and Marres, 1987) and protozoae which possess a quinol oxidase which transfers electrons from ubiquinol to oxygen (Clarkson *et al.*,1989).

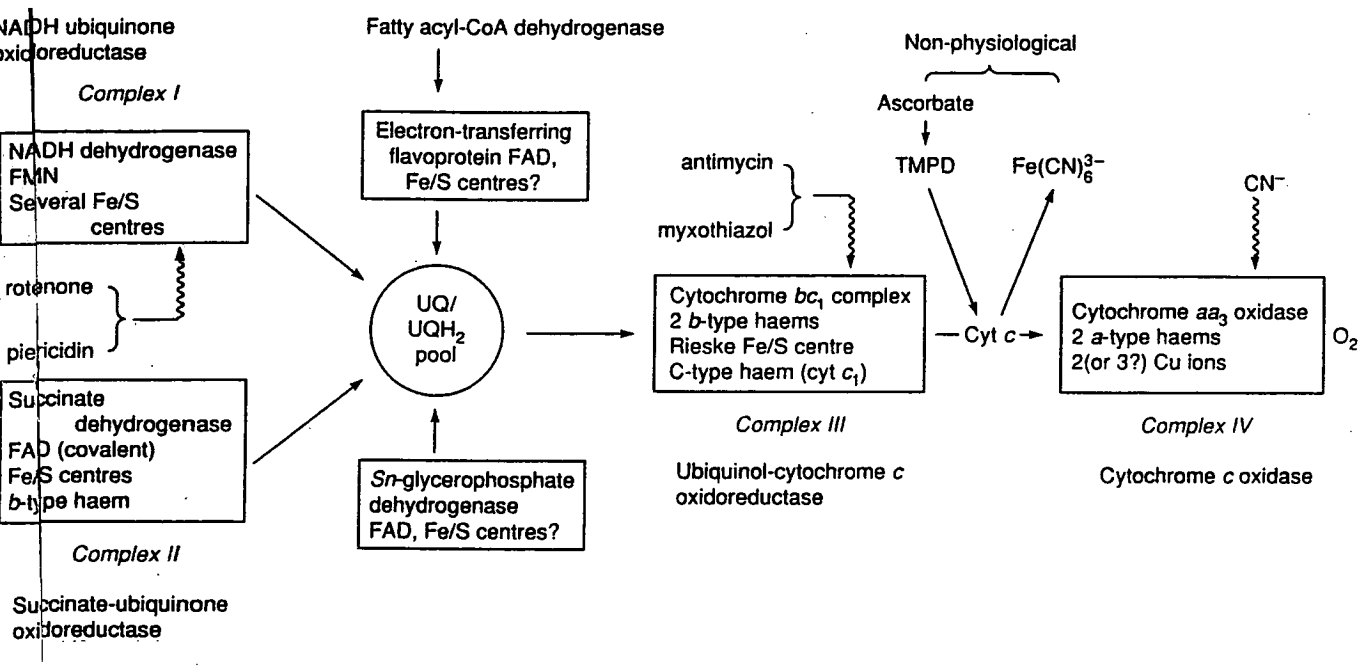

Fig. 1.8. An overview of the redox carriers in the mitochondrial respiratory chain and their relation to the four respiratory chain complexes (Nicholls and Ferguson, 1992). 'Wavy arrow' = site of action of an inhibitor.

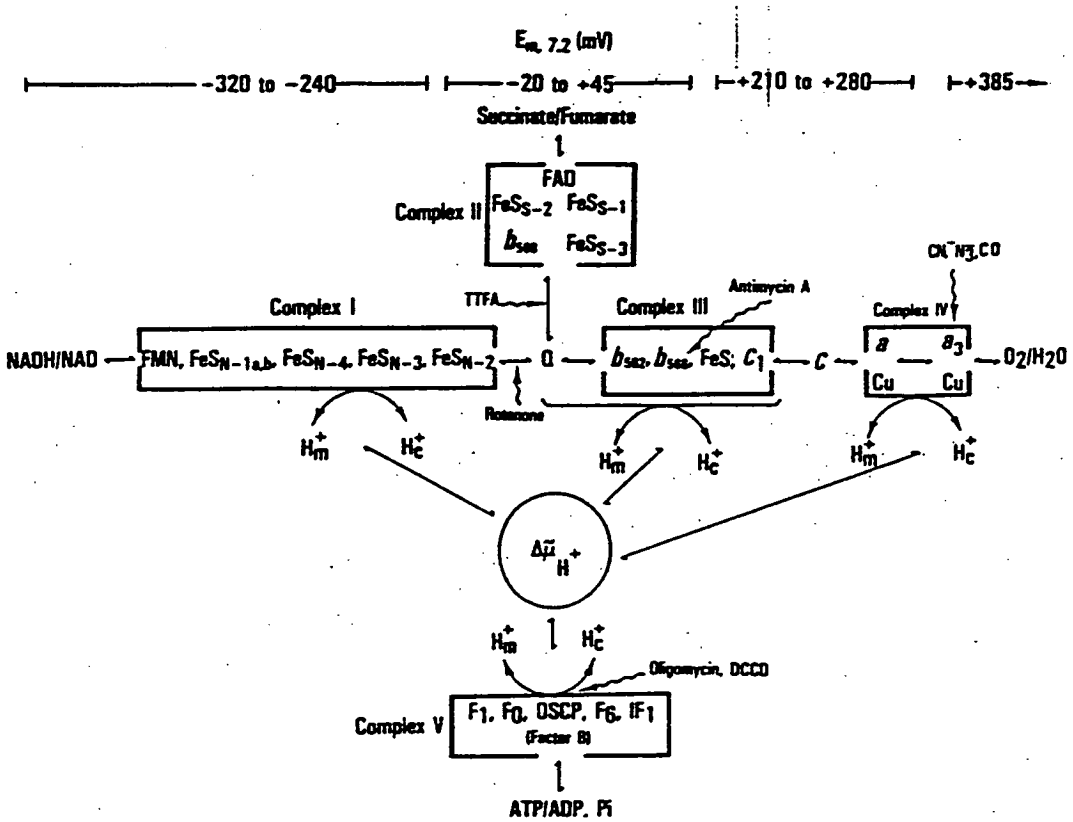

Fig. 1.9. Profile of the mitochondrial electron transport-oxidative phosphorylation system (Hatefi, 1985).

Bacterial aerobic respiratory systems have greater diversity of electron transfer pathways than mitochondrial respiratory systems, and have exploited unique terminal oxidases, depending on the natural habitat of the bacteria and their modes of aerobic respiration. Fig. 1.10 shows the relatively simpler respiratory chain of *E. coli*, while Fig. 1.11 shows a different and more complex system present in *P. denitrificans*. The respiratory system of most bacteria are branched at both the dehydrogenase and oxidase sites as there is more than one terminal oxidase in the cytoplasmic membrane. The different dehydrogenases included NADH-ubiquinone oxidoreductase, hydrogenase and succinate dehydrogenase. There are two main recognized groups of terminal oxidases: Class I are cytochrome *c* oxidases while Class II are quinol oxidases. Class I oxidases receive electrons from ferrocytochrome *c* and reduce molecular oxygen to water. Oxidases from Class I are further subdivided into three subgroups: Class IA enzymes contain haem *a* and Cu^{2+} and Class IB enzymes contain haem *b* or haem *o*. Recently-discovered Class IC enzymes possess haem *b*, haem *c* and Cu^{2+}. Quinol oxidases (Class II) are unique to bacteria. They receive electrons from ubiquinols and/or menaquinols and transfer them to molecular oxygen. These enzymes dispense entirely with haem *a*, but contain either haem *b*, haem *o* and Cu^{2+} (Class IIA), or haem *b* and haem *d* (Class IIB) (Anraku, 1988). To fully illustrate the diversity of bacterial electron transport systems, well-characterized pathways in *E. coli* and *P. denitrificans* will be described further in more detail.

In *E. coli* (Fig. 1.10), NADH dehydrogenase and succinate dehydrogenase donate their electrons to a ubiquinol pool that transfers the electrons directly to 3 different terminal quinol oxidases, cytochrome *bd*-I, cytochrome *bd*-II and cytochrome *bo*. Cytochrome *bd*-I (Class IIB) comprises 2 subunits with 2 haems *b* and 1 or 2 haems *d* (Bebbington and Williams, 1993).

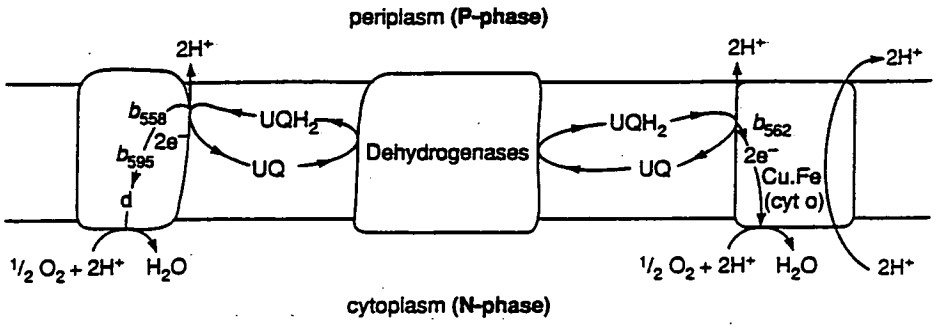

Fig. 1.10. The *E. coli* aerobic electron-transfer chain from ubiquinol to oxygen (Nicholls and Ferguson, 1992).

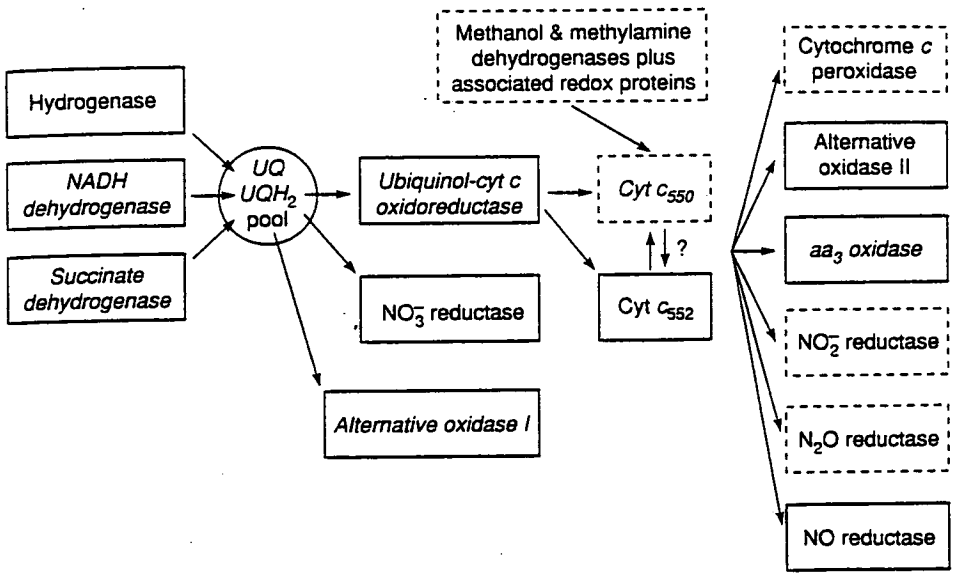

Fig. 1.11. Organization of electron transport components in *P. denitrificans* (Nicholls and Ferguson, 1992).

Cytochrome *bd*-I has a higher affinity for oxygen than cytochrome *bo*, making it better adapted to scavenging oxygen in a low oxygen environment. Cytochrome *bd*-I is encoded by the *cydAB* genes while cytochrome *bd*-II (not shown in Fig. 1.10), a newly discovered quinol oxidase in *E. coli* is encoded by the *appBC* genes (Sturr *et al.*, 1996). The latter was identified and sequenced, with a higher homology to the former. However, cytochrome *bd*-II is still not very well characterized and it is unclear if it contains the same number and types of haem groups. Cytochrome bo_3 (Class IIA) is a five subunit complex with low affinity for oxygen but is extremely efficient as it functions as a proton pump. It contains a low spin haem and a high spin haem in cytochrome $b_{563.5}$ and *o* respectively as well as a Cu_B. This cytochrome *bo* belongs to the aa_3-type cytochrome *c* oxidase superfamily but differs slightly from the other members in that it does not contain Cu_A but Cu_B instead (Minigawa *et al.*, 1992; Salerno *et al.*, 1990; Au *et al.*, 1985; Nakamura *et al.*, 1989).

In the more complex *P. denitrificans* pathway (Fig. 1.11), ubiquinone accepts electrons from NADH dehydrogenase, hydrogenase and succinate hydrogenase and transfers them to either ubiquinol cytochrome *c* oxidoreductase (cytochrome bc_1) or quinol reductase cytochrome bb_3. The terminal quinol oxidase cytochrome bb_3 (also known as cytochrome *o*, ba_3 or b_o) functions as a proton pump, and comprises 3 subunits encoded by the *P. dentrificans cyoABC*, and is highly homologous to cytochrome bo_3 from *E. coli*. It has 2 protohaems (subunit I) and a Cu_A (subunit II) for prosthetic groups. Electrons passed on to cytochrome bc_1 however, are subsequently donated to cytochrome c_{552} which eventually transfers the electrons to 2 different cytochrome *c* oxidases, cytochrome aa_3 and cytochrome cbb_3. Both cytochrome aa_3 and cytochrome cbb_3 couple proton translocation across the membrane with oxygen reduction. Cytochrome aa_3 belongs to the aa_3-type cytochrome oxidase superfamily (Class IA) and comprises 3 subunits in which subunit I contains 2 haems *a* and a Cu_B while subunit II contains Cu_A involved in the oxidation of cytochrome c_{552}. One high-spin haem *a* and the Cu_B forms the oxygen

reduction catalytic site. A new alternative *cbb*$_3$-type cytochrome *c* oxidase (Class IC) is also found in *P. denitrificans*. This cytochrome complex contains 3 subunits with 2 cytochromes *c* and 1 cytochrome *b*. Prosthetic groups of cytochrome *cbb*$_3$ include a haem *b*, a haem *c* and Cu_B (de Gier *et al.*, 1994).

1.9 Complex I and H^+-translocating NADH-ubiquinone oxidoreductases

In eukaryotes, the inner membranes of mitochondria contain three multi-subunit enzyme complexes that act successively to transfer electrons from NADH to oxygen, which is reduced to water (Fig. 1.12). The first enzyme in the electron transfer chain, NADH-ubiquinone oxidoreductase, removes electrons from NADH and passes them via a series of enzyme-bound redox centres (FMN and Fe-S clusters) to the electron acceptor ubiquinone. For each pair of electrons transferred from NADH to ubiquinone it is usually considered that four protons are removed from the matrix (Walker, 1992).

The structure, mechanism and evolution of complex I were derived from:

- the primary structures of bovine mitochondrial enzyme, *Neurospora crassa* enzyme and bacterial sources, and homology between subunits of different species;
- the resolution of bovine complex I and *N. crassa* complex I into defined sub-complexes;
- the electron microscopic studies of the *N. crassa* enzyme.

1.9.1 Purification of complex I

Hatefi and colleagues (1962) purified complex I from bovine heart mitochondria, providing an active although polydisperse enzyme that can be assayed conveniently by its ability to transfer electrons to ubiquinone-1; this activity can be inhibited by rotenone or piericidin A. This preparation contained a number of impurities such as transhydrogenase and cytochrome oxidase subunits. The idea was adopted that copurification of subunits with the complex under different conditions of purification was evidence that they are part of the assembly, even though their roles may be obscure. In addition, comparison of the subunit compositions and sequences of subunits present in preparations of enzyme from different species, would indicate which subunits are truely part of the complex I assembly.

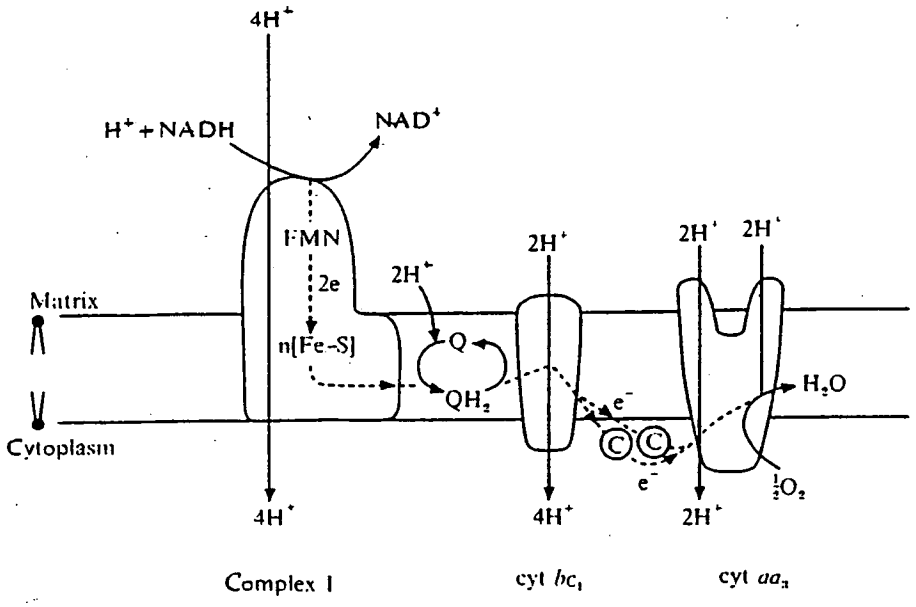

Fig. 1.12. Electron transfer coupled to proton translocation in the mitochondrial electron transfer chain (Walker, 1992).

More recently, complex I is now routinely purified by extraction from membranes with dodecyl-β-D-maltoside and purified by chromatographic methods, producing a monodisperse complex with fewer contaminants (Finel *et al.*, 1992; Buchanan *et al.*, 1996).

Purified complex I was fragmented with the chaotropic anion, perchlorate, producing soluble material (flavoprotein fraction and iron protein fraction) and a precipitate which is known as the hydrophobic protein fraction. The latter fraction actually contains globular water-soluble subunits as well as hydrophobic ones.

The bovine heart complex (*Bos taurus*) comprises at least 42 subunits grouped into the above mentioned three fractions :

- FP (flavoprotein)
- IP (iron-sulphur protein) and
- HP (hydrophobic protein-ND subunits). (Walker, 1992)

In mammalian complex I, there are seven mitochondrial-encoded subunits ND1-6 and ND4L which are all hydrophobic intrinsic membrane polypeptides. In addition to these 7 subunits, there are at least 34 nuclear-encoded subunits in the bovine complex I (Walker, 1992) (Table 1.1 and 1.2).

Subunit	M_r by gel (kDa)	M_r from sequence	No. of amino acids	Transmembrane α-helices
ND1	30	35698.0	318	8
ND2	30	39282.1	347	8
ND3	15	13082.6	115	3
ND4	39	52127.1	459	12
ND4L	10	10825.2	98	3
ND5	50	68341.5	606	13-14
ND6	n.d.	19105.6	175	4-5

Table 1.1. Properties of subunits of bovine complex I that are encoded in mitochondrial DNA (Walker, 1992).

Subunit	M_r by gel (kDa)	M_r from sequence	No. of amino acids	Post-translational modifications
75 kDa (IP)	75	76960.2	704	[4Fe-4S], [2Fe-2S]
51 kDa (FP)	51	48416.1	444	[4Fe-4S]
49 kDa (IP)	49	49174.4	430	None known
42 kDa	42	36692.8	320	None known
39 kDa	39	39115.1	345	None known
30 kDa (IP)	30	26431.8	228	None
24 kDa (FP)	24	23814.4	217	[2Fe-2S]
B22	22	21700.6	178	*N*α-acetyl
TYKY	23	20195.9	176	2 x [4Fe-4S]
PDSW	22	20833.6	175	None
PSST	20	20077.5	178	Fe-S protein (?)
PGIV	19	19959.9	171	Fe-S protein (?)
ASHI	19	18737.0	158	None
SGDH	16	16726.3	143	None
B18	18	16476.5	136	*N*α-myristyl
18 kDa (IP)	18	15337.2	133	None
B17	16.5	15434.9	127	*N*α-acetyl
B15	15	15095.1	128	*N*α-acetyl
B14	14	14964.3	127	*N*α-acetyl
B13	13	13226.4	115	*N*α-acetyl
15 kDa (IP)	15, 13	12536.4	105	None
B8	8	10990.6	98	*N*α-acetyl
B12	12	11009.4	97	Modified
13 kDa (IP)	13	10535.7	96	None
SDAP	8	10109.5	88	Pantethenic acid
B9	9	9217.7	83	Modified
MLRQ	9	9324.7	82	None
10 kDa (FP)	10	8437.3	75	None
AGGG	7.9	8493.3	72	None
MWFE	7.5	8135.4	70	None known
MNLL	7	6966.1	57	None
KFYI	6	5828.7	49	None

Table 1.2. Properties of nuclear-encoded subunits of bovine complex I (Walker, 1992).

1.9.2 Sequence identification

The mitochondrial subunits were detected by antibodies raised with peptides based on sequences predicted from the mitochondrial sequences and *N*-terminal sequenced (Gibb and Ragan, 1990), except for ND6 sequences, which have been determined by sequencing following the removal of their *N*-α-formyl groups (Skehel and Walker, unpublished work). *N*-terminal sequence for the mitochondrial complex I subunits had been difficult to determine because these subunits did not associate with particular bands in stained polyacrylamide gel analyses of the enzyme complex. That is due to the extreme hydrophobic nature of these subunits, which causes faint staining with Coomassie Blue dye and gives rise to diffuse bands in denaturing SDS gels. The problem is further compounded by the fact that these hydrophobic proteins migrate to anomalous molecular weights on SDS gels and their true molecular weights cannot be determined.

For the nuclear-encoded subunits, fragments of protein sequences determined directly from the proteins, were used to design mixed oligonucleotide primers and probes for polymerase chain reactions using poly(A^+) bovine heart cDNA as template (Fearnley *et al.*, 1989, 1991; Pilkington and Walker 1989; Runswick *et al.*, 1989, 1991; Pilkington *et al.*, 1991a, b; Dupuis *et al.*, 1991a, b; Skehel *et al.*, 1991; Arizmendi *et al.,* 1992; Walker *et al.*, 1992). In the case of proteins with free α-NH_2 groups, partial protein sequence were determined by first separating the subunits by gel electrophoresis, then transferring them to a poly(vinylidene difluoride) membrane before subjecting the protein to Edman degradation. Post-translationally modified subunits were purified by chromatography, fragmented, the fragments fractionated (usually by HPLC or by gel electrophoresis), and then partial sequences were determined on internal peptides.

1.9.3 Post-translational modifications

At least 10 subunits of bovine complex I are post-translationally modified. With the accuracy of the electro-spray mass spectrometry, the mass difference between the post-translationally modified protein and the mass calculated from its sequence were used to deduce the nature of the modification (Table 1.2). The *N*-terminals of B22, B17, B15, B14, B13 and B8 appear to be α-*N*-acetylated (Walker, 1992). B18 was suggested to be α-*N*-myristylated subunit and it was suggested the myristyl moiety helps anchor B12 in the inner mitochondrial membrane (Towler *et al.*, 1988). B12 and B9 are modified but their modifications have not been determined fully. Data indicates that the *N*-terminal residue of B12 is *N*-acetylated while other unidentified amino acids are methylated (Runswick, Fearnley and Walker, unpublished results). An unusual modification in SDAP produces a covalently bound pantethenic acid which has a possible role as an acyl carrier protein. 49kDa (IP), 42kDa, 39kDa, 30kDa (IP), PDSW, ASHI, SGDH, 18kDa (IP), 15kDa (IP), 13kDa (IP), MLRQ, 10kDA (FP), AGGG, MWFE, MNLL, KFYI are not modified.

1.9.4 Homology to *Alcaligenes eutrophus* NAD^+-reducing hydrogenase

Interestingly, the *hoxF* gene in *Alcaligenes eutrophus* codes for the α subunit of a water-soluble NAD^+-reducing hydrogenase which has good similarity to sizeable stretches of the 24 kDa (Pilkington and Walker, 1989) and the 51 kDa (Pilkington *et al.*, 1991a) from FP of the bovine complex I while the γ subunit (*hoxU*) corresponds to the 75 kDa (1-200) (Runswick *et al.*, 1989; Pilkington *et al.*, 1991a) from IP of complex I (Fig. 1.13). This relationship implies that the 24 kDa, 51 kDa and 75 kDa subunits of complex I form a structural unit that is involved in NAD^+/NADH oxidoreductase activity in the first step of electron transport (Pilkington *et al.*, 1991a). Similar relationships were observed between the hydrogenase subunits and the homologues of the 51 kDa subunit in *P. denitrificans* (Xu *et al.*, 1991a) and the 75 kDa and 51 kDa subunits in *N. crassa* (Preis *et al.*, 1991).

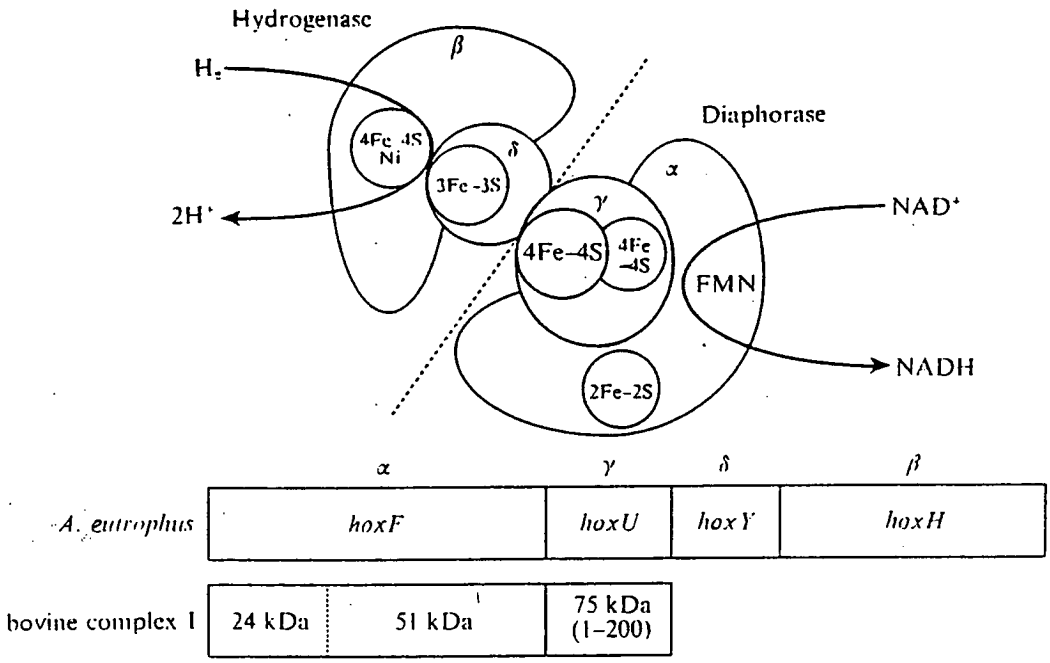

Fig. 1.13. The structure and catalytic model of the NAD^+ reducing hydrogenase from *A. eutrophus* and a diagram illustrating the subunits of *Bos taurus* complex I which correspond to the subunits encoded by the *hoxS* operon (Walker, 1992).

From these comparisons and other features, it is believed that the *B. taurus* 51 kDa subunit of complex I catalyses NADH oxidation, transferring electrons from NADH to FMN. Comparison of the *B. taurus* 51 kDa of complex I with homologues such as *Paracoccus denitrificans* 50 kDa corresponding subunit and the 51 kDa of *Neurospora crassa* and the *A. eutrophus* HoxF (153-602), shows a number of conserved amino acids, especially at the putative NADH binding site, the FMN binding site and the [4Fe-4S] cluster site, with the conserved Cys-X-X-Cys-X-X-Cys motif. The homologous regions of the γ subunit of the *A. eutrophus* enzyme and the 75 kDa subunit of IP contain ligands for a second and possibly third [4Fe-4S] centre. Finally, homologous regions of the 24 kDa peptide of FP from several sources including *Paracoccus* and the α subunit of *A. eutrophus* H_2-NAD^+ oxidoreductase, contain Cys residues which could contribute to a fourth FeS centre (probably [2Fe-2S] type) (Nicholls and Ferguson, 1992).

The NADH-binding site of complex I is considered to lie within the 51 kDa subunit. The likelihood of a sequence folding into a β-sheet:α-helix:β-sheet nucleotide binding fold depends on the comparison of the sequence with a 'core' of four invariant residues consisting of three glycines and an acidic amino acid found in NADH-binding sites of known structure, and seven additional positions are examined for the conservation of particular classes of amino acids (Wierenga *et al.*, 1986). From alignments with sequences in NAD^+-binding sites in three dehydrogenases with known structure, the ADP-binding pocket of the bovine 51 kDa subunit was identified (Walker, 1992).

FMN is usually considered the most likely immediate oxidant of NADH. There are three known classes of FMN-binding sites. One class is the $(\beta\alpha)_8$ flavoenzyme family where the FMN lies at the end of an 8-stranded α–β barrel and is between five α-helices in flavocytochrome b_2 (Xia and Matthews, 1990) and glycolate oxidase (Lindqvist, 1989), or three α-helices in trimethylamine dehydrogenase (Lim *et al.*, 1986). The flavodoxins comprise the second class of FMN-binding site. FMN is bound in a β–α–β fold similar to the ADP fold described

above but without the characteristic pattern of amino acids (Mayhew and Ludwig, 1975; Smith *et al.*, 1983). The third class is exemplified by phthalate dioxygenase reductase (PDR) which catalyses electron transfer from NADH to phthalate dioxygenase via FMN and a [2Fe-2S] cluster. The NADH-binding domain is folded into a central five-stranded parallel β-sheet flanked on each side by an α-helix, and is similar to nucleotide-binding domains in dehydrogenases. FMN is bound to the edge of an antiparallel β barrel which is related to a structure in the FAD-binding flavoenzyme, ferredoxin reductase (Karplus *et al.*, 1990). Of all three classes, PDR is structurally most similar to the 51 kDa subunit of complex I. The region of the 51 kDa subunit involved in binding FMN is most likely to be in the highly conserved glycine rich sequence encompassing amino acids 180-234. The 51 kDa subunit appears to contain at least three domains binding NADH, FMN and an Fe-S cluster, arranged in that linear order in the sequence from *N*- to the *C*-terminus (Walker, 1992).

A 39 kDa subunit of complex I contains a segment of sequence which fits the nucleotide binding site fingerprint associated with the NADH-NAD^+, or DD, transhydrogenase activity in complex I (Fearnley *et al.*, 1991) and a similar sequence is also present in the homologous 40 kDa subunit from *N. crassa* complex (Fearnley and Walker, 1992; Roehlen *et al.*, 1991), indicating that these subunits may have a potential NADH binding site. Moreover, the 39 kDa subunit is significantly related to 3β-hydroxy-5-ene steroid dehydrogenases throughout most of its sequence although the significance of this relationship is not understood. The fungal 40 kDa subunit has been proposed to be related to the mitochondrial processing peptidase and to the processing enhancing peptidase (Roehlen *et al.*, 1991), which co-operate in the processing of mitochondrial import precursor proteins. These proteins belong to the insulinase protease super-family which includes core proteins I and II of mitochondrial cytochrome *c* reductase (Walker, 1992).

1.9.5 Other subunits of complex I

The 33 kDa (ND-1) and 15 kDa subunits of bovine complex were thought to contain the ubiquinone binding site but the evidence is rather inconclusive. ND-1 sequence was related to a bacterial glucose dehydrogenase (Friedrich *et al.*, 1990). It was identified by photoaffinity labelling with a photoactivatable analogue of rotenone (Earley and Ragan, 1984) and a photoactivatable inhibitor (Earley *et al.*, 1987). A 15 kDa subunit was found upon mild dissociation which resulted in this IP fragment subunit remaining bound to ubiquinone (Suzuki and Ozawa, 1986). Its identity is unclear, as there are more than 1 candidate at this molecular weight present in the IP of Complex I.

Results from experiments using the carboxyl group modifying reagent, DCCD, a protonophore, indicate that proton translocation occurs in up to 6 subunits of complex I. Some of the subunits identified to be involved in proton translocation were the 29 kDa, 49 kDa, 14 kDa and 21 kDa subunits. The sequence of 21 kDa ASHI (Walker *et al.*, 1992) indicates that it has one transmembrane α-helix and the proposed helical region contains a single glutamic acid residue in a region which is related to a sequence that contains a site of modification by DCCD of cytochrome oxidase in subunit III (Walker, 1992).

1.9.6 Prosthetic groups and catalytic mechanism

In order to understand the electron transfer and the mechanism of catalysis in complex I, the relative positions of the various subunits within the complex and their prosthetic groups must be known. The electron carriers of complex I are contained predominantly in 2 extramembranous subcomplexes, FP and IP (Table 1.3). FP contains the 51, 24 and 9 kDa subunits. The 51 kDa subunit carries the NADH binding site and contains FMN and a tetranuclear iron-sulphur cluster. The 24 kDa subunit contains a binuclear iron-sulphur cluster. IP contains at least 7 subunits, namely, the 75, 49, 30, 18, 15, 13 and 11 kDa subunits. A tetranuclear and very likely a binuclear iron-sulphur cluster are present in the 75 kDa subunit.

Table 1.3. Distribution of iron-sulphur clusters in subunits of Complex I

Subunit	Number of conserved cysteine residues in DNA sequence	Proposed cluster types from sequence	Iron-sulphur cluster types identified from EPR	Conclusion
75 kDa (IP)	11	1 x [4Fe-4S] 1 x [2Fe-2S]	1 x [4Fe-4S] 1 x {2Fe-2S]	N-2 or N-4
51 kDa (FP)	4	1 x [4Fe-4S]	1 x [4Fe-4S]	N-3
24 kDa (FP)	3	1 x [2Fe-2S]	1 x [2Fe-2S]	N-Ib
TYKY (23 kDa)	8	2 x [4Fe-4S]	-	N-2 or N-4
PSST (20 kDa)	3	1 x [4Fe-4S]	-	N-2 or N-4
PGIV (19 kDa)	8	unknown	-	

FP and IP make contact through the 51 and 75 kDa subunits, as observed in cross-linking studies described below. The remaining HP fraction contains 31 subunits, is largely membrane-intercalated and contains 2 iron-sulphur subunits, the 23 and possibly 20 kDa subunits. By radioimmunoassay, there are 2 mol of the 15 kDa subunit, 1 mol each of the FP subunits and the four largest IP subunits per mol of complex I. The stoichiometry of the 11 kDa and 13 kDa subunits could not be determined due to co-migration during gel electrophoresis (Belogrudov and Hatefi, 1994).

Cross-linking studies showed that the three FP subunits are juxtaposed to one another, and only the 51 kDa subunit of FP is in close proximity to only the 75 kDa subunit of IP (Yamaguchi and Hatefi, 1993). The 75 kDa subunit cross-linked to the 30 kDa and the 13 kDa subunits, the 49 kDa subunit cross-linked to the 30 kDa, 18 kDa and 13 kDa subunits, and the 30 kDa subunit cross-linked to the 18 kDa and 13 kDa subunits. No cross-linked products of 75+49, 75+18, or 18+13 kDa subunits were detected. The results are consistent with the occurrence of potential electron carriers in FP and IP subunits. These electrons carriers are FMN and one iron-sulphur cluster in the 51 kDa subunit, one iron-sulphur cluster in the 24 kDa subunit and apparently two iron-sulphur clusters in the 75 kDa (Yamaguchi and Hatefi, 1993).

When complex I was reduced by NAD(P)H, this appeared to cause conformational changes involving proximities among and between the FP, IP and HP subunits. Energy coupling and transfer occurs via conformational energy transfer from FP and IP to HP, where proton translocation is effected (Belogrudov and Hatefi, 1994). Supporting this evidence, the thermodynamic analysis of flavin in complex I also suggests a conformational change of the complex due to substrate binding (Sled *et al.*, 1994). Ubisemiquinones were obligatory intermediates in electron transfer from NADH to ubiquinone (De-Jong *et al.*, 1994).

From sequence of subunits available from complex I, and assuming one copy of each subunit were present, the calculated molecular weight would be 880 kDa. The molecular weight of bovine complex I was estimated to be 670-890 kDa from its

FMN content (Ragan, 1976). Ragan (1987) suggested the active enzyme was dimeric and this was reinforced by evidence from van Belzen *et al.* (1990) when they titrated NADH-oxidation activity in sub-mitochondrial particles with inhibitor piericidin A. Later evidence disagrees and suggests that the minimal functional unit of complex I must be a heterodimer because the concentration of cluster N-1b is half that of cluster N-2 (van Belzen *et al.*, 1992).

1.9.7 Inhibitors

Due to the lipophilic nature of ubiquinone, the site at which it is reduced has been assumed to be within the membrane domain of the enzyme. 2 main classes of complex I inhibitors exist, divided by their specificity and mode of action on this ubiquinone binding site. Class I (such as piericidin A) inhibitors inhibit in a competitive manner with regard to ubiquinone. Class II (e.g. rotenone) inhibitors are non-competitive. All inhibitors affect electron transfer from the high-potential iron-sulphur cluster N-2 to ubiquinone and bind close to ubiquinone. Class I inhibitors appear to act directly at the ubiquinone-catalytic site (Friedrich *et al.*, 1994), while non-competitive class II inhibitors are thought to cause steric hinderance or form a conformational change preventing passage of electrons to ubiquinone. Both rotenone and Q-binding sites must be occupied for complete inhibition of NADH oxidation (Singer and Ramsay, 1994). Another inhibitor, diphenyleneiodonium, inhibits reduction of iron-sulphur clusters in the mitochondrial NADH-ubiquinone oxidoreductase (complex I) when incubated together in the presence of NADH (Majander *et al.*, 1994).

Natural substances (acetogenins) from the family *Annonaceae* are powerful inhibitors of mitochondrial complex I. Rolliniastatin-1 and Rolliniastatin-2 are more powerful than piericidin in terms of inhibitory constant and protein-dependence of their titres in bovine sub-mitochondrial particles. Squamocin and octivarin have a lower inhibitory constant than piericidin but a larger protein-dependence of the titre. They behave like rotenone. Rolliniastatin-2 has properties mutually exclusive to that

of piericidin and mutually non-exclusive to rotenone with its inhibition site not overlapping that of rotenone (Degli-Eposti *et al.*, 1994).

It was recognized that millimolar concentrations of Ca^{2+} drastically reduce the rate of the turnover-dependent activation of NADH-quinone reductase. Ca^{2+} increases the reactivity of the enzyme sulphydryl group in deactivated preparations towards *N*-ethylmaleimide. Hence it was postulated that the Ca^{2+} content in the mitochondrial matrix may play an important role in the control of NADH oxidation of the respiratory chain (Kotlyar *et al.*, 1992).

1.9.8 Structural resolution

1.9.8.1 *Bos taurus*

Bovine complex I is composed of a peripheral part and a membrane part which are arranged perpendicularly to each other to give the complex an unusual L-shape. The peripheral part protrudes into the matrix space and constitutes the proximal segment of the electron pathway with the NADH-binding site, the FMN and at least three iron-sulphur clusters. The membrane part constitutes the distal segment of the electron pathway with at least one iron-sulphur cluster and the ubiquinone-binding site. Both parts are assembled separately and relationships of the major structural modules of the two parts with different bacterial enzymes suggest that both parts also emerged independently in evolution. This assumption is further supported by the conserved order of the bacterial complex I genes, which correlates with the topological arrangement of the corresponding subunits in the two parts of complex I (Friedrich *et al.*, 1993).

The structure of complex I was resolved by Finel *et al.* (1992). Firstly, complex I was purified from bovine heart mitochondria by solubilization with n-dodecyl β-D-maltoside (lauryl maltoside), ammonium sulphate fractionation, and chromatography on Mono Q in the presence of the detergent. Complex I was dissociated in the presence of N,N-dimethyldodecylamine N-oxide and β-mercaptoethanol. Bovine complex I was split with detergent LDAO, into 2

subcomplexes I_α and I_β, similar to those in *N. crassa* (Finel *et al.*, 1994) Figure 1.14 illustrates the distribution of various subunits in the L-shaped structure. Subcomplex I_α comprises of 23 mainly hydrophilic proteins from the FP, IP fractions and some proteins from HP such as ND2, 39 kDa and 42 kDa (Table 1.4). It can transfer electrons from NADH to coenzyme Q_1 and retains a substantial portion of the electron pathway of complex I. No known activity is associated with I_β, which is embedded in the membrane, comprising of ND4, ND5 and at least 11 other proteins, mostly from the HP fraction (Table 1.5). A scheme is proposed in Figure 1.15, depicting the catalytic reactions and electron transfer through the L-shaped complex I, taking into account of the positions of catalytic sites and prosthetic groups in the various subunits in the I_α and I_β fragments.

By modification of the above procedure, enzymatically active subcomplexes were purified by sucrose-gradient centrifugation in the presence of detergents (Finel *et al.*, 1994). These active subcomplexes, $I_{\lambda IS}$ and $I_{\lambda S}$, catalyse ferricyanide and ubiquinone-1 (Q-1) reduction at similar rates to complex I but do not catalyse decylubiquinone reduction and is rotenone-insensitive. The smallest subcomplex, $I_{\lambda S}$ contains only 13 subunits compared to 22 in I_α, but still retains the 75, 51, 49, 30, 24, 23 (TYKY) and 20 kDa (PSST) subunits which are suggested to form a functional core that comprises the EPR-detectable Fe-S clusters N-1 to N-4 (Table 1.3), and FMN.

Subunit	Properties
75 kDa (IP)	Contains [4Fe-4S] and [2Fe-2S] clusters
51 kDa (FP)	Contains NADH, FMN sites; [4Fe-4S] cluster
49 kDa (IP)	No obvious sites for [Fe-S] cluster
42 kDa	-
39 kDa	Has potential NADH binding site
30 kDa (IP)	No obvious sites for [Fe-S] cluster
24 kDa (FP)	Contains [2Fe-2S] cluster
TYKY	Binds 2 x [4Fe-4S] clusters
PSST	Possible Fe-S protein
PGIV	Possible Fe-S protein
18 kDa (IP)	-
B14	-
15 kDa (IP)	-
B13	-
13 kDa (IP)	-
B8	-
SDAP (also in I_β)	Acyl carrier protein
MLRQ	1 hydrophobic segment
B9	1 hydrophobic segment
10 kDa (FP)	No cysteine residues
MWFE	1 hydrophobic segment
ND2	8 hydrophobic segments

Table 1.4. Properties of bovine complex I subunits detected in bovine subcomplex I_α (Walker, 1992).

Subunits	Hydrophobic segments	Comments
B22	0	
PDSW	1	
ASHI	1	
SGDH	1	
B18	0	N-α-myristylated
B17	1	
B15	1	
B12	0	
SDAP (also in I_α)	0	Acyl carrier protein
AGGG	1	
MNLL	1	
ND4	14 approx.	
ND5	15 approx.	

Table 1.5. Subunits detected in bovine subcomplex I_β (Walker, 1992).

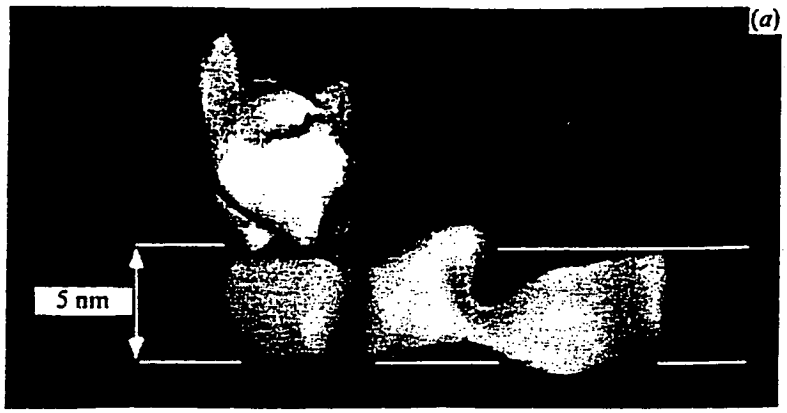

Fig. 1.14. Structural model with montage views of reconstructions of the extrinsic and membrane arms of complex I from *N. crassa* (Walker, 1992).

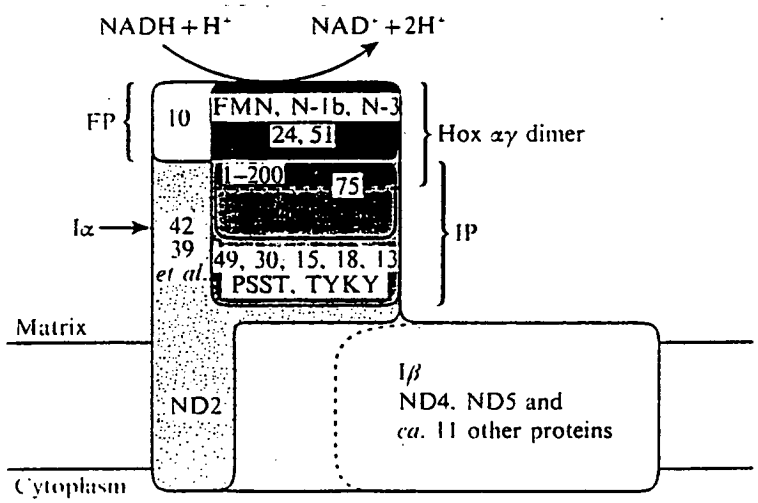

Fig. 1.15. Arrangement of some subunits in bovine complex I based upon the polypeptide compositions of I_α and I_β, of the FP and IP fragments, and the relationship between the αγ dimer part of the hydrogenase from *A. eutrophus* and the 24 kDa, 51 kDa and residues 1-200 of the 75 kDa subunit of bovine complex I (Walker, 1992).

1.9.8.2 *Neurospora crassa*

The extrinsic membrane domain of *N. crassa* complex I was likewise found to be an L-shaped membrane-bound enzyme (Fig. 1.15) in which the extrinsic peripheral arm protrudes into the mitochondrial matrix, comprising subcomplexes I_α and I_β isolated by chromatography, with various groups of subunits being associated within subcomplex I_α (Leonard *et al.*, 1987; Hofhaus *et al.*, 1991). An important feature of this model is that it places all of the known redox centres of complex I outside the lipid bilayer. Subcomplex I_α catalyses electron transfer from NADH to ubiquinone-1. It is composed of about 22 different and mostly hydrophilic subunits and contains 2.0 nmol of FMN/mg protein. Among its subunits is the 51 kDa subunit which binds FMN and NADH and probably contains a [4Fe-4S] cluster also. Three other potential Fe-S proteins, the 75 and 24 kDa subunits and a 23 kDa subunit (*N*-terminal sequence TYKY) are also present. Subcomplex I_β contains about 15 different subunits. The sequences of many of them contain hydrophobic segments that could be membrane spanning, including at least two mitochondrial gene products, ND4 and ND5 (Fig. 1.14). The role of I_β is yet to be elucidated. The L-shaped structure of complex I in *N. crassa* is very similar to that in *B. taurus*, with homologous corresponding subunits forming the I_α and I_β fragments.

1.9.9 Electron transfer mechanism based on the location of Fe-S clusters within the Complex I structure

The coupling ratio is $4H^+/2e^-$ by consensus but other ratios have been suggested depending on the models proposed based on the arrangement of the complex (Fig. 1.16 and Fig. 1.17). The loop scheme in Fig. 1.17a has been generally disregarded as it predicted a $2H^+/2e^-$ ratio (Mitchell, 1966).

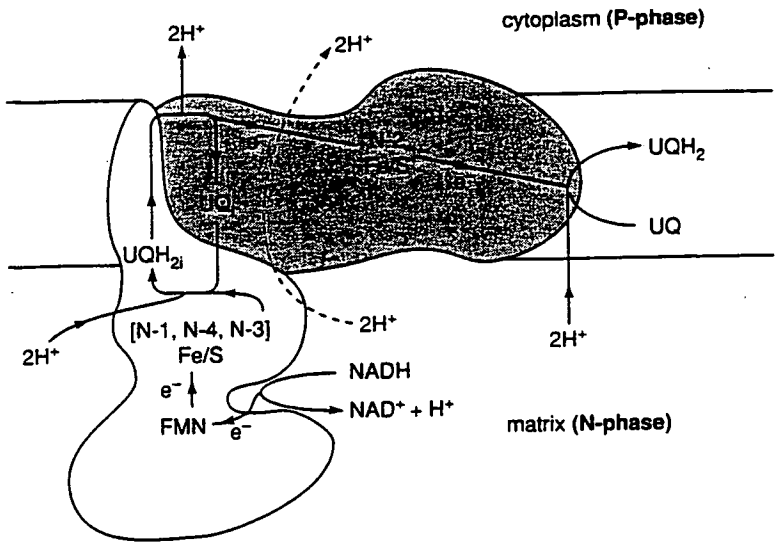

Fig. 1.16. A structural model for the mitochondrial NADH-UQ oxidoreductase (complex I) demonstrating catalytic reactions, proton translocation and electron transfer through the various iron-sulphur clusters (Nicholls and Ferguson, 1992).

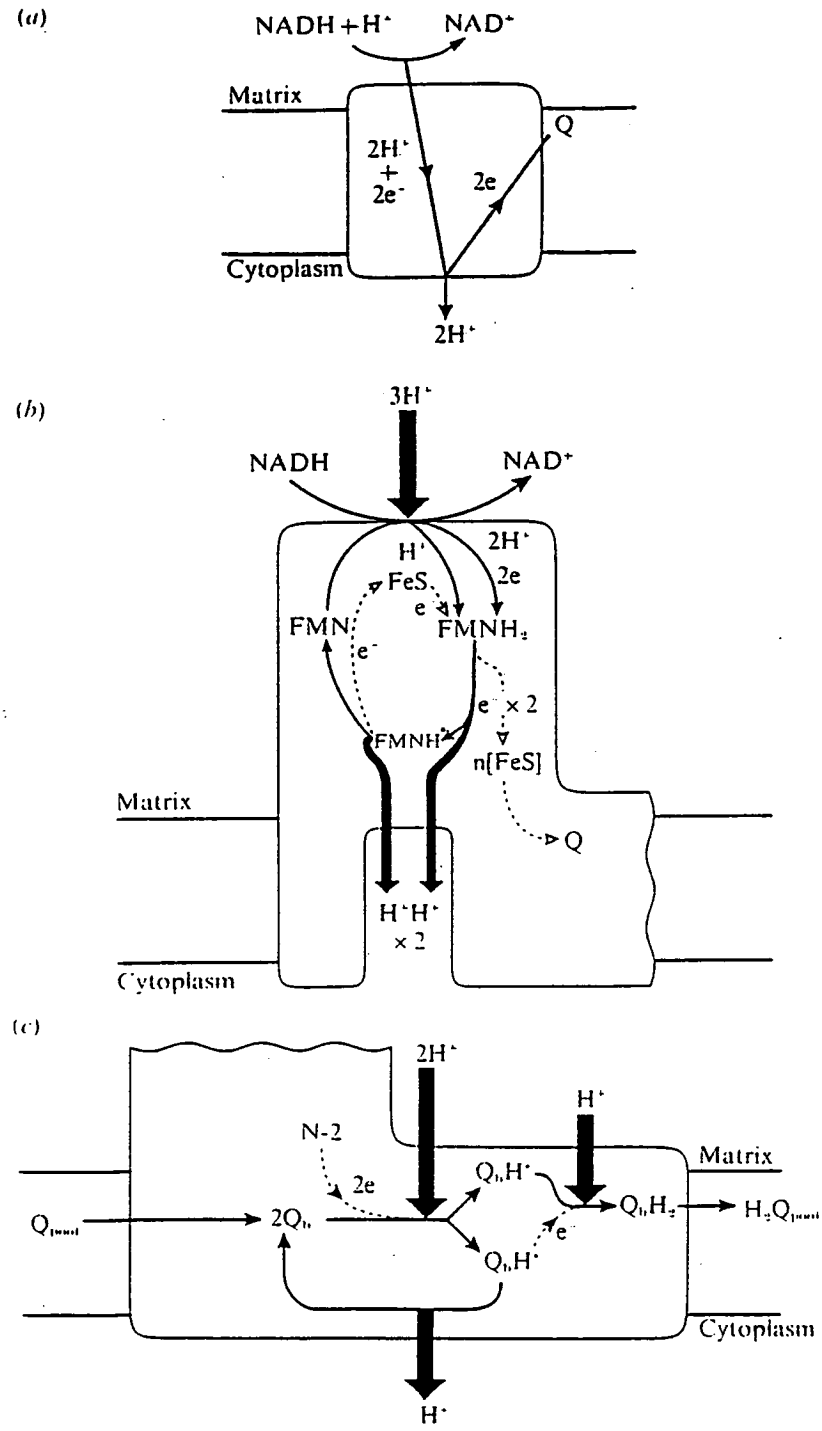

Fig. 1.17. Models for energy transduction coupled to proton translocation in complex I (Walker, 1992). (a) Loop mechanism (Mitchell, 1966); (b) a possible mechanism of redox-linked proton translocation between NADH and FMN drawn as an analogue of the *b* cycle in cytochrome *bc1* (Krishnamoorthy and Hinkle, 1988); (c) proton translocation between Fe-S cluster N-2 and the ubiquinone pool (Kotlyar et al, 1990).

Based on the mid-point potentials of the Fe-S clusters (Table 1.6), one of the models proposed is that FMN receives 2 electrons from NADH and transfers them as single electrons in 2 steps to the cluster N-1b. N-1b, together with N-3 and N-4, to form an isopotential pool for electrons that are finally donated to the high potential cluster N-2 which subsequently reduces ubiquinone (Burbaev *et al.*, 1989).

Energy transduction was thought to occur between FMN and the isopotential clusters (N-1, N-2 and N-4), with the FMN participating in a proton translocating flavin cycle, whereby reoxidation of $FMNH_2$ is coupled to proton translocation (Weiss *et al.*, 1991, Krishnamoorthy and Hinkle, 1988) (Fig. 1.17b). Another possible theory states that NADH transfers electrons one at a time to the low potential iron-sulphur clusters, and they are responsible for the reduction of $FMNH_2$ to FMN, via an internal Q-cycle (Weiss *et al.*, 1991). A second probable site of energy transduction is between the isopotential clusters and cluster N-2, involving an internal Q-cycle, similar to the one operating in the cytochrome bc_1 complex (Trumpower, 1990). A third possible site was suggested to exist between the N-2 cluster and the quinone pool, with protonated quinones involved in the mechanism (Kotlyar *et al.*, 1990) (Fig 1.17c).

Species	Cluster	Cluster type	g values ($g_{x,y,z}$)	E_m (mV)
Bos taurus	N-1a	[2Fe-2S]	1.91, 1.95, 2.03	-370
	N-1b	[2Fe-2S]	1.92, 1.94, 2.02	-245
	N-2	[4Fe-4S]	1.92, 1.92, 2.05	-120
	N-3	[4Fe-4S]	1.86, 1.93, 2.04	-245
	N-4	[4Fe-4S]	1.87, 1.93, 2.10	-245
Neurospora crassa	N-1	[2Fe-2S]	1.933, 1.935, 2.019	-350
	N-2	[4Fe-4S]	1.916, 1.925, 2.051	-150
	N-3	[4Fe-4S]	1.867, 1.928, 2.044	-230
	N-4	[4Fe-4S]	1.884, 1.920, 2.044	-300
Paracoccus denitrificans	N-1a	[2Fe-2S]	1.918, 1.937, 2.029	-150
	N-1b	[2Fe-2S]	1.929, 1.941, 2.019	-260
	N-2	[4Fe-4S]	1.919, 1.923, 2.050	-130
	N-3	[4Fe-4S]	1.861, 1.935, 2.014	-240
	N-4	[4Fe-4S]	1.878, 1.935, 2.093	-270
Thermus thermophilus HB-8	N-1a	[2Fe-2S]	1.93, 1.94, 2.02	-274
	N-2	[4Fe-4S]	1.89, 1.95, 2.04	-304
	N-3	[4Fe-4S]	1.80, 1.83, 2.06	-289
Escherichia coli	N-1	[2Fe-2S]	1.92, 1.935, 2.03	-220
	N-2	[4Fe-4S]	1.90, 1.91, 2.05	-240

Table 1.6. Properties of the Fe-S clusters of NADH-ubiquinone oxidoreductases in various species (Walker, 1992).

1.9.10 Homology and evolution

In chlororespiration in plants, an electron transport chain operates in the dark and under aerobic conditions at about 10% of the rate of respiration in mitochondria (Peltier *et al.*, 1987), whereby electrons from NADH, NADPH and also succinate (Willeford *et al.*, 1989) flow into the plastoquinone pool and thence to an unidentified terminal oxidase. Interest in chlororespiration has been stimulated by the surprising discovery in chloroplast genomes of higher plants, of open reading frames (potential genes) for homologues of ND1-ND6 and ND4L, the seven hydrophobic subunits of mitochondrial complex I encoded in mitochondrial DNA (Matsubayashi *et al.*, 1987). Chloroplast genomes also contain homologues of four nuclear-encoded polypeptides of bovine complex I, namely the 49 kDa (IP), 30 kDa (IP), TYKY and PSST subunits (Fearnley *et al.*, 1989; Pilkington *et al.*, 1991b; Dupuis *et al.*, 1991a; Arizmendi *et al.*, 1992) and similar relationships exist with the *N. crassa* homologues of the 49 kDa and 30 kDa subunits (Preis *et al.*, 1990; Videira *et al.*, 1990).

A possible mechanism of evolution of a multisubunit assembly such as complex I, is that the present day assembly may have arisen by accretion of its various component activities. For example, the electron pathways of complex I and its proton-pumping activities may have evolved independently as separate structural modules for a time and then the modules may have come together to make up the present-day enzyme (Walker, 1992). An example of modular evolution is found in bacteriophages whereby genes for the components of the head cluster together as do those that encode protein that form the tail. It was proposed that lambdoid phages interchange these gene clusters for heads and tails in interbreeding phage populations, and so evolution operates not at the level of intact virus, but at the level of the individual functional units, the 'modules' (Botstein, 1980). Another example is the ATP synthase. In many bacteria species, there is a gene cluster encoding the five different subunits of the F_1 sector and another gene cluster encoding the 3 or 4 subunits of the F_0 sector. The conservation of gene orders for the ATP synthase subunits was interpreted as support for modular evolution, whereby F_1 and F_0 parts evolved separately as a proton

channel module (to relieve cellular acidification by fermentation) and a cytoplasmic ATPase module respectively. These two subunits then associated to form an ATP-driven proton pump, which was subsequently able to harness redox energy to become an ATP synthase (Walker *et al.*, 1984; Walker and Cozens, 1986).

Modular evolution of complex I is supported by the structural module that was common to both complex I and NAD^+-reducing hydrogenase from *A. eutrophus*. Biosynthetic studies of the *N. crassa* complex I revealed that extrinsic and intrinsic sectors of complex I assembled independently (Tuschen *et al.*, 1990; Nehls *et al.*, 1992).

It was proposed that complex I subunits that are involved in substrate and co-factor binding are very likely to be present in the minimal enzyme exemplified by the bacterial complexes. These are the 51, 24 amd 75 kDa subunits and subunit TYKY. Those that are conserved in a wide range of species but for which as yet there are no clearly defined functions are also likely to be in the minimal enzyme. These are the 49 kDa, 30 kDa and the PSST subunits and the hydrophobic subunits ND1-ND6 and ND4L. Hence the minimal enzyme has at least 14 different subunits. The *P. denitrificans* NUO contains 14 subunits encoded by a gene cluster, as does that of *Escherichia coli,* all subunits of which have homologues with the mitochondrial complex I. For both the eukaryotic complex I and its prokaryotic counterpart, the gene order in the locus is conserved and correlates with the topological arrangement of the encoded subunits, therefore supporting the concept of modular evolution.

It has been suggested that the supernumerary subunits (i.e. those subunits in the mitochondrial enzymes that have no counterparts in the simpler bacterial complexes) might be involved in facilitating the co-assembly of the group of subunits that originate from the mitochondrial genome, with the group that are products of nuclear genes and are imported into the organelle, and there is evidence in the cytochrome bc_1 complex, for example, that supernumerary subunits are required for correct assembly to take place. An acyl carrier protein is associated with complex I in *N. crassa* and it participates in a cerulenin-sensitive, *de novo* fatty acid synthesis that

is independent of the fatty acid synthetase complex present in the cytoplasm. It is suggested that the purpose of this pathway is to satisfy the needs of the mitochondrion by providing myristate for incorporation into mitochondrial lipids.

Other energy-transducing enzyme complexes (complex III and cytochrome oxidase) are only composed of three subunits. This poses the question why Complex I is such an intricate and complex structure. Ragan (in 1987 review) attempts to answer this by proposing that some polypeptides of complex I do not have a role in the catalytic function of the enzyme, but serve instead as receptors for other dehydrogenases. This hypothesis stems from reports that several TCA cycle dehydrogenases in the mitochondria appear to channel NADH to Complex I (Sumegi and Srere, 1984; Yagi, 1993).

1.9.11 Medical implications

A wide range of rare human diseases is associated with defects in the generation of ATP in mitochondria caused by changes in mitochondrial DNA sequence. All mitochondrial DNA molecules originate from the ovum during zygote formation and so the diseases are transmitted in a non-Mendelian maternal manner. Cells may be heteroplasmic in mitochondria DNA and this may shift towards pure mutant or pure wild type during cellular replication. Deleterious mutations in mitochondrial genes occur much more frequently than in nuclear genes and the mitochondria is said to have no DNA repair mechanism (Finel *et al.,* 1994). About 38% of the mitochondrial genome codes for components of complex I and defects arising in this enzyme are amongst the most common.

As the central nervous system is more dependent on mitochondrial energy than any other tissue, it is the most severely affected by mitochondrial defects. Skeletal muscle is also seriously affected, followed with decreasing severity, by heart, kidney and liver. The mitochondrial encephalomyopathies which affect the central nervous system primarily are amongst the most common forms of this disease (transition mutations). Accumulation of mitochondrial mutations and the subsequent cytoplasmic

segregation of these mutations during life have been proposed to lead to the progressive loss of respiratory function in cells and is an important contributor to the process of ageing and to several human degenerative diseases. Parkinson's disease is linked to complex I deficiency. There is multiple respiratory failure in skeletal muscle and multiple system atrophy. Another familiar disease, Huntington's disease, is characterized by progressive motor and cognitive impairment whereby depressed levels of complex I leads to a decrease in available ATP or that diversion of high energy electrons from their normal path through complex I might generate free radicals and impair glutamate metabolism leading to neuronal damage (Walker, 1992).

Experiments demonstrated reduced enzyme activity correlated with the decrease of 4 mitochondrial DNA-encoded subunits of complex I and the decrease of other complex I subunits in skeletal muscle of patients affected by mitochondrial myopathies (Bentlage *et al.*, 1995). Seven human cell-line VA(2)B rotenone-insensitive mutants were found to be respiration-deficient, of which six exhibited defect in complex I. Molecular analysis reveal that 2 mutants had frameshifts in ND4 and 2 had frameshifts in ND5 (Hofhaus and Attardi, 1995). In a novel therapy recently, patients with Alzheimer-type dementia were treated with NADH, increasing the availability of substrate to compensate for the reduced levels of their complex I enzyme (Birkmayer, 1995).

1.10 Bacterial NADH-ubiquinone oxidoreductases

Initially, much research concentrated on the eukaryotic NADH-ubiquinone oxidoreductase, complex I, spurred on by medical interest due to its association with mitochondrial encephalomyopathies and ageing. Since Bragg and Hou reported the presence of NADH dehydrogenase activity in several *E. coli* membrane homogenate fractions in 1967, a flood of research into bacterial NADH-ubiquinone oxidoreductases (NUO) has ensued. This led to the discovery and identification of 3 types of bacterial NUOs (Yagi, 1993). The first of these enzymes (designated NADH dehydrogenase 1 (NDH-1)) is a multi-subunit complex and bears an energy coupling site for H^+. NADH dehydrogenase 2 (NDH-2) on the other hand, lacks an energy coupling site, and is comprised of a single polypeptide (Table 1.7). To date, NDH-1 type enzymes have been isolated from *P. denitrificans, Thermus thermophilus, E. coli* and *V. alginolyticus*, whereas the NDH-2 enzymes have been isolated from a large number of bacteria and eukaryotes.

NDH-1 contains non-covalently bound FMN and iron-sulphur clusters as prosthetic groups (Yagi, 1991, 1986, Hayashi, Miyoshi *et al.,* 1989) whereas NDH-2 bears non-covalently bound FAD and has no iron-sulphur clusters (Yagi *et al.*, 1988, Yagi, 1989, 1991). NDH-1 tends to be inhibited by one or more of the potent mitochondrial complex I inhibitors such as rotenone, piericidin A, capsaicin and DCCD (Yagi, 1987), which have no effect on NDH-2. There are no known specific inhibitors for NDH-2 to date. NDH-2 type enzymes of plant and fungal mitochondria can be further subdivided into two groups: one which directs to the cytoplasmic side and the other which faces to the matrix side (Rasmusson and Møller, 1991).

The last type of NADH dehydrogenase is termed Na^+-NQR (sodium-translocating NADH-quinone reductase) and was isolated and characterised by Unemoto and Hayashi (1989) from *V. alginolyticus*. It is coupled to a Na^+ gradient (rather than a H^+ one), bears an FAD prosthetic group and is composed of 6 subunits distinct from the 14 found in NDH-1 of *E. coli* and *P. denitrificans*. This third type of enzyme will be further discussed below in section 1.12 and 1.13.

Table 1.7. Comparison of NADH-ubiquinone oxidoreductases (Bourne and Rich, 1992).

Type	**NDH-1**	**NDH-2**	**Na^+-NQR**	**Complex I**
Source	Bacterial	Bacterial Mitochondrial	Bacterial	Mitochondrial
Coupling ion	H^+	Not coupled	Na^+	H^+
Redox centres	FMN Fe-S	FAD	FAD	FMN Fe-S
No. protein subunits	14	1	6	34 (n) + 7 (m)
Oxidation of:				
deamino-NADH	Yes	Variable (Yes in *V. alg.)*	Yes	Yes
NADPH	No	No	No	No
thio-NADH			Yes	
APAD			No	
Inhibition by:				
Ag^+	No	No	Yes	No
Rotenone	Yes	No	No	Yes
HQNO/NQNO	Yes	No	Yes	Yes
Capsaicin	Yes	No	No	Yes
Flavone	Yes (in eukaryotes)	No	No	Yes
Piericidin A	Yes	No	No	Yes

The energy coupling observed in Complex I, NDH-1 and Na^+-NQR which contain Fe-S prosthetic groups, but absent in NDH-2 which does not comprise of such groups, suggests that the Fe-S clusters are essential and perhaps indispensable components of the energy coupling site (Yagi, 1991). The high potential FeS cluster (N2) present in *Paracoccus* NDH-1 but not detected in *E. coli* or *Thermus* NDH-1, was shown to play a role in H^+ translocation, based on the demonstration that E_m values of this cluster are dependent on the energized state or the pH of the membrane (Yagi, 1993).

It is evident that the distribution of these three types of NADH dehydrogenases in different bacteria vary greatly. *P. denitrificans* membranes appears to bear only NDH-1, while *Bacillus subtilis* and *Sulfolobus acidocaldarius* membranes were reported to only contain NDH-2. But both NDH-1 and NDH-2 are found in *T. thermophilus, E. coli, Thermus aquaticus, Rhodobacter* and *Synechocystis*. *Vibrio alginolyticus* membranes have all three types of NADH-ubiquinone oxidoreductases (Yagi, 1993).

1.11 Comparisons between bacterial NDH-1 and eukaryotic complex I

It was discovered that structural genes encoding NDH-1 subunits in *P. denitrificans* and *E. coli*, constitute a single gene cluster that is composed of 14 structural genes (Xu *et al.*, 1991a, 1992b, 1993, Weidner *et al.*, 1993). All 14 encoded subunits have distinct homologues with all 7 hydrophobic mitochondrial-encoded complex I subunits and some of the 35 or more nuclear-encoded complex I subunits in *Bovine taurus*. Table 1.8 summarises the comparisons between the bacterial NDH-1 subunits and the homologous complex I counterparts (Yagi, 1993). Paracoccus NDH-1 has a relatively simple structure compared with complex I, though it is greatly similar to complex I in terms of EPR-visible FeS clusters. These fourteen genes code for the minimal number of subunits required for a functional NADH-ubiquinone oxidoreductase and the gene order in the *nuo* locus is conserved in comparison to other bacterial genomes and the chloroplast genome of higher plants (Weidner *at al.*, 1993). To some extent, the gene order correlates with the topological arrangement of the encoded subunits.

Escherichia coli	NUO 1	NUO 2	NUO 3	NUO 4	NUO 5	NUO 6	NUO 7	NUO 8	NUO 9	NUO 1	NUO 11	NUO 12	NUO 13	NUO 14
Paracoccus denitrificans	NQO 7	NQO 6	NQO 5	NQO 4	NQO 2	NQO 1	NQO 3	NQO 8	NQO 9	NQO 1	NQO 11	NQO 12	NQO 13	NQO 14
Bos taurus	ND 3	20 kD	30 kD	49 kD	24 kD	51 kD	75 kD	ND 1	23 kD	ND6	ND 4L	ND 5	ND 4	ND 2
	HP	IP	IP	IP	FP	FP	IP	HP		HP	HP	HP	HP	HP
Comments		homologous to *ndhK* of chloroplast and *Paramecium* mitochondrial DNA			peripheral protein	NADH oxidation	e^- carrier and structural protein		homologous to *ndhI* of chloroplast					
Catalytic centres					[2Fe-2S]	[4Fe-4S] NADH FMN	[4Fe-4S] [2Fe-2S]		[4Fe-4S]					

IP: Iron-sulphur protein

FP: Flavoprotein

HP: Hydrophobic protein

Table 1.8 Corresponding subunits encoded by the proton-translocating NADH-ubiquinone oxidoreductase in *E. coli, P. denitrificans* and *B. taurus.* The polypeptide subunits of *E. coli* and *P. denitrificans* are listed according to their gene order in the *nuo* or *nqo* clusters, which are highly conserved in both bacteria. ND 1 to ND 6 are encoded by the mitochondria in *B. taurus,* while the others are nuclear-encoded.

The 50 kDa polypeptide of *Paracoccus* NDH-1 has been identified as the NADH-binding subunit by direct photoaffinity labelling with [^{32}P]NAD(H). Immuno-crossreactivity and high amino acid sequence identity (64% identity) with bovine and *N. crassa* counterparts have confirmed this observation (Yagi and Dinh, 1990). In addition, FeS clusters were detected using EPR spectra analysis.

A 25 kDa subunit from *P. denitrificans* was shown to be homologous to the FP fragment 24 kDa subunit of bovine complex I (Xu *et al.*, 1991a). EPR studies on overexpressed 25 kDa subunit indicates that it contains a single [2Fe-2S] cluster that is consistent with coordination by two cysteinyl residues at both the reducible and the nonreducible iron sites and reveal a striking similarity between the properties of the [2Fe-2S] cluster in the *P. denitrificans* NDH-1 25-kDa subunit and those of the subclass of ferredoxin-type [2Fe-2S] centers typified by *Clostridium pasteurianum* 2Fe ferredoxin. The four cysteines residues involved in cluster ligation in these proteins have been tentatively identified based on sequence homology considerations (Crouse *et al.*, 1994). Using UV-visible and EPR spectroscopy of site-directed mutants, the 4 conserved residues that coordinate the [2Fe-2S] cluster in the 25 kDa subunit were found to be C96, C101, C137 and C141 (Yano, Sled *et al.*, 1994).

Expression of the flavoprotein subcomplex composed of 50 kDa (NQO1) and 25 kDa (NQO2) subunits of *P. denitrificans* in *E. coli*, was achieved for EPR studies, which revealed the presence of a [2Fe-2S] and 2 [4Fe-4S] (reconstituted) clusters. Incorporation of FMN and [4Fe-4S] was postulated to require some specific *P. denitrificans* genes/ gene products or interaction with neighbouring NQO subunits as overexpressed subunits had to be reconstituted for EPR studies. This FP subcomplex catalyses electron transfer from NADH and dNADH to a variety of electron acceptors, with FMN being the primary electron acceptor from NADH (Yano *et al.*, 1996).

The 66 kDa subunit of NDH-1 (NQO3) of *P. denitrificans* was expressed in the cytoplasm of *E. coli* and purified by ammonium sulphate fractionation and anion-exchange chromatography. Chemical analyses, UV-visible and EPR spectroscopic studies showed that NQO3 contained at least 2 distinct iron-sulphur clusters, a [2Fe-

2S] and a [4Fe-4S]. The tetranuclear [4Fe-4S] site is sensitive to oxidants and converts to a [3Fe-4S] form. From the primary sequence of NQO3, a consensus motif (Cys-158, -161, -164, and -208) for the [4Fe-4S] cluster has been identified. The [2Fe-2S] motif could not be unambiguously identified although there are 8 Cys and 2 His residues which may be likely candidates (Yano *et al.*, 1995). The iron-sulphur clusters of this subunit appear to be clustered at the *N*-terminal region which bears structural similarity to the γ-subunit of *A. eutrophus* NAD^+-reducing hydrogenase. This γ-subunit, which contains 11 of the 12 conserved Cys residues in NQO3 and its homologues (Xu *et al.*, 1992a), is thought to bear iron-sulphur clusters that participate in wiring electrons from the hydrogenase part of the βδ-heterodimer subunits to the NADH-binding site of α-subunit (Schneider *et al.*, 1984). It was proposed that the iron-sulphur domain of NQO3 interacts with FP, most likely with NQO1. It was also speculated that this *N*-terminal domain together with the relatively hydrophobic *C*-terminal (residues 266-673) of NQO3 is involved in linking the hydrophilic section (FP, IP) of NDH-1 to the hydrophobic section (HP subunits) (Yano *et al.*, 1995).

The apparent lack of lower molecular mass (18 kDa, 15 kDa, 13 kDa(A), or 13 kDa(B)) HP mitochondrial counterparts in bacterial respiratory chain complexes is not unique to NADH-ubiquinone oxidoreductases. For example, although bacterial complex III contains homologues to the mitochondrial complex III cytochrome *b*, cytochrome c_1 and FeS protein, it lacks homologues to the smaller 14 kDa, 12 kDa, 11 kDa and 8 kDa polypeptides. Hence it was deduced that these low molecular weight polypeptides assist in the assembly of complex I in the mitochondria rather than in its catalytic function (Yagi, 1993).

1.12 NADH dehydrogenases of *V. alginolyticus*

The Na^+ pump of *V. alginolyticus* is coupled to respiration by a membrane bound NADH-ubiquinone oxidoreductase (Na^+-NQR) (Tokuda and Unemoto, 1984). *V. alginolyticus* has a Na^+-dependent NADH-ubiquinone oxidoreductase functioning as a Na^+ pump (Na^+-NQR), a H^+-dependent NADH-ubiquinone oxidoreductase functioning as a H^+ pump (NDH-1) and a non-coupled NADH dehydrogenase (NDH-2) (Hayashi 1991, Tokuda and Unemoto, 1982), unlike *E. coli* which only has NDH-1 and NDH-2 (Table 1.4). NDH-2 is not energy-linked and is unable to generate a membrane potential; does not require salts for its activity and the pH optimum for activity is lower than that of Na^+-NQR (pH 6.8 to 7.8). NDH-2 is insensitive to preincubation with NADH and unable to utilise deamino-NADH as a substrate. In addition, NDH-2 is insensitive to strong Na^+-NQR inhibitors, like HQNO or NDH-1 inhibitors, such as piericidin and rotenone, and lacks sodium or proton dependent activity (refer to Table 1.7 and 1.9). Na^+-NQR is sensitive to preincubation with NADH, able to utilise deamino-NADH as a substrate and functions as a sodium pump. NDH-2 reduces menadione and ubiquinone by a two electron pathway while the NADH-reacting FAD-containing β-subunit of Na^+-NQR reduces quinones in a one electron pathway with the formation of semiquinone radicals intermediates that may be essential to the mechanism of the sodium pump (Hayashi, 1992). The NDH-1 of *E. coli* which functions as a proton pump was also sensitive to pre-incubation with NADH and reduces quinone by a one electron pathway. The *E. coli* NDH-1 was also similar to the *V. alginolyticus* NDH-1, therefore the formation of semiquinone radicals as an intermediate is likely to be a common mechanism to functioning as either proton or sodium pump (Unemoto, 1992). The respiratory chain of *V. alginolyticus* is composed of quinone, menaquinone and cytochromes *b, c, d* and *o* (Unemoto and Hayashi, 1989). The electron transfer pathway from NADH to ubiquinol is formulated in Fig 1.18.

Type of NADH quinone reductase	*V. alginolyticus*	*E. coli*	Substrate
Na^+-NQR	Na^+ dependent pump	Not present	NADH and deamino-NADH
NDH-1	H^+ dependent pump	H^+ dependent pump	NADH and deamino-NADH
NDH-2	No pump	No pump	NADH only

Table 1.9. Comparison of NADH-quinone reductases in *V. alginolyticus* and *E. coli.*

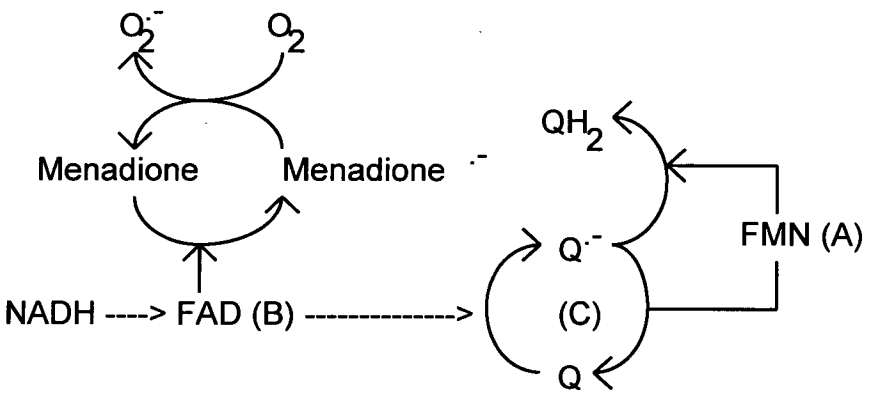

Fig. 1.18. Electron transfer pathway in Na^+-dependent NADH-ubiquinone oxidoreductase. Curved arrows indicate chemical reactions and straight arrows indicate electron transfer.

1.13 Sodium-translocating NADH-ubiquinone oxidoreductase of *Vibrio alginolyticus*

Previous biochemical studies revealed that *V. alginolyticus* can generate a Na^+ electrochemical potential at alkaline pH by aerobic respiratory electron transport and is not inhibited by the protonophore carbonyl cyanide *m*-chlorophenylhydrazone (CCCP) at alkaline pH (Tokuda and Unemoto, 1981; Tokuda and Unemoto, 1982). This Na^+ motive force plays a central role as a primary pump in *V. alginolyticus*, driving ATP synthesis, solute transport and flagellar motion through Na^+ dependent coupling (Tokuda and Unemoto, 1984). This Na^+ cycle co-exists and operates simultaneously with a H^+ cycle on the membranes of *V. alginolyticus* (Smirnova, 1988; Vagina, 1989). A K^+ transport system is also present in *V. alginolyticus,* discovered when a *trkA*-like gene (71% DNA homology to *E. coli trkA* and 79% identity to the TrkA protein) was found to complement an *E. coli* mutant, TK420, defective in K^+ transport genes (*kdpABC, trkD, trkA*) (Nakamura *et al.*, 1994b; Nakamura *et al.*, 1994c).

Tokuda isolated *V. alginolyticus* Na^+ pump mutants with significantly reduced Na^+ pump activity and Na^+-independent NADH oxidase activity (Tokuda, 1983). Further analysis of these mutants by Tokuda *et al.* (1987) suggested that the Na^+ pump genes are located on a plasmid as the recovery of Na^+ pump activities in a mutant lacking in three subunits appeared to be conjugation-dependent. However later experiments revealed that a plasmid-cured strain of *V. alginolyticus* 138-2 retained its respiration-driven sodium pump irrespective of the absence or presence of plasmids, suggesting strongly that the genes for the sodium pump were encoded by chromosomal DNA (Nakamura *et al.*, 1993).

1.13.1 Purification, identification and catalytic mechanism

The Na^+-dependent NADH-ubiquinone oxidoreductase was purified from the membranes of *V. alginolyticus* and shown to be composed of 3 subunits α, β and γ with apparent M_r of 52,000, 46,000 and 32,000 respectively (Hayashi and Unemoto, 1986). We have found 4 subunits which were designated A, B, C1 and C2 with M_r of 55,000, 50,000, 33,000 and 30,000 respectively (Beattie *et al.*, 1994). Earlier biochemical studies by Hayashi and Unemoto, led them to propose a model for electron transfer in which the FAD-containing β subunit, an NADH dehydrogenase, accepts electrons from NADH and reduces menadione or quinone by a one-electron transfer reaction to produce semiquinones (Fig 1.19). This reaction is independent of Na^+ but is irreversibly inhibited by Ag^+, which is not known to inhibit any other types NADH dehydrogenases (Table 1.7). The reduction of hydrophobic quinones, such as ubiquinone, is dependent upon Na^+ and is catalysed by the α subunit in the presence of β (Fig 1.19) (Hayashi and Unemoto, 1986, 1987, Unemoto and Hayashi, 1989). This complex is very different, unique and distinct from the NDH-1 and Complex I enzymes; Na^+-NQR is not inhibited by classical mitochondrial respiratory inhibitors such as rotenone, piericidin A and capsaicin (Bourne and Rich, 1992, Table 1.7).

The A or α FMN prosthetic group-containing subunit was identified as the Na^+ pump and the β subunit that contains one non-covalently bound FAD, is the NADH dehydrogenase that oxidises NADH (refer to Fig 1.19).

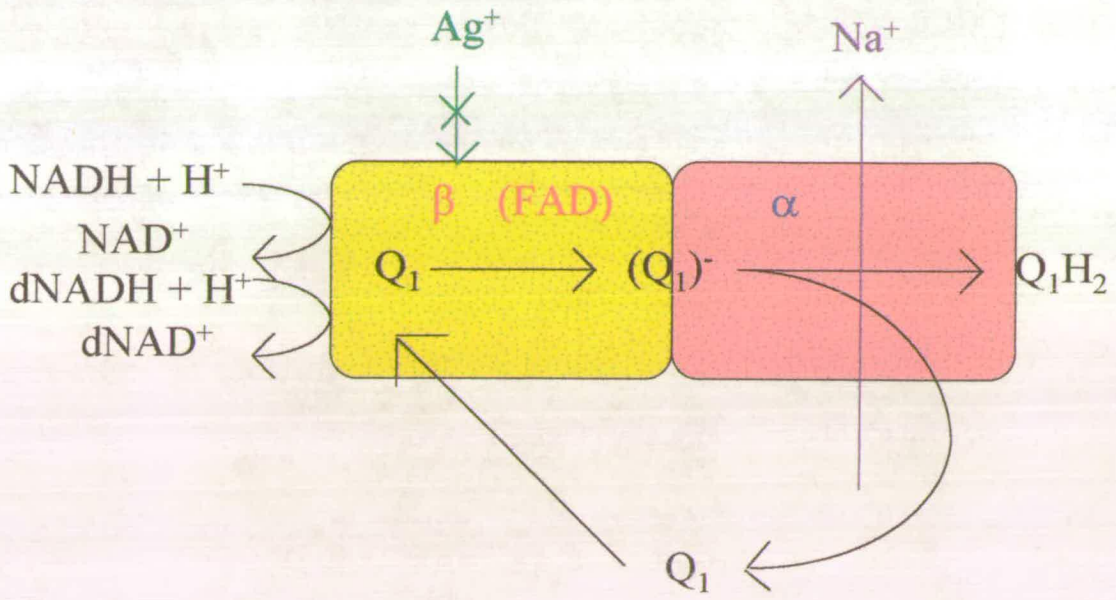

Figure 1.19. Schematic diagram of α and β subunits of NADH-quinone oxidoreductase of *V. alginolyticus* (Tokuda and Kogure, 1989). Catalytic reactions and inhibitor specificities are indicated.

The β subunit (NADH dehydrogenase) accepts electrons from NADH and reduces menadione or quinone by a one-electron transfer reaction to produce semi-quinones. This reaction is independent of Na^+, insensitive to respiratory inhibitor, 2-heptyl-4-hydroxyquinoline-N-oxide (HQNO) (Tokuda and Unemoto, 1982, 1984) but sensitive to Ag^+, Pb^{2+}, Zn^{2+}, Cu^{2+}, Cd^{2+}, and *p*-mercuribenzoate (Bourne and Rich, 1992). Ag^+ was found to be a specific and competitive inhibitor for the active site of the β-subunit (Unemoto, 1993). However, the rapid reduction and dismutation of ubisemiquinone radicals to ubiquinol and ubiquinone is specifically Na^+-dependent, ATP-independent (arsenate-insensitive) and HQNO-sensitive and is probably catalysed by the α subunit (sodium pump) in the presence of the β subunit (Unemoto and Hayashi, 1979, Hayashi and Unemoto, 1987). An artificial electron donor, N,N,N',N'-tetramethyl-*p*-phenylenediamine is able to reverse the effects of HQNO on the Na^+ pump.

The function of the NADH oxidase as an Na^+ pump was directly demonstrated by Na^+ accumulation in inverted bacterial vesicles and reconstituted proteoliposomes during NADH oxidation. Inhibition of the NADH oxidase with HQNO prevented the accumulation of Na^+ (Tokuda, 1984). Pfenninger-Li *et al.* (1996) demonstrated that the Na^+-dependent step in the electron transfer catalyzed by NADH-ubiquinone oxidoreductase is the reduction of ubisemiquinone to ubiquinol. Reconstitution of the purified quinone reductase into proteoliposomes, resulted in NADH oxidation by ubiquinone-1 was coupled to Na^+ transport with an apparent stoichiometry of 0.5 Na^+ per NADH oxidized. This transport was stimulated by valinomycin ($+K^+$) or by CCCP, therefore clearly indicating that the Na^+ transport is a primary event and does not require the intermediate formation of a proton gradient. The role of the γ subunit is unclear but it increases the affinity of the β subunit for quinones. In addition, it plays an important role in the interaction of quinones with β as well as the electron transfer reaction from the β to α subunit (Unemoto and Hayashi, 1989).

The α, β and γ subunits were found in stoichiometrically equimolar amounts but the M_r of the entire enzyme complex was twice that of the total of each individual

subunit, therefore it was initially inferred that the active complex probably exists as a dimer $\alpha\beta\gamma$ or as $\alpha_2\beta_2\gamma_2$.

A similar catalytic mechanism is also observed in the Na^+-translocating NADH-ubiquinone oxidoreductase of *Klebsiella pneumoniae* (Dimroth, 1989). This Na^+-NQR is widely distributed among Gram-negative marine bacteria such as *Alcaligenes, Alteromonas, Flavobacterium, Vibrio* (Tokuda and Kogure, 1989) and shares common properties such as Na^+-dependence, Ag^+-sensitivity and sensitivity to HQNO. An Na^+-NQR also exists in *Haemophilus influenzae* Rd. Venter and coworkers (Fleischmann *et al.*, 1995) and Hayashi and colleagues (1996) have sequenced the entire *nqr* operon and found it to be almost identical to that found in *V. alginolyticus. H. influenzae* is not a marine halophile but some strains of *Haemophilus* require 1.0-1.5% (w/v) NaCl for optimum growth (Rimler *et al.*, 1977). The use of a Na^+-coupled NQR in *H. influenzae*, which grows in blood, is not surprising, as animal cells are long known to utilize a Na^+-ATPase due to high Na^+ levels in blood.

1.13.2 Related work on Na^+-NQR in *V. harveyi*

Andrew Stevenson (Stevenson, 1991, 1994) performed transposon mutagenesis and chemical mutagenesis to generate Na^+ pump-deficient *V. harveyi* mutants which were selected using CCCP at pH 8.5. CCCP acts as a proton uncoupler and hence cells can only generate membrane gradients by using a Na^+-based metabolism at pH 8.5. Na^+ pump mutants would therefore be unable to grow at pH 8.5 in the presence of CCCP. However, all of the 16 CCCP-sensitive transposon mutants obtained were shown to have wild-type NADH/ deamino-NADH oxidase activities. It was therefore concluded that they were not defective in Na^+-NQR. This indicates that the transposons have possibly integrated at the genes for Na^+-dependent V-ATPase or other Na^+-dependent enzymes, creating mutations in their Na^+-translocating subunits, rather than in that of Na^+-NQR. He also purified the NADH-ubiquinone oxidoreductase complex from *Vibrio harveyi* using detergent extraction,

ion-exchange chromatography and gel filtration. Zymogram stains used to visualize enzyme activity on PAGE gels, indicated an M_r of 254 kDa for the complex.

1.13.3 Objectives of the project

The principal aims of this project were to accomplish:

1. Cloning and sequencing of the genes corresponding to all subunits of the Na^+-NQR complex of *V. alginolyticus*
2. Identification of the promoter region 5' to *nqrA* and determine if the gene cluster is organized as an operon
3. Sequence analysis by comparison of Nqr sequence to known sequences in databases and identification of possible co-factor binding sites by homology in specific regions
4. Expression of the NqrF polypeptides in *E. coli*
5. Purification of NqrF
6. Molecular and biochemical characterisation of NqrF
7. Fusion of NqrF to β-lactamse in pJBS633 to determine membrane topology of the polypeptide.

Chapter 2

Materials and methods

2.1 List of host strains and plasmids

Host strains

E. coli DH5α™: F^-, *rec*A1, *sup*E44, *end*A1, *deo*R, *pho*A, *hsd*R17 (r^-_K,m^+_K), *gyr*A96, *rel*A1, *thi*-1, (*argF-lacZYA*)U169, ϕ80*lacZ*M15 (Life technologies).

E. coli DH5αF'IQ™: F', *rec*A1, *sup*E44, *end*A1, *deo*R, *pho*A, *hsd*R17(r^-_K,m^+_K), *gyr*A96, *rel*A1, *thi*-1, (*arg*F-*lac*ZYA)U169, ϕ80*lacZ*M15/F', *pro*AB^+, *lac*$I^qZ\Delta M15$, *zzf*::*Tn5*[km^r] (Life technologies).

E. coli K12 strain HMS174: F^-, *rec*A1, *hsd*R, (r^-_{K12},m^+_{K12}), rif^r (Novagen).

E. coli B strain BL21(DE3): F^-, *omp*T, *hsd*S, *gal*, (λ*cIts*857, *ind*1, *Sam*7, *nin*5, *lac*UV5-T7 gene*1*) (Novagen).

E. coli B strain BL21(DE3)p*LysS*: F^-, *ompT*, $hsdS_B$ (r_B^-,m_B^-), *gal*, *dcm*(DE3)p*LysS*(cm^r) (Novagen).

Plasmids

pTZ18R (Fig. 2.1)

pTZ19R (Fig. 2.2)

pSL1180 (Fig. 2.3)

pSL1190 (Fig. 2.4)

pBluescript KS^- (Fig. 2.5)

pET16-b (Fig. 2.6)

pT7-7 (Fig. 2.7)

pJBS633 (Fig. 2.8)

Fig. 2.1. Plasmid map of pTZ18R.

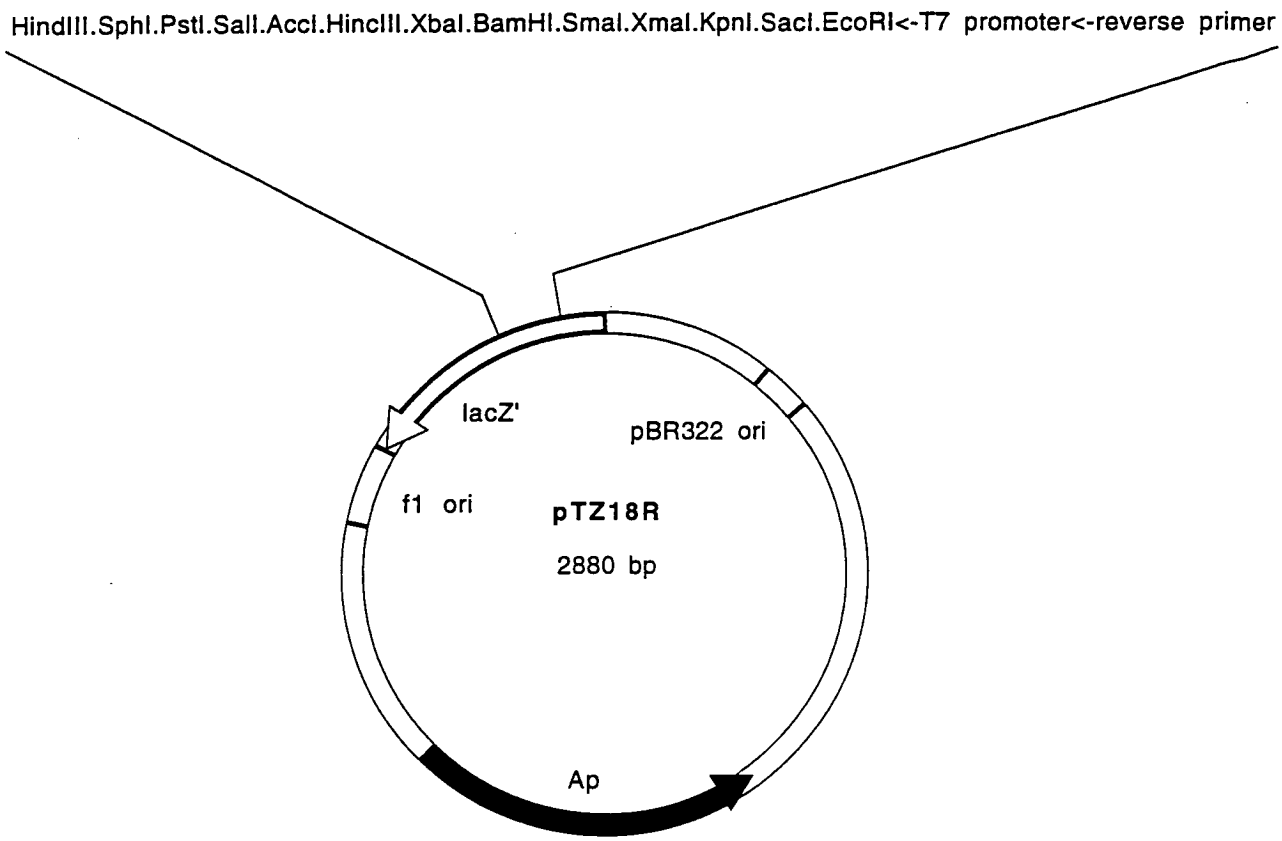

Plasmid name: pTZ18R
Plasmid size: 2880 bp
Constructed by: Mead
Construction date: 1986
Comments/References: Mead (1986) Protein engineering 1: 67. Derivative of pUC18.

Fig. 2.2. Plasmid map of pTZ19R.

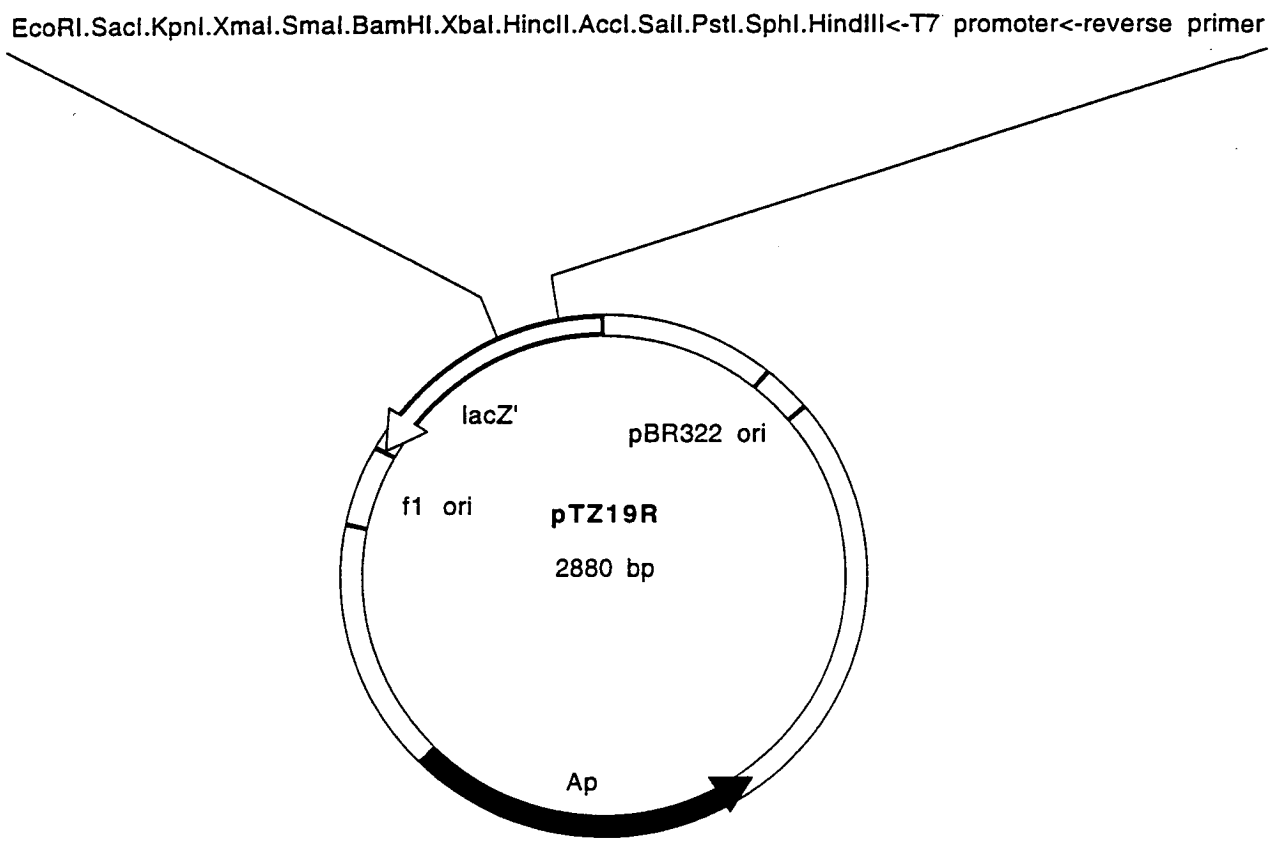

Plasmid name: pTZ19R
Plasmid size: 2880 bp
Constructed by: Mead
Construction date: 1986
Comments/References: Mead (1986) Protein Engineering 1: 67. Derivative of pUC19.

Fig. 2.3. Plasmid map of pBluescript KS-.

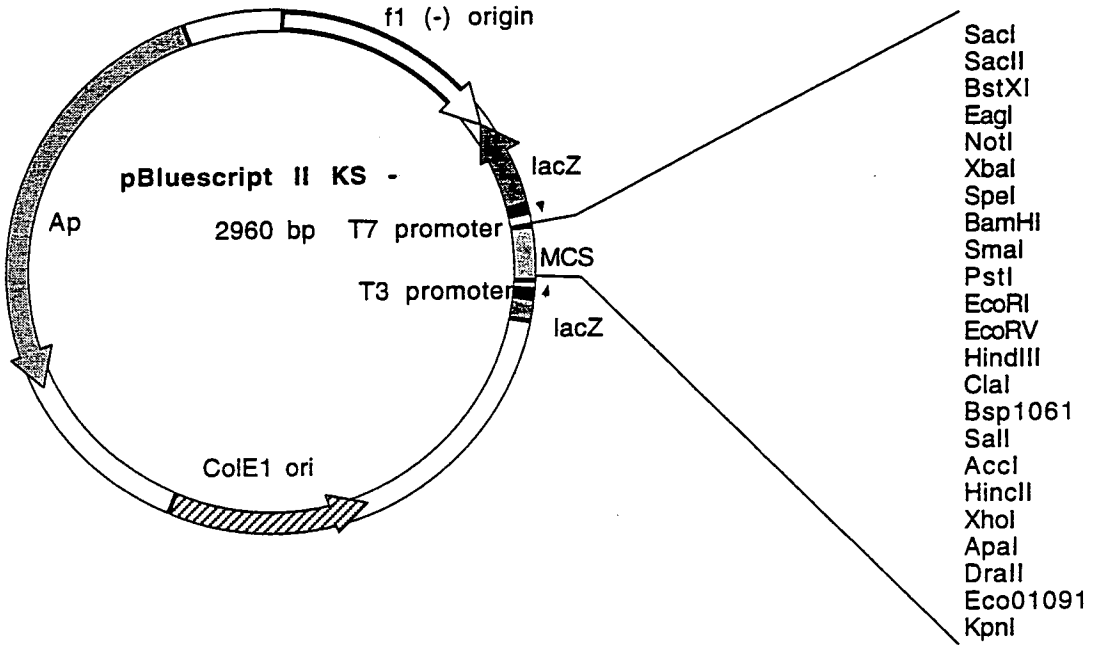

Plasmid name: pBluescript II KS -
Plasmid size: 2960 bp
Constructed by: Short
Construction date: 1988
Comments/References: Short et al (1988) Stratagene Cloning Systems product literature.

Fig. 2.4. Plasmid map of pSL1180.

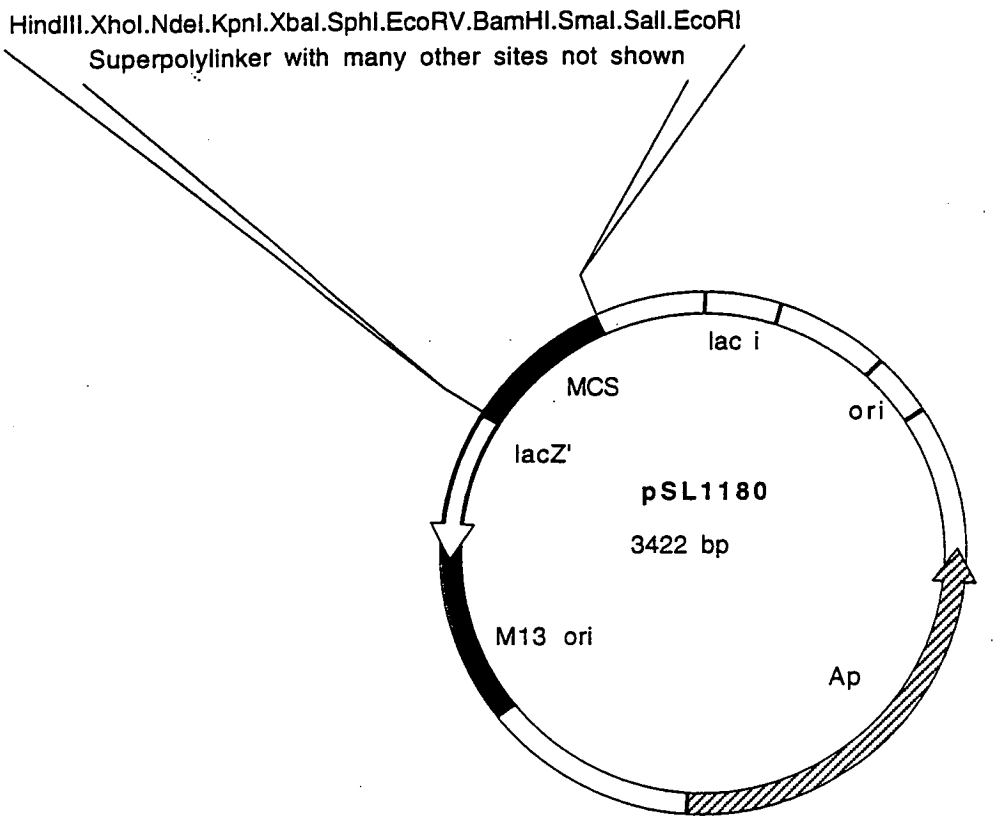

Plasmid name: pSL1180
Plasmid size: 3422 bp
Constructed by: Brosius
Construction date: 1989
Comments/References: Brosius (1989) DNA 8: 759. Superlinker phagemid.

Fig. 2.5. Plasmid map of pSL1190.

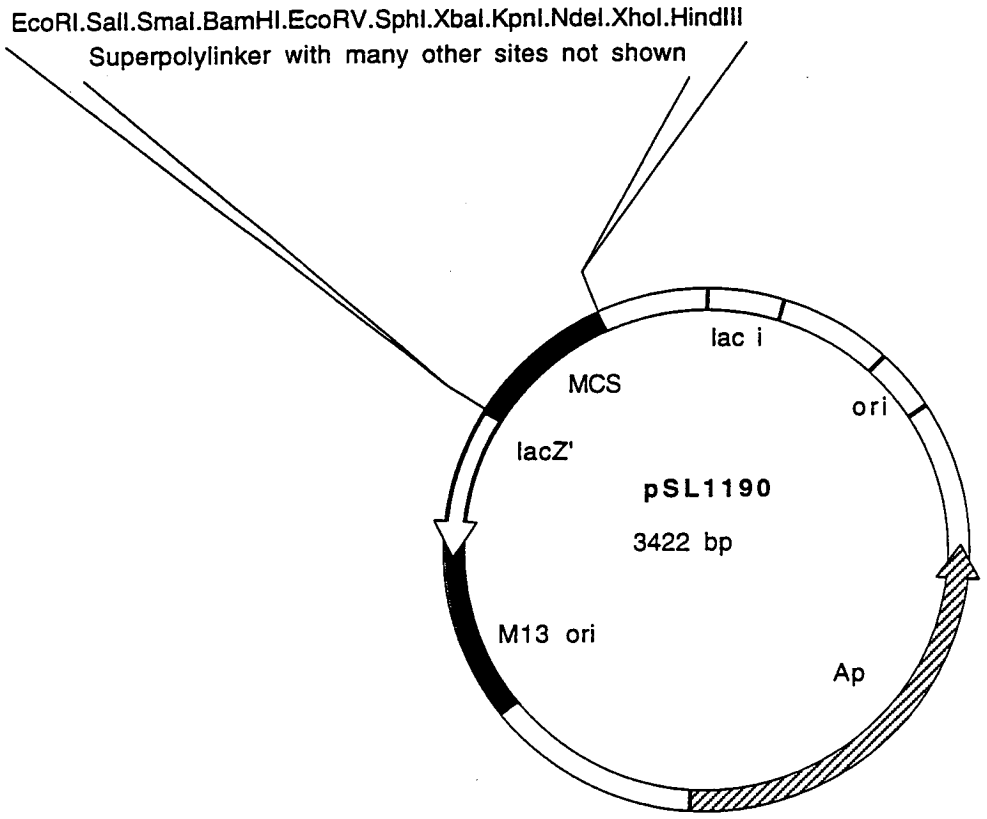

Plasmid name: pSL1190
Plasmid size: 3422 bp
Constructed by: Brosius
Construction date: 1989
Comments/References: Brosius (1989) DNA 8: 759. Superlinker phagemid.

Fig. 2.6. Plasmid map of pET16-b.

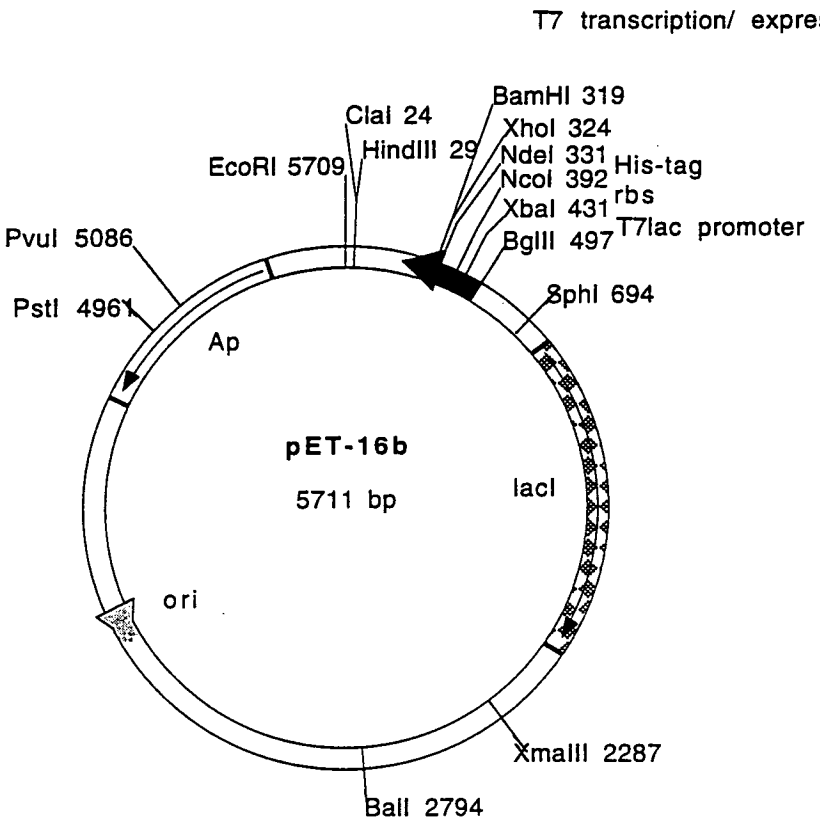

Plasmid name: pET-16b
Plasmid size: 5711 bp
Constructed by: Studier
Construction date: 1986
Comments/References: Studier and Moffat (1986) Journal of Molecular Biology 189: 113. Studier (1991) Journal of Molecular Biology 219: 37-44. Studier, Rosenberg, Dunn and Dubendorff (1990) Methods in enzymology 185: 60-89. T7 lac expression vector.

Fig. 2.7. Plasmid map of pT7-7.

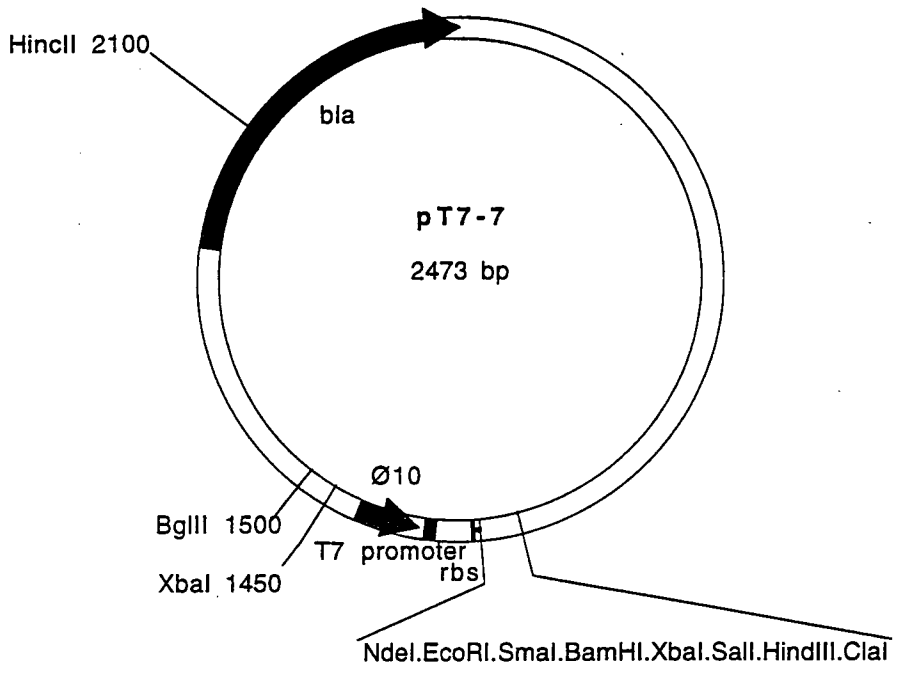

Plasmid name: pT7-7
Plasmid size: 2473 bp
Constructed by: Tabor
Construction date: 1990
Comments/References: Tabor (1990) Current Protocols in Molecular Biology pp 16.2.1-16.2.11. Green Publishing and Wiley-Interscience, New York. T7 expression vector.

Fig. 2.8. Plasmid map of pJBS633.

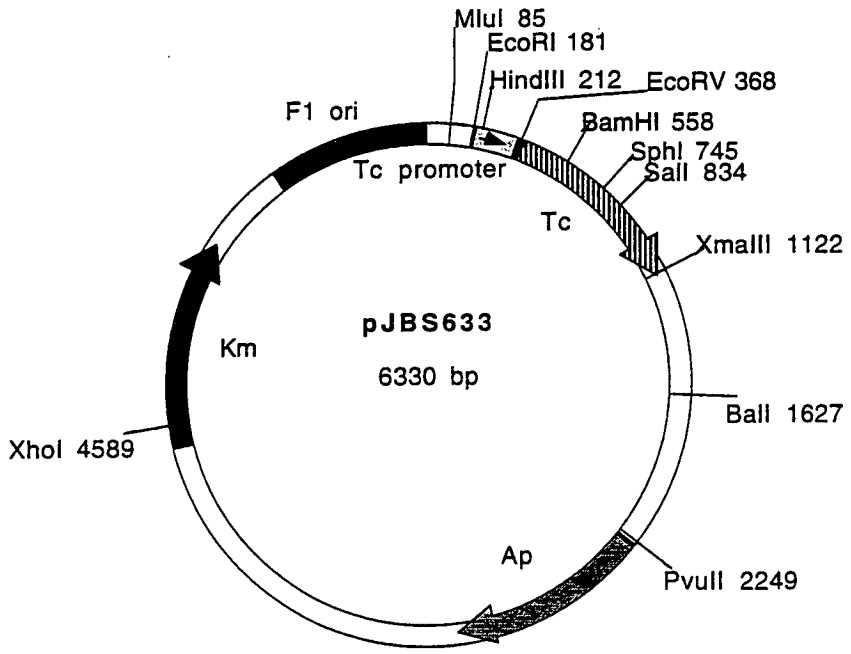

Plasmid name: pJBS633
Plasmid size: 6330 bp
Constructed by: Broome-Smith
Construction date: 1986
Comments/References: Broome-Smith and Spratt (1986) Gene 49: 341-349. blaM translational fusion vector.

2.2.1 Purification of plasmid DNA using QIAGEN kits

1. A single colony was picked and grown overnight in LB broth + appropriate antibiotic at 37°C. It was diluted 1:10 and grown until A_{600} was 1.0-1.5.

2. Cells from 30 ml culture were poured into a 30 ml sterile Corex tube and harvested by centrifuging for 15 min at 6000 rpm, 4°C in a Sorvall RC-5B refrigerated superpeed ultracentrifuge, using an SS-34 rotor.

3. The bacterial pellet was resuspended in 4 ml buffer P1 (50 mM Tris-HCl, 10 mM EDTA, pH 8.0) containing 100 μg/ml RNase to give a homogenous non-clumped cell suspension.

4. Buffer P2 was checked for precipitation of SDS and if necessary warmed. An aliquot of 4 ml of buffer P2 (200 mM NaOH, 1% (w/v) SDS) was added, mixing gently by inversion (4-6 times). No vortexing was done as this would shear the genomic DNA. Incubation at room temperature proceeded for 5 min but not longer. Lysis was evident by the viscosity.

5. Next, 4 ml of chilled buffer P3 (3 M potassium acetate, pH 5.5) was added. The solution became cloudy and viscous and was mixed by inversion 5-6 times to avoid precipitation of potassium dodecylsulphate and then incubated on ice for 15-20 min.

6. The solution was remixed and centrifuged at 15 000 rpm for 30 min at 4°C using the same centrifuge and rotor. It was recentrifuged for a further 15 min if the supernatant was not clear.

7. The QIAGEN tip was prepared by equilibrating with 4 ml buffer QBT (750 mM NaCl, 50 mM MOPS, 15% (v/v) ethanol, 0.15% (v/v) Triton X-100, pH 7.0). The column emptied by gravity flow, leaving it covered with a small amount of buffer, which prevented it from drying out.

8. The 12 ml sample was applied to the column.

9. The column was washed with 10 ml QC (1.0 M NaCl, 50 mM MOPS, 15% (v/v) ethanol, pH 7.0) twice, emptying by gravity flow.

10. DNA was eluted with 5 ml buffer QF (1.25 M NaCl, 50 mM Tris-HCl, pH 8.5) by gravity flow.

11. Precipitation of DNA was achieved by addition of 0.7 volume (approx. 3.5 ml) isopropanol at room temperature to avoid salt precipitation. This was centrifuged immediately at full speed (10 000 rpm) at 4°C for 30 min using an SS-34 rotor with the Sorvall RC-5B centrifuge.

12. After a wash with 5 ml cold 70% (v/v) ethanol, it was centrifuged again for 30 min to remove salt from the pellet and air-dried for 10 min.

13. DNA was resuspended in 200 µl of TE (10 mM Tris-HCl, pH 8.0, 1 mM EDTA) and stored at 4°C. 2 µl was used for gel electrophoresis on a 1% (w/v) agarose gel.

14. DNA quality was assessed by $A_{260/280}$ ratio (optional).

2.2.2 Novagen plasmid miniprep

1. Using a sterile loop, toothpick or pipette tip, a well-isolated colony was transferred into 3 ml of LB broth supplemented with appropriate selection in a bijou bottle. This was capped loosely and incubated with shaking at 37°C, 6 h to overnight.

2. 1.5 ml of culture was transferred into a 1.5 ml microcentrifuge tube and centrifuged at 12 000 g for 1 min.

3. The medium was removed by aspiration, to leave the pellet as dry as possible.

4. Cells were completely resuspended in 100 µl of ice-cold 50 mM glucose, 25 mM Tris-HCl, pH 8.0, 10 mM EDTA.

5. 200 µl of freshly prepared 0.2 M NaOH, 1% (w/v) SDS was added, mixed by inversion and sat on ice for 3 min.

6. 150 µl of ice-cold 3 M sodium acetate, pH 5.2 was added, mixed by inversion and left on ice for 5 min.

7. After centrifugation at 12 000 g for 5 min, the clear supernatant was transferred to a fresh tube, avoiding the pellet, which tended to break up easily.

8. Phenol/chloroform extraction was performed by adding 400 µl phenol:chloroform:isoamyl alcohol (25:24:1), vortexing for 30 s, and finally centrifuging at 12 000 g for 1 min at room temperature.

9. The top aqueous phase was transferred to a fresh tube and 800 µl ethanol added before vortexing. This was left at room temperature for 2 min and centrifuged at 4 °C, 12 000 g for 5 min.

10. The supernatant was decanted and 400 µl ethanol added to the pellet. After a brief spin, the ethanol was poured off and the pellet allowed to air dry in an inverted position for about 10 min.

11. The pellet was resuspended in 30 µl of TE buffer (10 mM Tris-HCl, pH 8.0, 1 mM EDTA) containing 20 µg/ml RNase A and incubated at 37°C for 15 min. A yield of about 1-2 µg plasmid DNA was expected.

12. At this point the DNA could be used for transformation or analyzed by restriction digestion. For transforming into an expression host, 1 µl of a 50-fold dilution (approx. 1 ng) of plasmid in sterile water or TE was used.

13. For sequence analysis the preparation must be further processed to remove RNA breakdown products. This was easily accomplished by precipitation with polyethylene glycol. 10 µl of 30% (v/v) PEG-8000, 1.5 M NaCl (prepared from autoclaved stocks of 50% PEG and 5 M NaCl to avoid possible DNase contamination) was added, vortexed thoroughly, and incubated on ice for 60 min.

14. After centrifuging at 12 000 x g at 4°C for 10 min, the supernatant was carefully removed, leaving the small transparent DNA pellet behind. This pellet was successively rinsed with 70% (v/v) ethanol and then 100% (v/v) ethanol as above and allowed to air dry.

15. Finally the DNA was resuspended in 20 µl TE. The plasmid was then suitable for alkaline denaturation and double-stranded sequencing.

2.2.3 Birnboim and Doly large scale plasmid preparation

1. 5 ml of LB-medium (containing the appropriate selective antibiotic) was inoculated with a single colony-purified bacterial colony and incubated at 37°C with shaking overnight.

2. 250 ml of LB (containing the appropriate selective antibiotic) was inoculated using 1 ml of the saturated overnight culture and incubated at 37°C with shaking overnight.

3. The culture was harvested by spinning at 7 000 rpm for 10 min in a Sorvall RC-5B refrigerated superspeed centrifuge using a GS-3 rotor.

4. The supernatant was discarded and the cells resuspended in 20 ml of 25 mM Tris-HCl, pH 8.0, 50 mM EDTA, pH 8.0.

5. 40 ml of freshly prepared 200 mM NaOH, 1% (w/v) SDS was added, the suspension thoroughly mixed by swirling and placed on ice for 10 min.

6. 30 ml of ice-cold 5 M potassium acetate, pH 5.5, was added, the lysed cells mixed by swirling and replaced on ice for 5 min.

7. Chromosomal DNA and cell debris were removed by spinning at 10 000 rpm for 15 min in a Sorvall RC-5B refrigerated superspeed centrifuge using a GS-3 rotor and transferring the supernatant to a fresh GS-3 bottle with a pipette.

8. 0.6 volumes of isopropanol was added, mixed well and left at room temperature for 10 min.

9. The DNA was sedimented by spinning at 10 000 rpm for 15 min in a Sorvall RC-5B refrigerated superspeed centrifuge using a GS-3 rotor.

10. The supernantant was discarded and the pellet dissolved in 5 ml of 1 x TE. 2.4 ml of 8 M ammonium acetate was added, mixed well and placed on ice for 20 min.

11. The solution was spun at 10 000 rpm for 15 min in a Sorvall RC-5B refrigerated superspeed centrifuge using a GS-3 rotor and the supernatant transferred to sterile-baked 30 ml glass Corex tubes.

12. The DNA was precipitated by adding 2.5 volumes of ice-cold ethanol, mixing gently by inversion and placing the tube at -20°C for 15 min.

13. The DNA was sedimented by spinning at 10 000 rpm for 15 min in a Sorvall RC-5B refrigerated superspeed centrifuge using a SS-34 rotor.

14. The DNA pellet was resuspended in 750 µl of 1X TE/RNase, transferred to an eppendorf and incubated at 37°C for 30 min.

15. Protein debris was removed by sequential phenol, phenol/chloroform and chloroform extractions.

16. The DNA was precipitated by adding 0.1 volume 3 M sodium acetate, pH 5.2, and 2.5 volumes of ice-cold ethanol, mixing gently by inversion and placing the tube at -20°C for 15 min.

17. The DNA was sedimented by spinning at 12 000 g for 15 min at 4°C in a benchtop microfuge.

18. The DNA was resuspended in 1 ml 1X TE.

2.3 Restriction digests of DNA

1. Digestions were set up in small Eppendorf tubes, adding the various components usually in the order indicated.

Single digest

Sterile distilled water	10X Buffer	DNA	Restriction enzyme
add to 10 µl	1 µl	0.1 - 1 µg	1 µl
or			
add to 20 µl	2 µl	0.1 - 1 µg	1 µl
(for more dilute DNA samples)			

2. After sealing the tubes, they were spun in the microfuge for about 5 s and placed in a rack in a 37°C water bath for 2 h. 3 µl of loading buffer (0.1% Bromophenol blue, 20% (v/v) glycerol, 10 mM EDTA) was then added.

3. Double digest

Sterile distilled water	10X Buffer	DNA	Restriction enzymes
Add to 10 µl	1 µl	100 ng - 1 µg	1 µl of X-> 1 µl of Y
or			
Add to 20 µl	2 µl	100 ng - 1 µg	1 µl of X-> 1 µl of Y

If the two different restriction enzymes have compatible buffers, they were both added at the same time and digestion proceeded for 2 h.

But otherwise, the restriction enzyme X with the lower salt buffer was added first and mixed well in the microfuge. After incubation at 37°C for 2 h, the salt concentration and/ or Tris-HCl concentration was increased in the buffer before the second restriction enzyme Y was added, the tubes spun briefly and incubated for another 2 h at 37°C before adding 3 µl of the loading buffer.

If the two restriction enzymes have totally incompatible buffers, the DNA was ethanol precipitated after the first digest, resuspended in TE, then proceeding with the second digest.

Considerations

The two restriction sites must not be too close to each other. If they are, they are checked that they have the required number of bases (different for each restriction enzyme) at each end of the cleavage site for efficient cutting by the particular restriction enzymes involved.

The relative volumes of each component added would depend on the concentration of DNA and buffer. It is important to remember that 1 unit of restriction enzyme will digest 1 µg DNA. The buffer must be diluted to 1X in the final volume, i.e. if a 10X buffer is used, 2 µl of the buffer is required when the total volume is 20 µl. About 3 µl of loading buffer is required for every 20 µl of digest. Number of samples from each digest, concentration of original DNA stock and size of wells determine the total volume of digests required.

N.B. Concentration of DNA and amount used for restriction is empirically determined and also dependent on the number of fragments to be fractionated on the gel.

Standard markers: λ*Hin*dIII, λ*Bst*EII

Restricted λ DNA markers were heated up to 65°C and plunged straight into ice before loading onto the gel, otherwise *cos* ends would ligate and hence give rise to a different banding pattern on the gel.

2.4 Creation of blunt-ends by end-filling

1. DNA was digested with the appropriate enzymes and heated at 65°C for 20 min.

2. This DNA was ethanol precipitated and resuspended in 10 µl dH_2O.

3. 1 µl NEB Klenow DNA polymerase and 33 µM of each dNTP (in total reaction mix) were added and made up to 20 µl total reaction mix with dH_2O and 2 µl 10X NEB Klenow reaction buffer and incubated at 25°C for 15 min.

4. The reaction was stopped by adding 0.4 µl of 0.5 mM EDTA (10 mM final concentration) and heating at 75°C for 10 min.

5. Ethanol precipitation of the DNA and resuspending in dH_2O was carried out before proceeding with ligation or further digests.

2.5 Agarose gel electrophoresis

1. The appropriate amount agarose was dissolved completely in 1X TAE buffer (10X TAE stock: 48.4 g Tris base, 11.4 ml glacial acetic acid, 20 ml 0.5 M EDTA, add distilled water to 1 ℓ; diluted to 1X TAE before use) in a screw-top flask, using a microwave oven.

For example, if a large 0.8% agarose gel is required, dissolve 0.8 g agarose in 100 ml TAE, whereas if a mini 0.8% agarose gel will be used, dissolve 0.2 g agarose in 25 ml TAE. The concentration of the gel (% agarose) selected will depend on the size of the DNA fragments to be separated.

2. The agarose was cooled slightly and 2.5 μl (for minigels) or 10 μl (for large gels) of 10 mg/ml ethidium bromide were added to the agarose solution.

3. The agarose was poured into the gel plate (with the ends taped and comb in place) carefully, ensuring that there were no air bubbles and left to set for 20-30 min. When the gel was set, the comb and tape were removed and the gel placed into the electrophoresis tank fully filled with 1X TAE.

4. All restriction digests and λ markers with loading buffer were pipetted into the wells.

5. The tank was connected to a power supply, and electrophoresis progessed overnight at 25 V or 10 mA. A higher voltage may be used to speed up the electrophoresis process but this will give poorer resolution.

2.6 Fluorescence detection

The DNA fragments were run on a gel incorporated with ethidium bromide. Ethidium bromide will bind to the DNA fragments and fluoresces under U.V. illumination, so that clear bands may be seen on the gel, allowing their sizes to be elucidated. After electrophoresis, agarose gels were placed on a U.V. transilluminator, and after focussing the camera, photographs were taken.

Restriction fragment size mapping

From the photograph, the distance migrated by each fragment was measured. The distance migrated by each of the fragments from the DNA markers can be plotted against their known fragment sizes in kb. [Plot molecular weight (kb) on the logarithmic axis and distance migrated (mm) along the linear axis of the log graph

paper] Once the calibration curve was plotted, sizes of the other DNA fragments from the same gel may be determined.

2.7 DNA extraction from agarose gels

2.7.1 Purification of DNA using QIAEX gel extraction kit

1. DNA fragments were excised by cutting out gel slices containing DNA of interest, under U.V. illumination.

2. 300 µl of QX1 was added per 100 mg gel.

3. QIAEX beads were suspended by vortexing 1 min.

4. 10 µl of QIAEX was added for every 5 µg DNA and vortexed. This was incubated at 50°C for 10 min and vortexed every 2 min to keep QIAEX in suspension.

5. Samples were centrifuged for 30 s in a microfuge.

6. Pellets were washed twice in 500 µl of QX2 and centrifuged for 30 s in a microfuge each time and supernatant was removed each time.

7. Pellets were then washed twice in 500 µl of QX3, centrifuged for 30 s in a microfuge each time to remove the supernatant. Ethanol-containing QX3 was completely removed to allow proper drying and prevent enzymatic inhibition by ethanol in subsequent reactions.

8. Pellets were air-dried for 10-15 min.

9. 20 µl of TE was applied to resuspend the pellet in order to elute the DNA. Tubes were incubated at room temperature for 5 min and vortexed every 2 min. For each

additional 6-10 µl of QIAEX added, an extra 10-20 µl of TE was added and incubatde 10 min for complete elution. The DNA can be eluted in minimum volume of 10 µl but may result in lower recovery of DNA from QIAEX particles.

10. After centrifugation for 30 s, the supernatant containing the DNA was transferred into a clean tube.

11. Optional: repeat elution and combine eluates.

2.7.2 QIAquick Gel Extraction kit

1. The DNA fragment was excised from the agarose gel with a clean, sharp scalpel and weighed in a tube.

2. 3 volumes of Buffer QX1 to 1 volume of gel (100 mg ~ 100 µl) was added.

3. The tubes were incubate at 50°C for 10 min. To help dissolve the gel slices, flicking and inverting the tube every 2-3 min during incubation was done. (For >2% agarose gels, increase incubation time to 20 min).

4. 1 gel volume of isopropanol added and mixed.

5. A QIAquick spin column was placed in a 2 ml collection tube and the sample loaded into the spin column. This was centrifuged at 13 000 rpm for 1 min in a microfuge.

6. Flow-through was discarded and the QIAquick column returned onto the same collection tube.

7. (Optional) 0.5 ml of Buffer QX1 was added to the Qiaquick column and centrifuged for 1 min.

8. To wash, 0.75 ml of Buffer PE was pipetted into QIAquick column and centrifuged for 1 min.

9. Again the flow-through was discarded and the QIAquick column centrifuged for an additional 1 min at 10 000 x g (~13 000 rpm).

10. QIAquick column was placed in a clean 1.5 ml microfuge tube.

11. To elute, 50 µl of 10 mM Tris-HCl, pH 8.5 or H_2O was added to the centre of the QIAquick column and centrifuged for 1 min at maximum speed. Alternatively, for increased DNA concentration, 30 µl elution buffer was added, stood for 1 min, and then centrifuged for 1 min.

2.8 Ligation

Considerations

DNA was ethanol precipitated and resuspended in a small volume if the DNA was at low concentration. DNA has to be concentrated as ligation volume must be small to efficiently allow insert and vector to anneal together.

Heat-labile phosphatase was used to to remove phosphate from all blunt ends or sticky ends of vectors digested by single enzymes, to prevent re-ligation of the vector.

Insert:vector concentration is approximately 3:1 for blunt ends and 1:1 for sticky ends.

The total volume of ligation must be small, 10-15 µl.

Table 2.1. Requirements for cloning dependent on foreign DNA termini (Sambrook *et al.*, 1989)

Termini carried by fragment of foreign DNA	**Requirements for cloning**	**Comments**
Blunt-ended	high concentrations of DNAs and ligase phosphatase treatment of linear plasmid DNA	background of non-recombinant clones can be high restriction sites at junctions between plasmid and foreign DNAs may be eliminated recombinant plasmids may carry tandem copies of foreign DNA
Different protruding termini	for maximum efficiency requires purification of plasmid vector after digestion with two restriction enzymes	restriction sites at junctions between plasmid and foreign DNAs are usually conserved background of nonrecombinant clones is low foreign DNA is inserted in only one orientation within recombinant plasmid
Identical protruding termini	phosphatase treatment of linear plasmid DNA	restriction sites at junctions between plasmid and foreign DNAs are usually conserved foreign DNA can be inserted in either orientation recombinant plasmids may carry tandem copies of foreign DNA

Concentration by ethanol precipitation of DNA

To dilute DNA, 2 volumes of 100% (v/v) cold ethanol and 0.1 volume of 3 M sodium acetate pH 5.2 were added and left on ice for 30 min. The mixture was spun for 30 min at 4°C in microfuge. Finally the supernatant was decanted and the pellet resuspended in a small volume of TE.

Dephosphorylation of 5' phosphate of vector to prevent cohesive ends from self religating

After digestion of vector by the appropriate restriction enzyme, 1 µl of 1 U/µl shrimp alkaline phosphatase or calf intestine phosphatase was used to treat per 10 µl of the digestion, and incubated at 37°C for 30 min. The phosphatase was inactivated by incubation at 65°C for 15 min with 2 µl of 200 mM EGTA.

Ligation of cohesive-termini

Controls were set up to determine if restriction digests were efficient (1), and if phosphatase reaction was effective or test the tendency for the cut vector to re-ligate (2).

1. Control - cut vector alone without ligase
2. Control - cut vector with ligase
3. vector with a small amount of insert
4. vector with more insert

Assuming insert and vector DNA concentrations are both at 100 ng/µl, ligations (1-4) were set in the following way:

	1	2	3	4
dH_2O	8 µl	6 µl	4 µl	-
10X buffer for ligase	-	1 µl	1 µl	1 µl
vector (200 ng)	-	2 µl	2 µl	2 µl
DNA insert (200 - 600 ng)	-	-	2 µl	6 µl
ligase (1 U or more)	-	1 µl	1 µl	1 µl
Total volume	10 µl	10 µl	10 µl	10 µl

Ligation of blunt-ended DNA

This requires: 1. low concentration (0.5 mM) of ATP

2. absence of polyamines such as spermidine

3. very high concentrations of ligase (50 Weiss units/ml)

4. high concentrations of blunt-ended termini

Good ligation of blunt-ended termini was acheived by using polyethylene glycol (PEG 8000) or hexamminecobalt chloride: (1) they accelerate rate of ligation by 1-3 orders of magnitude, allowing ligation at low enzyme and DNA concentrations; (2) they alter distribution of ligation products so that intramolecular ligation is suppressed and ligation products are created exclusively by inter-molecular joining events. All DNA products are linear multimers.

All ligations were carried at 16°C for 30 min.

2.9 Competent cells preparation and transformation

2.9.1 $CaCl_2$ combined with heat-shock method

1. Culture of strain in 5 ml of LB was grown to stationary phase.

2. Culture was diluted 1:100 into 25 ml of fresh medium and grown shaking until A_{600} reached 0.3, whereby cell culture was poured into an ice-cold sterile Corex tube and sat on ice for 10 min.

3. Cells were spun down at 4000 rpm for 10 min, 4°C.

4. The supernatant was removed and the cell pellet resuspended in 5 ml sterile ice-cold 100 mM calcium chloride, and left on ice for 30 min.

5. Another spin at 4000 rpm for 10 min, 4°C was carried out.

6. Again, supernatant was decanted and the competent cells resuspended in 1 ml 100 mM calcium chloride and stored on ice, ready to be used.

7. Cells may be stored frozen in this state in 0.5 ml portions at -70°C or snap frozen in dry-ice ethanol.

Transformation by heat-shock

8. Using a chilled sterile pipette tip, 200 µl of the competent cell suspension was transferred into a sterile microfuge tube. DNA, no more than 50 ng in a volume of 10 µl (5 µl of ligation mix), was added to each tube, swirled gently and left on ice for 30 min.

9. In addition to the ligation controls, transformation controls were also set up as follows:
   - competent cells receiving known amount of uncut plasmid
   - competent cells receiving no plasmid

10. These tubes were transferred to 42°C for 5 min without shaking, and rapidly placed in an ice bath after heat-shock.

11. 800 µl LB broth + glucose (0.4 ml 20% (w/v) glucose into 10 ml LB broth) was added to each tube and incubated for 45 min or longer, at 37°C, shaking (to encourage expression of antibiotic-resistance genes and increase transformation efficiency).

12. Cells were spun in microfuge for 15 s, 500 µl of supernatant removed and the pellet was resuspended in remaining solution.

13. Up to 200 µl of transformed cells were spread onto appropriate selection plates, which were incubated overnight at 37°C.

LB broth

950 ml deionised water

10 g bacto-tryptone

5 g bacto-yeast extract

10 g NaCl

Adjust pH to 7.0 with 5 M NaOH (approx. 0.2 ml). Adjust volume to 1 ℓ with deionised water. Sterilise by autoclaving for 20 min at 15 lb/ sq. in. on liquid cycle.

2.9.2 1-step preparation of competent cells for transformation

(Derived form Chung *et al.*, 1989)

1. Inoculum was grown in 5 ml of LB broth (with appropriate selection, i.e. antibiotic) at 37°C overnight.

2. This was diluted 1:100 into fresh 25 ml LB broth to A_{540} 0.05-0.1 (540 nm at filter 2) and grown at 37°C shaking, until A_{540} 0.3-0.4 was reached.

3. Cells were cooled on ice for 10 min, then centrifuged at 5 000 rpm for 10 min, room temperature.

4. Pellets were resuspended in 1 µl of TSS (950 µl of TSS + 50 µl DMSO) and placed on ice. These cells were competent.

5. Plasmid DNA (approx. 10 ng) were added to 100 µl of the cell suspension and placed on ice for further 30 min.

6. 900 µl of L-broth containing 0.36% (w/v) glucose was added and incubated shaking at 37°C to express phenotype for 1 h.

7. Cells were spun down for 15 s in a microfuge and 0.5 ml of the supernantant removed before the cell pellet was resuspended.

8. 100 µl was spread on LB agar with the appropriate selection and incubated overnight at 37°C.

2.10 Sequencing

Preparing the plates

Plates were carefully and thoroughly washed with detergent, rinsed and cleaned with ethanol before drying. One plate was usually siliconised by wiping over with dimethyldichlorosilane, allowed to dry for 5 min and then rinsed with water (to avoid HCl being formed during electrophoresis). Spacers were positioned correctly beween the plates before the sides and bottom of the 2 plates were properly taped up.

Pouring the gel

A 6% acrylamide gel solution was made up as follows:

Protogel (30% (w/v) acrylamide/bisacrylamide)	12 ml
Urea	25.2g
10 X TBE	6 ml

TBE (121g Tris base, 7.4g EDTA 53.4g Boric acid, make up to 1 ℓ, pH should be 8.3)

Add approx. 22 ml of water to make up to 60 ml

This mixture was placed at 37°C for a few min (it is an endothermic reaction), then stirred gently for 10 min (Covered with tin foil and stirred gently because oxygen inhibits the polymerization). When dissolved, 142.5 µl 10% fresh AMPS and 142.5 µl TEMED were added to the gel solution which would usually set in an hour.

A 25 ml pipette was used to add the gel mix. The gel mix was poured down one corner, taking care to avoid the formation of air bubbles. The flat side of comb was edged in 0.2 inch at the top and plates were laid onto a rack while the gel set. The exposed top of the plates were covered with Saran wrap and clamped together over the spacers or as far in as possible at the top.

Sequencing reactions

(1) Promega Taq track sequencing kit

A. Alkaline denaturation of supercoiled plasmid DNA.

1. 4 μg (approximately 2 pmol) of supercoiled plasmid DNA and deionized water was added to a microcentrifuge tube to a final volume of 18 μl.

2. 2 μl of 2 M NaOH, 2 mM EDTA was included and incubated for 5 min at room temperature to denature the DNA.

3. To neutralize the reaction, 8 μl of 5 M ammonium acetate, pH 7.5 was added and the tube vortexed.

4. 112 μl of 100% ethanol was introduced to precipitate the DNA and the reaction mix was vortexed.

5. The tube was centrifuged for 10 min at top speed in a microcentrifuge.

6. After decanting the supernatant, the pellet was washed with 1 ml of 70% (v/v) ethanol and centrifuged for 1 min.

7. The supernatant was removed and the pellet dried. The dried pellet was resuspended in 16 μl of distilled water for sequencing with *Taq* DNA polymerase.

B. Annealing the double-stranded template and primer

The primer was annealed with double-stranded DNA plasmid template in a molar ratio of approximately 1:1. For each set of four sequencing reactions, the following reagents were mixed in a microcentrifuge tube:

Denatured plasmid ds DNA (approx. 4 μg of a 3.5 kb template)	1.6 pmol (16 μl)
Primer (approx. 16 ng of a 24mer)	2 pmol (2 μl)
Taq DNA polymerase 5X buffer	5.0 μl
Extension/labelling mix	2.0 μl
Sterile H_2O	to final volume 25 μl

Incubation proceeded at 37°C for 10 min.

C. Extension/labelling reaction

1. 0.5 μl of [α-^{35}S]dATP (1,000 Ci/mmol, approx. 10 μCi/μl) or 0.5 μl of [α-^{32}P]dATP (800 Ci/mmol, approx. 10 μCi/μl) was added to the annealed primer template mixture.

2. 1 μl of Sequencing Grade *Taq* DNA polymerase (5 U/μl) was introduced and mixed briefly by pipetting up and down.

3. This was incubated at 37°C for 5 min.

D. Termination reaction

1. For each set of sequencing reactions, four microcentrifuge tubes (G, A, T, C) were labelled and 1 μl of the appropriate d/ddNTP Mix was added to each tube. These tubes were stored on ice or at 4°C until just before completion of the extension/labelling reaction.

2. When the extension/labelling reaction was complete, 6 µl were aliquoted to each tube containing the d/dNTP Mix (G, A, T, C). This was mixed briefly by pipetting up and down followed by a brief spin to ensure that no liquid was left on the tube walls.

3. The tubes were incubated at 70°C for 15 min.

4. Then 4 µl of Stop Solution was added to each tube and stored at -20°C.

5. These reactions were heated to >70°C for 2-5 min immediately before loading on a sequencing gel. 2.5-3.0 µl of each reaction was normally loaded on the gel.

(2) Pharmacia T7 sequencing kit

1. To denature template, 2 µl 2 M NaOH was added to 8 µl of template DNA (or 8 µl total DNA + H_2O) in a microcentrifuge tube. The tube was flicked to mix, spun if necessary, and left at room temperature for 10 min.

2. 7 µl 3 M NaOAc, pH 5.2, 4 µl dH_2O and 120 µl ethanol were added to precipitate the denatured DNA and this was placed on ice for 15-20 min before a spin for 15 min at 4°C. The DNA pellet was dried and redissolved in 10 µl dH_2O.

3. For annealing the primer to the template, 2 µl primer, 2 µl annealing buffer and 10 µl template were mixed by flicking and spun briefly before incubation at 65°C for 5 min. This was followed by another incubation at 37°C for 10 min and a final incubation at room temperature for 10 min. The samples were spun briefly.

4. The T7 DNA polymerase was diluted with dilution buffer as directed for the labelling reaction and primer extension. The 14 µl annealed template/primer was

added to a pre-mixed solution of 3 µl labelling mix, 1 µl labelled dNTP ([α-^{35}S]dATP) and 2 µl diluted T7 DNA polymerase. This was mixed by pipetting and spun briefly before incubation at room temperature for 5 min. 2.5 µl of 'T, G, C, A Short mix' nucleotides were dispensed for each template and incubated at 37° C for 2 min (last 2 min of 5 min labelling reaction). 4.5 µl of the labelling reaction was added to each of the four nucleotide mixes and returned to 37°C for 5 min.

5. The termination reaction comprised adding 5 µl Stop solution to each tube. Samples could be frozen at this stage. (-20°C). To prepare samples for loading, 3-5 µl of each reaction was transferred to a fresh eppendorf tube, heated to 75-80°C for 2 min before loading.

Preparation of gel for loading

Plates and combs were wiped clean to remove any crystallised urea. The tape was removed followed by the combs. The plates containing the polyacrylamide gel, were placed in the electrophoresis tank and clamped tight. After closing the drain tap, 1X TBE was added to top tank and checked for leaks. The well left by the flat side of the combs were washed using with a Pastuer pipette. Combs were then inserted so that the teeth were just pressing into the gel. If no leaks were obvious, 1X TBE was added to the bottom tank and leads were connected to the power supply set at 65 V for pre-electrophoresis for 1 h before sample loading. Wells were washed out again with the pipette prior to loading.

Fixing and drying down of the gel

The gel was removed from tank and the spacers and combs taken out. The plates were gently prised apart from a corner with a ruler. A small portion of gel from top right hand corner was removed as an orientation mark. Placing the gel with the plate into a large container containing fix solution (10% (v/v) acetic acid, 12% (v/v) methanol),

fix solution was pipetted over gel occasionally to remove urea. The fixed gel was lifted out carefully after 15 min. (Fixing of the gel is an optional step.)

A piece of card (3M blotting paper) was wet with water and laid over the gel, starting at the top edge, bringing it down the length of gel slowly to displace air and flatten out wrinkles in gel. This was blot dry with dry blotting paper and lifted carefully to lie the gel side up on the glass plate. A piece of Saran wrap was put over the gel and this was then dried using a gel drier.

The dried gel was placed in a cassette with a piece of X-ray film and stored at room temperature, exposed and developed after a period of time depending on cps checked with a Geiger counter.

2. 11 Unidirectional digestion of DNA with Exonuclease III and S1 nuclease and *bla*M fusions in pJBS633

This method was described by Henikoff (1984, 1987) and the solutions below were used:

10X Exonuclease III buffer

0.66 M Tris-HCl (pH 8.0)

66 mM $MgCl_2$

S1 reaction mixture

H_2O	172 µl
10X S1 buffer	27 µl
S1 nuclease	60 U

10X S1 buffer

5 M NaCl	5.0 ml
3 M potassium acetate (pH 4.5)	1.1 ml
Glycerol	5.0 ml
1 M $ZnSO_4$	20 µl

S1 Stop mixture

0.3 M Tris base

50 mM EDTA (disodium salt)

Klenow mixture

H_2O	20 µl
1 M $MgCl_2$	6 µl
0.1 M Tris-HCl (pH 7.6)	3 µl
Klenow fragment	3 U

10 μg of pKT05 plasmid DNA (pJBS633 with insert of *nqr*E and *nqr*F) was digested completely using two restriction enzymes, one of which leaves a 4 base 3' protrusion (*Sph*I) that protects the vector DNA on that end from exonuclease III digest, while the other enzyme produces a 5' protrusion (*Bfr*I) between the *Sph*I site and the target sequence and is hence susceptible to exonuclease III digestion. The DNA was then purified by phenol/chloroform extraction and ethanol precipitated. The dried DNA pellet was then resuspended in 40 μl of 1X exonuclease III buffer and stored on ice.

7.5 μl of S1 reaction mix was added to 16 eppendorf tubes and placed on ice. The plasmid DNA in the 1X exonuclease III buffer was incubated at 37°C and 2.5 μl of the DNA solution was transferred into the first eppendorf tube containing the S1 reaction mix. To the remainder of the DNA solution, approximately 300-400 U of exonuclease III was added. The tube was vortexed briefly and returned to the 37°C water bath immediately. At intervals of 30 s, 2.5 μl samples of the DNA solution were removed and placed in successive eppendorf tubes containing the S1 reaction mix. After all the samples were taken, the tubes were incubated for 30 min at 30°C to remove single stranded DNA before 1 μl of S1 stop solution was added to each of the tubes and incubated at 70°C for 10 min. This inactivates the S1 nuclease and any residual exonuclease III. Portions of each sample were analysed by agarose gel electrophoresis. Samples containing DNA fragments of the desired size were pooled and 1 μl of Klenow mixture was added for each 10 μl of pooled sample. The pooled samples were incubated for 5 min at 37°C. During this incubation, in the absence of dNTPs the 3'->5' exonuclease activity of the Klenow fragment of *E. coli* DNA polymerase I removes any remaining protruding 3' termini from the digested DNA. For each 10 μl of pooled sample, 1 μl of 0.5 mM dNTPs was added and left at room temperature for 15 min.

The samples were phenol/chloroform extracted, ethanol precipitated and cut with *Pvu*II followed by another phenol/chloroform extraction and ethanol precipitation. The pellet was resuspended in 10 μl dH_2O. 3 μl was analysed by gel

electrophoresis while the rest was religated. The DNA was cut again with *Pvu*II (to removed DNA undigested by the initial restriction enzymes and exonuclease III) before being transformed into *E. coli* DH5α and plated onto LB + kanamycin (50 μg/ml) plates.

Plasmid pJBS633 contains a tetracycline promoter just before the target gene cloning site and has a *Pvu*II site just before the mature β-lactamase coding sequence (lacks a promoter and will not be transcribed in the absence of an in-frame fusion). Beta-lactamase will only be able to protect cells from ampicillin if translocated to the periplasm where it cleaves β-lactams before they interfere with the cells' peptidoglycan synthesis.

To screen for in-frame fusions to *bla*M, kanamycin-resistant transformants were plated at high inoculum (patched with toothpicks) onto LB + ampicillin (200 μg/ml) plates. Even proteins fused at the cytoplasmic region to *bla*M, will produce colonies at high inoculum because some cells would lyse and release their cytoplasmically located β-lactamase fusion protein and protect neighbouring cells from ampicillin. But when single cells are plated on ampicillin (4 μl of a 10^5 dilution of an overnight culture spotted onto a LB + 200 μg/ml ampicillin plate), only periplasmically fused *bla*M fusions will protect cells from the ampicillin.

These transformants were then sequenced across their fusion junctions using the mature β-lactamase universal primer (refer to table 3.1 for primer sequence) 40 nucleotides from the junction.

2.12 PCR

Genes n*qr*A-*nqr*F were cloned into pET16b using PCR to engineer an *Nde*I site at the N-terminal region. An 0.12 kb *Nde*I/*Sph*I PCR fragment generated by restriction of the PCR product, was then cloned into pSL1190. Following this, the next connecting fragment of 3.8 kb was cut with *Sph*I/*Kpn*I, cloned into pSL1190, cut with *Sph*I/*Xho*I, cloned just behind the PCR fragment in pSL1190 cut with *Sph*I/*Sal*I (complementary ends to *Xho*I). This recombinant plasmid is finally cut with *Nde*I/*Kpn*I and cloned into the 2.3 kb *Kpn*I/*Sal*I pET16b plasmid (pKT02) cut also with *Nde*I/*Kpn*I.

In addition, *nqr*F was cloned into pET16b using its translational start site *Nde*I. The *Nde*I site was engineered into *nqr*F using PCR, as above with *nqr*A. The 0.08 kb N-terminal region of *nqr*F is cut with *Nde*I and *Hin*dIII, and ligated to its C-terminal region from cutting 2.3 kb *Kpn*I/*Sal*I previously cloned into pET16b (pKT02) with *Nde*I and *Hin*dIII. The resulting plasmid was termed pKT03. Expression from pKT03 results in a His-tagged catalytic subunit which can then be easily purified in one step with its His·Tag binding to a nickel chelation column. A point of concern would be that the conformation of the protein purified this way may not be a native natural form, and activity may be lost due to the presence of the tag although the tag is cleavable with Factor Xa. This may affect biochemical work in future when kinetics experiments will be done.

Primers

All PCR primers were designed with the following requirements: (1) not GC rich (problems with high annealing temperatures); (2) must not form primer dimers (no possibility of more than three consecutive bases on primers complementing and pair with each other); (3) annealing temperatures of each pair of primers must not be too different; (4) at least 16 bases, optimum 20-24; (5) must not fold into hairpin loops with energy less than 0, and have a free 3' tail. The Wisconsin GCG8 package

contains FOLDRNA and PRIME programmes which were used for aiding primer design.

*nqr*A

Primers to create *Nde*I site at ATG codon in *nqr*A

Primer 1:

---*Nde*I---

5' AGGACTGCCATATGATTACAATAAA 3' 25 nucleotides

-----8bp------- ----------*nqr*A----------

for efficient *Nde*I

cleavage close to end

of DNA fragment

Fold energy = 2.1

```
          10
AGGACUGCCA       GAU
                UAU
                AUA       U
          ----AA        ACA
               20
```

Annealing temperature = [A+T] x2 + [G+C] x4 = (17x2)+(8x4) = 66°C

Primer 2:

5' CACCAACGCGGACATG 3' 16 nucleotides

Primer that anneals to sequence downstream of *Sph*I in *nqr*A

Fold energy = 1.5

```
       --CA     AA
            CC
            GG     C
ACGUACA  10 CG
```

Annealing temperature = (10x4)+(6x2) = 52°C

Primers to create *Nde*I site at ATG codon in *nqr*F:

Primer 3:

---*NdeI*---

5' GATGCAATCATATGGACATTATTC 3' 24 nucleotides

----8 bp----- ---*nqr*F sequence---

for efficient *Nde*I

cleavage close to end

of DNA fragment

Fold energy = 1.1

```
          --    AU
 ----GAUG  CA     C
     UUAC  GU     A
CUUA      AG   AU
  20              10
```

Annealing temperature = (8x4)+(16x2) = 64°C

Primer 4:

5' CCGGCTAGAGCACTCA 3' 16 nucleotides

Primer just downstream of *Hin*dIII in *nqr*F

Fold energy = 2.4

```
  -----C    GC
        CG
         GC    U
ACUCAC    GA
```

Annealing temperature = (10x4)+(6x2) = 52°C

Using the higher annealing temperature of each pair of primers calculated above, the primers were annealed to the DNA template in the proportions in the PCR reaction mix (below) and put through several cycles in the PCR thermal reactor.

PCR reaction mixtures

10x buffer	5 µl
10 mM dNTPs	1 µl
25 mM $MgCl_2$	2 / 3 / 4 µl
Primers (30 ng/µl)	1 µl of each primer (0.1-0.5 µM)
DNA template (in plasmid or linear, 10 ng/µl)	1 / 2µl (i.e.10-20 ng)
Taq polymerase (2U/µl)	0.5 µl (1U)
H_2O	add to 50 µl reaction volume
Sterile mineral oil	2-3 drops

Hybaid PCR thermal reactor programmed for:

	Denaturation	Annealing	Polymerization
First cycle	94°C 5 min	62°C 1 min	72°C 30 sec
Subsequent 28 cycles	94°C 1 min	62°C 1 min	72°C 30 sec
Last cycle	94°C 1 min	62°C 1 min	72°C 10 min

The DNA template for *nqr*A was 2.0 kb *Hin*dIII, while 1.9 kb *Xba*I/*Sal*I was used for *nqr*F. Primers 1, 2 were used for *nqr*A and primers 3, 4 for *nqr*F. On running 2 μl samples of PCR products from N-terminal regions of *nqr*A and *nqr*F on 2% agarose gels, a clear distinct 140 bp band was observed for all *nqr*A samples except for the blank (no DNA template) and a weak 180 bp band for a few *nqr*F samples, except for the blank. There was no evidence of primer-dimers or non specific priming as only a single clean band was obvious in all samples.

2.13 Protein overexpression system using a T7 polymerase system

1. 5 ml LB + Cm + Amp was inoculated with a single colony of BL21(DE3)p*LysS* harbouring the gene(s) to be overexpressed on a pT7 vector. A similar culture carrying only the parental plasmid was also set up. Both were grown overnight at 37°C with shaking.

2. Cells were spun down and resuspended in 1 ml of the same medium. 0.5 ml of this culture was inoculated into 24.5 ml of mimimal medium (300 ml dH_2O, 80 ml 5X Spitzizen salts, 10 ml 20% (w/v) glucose, 0.1 ml thiamine B1 (5 mg/ml), 0.2 ml ampicillin (100 mg/ml), 0.4 ml chloramphenicol (20 mg/ml), and grown at 37°C until an A_{600} of 0.6-0.8 was reached.

3. To induce overexpression, four 0.5 ml aliquots of cells from each culture were obtained and 3 µl of IPTG (20 mg/ml, final concentration 0.5 mM; or 6 µl for pT7*lac* vectors, final concentration 1 mM) added to three of them (the fourth aliquot is an uninduced control). These were then incubated at 37°C (note: IPTG M_r 238.3).

4. At 1, 2, and 3 h intervals post-induction, one of the tubes were removed and cooled on ice. After a spin, the supernatant was removed and cells were resuspended in 100 µl of 1X sample buffer by vortexing well.

5. Samples were boiled for 5 min and 5 µl loaded onto a polyacrylamide gel.

2.14 Radiolabelling of proteins that are overexpressed using a T7 polymerase system

1. 5 ml LB + Cm + Amp was inoculated with a single colony of BL21(DE3)p*LysS* harbouring the gene(s) to be overexpressed on a pT7 vector. A similar culture carrying only the parental plasmid was also set up. Both were grown overnight at 37°C with shaking.

2. Cells were spun down and resuspended in 1 ml same medium. 0.5 ml of this culture was inoculated into 24.5 ml of mimimal medium, and grown at 37°C until A_{600} 0.6-0.8 was reached.

3. To induce overexpression, four 0.5 ml aliquots of cells from each culture were obtained, and 3 µl of IPTG (20 mg/ml, final concentration 0.5 mM; or 6 µl for pT7*lac* vectors, final concentration 1 mM) was added to two of them. Incubation continued at 37°C for 30 min.

4. 1 µl rifampicin (100 mg/ml; final concentration 200 µg/ml) was added to one IPTG-treated sample and one non-IPTG-treated sample:

   -I/-R, -I/+R, +I/-R, +I/+R (where I = IPTG; R = rifampicin)

5. Samples were incubated for 45 min.

6. Each sample was pulse-labelled with 5 µCi of labelled amino acid for 5 min.

7. After cooling tubes on ice, they were spun down, the supernatant removed and cells resuspended in 100 µl of 1X sample buffer by vortexing well.

8. Samples were boiled for 5 min and before loading 5 µl onto a polyacrylamide gel.

9. The gel was dried down and a film placed over gel.

2.15 Cell fractionation

Spheroplasts of *E. coli* were prepared by a modification of the method of Birdsell and Cota-Robles (1967).

1. A 2 ℓ culture of *E. coli* BL21 (DE3) p*LysS* expressing NqrE and NqrF from pET16b, upon reaching A_{600} 0.6-0.8, was harvested by centrifugation at 10 000 g for 15 min at 4°C and washed once in 10 mM Tris-HCl, pH 7.5, containing 0.1 M NaCl.

2. The washed cells were resuspended in 25 ml 10 mM Tris-HCl, pH 8.0, containing 0.5 M sucrose to give a protein concentration of approximately 3 mg/ml. This suspension was then incubated statically for 5-10 min at 20°C.

3. Lysozyme was added to a final concentration of 30 µg/ml and incubated for a further 10 min.

4. An equal volume of 10 mM Tris-HCl, pH 8.0, was added with continuous stirring and incubated at 20°C for 5-10 min after which EDTA (100 mM, pH 8.0) was added to a final concentration of 1 mM (0.5 ml per 50 ml).

5. Throughout these stages, spheroplast formation was monitored by phase-contrast microscopy. After EDTA addition, spheroplast formation should be 95-100% complete within 15 min.

6. $MgSO_4$ was immediately added to a final concentration of 50 mM to counteract any inhibitory effects of EDTA (5 ml of a 0.5 M stock solution per 50 ml mixture).

7. The spheroplasts were harvested by centrifuging the spheroplast suspension at 17 000 g for 15 min (12 500 rpm in the Sorvall 8 x 50 head). The supernatant is the periplasmic fraction.

8. The pellet was gently resuspended in 10 ml MacLeod Buffer B (10 mM Tris-HCl, pH 7.5, 0.3 M NaCl, 50 mM Mg SO_4, 10 mM KCl).

9. The cells were then disrupted by sonication of 3 x 30 s bursts with 30 s cooling gaps in between.

10. Whole cells and cell debris were then removed by centrifuging at 10 000 g for 15 min at 9 000 rpm in a Sorvall 8 x 50 ml head.

11. The cell-free supernatant was spun in a Beckman TL-100, using the TL100-2 rotor, at 45,000 rpm, 4°C, 1 h.

12. The cytoplasmic supernatant was collected and the membrane pellet was solubilized in 10 mM NaCl, 20 mM Tris-HCl, pH 7.5, 5 mM EDTA, 1% (v/v) Triton X-100, 10% (v/v) glycerol and 1 mM PMSF (solubilization buffer), for 1 h at 4°C.

13. This was then centrifuged in the Beckman at 80 000 rpm, 1.5 hours, 4°C. The supernantant is the membrane fraction. The pellet was redissoved in fresh solubilization buffer and this represented the outer membrane fraction.

Alkaline phosphatase assay (periplasm)

Alkaline phosphatase was assayed as the rate of hydrolysis of *p*-nitrophenyl phosphate (Thompson and MacLeod, 1974). The reaction mix (2 ml) contained 10 mM *p*-nitrophenyl phosphate, Tris-salts buffer, pH 8.8 and the reaction was started by the addition of 50-100 µl of the enzyme source. The reaction was monitored as the increase in absorbance at 420 nm owing to nitrophenol and the rate was calculated assuming 1 O.D. unit = 1 µmol nitrophenol.

Isocitrate dehydrogenase (cytoplasm)

Isocitrate dehydrogenase was assayed by the formation of NADPH from NADP (Reeves *et al.*, 1971). The assay mix contained 20 mM Tris-HCl buffer, pH 7.5, 2 mM $MnCl_2$, 0.5 mM $NADP^+$, 0.5 mM isocitrate and 50 µl enzyme in a total volume of 1 ml. The reaction was started by the addition of isocitrate and activity was determined from the increase in absorbance at 340 nm due to NADPH formation using the extinction coefficient 6.22 x 10^3 $M^{-1}cm^{-1}$.

Succinate dehydrogenase (membrane)

Succinate dehydrogenase was assayed as the reduction of ferricyanide using the method described by Veeger *et al.* (1969). The reaction mix contained 100 mM phosphate buffer, pH 7.6, 1 mM EDTA, 1 mM KCN, 40 mM succinate, 0.1% (w/v) bovine serum albumin (BSA), 1.25 mM $K_3Fe(CN)_6$ in a total volume of 2.9 ml. The reaction was started by the addition of 50 µl of enzyme and the decrease in absorbance at 455 nm was monitored. The acitivity was calculated as µmol succinate reduced min^{-1} assuming the extinction coefficient for ferricyanide was 150 $M^{-1}cm^{-1}$ and 1 mol succinate reduced 2 mol $K_3Fe(CN)_6$.

2.16 Expression, sonication and membrane extraction

15 *l* of fresh transformants of BL21(DE3)p*LysS* were grown in a 50 *l* aerated fermenter containing LB broth supplemented with 150 µg/ml of carbenicillin, 15

μg/ml ferric citrate and 15 μM sodium sulphide, from 5 ml (500 ml) overnights. They were incubated at 25°C in shaking water baths until A_{600} reached 0.6 whereby cells were induced by adding to 1 mM IPTG and 0.2 mM PMSF. Three to four hours after induction, cells were harvested by centrifugation and resuspended in 10 mM Tris pH 8.0, 5 mM EDTA, 10% (v/v) glycerol, 1 mM DTT, 1 mM PMSF. Cells were homogenised and lysozyme was added to a final concentration of 30 μg/ml and incubated at 37°C for 30 min. Lysed cells were then sonicated for four bursts of 30 s at power 8 with 1 min gaps between, cooled by an ice-salt-ethanol mixture. The thick opaque mixtures became translucent and fluid and a quick centrifugation was done to remove unbroken cells. High speed centrifugation at 40 000 rpm, 1.5 h at 4°C (Beckman with TL-100 rotor) pelleted the membranes, separating them from the soluble cytoplasmic fraction (supernantant). Membrane proteins were then solubilized for 1 h at 4°C in solubilization buffer (10 mM NaCl, 20 mM Tris HCl pH 7.5, 5 mM EDTA, 10 mM NaCl, 10% (v/v) glycerol, 1 mM PMSF, 1 mM DTT, 1.0% (v/v) Triton X-100). The mixture was then centrifuged at 100 000 rpm for 1 h at 4°C. The detergent-containing supernatant is the membrane fraction while the pellet contains membrane debris and outer membrane components. Fractions were then run on 10% (w/v) native PAGE gels and 10% (w/v) SDS-PAGE gels to view the distribution of proteins in the various cell fractions.

First column

Ion exchange chromatography

2.17 DEAE sepharose CL-6B chromatography (Pharmacia)

Membrane preparations were loaded onto a DEAE sepharose fast flow column in a 21 cm x 2.5 cm bed volume, equilibrated with 50 mM Tris-HCl, pH 8.0, 5 mM EDTA, 10% (v/v) glycerol, 0.1 mM PMSF, 1 mM DTT and 0.1% (w/v) Triton-X-100. Elution of proteins at 80 ml/h from the DEAE sepharose column was employed with the creation of 4 bed volumes of an increasing linear gradient from 0 to 0.5 M NaCl.

Second columns

Hydrophobic interaction chromatography

2.18 Phenyl sepharose chromatography (Pharmacia)

Pooled DEAE sepharose fractions were injected into a 10 cm x 1.6 cm (20 ml bed volume) phenyl sepharose column with a flow rate of 30 ml/h. The column was equilibrated with 50 mM Tris-HCl, pH 7.5, 5 mM EDTA and 0.1% (v/v) Tween 80. For this hydrophobic interaction chromatography, 4 bed volumes of an increasing linear gradient of 0 to 1% (w/v) Triton X-100 was used.

Pooled DEAE sepharose fractions were again run through the phenyl sepharose column, eluting from 2 M NaCl (to promote binding to hydrophobic column) to 0 M NaCl in 0.1% (v/v) Tween 80, 50 mM Tris-HCl, pH 7.5, 5 mM EDTA buffer and subsequently eluted with an increasing Triton X-100 gradient from 0- 1% (v/v).

2.19 Mono Q chromatography (Pharmacia)

Mono Q HR 5/5 was provided as a pre-packed FPLC column. Chromatography was carried out at a flow rate of 60 ml/h equilibrated with 20 mM Tris-HCl, pH 8.0, 0.1% Triton X-100 and eluted with an increasing gradient of 5 bed volumes of 0 to 1 M NaCl.

2.20 Hydroxyapatite chromatography (Pharmacia)

Pooled fractions from the DEAE sepharose column was put through a 15 cm x 2.5 cm hydroxyapatite column equilibrated with 10 mM potassium phosphate buffer, pH 6.5, 100 mM NaCl, 10% (w/v) ethylene glycol, 1% (w/v) Triton X-100, 3 mM sodium azide. After a wash to remove unbound proteins with the equilibration buffer, a 1.0 M NaCl wash was incorporated to elute neutral but not acidic proteins. Elution was accomplished with a phosphate gradient increasing from 0.02 M to 0.5 M at 50 ml/h.

Final columns

2.21 Octyl sepharose chromatography (Pharmacia)

A 30 ml bed volume column was run at 30 ml/hr in a 50 mM Tris-HCl pH 7.5, 5 mM EDTA, 0.1% Tween 80 buffer. It was loaded with pooled hydroxyapatite fractions. Two 4X Vt gradients were employed in combination, a decreasing NaCl gradient from 3 M to 0 M and an increasing detergent gradient from 0 to 2% (v/v) Triton X-100.

2.22 Dye Affinity chromatography

Mimetic Blue-2 (0100-0025) and Mimetic Green-1 (0080-0025) (Affinity Chromatography Ltd)

A MIMETIC screening kit (PIKSI) was used to test the suitability of mimetic triazine dyes for chromatography. Hydroxypatite fractions were loaded onto the twelve 1 ml test columns pre-equilibrated with 20 mM potassium phosphate, pH 6.5. The test columns were washed with 1 ml equilibration buffer after loading and eluted with 5 ml phosphate buffer with 1 M NaCl. The Mimetic Blue-2 and Mimetic Green-1 affinity columns gave the best results and demonstrated good binding and elution of NqrF. These were hence scaled up to 12.5cm x 1.6 cm (25 ml) dye columns which were equilibrated with (or pH 8.0), 10% glycerol, 0.1% (w/v) CHAPS (0.1% (v/v)

Triton X-100 or 0.1% (w/v) laurylsulphobetaine), washed with start buffer and finally eluted with 4 bed volumes of 0 to1.0 M NaCl at 25 ml/h.

2.23 1-step purification

His.Trap chelating column, 1 ml (Pharmacia)

Buffers

Start buffer: 10 mM imidazole, 20 mM PO_4, 0.5 M NaCl, pH 8.0, 0.05% (w/v) CHAPS

Elute buffer: 500 mM imidazole, 20 mM PO_4, 0.5M NaCl, pH 8.0, 0.05% (w/v) CHAPS

10 ml of freshly-made 1 M imidazole was filter-sterilized.

Column preparation

1. The top cap was removed and a drop of distilled water applied to top to avoid bubbles. After connecting a luer adaptor or tubing from pump to top of column, another drop of distilled water was applied. The twist-off end below was then removed.

Using a syringe:

2. the column was washed with 5 column volumes of distilled water
3. 0.1 M nickel sulphate solution was loaded onto the column (0.5 ml/ 1 ml column)
4. the column was washed with 5 column volumes of distilled water.

Basic purification protocol

- Flow rate was kept at 1-4 ml/ min or 2 drops/ s
- Blanks were run to determine background
- Sample were centrifuged or filtered if particles were present or it was cloudy
- It was ensured that the pH of sample was equal that of buffer
- No chelating agents (EDTA, EGTA) or reducing agents (DTE, DTT) were used in purification.

Using a syringe:

1. The column was equilibrated with 5 column volumes of start buffer, 4 ml/min maximum, at 4°C
2. Sample was applied using pump or syringe, 2 ml/min max. and stood at 4°C for 30 min to improve binding
3. 10 column volumes of start buffer were used to wash through the column or until no material emerged from the effluent at 4 ml/min maximum
4. Elution proceeded with 1-3 column volumes of elution buffer using a step or linear gradient, 2 ml/min maximum; lower flow rates were used to give higher resolution
5. The eluate was collected
6. Purification was checked by running samples on SDS-PAGE
7. Re-equilibration was then carried out using 5 column volumes of start buffer if using same metal ion.\
8. If another metal ion was desired, the column was first stripped of existing metal ion by washing with 5 column volumes of start buffer with 0.05 M EDTA, then washed with 5 column volumes of distilled water and recharged with the new ion.

2.24 Gel permeation chromatography

Sephadex desalting column (Pharmacia)

Samples from the dye columns were pre-incubated with 1 mM FAD for 1 hour at 4°C and were put through a 30 ml bed volume desalting column which was equilibrated with 20 mM Tris-HCl, pH 7.5, 0.1% laurylsulphobetaine, 0.1 M NaCl. The same buffer was used to wash proteins out at 60 ml/h after samples were loaded. This column was also used to remove excess FAD from reconstituted samples of NqrF.

2.25 Isoelectric focussing (Moredun Research Institute)

Pooled hydroxyapatite fractions were focussed across a liquid pH gradient in a MinipHor isoelectric focussing cell (Anachem). 21 ml of dialysed hydroxyapaptite fractions with NADH dehydrogenase activity were mixed with 1% ampholytes (pH 4-5, pH 5-6 (Anachem)), 10% (v/v) glycerol and 0.1% (v/v) Triton X-100 in a 32 ml final volume, and loaded into the MinipHor focussing cell as described by the manufacturer. The apparatus was run with cooling at 1000 V, 40 W, 200 mA until readings stabilized (approximately 35 min), then for a further 20 min and finally for 10 min at 500 V. Twenty fractions were collected spanning the pH gradient, and the pH of each fraction was measured using a tapered pH electrode. The fractions were then analyzed by SDS-PAGE, native PAGE and NADH menadione oxidase assays.

2.26 Protein determination

Protein determination was done using a modified Lowry method (Peterson *et al.*, 1977). Samples to be assayed were diluted in distilled H_2O to give a protein concentration of approximately 50-200 µg/ml in a final volume of 200 µl. Samples were mixed with 50 µl of 0.15% (w/v) Deoxycholate and incubated at room temperature for 10 min. An aliquot of 50 µl of 72% (w/v) TCA was then added before the samples were mixed and centrifuged for 15 min at 12 000 g in a Sorvall Micro spin 12 microfuge. The supernatant was removed and the pellet resuspended in 200 µl of distilled H_2O. Samples containing 50, 100, 150 and 200 µg/ml of BSA in a final volume of 200 µl, were also prepared to establish a standard curve. Next, 600 µl of a freshly prepared solution containing 2% (w/v) Na_2CO_3, 1% (w/v) SDS, 0.16% (w/v) sodium tartrate, 0.4% (w/v) NaOH and 0.04% (w/v) $CuSO_4$ was added to each sample and mixed thoroughly. Samples were incubated at room temperature for 45 min. The A_{660} of the samples were measured and the protein concentrations were determined from the BSA standard curve plot of A_{660} vs µg/ml protein. All samples were assayed at least twice and an average value used.

2.27 NADH/dNADH menadione oxidase assays

Samples were pre-incubated at room temperature with 20 mM KCN for 10 min. These were then added to a 1 ml fresh assay mixture containing 20 mM Tris-HCl pH 7.5, 0.2 mM NADH, 0.4 M NaCl. Decrease in absorbance of the NADH or dNADH at 340nm was measured immediately after the addition of 100 μM menadione.

Activity was calculated using Beers law:

$AU = \varepsilon.c.x$

where AU is the absorbance, c is the concentration in M, x is the pathlength of the cuvette in cm (usually 1 cm), and for NADH at 340 nm, $\varepsilon = 6\ 220\ M^{-1}cm^{-1}$.

Therefore,

Rate in μmole NADH/min/mg (U) = (Rate in change in absorbance units/min) x (1000/6220) x 1 x (1000/ μl of sample used in assay) x (1/concentration of sample in mg/ml)

All samples were assayed at least twice and an average value obtained.

2.28 Zymogram stain

NADH or dNADH oxidase activity was visualised in native gels using a zymogram stain. In the presence of NADH or dNADH, the NADH-ubiquinone oxidoreductase can reduce dinitrotetrazolium blue from yellow to a deep blue/purple colour. After electrophoresis, gels were incubated in 20 ml of a solution containing 50 mM Tris-HCl pH 7.5, 0.4 M NaCl, 6 mg NADH or dNADH and 7 mg dinitrotetrazolium blue at 30°C. When colour had developed sufficiently, the gel was then transferred to 0.5% (v/v) acetic acid to prevent further reaction.

2.29 Polyacrylamide gel electrophoresis

The Bio-Rad Mini-Protean II Dual Slab Cell was used to run mini-gels for SDS or native PAGE. The gel plates were assembled, filled with gel solution and run according to manufacturer's instructions. For the viewing Nqr proteins, 10% (w/v) gels were most appropriate as they gave good resolution bands between the range of 16 to 68 kDa. Reagents and gel preparation were made according to the Laemmli buffer system (Laemmli, 1970). A discontinuous buffer system was employed. The buffers and reagents used are detailed as below.

Preparation of polyacrylamide gels

Resolving gel (10% (w/v))

Distilled water	4.0 ml
1.5 M Tris-HCl, pH 8.8	2.5 ml
10% (w/v) SDS stock (stored at room temp.) or 10% (v/v) Triton X-100	100 µl
Protogel 30% (w/v) acrylamide/bisacrylamide stock	3.33 ml
10% (w/v) fresh ammonium persulfate	50 µl
TEMED	5 µl

Total volume of 10 ml, sufficient for pouring 2 mini resolving gels.

Stacking gel (4.0% (w/v))

Distilled water	3.05 ml
0.5 M Tris-HCl, pH 6.8	1.25 ml
10% (w/v) SDS stock (stored at room temp.) or 10% (v/v) Triton X-100	50 µl
Protogel 30% (w/v) acrylamide/bisacrylamide stock	0.65 ml
10% (w/v) fresh ammonium persulfate	31.25 µl
TEMED	6.25 µl

Total volume of 5 ml, sufficient for pouring 2 mini stacking gels.

SDS/Triton X-100/native sample buffer

(0.125 M Tris-HCl, pH 6.8, 2% (w/v) SDS (Sigma), 10% (w/v) glycerol (Fisons), 10% (w/v) β–mercaptoethanol, 0.01% (w/v) bromophenol blue)

Distilled H_2O	4.0 ml
0.5 M Tris-HCl, pH 6.8	1.0 ml
Glycerol	0.8 ml
10% (w/v) SDS or 10% (v/v) Triton X-100 or just distilled water	1.6 ml
2-β-mercaptoethanol	0.4 ml
0.05% (w/v) bromophenol blue	0.2 ml

5X Electrode (Running) buffer, pH 8.3

(0.025 M Tris base (BioRad), 0.19 M glycine (BioRad), 0.1% (w/v) SDS or Triton X-100)

Tris base	9 g
Glycine	43.2 g
SDS (or Triton X-100)	3 g (3 ml)

Make up to 600 ml with dH_2O and store at 4°C. Sufficient for eight runs.

Sample preparation and electrophoresis

Samples were diluted 1:1 with sample buffer and SDS samples were boiled at 100°C for 5 min before loading on gel. The reservoir tank was filled with 350 ml of 1X running buffer and gels were run at 200 V for 45 min at room temperature.

2.30 Method for silver staining of protein

A. Solutions The following solutions were prepared freshly for each gel using 'Analar' quality chemicals

a) Fixative A: 40% (v/v) methanol, 10% (v/v) acetic acid in distilled water.

b) Fixative B: 10% (v/v) ethanol, 5% (v/v) acetic acid in distilled water.

c) Oxidizer: potassium dichromate, 0.1 g in 100 ml distilled water containing 0.020 ml concentrated nitric acid.

d) Silver reagent: silver nitrate, 0.2 g in 100 ml distilled water.

e) Developer: sodium carbonate, 9 g in 300 ml distilled water containing 0.15 ml formaldehyde.

f) Stop: 0.5% (v/v) acetic acid in distilled water.

B. Protocol Reagents were added in the order given below.

Reagent	Volume (ml)	Incubation time
1. Fixative A	200	30 min/overnight
2. Fixative B	200	15 min
3. Fixative B	200	15 min
4. Oxidizer	100	5 min
5. Distilled water	200	5 min
6. Distilled water	200	5 min
7. Distilled water	200	5 min
8. Silver reagent	100	20 min
9. Distilled water	200	1 min
10. Developer	100	30 s
11. Developer	100	30 s
12. Developer	100	until developed
13. Stop	200	for storage

2.31 Coomassie brilliant blue staining

SDS polyacrylamide gels were stained 1/2 hour with 0.1% (w/v) Coomassie brilliant blue R-250 in fixative (40% (w/v) methanol, 10% (w/v) acetic acid) and destained with 40% (w/v) methanol, 10% (w/v) acetic acid to remove background (usually 1 to 3 h).

N.B. Coomassie brilliant blue solution must be filtered before use but may be re-used for staining many times.

2.32 PAGE and Electro-blotting for *N*-terminal Sequencing

PAGE

All reagents used must be as high a grade and as fresh as possible. Recommended acrylamide is BDH Electran molecular biology grade. The gel system is the usual Laemmli system with modifications as follows.

1. The stacking gel was poured with 0.375 M Tris-HCl, pH 8.8 resolving gel buffer. The entire gel was pre-run using stacking gel buffer (0.125 M Tris-HCl, pH 6.8, 0.1% (w/v) SDS) containing 50 μM glutathione until the bromophenol blue reached the gel interface. This allowed the glutathione to get into the gel and restore buffer ion concentration required for stacking.

2. This buffer was decanted and replaced with normal running gel buffer containing 70 μl of 100 mM sodium thioglycolate per 70 ml buffer (0.1 mM thioglycolate).

3. Samples were loaded and run as usual.

Blotting

Blotting onto ProBlott membrane (PDVF membrane) using CAPS buffer according to ABI instructions.

Solutions were prepared as follows:

a) 10X CAPS (100 mM, pH 11.0): dissolve 22.13 g CAPS in 900 ml deionized water. Titrate with 2N NaOH (about 20 ml) to pH 11.0 amd add deionized water to 1 ℓ. Store at 4°C.

b) Electroblotting buffer (1X in 10% (v/v) methanol): prepare 2 ℓ by mixing 200 ml 10X CAPS with 200 ml methanol and 1600 ml water.

At the end of the electrophoretic run, SDS gels were removed from the kit and thoroughly washed in dH_2O for a few times before soaking in electroblotting buffer (10 mM CAPS, pH 11.0, 10% (v/v) methanol) for 5 min.

PDVF membranes were cut to the exact size of the SDS gel and wet in 100% methanol for a few seconds and equilibrated in blotting buffer. Six Whatman No. 1 filter papers cut to the exact size of the gels were also soaked in blotting buffer. PDVF membrane with a mark on its lower left corner was placed over the gel in the correct orientation carefully, avoiding air bubbles. This was then sandwiched with three Whatman papers on each side, again avoiding air bubbles. This transblotting sandwich was then assembled in the Bio-Rad transblotting kit with the PDVF membrane facing the anode end and run at constant voltage of 10 - 12 V, 40 mA for 16 h at 4°C.

The PDVF membrane was removed from the sandwich, rinsed well with dH_2O and saturated with 100% methanol for a few seconds. It was stained with freshly prepared 0.1% (w/v) Coomassie brilliant blue R-250 in 40% (v/v) methanol, 10% (v/v) acetic acid for a maximum of 1 minute before destaining with 50% (v/v) methanol. The blot was finally rinsed extensively with dH_2O and bands of interest were excised and stored at -20°C.

2.33 Concentration with Centriplus concentrators (Amicon)

The pooled fractions from the final column were concentrated by a step gradient elution with 0.5 M NaCl from the DEAE sepharose column (optional) and then spun in an Amicon Centriplus concentrator 30 at 3 000 g, 75 min, 4°C. Samples were collected with a 4 min reversed spin at 2000 x g, 4°C.

2.34 Stability of NqrF under different conditions

Further experimentation was done to determine the stability of NqrF at different pH and storage temperatures in order to optimise recovery and preservation of catalytic activity. Crude membrane extracts were incubated overnight at various temperatures, at different pHs, and the effects on NqrF activity by the inclusion of sodium azide, PMSF, EDTA, glycerol, dithiothreitol, ferric citrate, sodium sulphide, FAD, and its solubility in detergents such as Triton X-100, Tween 80 and laurylsulphobetaine, were examined. All samples were measured for activity using the NADH menadione oxidase assay. The experiment was repeated thrice for each sample and the average value calculated.

2.35 Metallic cation inhibition

NqrF was incubated with 0.5, 1.0, 2.5, 5.0, 10.0 μM of Ag^{+}, Cu^{2+}, Cd^{2+}, Pb^{2+} and Zn^{2+} for 1 min at room temperature before NADH-menadione oxidase assays were used to determine the loss in activity compared with a control. Reversibility of inhibition was measured by adding 5 mM EDTA to the standard assay solution and incubating at room temperature for 5 min. The experiment was repeated thrice and the average value determined.

2.36 Cysteinyl inhibitors

Iodoacetic acid and *N*-ethylmaleimide were pre-incubated with NqrF in assay solution at concentrations of 1 μM, 10 μM, 100 μM and 500 μM, left at room temperature for 1 min before 100 μM menadione was added to start the reaction.

2.37 Inhibition by classical NADPH oxidoreductase and nitroreductase inhibitors

Dicoumarol, 4-nitrobezoic acid, nitrofurantoin and nitrofurazone were pre-incubated at various concentrations with NqrF to determine if they inhibit it. NADH menadione oxidase assays were used to calculate the activity of the samples. The experiment was repeated thrice for each sample and an average value calculated.

2.38 Substrate specificity

The affinity of NqrF for its substrate NADH and its analogue dNADH were measured by NADH/ dNADH menadione oxidase assays using several concentrations of NADH and dNADH, and K_m and V_{max} values were obtained. Electron acceptors such as menadione, ferricyanide and cytochrome *c* were also tested for their K_m and V_{max} values. The experiment was repeated thrice for each sample and an average value obtained.

2.39 Sodium ion dependence

Sodium ion dependence of the catalytic activity of NqrF was measured using 0.1, 0.2, 0.3 and 0.4 M NaCl in the standard assay solutions for NADH-menadione oxidase assays. The experiment was repeated thrice for each sample and an average value was calculated.

2.40 Absorbance spectrum of NqrF

A sample of oxidized NqrF was analysed for absorbance through wavelengths 190-600 nm using a Pye Unicam 8800 UV/visible stop-flow spectrophotometer. This sample was then partially reduced anaerobically by 1 mM NADH and the spectrum

recorded. Finally the sample was incubated with excess NADH for 20 min at room temperature before its spectrum was recorded

2.41 Flavin determination

The flavin in NqrF was identified by ascending paper chromatography on Whatman filter paper no. 1 using s-butanol/90% (v/v) formic acid/ H_2O (14:3:3 by vol.) as the solvent. Commercial preparations of FAD and FMN were used as standards. The experiment was repeated thrice for each sample and the average value used.

Chapter 3

Results and Discussion

Cloning and sequencing the *nqr* operon

3.1 Initial work on Na^+-NQR of *V. alginolyticus* (B. Ward and P. Beattie)

The NADH-ubiquinone reductase of *V. alginolyticus* was partially purified at Glynn Institute before a sample was sent to the ICMB in Edinburgh where further work was carried out (Beattie *et al.*, 1994). Four subunits were identified on PAGE gels: A- 55 kD, B- 50 kD, C1- 33 kD and C2- 30 kD and blotted onto PVDF membranes. The first 20 amino acids of the A and C subunits (the B subunit was N-terminally blocked) were determined using Edman degradation of protein extracted from SDS-PAGE gels. Low degeneracy oligonucleotide probes were designed, end-labelled with ^{32}P and used to isolate clones from an *Eco*RI library of wild type *V. alginolyticus* DNA in vector λNM1149 (refer to table 3.1) by plaque hybridization at low stringency. This library was prepared by growing *V. alginolyticus* and extracting chromosomal DNA, which was subsequently digested by *Eco*RI and ligated to *Eco*RI digested vector λNM1149 before being packaged into λ phage. The *E. coli* NM494 cells were infected with the phage and plated to give plaques. Plate lifts, using Hybond filters, were probed with the degenerate oligonucleotides. Positives plaques that hybridised to probes were purified, plated and reprobed. DNA was restricted by enzymes, run on gels and Southern blotted. A 10.7 kb insert which hybridised strongly to probe 1 (*nqr*A) was mapped using a series of restriction enzymes and 5 *Hin*dIII fragments of approximate sizes 2.85, 2.65, 2.0, 1.65 and 1.0 kb (Figure 3.1) obtained from the insert were subcloned. A 2.0 kb (actual size 1.9 kb) *Hin*dIII fragment from the *Hin*dIII digestion of this 10.7 kb insert was found to strongly hybridise with probe 1 (Figure 3.2) and therefore subcloned into the sequencing vector pTZ19R (Figure 2.2). DNA sequencing revealed that the first 250 bp of this 1.9 kb insert DNA were of λ origin, hence showing that this fragment is on the LHS of the original 10.7 kb fragment.

Table 3.1. Degenerate oligonucleotide probes designed from the *N*-terminal sequences of Nqr subunits.

Probe no.	Subunit	Amino acid sequence	Oligonucleotide sequence	No.
1	A	MITIKKG	ATGAT(CT)AC(ACGT)AT(CT)AA(AG)AA(AG)GG	64
2	C1	QKEETK	CA(AG)AA(AG)GA(AG)AC(AGCT)AA	32
3	C1	PQAEQV	CC(AGT)CA(AG)GC(AGT)GA(AG)CA(AG)GT	72
5B	C2	NNDSIG	AA(CT)AA(CT)GA(CT)AG(CT)AT(ACT)GGG	48

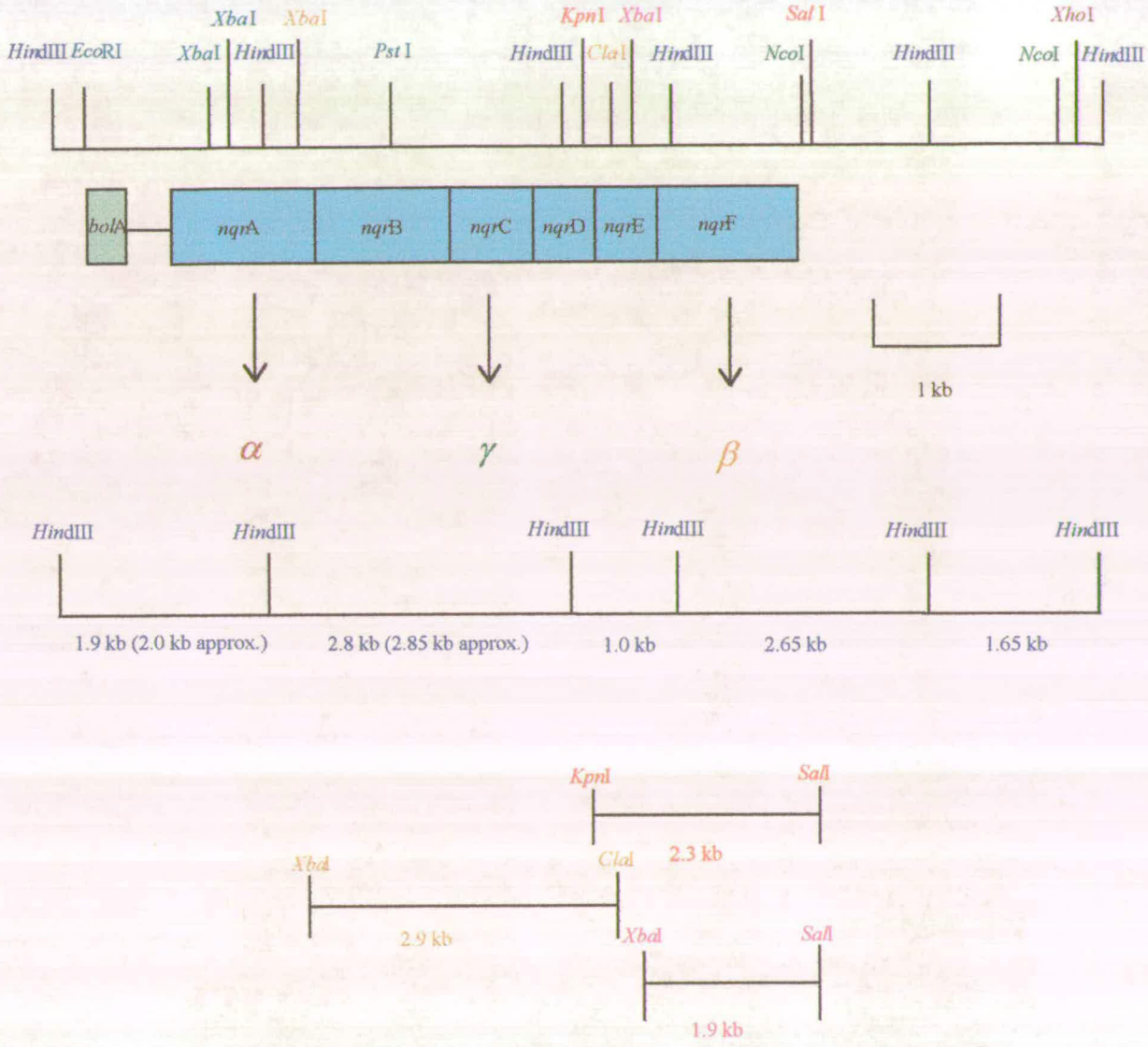

Figure 3.1 Restriction and gene map of *nqr* operon in *Vibrio alginolyticus*. Sizes of various important cloned fragments are also shown. NqrA corresponds to α subunit, NqrC to γ and NqrF to β.

Fig. 3.2 Identification of the *nqr*A gene on the 2.0 kb *Hin*dIII fragment of λNM1149 containing a 10.7 kb *Eco*RI insert of *Vibrio alginlyticus* DNA.

Various DNA fragments on a southern blot of the λNM1149 containing the 10.7 kb *Eco*RI *Vibrio* insert digested with various restriction enzymes, hybridised to probe 1. Probe 1 was derived from *N*-terminal sequence of *nqr*A. In particular, probe 1 was noted to hybridise to a 2.0 kb *Hin*dIII fragment, which was determined to contain at least the *N*-terminal sequence of *nqr*A.

(A) RESTRICTION OF DNA

(B) SOUTHERN HYBRIDISATION WITH PROBE 1

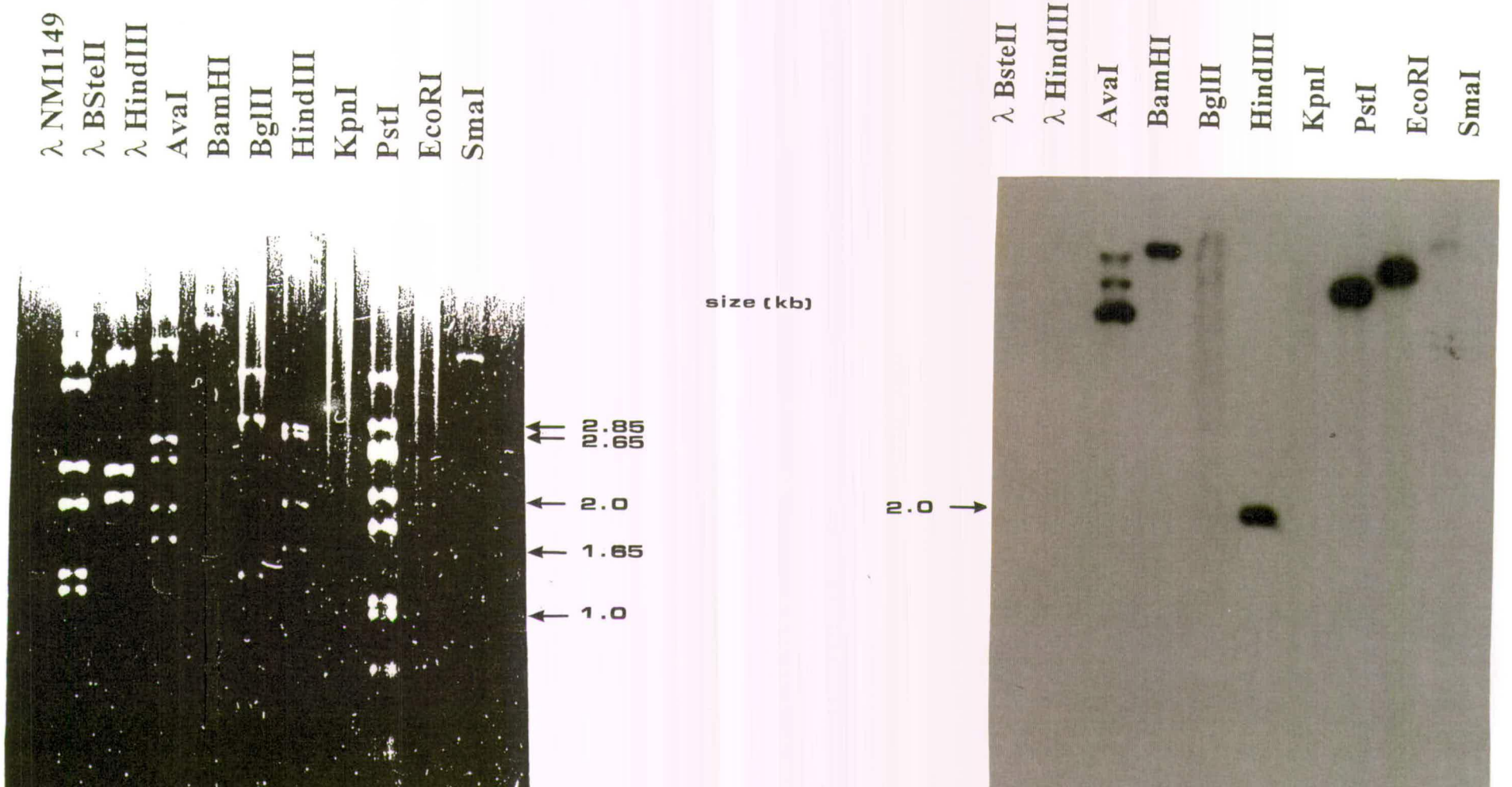

3.2 Cloning and sequencing

Analysis of the 10.7 kb clone revealed that it contained the *nqr*C gene as there was also good hybridisation with probe 5B (Table 3.1). This clone was then digested with different restriction enzymes and re-probed with probe 5B to locate *nqr*C. The *nqr*C gene was found on a 3.1 kb *Xba*I fragment from the 10.7 kb clone and a 2.2 kb *Xba*I/*Pst*I fragment from the same clone. This 3.1 kb fragment overlaps the 2.7 kb *Hin*dIII fragment (Fig. 3.1). Further mapping with probe 5 and 6 revealed that *nqr*C was close to *nqr*A. Probes 2 and 3 were designed from *N*-terminal sequence from weak bands obtained on SDS gel electrophoresis of partially purified Na^+-NQR complex and did not show significant hybridization to the 10.7 kb clone as they were likely to be contaminants.

The *nqr*A open reading frame extends for 843 bp to the end of the 1.9 kb *Hin*dIII fragment and comprised 63% of the *nqr*A gene. Further sequencing of the adjacent 2.8 kb (2.85 kb approx. size from gel) *Hin*dIII fragment, the overlapping 0.6 kb *Xba*I and the 0.9 kb *Xba*I/*Pst*I fragments, produced the remaining sequence of the 495 bp C-terminal portion (Fig. 3.1). Upstream of the *nqr*A gene, an ORF coding for a polypeptide of 102 amino acid residues was identified, which showed 71% identity with the *bol*A gene of *E. coli*.

Hybridisation experiments with probe 5B to detect the gene for the *nqr*C (γ2) subunit showed that this gene was located on a 3.1 kb *Xba*I fragment subcloned from the original 10.7 kb *Eco*RI clone. This fragment contained a unique *Pst*I site which divided the fragment into a 2.2 kb and an 0.9 kb fragment. Probe 5B reacted with the 2.2 kb fragment. Thus the *nqr*C gene was shown to map to the same region of the chromosome as the *nqr*A gene and on sequencing, an open reading frame about 768 bp was detected. It was in the same orientation as the *nqr*A gene and 1.3 kb downstream from the end of the *nqr*A gene (Fig. 3.1).

More open reading frames were detected on further sequencing of the region between *nqr*A and *nqr*C and the region immediately downstream of *nqr*C. The *nqr*B gene is located immediately downstream of *nqr*A and upstream of *nqr*C and extends

1278 bp from the 0.9 kb *Xba*I/*Pst*I fragment into the 2.2 kb *Pst*I/*Xba*I fragment. Downstream of *nqr*C, an open reading frame of 630 bp was found and this was termed *nqr*D (Beattie *et al.*, 1994).

The third 1.0 kb *Hin*dIII fragment, which follows the 2.8 kb *Hin*dIII fragment, was sequenced and produced the fifth open reading frame which was named *nqr*E. 0.3 kb *Cla*I and 0.24 kb *Cla*I/*Xba*I subclones obtained from this 1.0 kb *Hin*dIII fragment were sequenced. Subsequently, 2.3 kb *Kpn*I/*Sal*I and 1.9 kb *Xba*I/*Sal*I subclones were constructed to sequence across the *Hin*dIII region to determine the orientation of the fourth *Hin*dIII fragment (2.65 kb) and for expression of the *nqr*F gene, the last open reading frame of the *nqr* operon (Fig. 3.1). This fourth *Hin*dIII fragment was further subdivided into a 1.4 kb *Hin*dIII/*Sal*I clone and a 1.2 kb *Sal*I/*Hin*dIII clone for sequencing. The 1.4 kb *Hin*dIII/*Sal*I DNA contained most of the *nqr*F gene and terminator sequences at the end of the operon. A 2.3 kb *Nco*I fragment was cloned to sequence across the *Hin*dIII region between the fourth and fifth *Hin*dIII fragments and determine their orientations. To acquire the remaining sequence after the last *Hin*dIII site, an 0.8 kb *Xho*I/*Eco*RI fragment was cloned from the 10.7 kb λ clone for sequencing; this would represent the last portion of sequence just before the RH arm of the λ clone. All DNA of the *nqr* operon was cloned into various sequencing vectors such as pTZ18R (Fig. 2.1), pTZ19R (Fig 2.2), pBluescript KS- (Fig. 2.3), pSL1180 (Fig. 2.4), pSL1190 (Fig. 2.5), and sequenced on both strands using universal and reverse primers, and specific primers designed from *nqr* sequence (Table 3.2), purchased from OSWEL.

Table 3.2. List of primers.

Primer number	Primer sequence 5'->3'	Location
β	CTCGTGCACCCAACTGA	40 nucleotides from 5' fusion junction of β-lactamase gene
UP	GTAAAACGACGGCCAGT	Universal primer
KS	CGAGGTCGACGGTATCG	KS- primer
RP	AACAGCTATGACCATG	Reverse primer
fp2	CATCGCCAAGTTCATCA	191-208 of operon map
fp3	GGGCATTGATGTGGCAC	403-419
fp4	TGCGTCCTACCATGCATG	923-940
fp7	TGTTCAACATGCCATGGC	3118-3135
fp8	CCTAACAGTGTGCGTATC	4356-4373
fp9	GACCTGATTCTACCGAA	573-589
fp10	TCCTACCATGCATGTCC	927-943
fp11	TAGCAGCTAAGCCTGAG	1283-1299
fp12	CGCTCACTAGTAATGGTG	4058-4075
fp13	GCTGGGTGTTGTTATCGGG	3420-3438
fp14	CATTTTGAGCCTGGTGGT	2190-2207
fp15	GCTTTTCTGTATGGTGCG	2588-2605
fp16	GGTTCTGGACAGTTACATA	7982-7964
fp17	CAAGGCAGATTTAATTTA	8576-8559
fp18	GTTGAATTGATATGGGGA	6788-6771
fp19	GCCATCAGCAGTCATCGT	7663-7648

fp20	GCCATGCCTTTGTCTTCACC	7708-7648
fp21	AAGCCAGTGTAACCATCCC	6485-6467
fp22	CATTGAGTATGCACGGA	6066-6050
fp23	CCCCTTCACGCGCTTCACC	5743-5725
rp	CAGGAAACAGCTATGAC	4452-4461
rp2	GCCAGAGAGTCAACCAACT	8079-8094
rp3	GGGTTCTTTTTATCTTCAA	998-980
rp4	CTGTTTCTAGTTTAGTTG	4278-4261
rp5	GGAATACGCGAGATTTAT	675-658
rp7	GGCATACATCATCGACC	3837-3821
rp8	AACCCGATAACAACACCC	3440-3423
rp9	GGCATGTTGAACATTGGG	3130-3113
rp10	GCCACCTTTTCTCTGCACC	369-351
rp11	CAGTTAGCCAGTAGTGCC	2469-2452
rp12	GTACTCGTACTTACCTGG	2100-2083
rp13	GGTGAAGCGCGTGAAGGGG	5725-5743
rp14	TTTTCTCTCGCGCTCAAC	9342-9325
rp15	ACTCAATGGCTAACTAC	6059-6075
rp16	AAGAGCTAGCGGCACGAA	7216-7233
rp17	TACAGATGAAGAGCTAGCGG	7208-7227
rp18	GCTCACACATCTTCGACC	6290-6307
rp19	CCACCTATGATGAATGCG	6562-6579
rp24	TATGTAACTGTCCAGAACC	7964-7982

DNA was sequenced at least 4 times on each strand to give a good consensus. The *nqr* operon sequence has the EMBL nucleotide sequence database assession numbers Z37111 and D49364.

Results from Hayashi *et al.* (1995) concur with our sequence data that the *nqr* operon consists of 6 genes coding for 6 subunits, comprising of the 3 previously identified subunits α (NqrA), β (NqrB) and γ (NqrC) together with 3 further highly hydrophobic subunits, δ (NqrD), ε (NqrE) and ϕ (NqrF) (Beattie *et al.*, 1994, Hayashi *et al.*, 1995). The *nqr* operon is 5.7 kb in size. It initiates in the middle of the first *Hin*dIII fragment and terminates before *Sal*I site on the fourth *Hin*dIII fragment on the 10.7 kb λ clone.

DNA sequence data was computed via the University of Wisconsin Genetics Computer group, version 8.0 (gcg8) package and information was processed and analysed using various programmes in the package. Sequence analysis, database comparisons, translation, mapping of restriction sites, hydropathy plots etc., were achieved using these programs. Table 3.3 compiles the primary amino acid sequence data of the *nqr* operon. For the complete nucleotide sequence, please refer to attached publication at the back of the thesis (Beattie *et al*, 1994).

Table 3.3. Protein sequence encoded by *nqr* genes.

Subunit	Protein sequence
NqrA 446 aa 52 kDa	MITIKKGLDL PIAGTPSQVI NDGKTIKKVA LLGEEYVGMR PTMHVRVGDE VKKAQVLFED KKNPGVKFTA PAAGKVIEVN RGAKRVLQSV VIEVAGEEQV TFDKFEAAQL SGLDREVIKT QLVDSGLWTA LRTRPFSKVP AIESSTKAIF VTAMDINPLA AKPELIINEQ QEAFIAGLDI LSALTEGKVY VCKSGTSLPR SSQSNVEEHV FDGPHPAGLA GTHMHFLYPV NAENVAWSIN YQDVIAFGKL FLTGELYTDR VVSLAGPVVN NPRLVRTVIG ASLDDLTDNE LMPGEVRVIS GSVLTGTHAT GPHAYLGRYH QQVSVLREGR EKELFGWAMP GKNKFSVTRS FLGHVFKGQL FNMTTTTNGS DRSMVPIGNY ERVMPLDMEP TLLLRDLCAG DTDSAQALGA LELDEEDLAL CTFVCPGKYE YGTLLRECLD TIEKEG*
NqrB 426 aa 50 kDa	MPRYYREGRV IFMALKKFLE DIEHHFEPGG KHEKWFALYE AVATVFYTPG IVTNKSSHVR DSVDLKRIMI MVWFAVFPAM FWGMYNAGGQ AIAALNHMYA GDQLATVISG NWHYWLTEML GGTIAADAGV GSKMLLGATY FLPIYATVFL VGGFWEVLFC MVRKHEVNEG FFVTSILFAL IVPPTLPLWQ AALGITFGVV VAKEIFGGTG RNFLNPALAG RAFLFFAYPA QISGDVVWTA VDGFSGATAL SQWAQGGNGA LVNTVTGSPI TWMDAFIGNI PGSIGEVSTL ALMIGAAMIV YMRIASGRII AGVMIGMIAV STLFNVIGSD TNPMFNMPWH WHLVLGGFAF GMFFMATDPV SASFTNKGKW WYGILIGAMC VMIRVVNPAY PEGMMLAILF ANLFAPLFDH VVIEKNIKRR LARYGK*
NqrC 256 aa 32 kDa	MASNNDSIKK TLGVVIGLSL VCSIIVSTAA VGLRDKQKAN AVLDKQSKIV EVAGIDANGK KVPELFAEYI EPRLVDLETG NFTEGNASTY DQREASKDAE RSIALTPEED VADIRRRANT AVVYLVKDQD EVQKVILPMH GKGLWSMMYA FVAVETDGNT VSAITYYEQG ETPGLGGEVE NPSRRDQFIG KKLYNEDHQP AIKVVKGGAP QGSEHGVDGL SGATLTSNGV QHTFDFWLGD KGFGPFLAKV RDGELN*
NqrD 210 aa 29 kDa	MSSAQNVKKS ILAPVLDNNP IALQVLGVCS ALAVTTKLET AFVMTLAVTF VTALSNFSVS LIRNHIPNSV RIIVQMAIIA SLVIVVDQVL KAYLYDISKQ LSVFVGLIIT NCIVMGRAEA FAMKSAPVPS LIDGIGNGLG YGFVLITVGF FRELFGSGKL FGLEVLPLVS NGGWYQPNGL MLLAPSAFFL IGFLIWVIRI LKPEQVEAKE*
NqrE 193 aa 28 kDa	MEHYISLLVK SISSKHALSF FLGMCTFLAV SKKVKTSFGL GVAVVVVLTI AVPVNNLVYN LVLRENALVE GVDLSFLNFI TFIGVIAALV QILDRFFPPL YNALGIFLPL ITVNCAIFGG VSFMVQRDYN FAESIVYGFG SGVGWMLAIV ALAGIREKMK YSDVPPGLRG LGITFITVGL MALGFMSFSG VQL*
NqrF 407 aa 46 kDa	MDIILGVVMF TLIVLALVLV ILFAKSKLVP TGDITISVND DPSLAIVTQP GGKLLSALAG AGVEVSSACG GGGSCGQCRV KVKSGGGDIL PTELDHITKG EAREGERLAC QVAMKTDMDI ELPEEIFGVK KWECTVISND NKATFIKELK LQIPDGESVP FRAGGYIQIE APAHHVKYAD YDIPEEYRED WEKFNLFRYE SKVNEETIRA YSMANYPLEA GIIMLNVRIA TPPPNNPDVP PGIMSSYIWS LKEGDKCTIS GPFGEFFAKD TDAEMVFVGG GAGMAPMRSH IFDQLKRLHS KRKMSFWYGA RSKREMFYVE DFDMLQAEND NFVWHCALSD PLPEDNWDGY TGFIHNVLYE NYLRDHEAPE DCEYYMCGPP MMNAAVIGML KDLGVEDENI LLDDFGG*

3.3 Sequence analysis

3.3.1 *Nqr* operon

It is postulated that *nqr*B, *nqr*D, *nqr*E and *nqr*F constitute part of an *nqr* cluster together with *nqr*A and *nqr*C, as there are no intergenic regions within *nqr*A to *nqr*F and there appears to be a likely promoter region upstream of *nqr*A. Moreover, just upstream and adjacent to the putative *nqr* promoter region is the gene which codes for a 102 amino acid polypeptide that has 70% similarity to *E. coli bol*A. *Bol*A is believed to be involved in cell division in *E. coli*. Downstream of this gene, is a region of dyad symmetry followed by a T-rich region that is characteristic of a rho-independent transcriptional regulator. This is preceded by an A-rich sequence upstream of the GC-rich motif that is complementary to the T-rich tail. Such A-rich sequences are thought to increase the efficiency of termination. The location of this *bol*A terminator region within ORF1, a short reading frame found just before *nqr*A, makes it likely that a putative gene product of ORF1 is not produced as a translational product. Strong termination sequences of a transcriptional stop signal, a poly dT tail and a further 293 bp of non coding DNA, follows the end of *nqr*F and the next adjacent ORF after *nqr*F, codes for a polypeptide with high homology to Na^+/H^+ antiporters but is distinct from the previously sequenced Na^+/H^+ antiporter of *V. alginolyticus* (Nakamura *et al.*, 1994a).

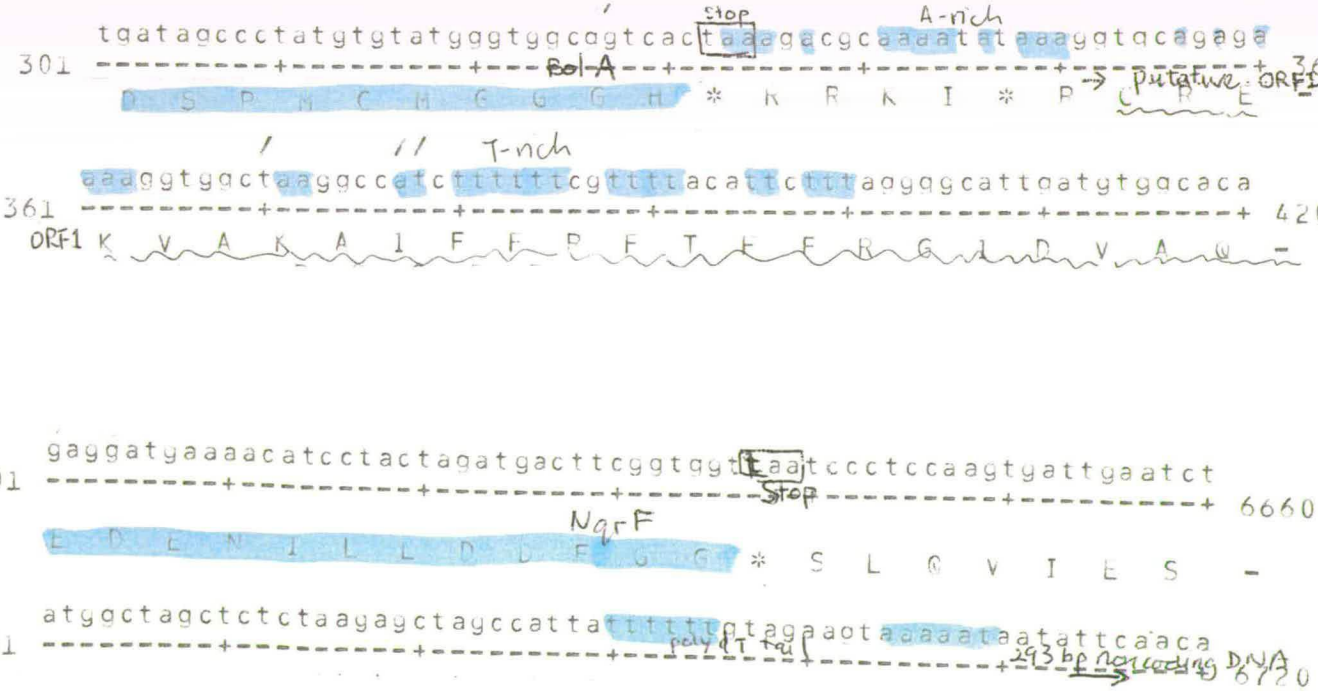

3.3.2 Presequence

The pre-sequence found just before *nqr*A was assessed to determine if it was a signal peptide, using von Heijne's (-3,-1) rule (von Heijne, 1986a). It did not meet the following basic requirements: 1) contain a small residue at position -1 (w.r.t. cleavage site); 2) the residue at position -3 must not be aromatic, or large and polar, and 3) there should be no proline residues from -3 through to +1.

This pre-sequence was about 32 amino acids long before the MITIKK... sequence of *nqr*A detected by Edman degradation previously. But the signal sequences of Gram-negative bacterial outer membrane proteins and periplasmic proteins are usually about 20-26 amino acids long (Oliver, 1985). It did not seem to possess a basic N-terminal region, a central hydrophobic region and a polar C-terminal region which are typical of a signal sequence.

Pre-sequence of NqrA:

MFKTTSKPDT DVVSKSYAIK RIFFPIKVVQ VR

3.3.3 Analysis of NqrA-NqrF

Sequence comparisons for Nqr A- NqrF using the MPsrch programme developed by J. Collins and S. Sturrock, Edinburgh University (http://www.dna.affrc.go.jp), with the SWISSPROT and Genpept database, showed high identity to the homologous Na^+-NQR found in *H. influenzae* and *E. coli* over a range of PAM values (40-350) (Table 3.4, 3.5 and 3.6). As the genomes of *H. influenzae* and *E. coli* have been recently sequenced, high homologies (80-90%) to the homologous Na^+-NQR counterparts in these bacteria have been found from database comparisons. With this method of sequence comparisons, PAM values of 250 were deemed suitable for NqrA-NqrE and Pam 180 was used for NqrF, with gap values of 7 for Pam 250 and gap values of 11 for Pam 180. In addition, significant similarities must have % Match values greater or equal to 30% to be meaningful. However, no significant homologies to subunits of Complex I were detected. NqrC has no obvious

similarity to related proteins other than to the homologous Na^+-NQR counterpart in the above mentioned bacteria (Tan *et al.*, 1996). A 48 kDa outer membrane protein in *Actinobacillus pleuropneumoniae* demonstrated 66% identity to NqrA. Interestingly, NqrB, NqrD and NqrE appear to have 25-38% similarities to regions of nitrogen fixing proteins RnfA- RnfF in *Rhodobacter capsulatus*. Note that many of the database sequences picked up in *V. alginolyticus, H. influenzae* and *E. coli* are duplicated many times, and were described as either hypothetical proteins, sequenced regions on a chromosome or certain homologues (i.e. a *H. influenzae* protein mistakenly described as a BolA homologue and another as a phenol hydroxylase homologue but are actually Nqr proteins). Detailed alignments of these comparisons of NqrA- NqrF to database sequences can be found in the appendix at the end of the thesis.

Table 3.4. Sequence homology of NqrA, NqrB, NqrC and NqrD polypeptides at PAM 250.

NqrA.

Statistics: Mean 68.447; Variance 700.150; scale 0.098

Pred. No. is the number of results predicted by chance to have a score greater than or equal to the score of the result being printed, and is derived by analysis of the total score distribution.

SUMMARIES

Result No.	Score	% Query Match	Length	DB	ID	Description	Pred. No.
1	2118	100.0	446	3	S51015(S510	NADH dehydrogenase (ub	2.48e-74
2	2118	100.0	446	6	VANQRBOL_2(	V;alginolyticus bolA,	2.48e-74
3	1550	73.2	449	6	APU24492_1(	Actinobacillus pleurop	5.52e-51
4	1550	73.2	449	1	APU24492_1	(U24492|gid:1185395)	5.52e-51
5	1534	72.4	447	6	HIU32702_4(	Haemophilus influenzae	2.49e-50
6	1534	72.4	447	1	HIU32702_4(	Haemophilus influenzae	2.49e-50
7	1166	55.1	358	2	HIU00070_69	Haemophilus influenzae	2.23e-35
8	1166	55.1	358	5	Y164_HAEIN	(P43955) HYPOTHETICAL	2.23e-35
9	320	15.1	73	5	Y165_HAEIN	(P43956) HYPOTHETICAL	1.35e-02
10	320	15.1	73	3	A64003(A640	hypothetical protein H	1.35e-02
11	241	11.4	65	1	HIU20229_1	(U20229|gid:644851) H	6.52e+00
12	241	11.4	65	6	HIU20229_1(	Haemophilus influenzae	6.52e+00
13	231	10.9	1263	5	RPOB_THEMA	(P29398) DNA-DIRECTED	1.38e+01
14	231	10.9	1263	6	TMRPO_3(X72	T;maritima ribosomal p	1.38e+01
15	231	10.9	1263	3	F44466(S414	DNA-directed RNA polym	1.38e+01
16	187	8.8	1232	5	TOP2_TRYCR	(P30190) DNA TOPOISOME	3.28e+02
17	187	8.8	1232	2	A48446(A484	DNA topoisomerase II -	3.28e+02
18	187	8.8	1232	7	TRBTOPOII_1	Trypanosoma cruzi DNA	3.28e+02
19	183	8.6	527	7	CEK08G2_5(Z	Caenorhabditis elegans	4.32e+02
20	183	8.6	527	1	CEK08G2_5(Z	Caenorhabditis elegans	4.32e+02

NqrB

Statistics: Mean 62.173; Variance 577.409; scale 0.108

Pred. No. is the number of results predicted by chance to have a score greater than or equal to the score of the result being printed, and is derived by analysis of the total score distribution.

SUMMARIES

Result No.	Score	% Query Match	Length	DB	ID	Description	Pred. No.
1	2237	100.0	426	3	S51016(S510	NADH dehydrogenase (ub	1.22e-88
2	2237	100.0	426	6	VANQRBOL_3(	V;alginolyticus bolA,	1.22e-88
3	1594	71.3	411	6	HIU32702_5(	Haemophilus influenzae	2.09e-59
4	1594	71.3	411	3	C64052(C640	nitrogen fixation prot	2.09e-59
5	267	11.9	352	6	ECAE000258_	Escherichia coli from	1.08e-01
6	234	10.5	304	6	RCRNFG_2(X7	R;capsulatus genes rnf	1.84e+00
7	234	10.5	304	2	RCRNFG_2(X7	R;capsulatus genes rnf	1.84e+00
8	231	10.3	358	6	RCRNFABCD_4	R;capsulatus rnfA, rnf	2.36e+00
9	231	10.3	358	2	RCRNFABCD_4	R;capsulatus rnfA, rnf	2.36e+00
10	229	10.2	358	6	HIU32841_9(	Haemophilus influenzae	2.80e+00
11	229	10.2	358	2	F64136(F641	nitrogen fixation prot	2.80e+00
12	216	9.7	378	6	ECAE000199_	Escherichia coli from	8.26e+00
13	216	9.7	378	6	D90735_7(D9	Escherichia coli genom	8.26e+00
14	216	9.7	378	1	APPB_ECOLI(	CYTOCHROME BD-II OXIDA	8.26e+00
15	215	9.6	512	5	NUOM_RHOCA	(P50974) NADH DEHYDROG	8.97e+00
16	215	9.6	512	2	NUOM_RHOCA(	NADH DEHYDROGENASE I C	8.97e+00
17	215	9.6	512	6	RCU25800_8(	Rhodobacter capsulatus	8.97e+00
18	214	9.6	911	5	B3AT_HUMAN	(P02730) BAND 3 ANION	9.75e+00
19	214	9.6	911	1	B3AT_HUMAN(	BAND 3 ANION TRANSPORT	9.75e+00
20	214	9.6	911	8	HUMAE1_1(M2	Human anion exchange p	9.75e+00

NqrC

Statistics: Mean 53.803; Variance 287.164; scale 0.187

Pred. No. is the number of results predicted by chance to have a score greater than or equal to the score of the result being printed, and is derived by analysis of the total score distribution.

SUMMARIES

Result No.	Score	% Query Match	Length	DB	ID	Description	Pred. No.
1	1168	100.0	256	3	S51017(S510	NADH dehydrogenase (ub	2.11e-74
2	1168	100.0	256	6	VANQRBOL_4(	V;alginolyticus bolA,	2.11e-74
3	1164	99.7	256	6	VIBNQR36_1(	Vibrio alginolyticus n	4.32e-74
4	1164	99.7	256	3	VIBNQR36_1(	Vibrio alginolyticus n	4.32e-74
5	1164	99.7	256	6	VIBNQRC_1(D	Vibrio alginolyticus N	4.32e-74
6	649	55.6	244	5	Y167_HAEIN	(P43957) HYPOTHETICAL	1.78e-34
7	649	55.6	244	3	B64003(B640	hypothetical protein H	1.78e-34
8	649	55.6	244	6	HIU32702_6(	Haemophilus influenzae	1.78e-34
9	137	11.7	761	4	MJU67561_5	(U67561|gid:1591827)	8.36e+01
10	137	11.7	521	7	CELW06B4_2(	Caenorhabditis elegans	8.36e+01
11	137	11.7	761	6	MJU67561_5(	Methanococcus jannasch	8.36e+01
12	137	11.7	521	1	CELW06B4_2	(U23522|gid:746549) C	8.36e+01
13	136	11.6	315	7	NSCHRIB_1(X	N;sylvestris DNA for 3	9.47e+01
14	136	11.6	315	7	NSRNP31_1(X	Tobacco mRNA for 31 kD	9.47e+01
15	136	11.6	315	5	RO31_NICSY	(P19683) CHLOROPLAST 3	9.47e+01
16	136	11.6	315	1	NSCHRIB_1(X	N;sylvestris DNA for 3	9.47e+01
17	128	11.0	395	5	ACTW_CAEEL	(P53489) ACTIN-LIKE PR	2.52e+02
18	128	11.0	395	2	ACTW_CAEEL(	ACTIN-LIKE PROTEIN C.	2.52e+02
19	128	11.0	395	7	CEK07C5_1(Z	Caenorhabditis elegans	2.52e+02
20	127	10.9	287	2	D90906_102(	Synechocystis sp; PCC6	2.84e+02

qrD

Statistics: Mean 56.202; Variance 421.175; scale 0.133

Pred. No. is the number of results predicted by chance to have a score greater than or equal to the score of the result being printed, and is derived by analysis of the total score distribution.

SUMMARIES

Result No.	Score	% Query Match	Length	DB	ID	Description	Pred. No.
1	999	100.0	210	6	VANQRBOL_5(	V;alginolyticus bolA,	2.51e-42
2	999	100.0	210	1	S51018(S510	NADH dehydrogenase (ub	2.51e-42
3	999	100.0	210	6	VIBNQR36_2(	Vibrio alginolyticus n	2.51e-42
4	787	78.8	208	3	HIU32702_7(	Haemophilus influenzae	1.04e-30
5	787	78.8	208	6	HIU32702_7(	Haemophilus influenzae	1.04e-30
6	510	51.1	123	5	Y169_HAEIN	(P43959) HYPOTHETICAL	7.26e-16
7	510	51.1	123	3	D64003(D640	hypothetical protein H	7.26e-16
8	364	36.4	231	6	D90806_11(D	E;coli genomic DNA, Ko	2.45e-08
9	364	36.4	231	6	D90807_6(D9	E;coli genomic DNA, Ko	2.45e-08
10	364	36.4	231	6	ECAE000258_	Escherichia coli from	2.45e-08
11	364	36.4	231	6	D90808_11(D	E;coli genomic DNA, Ko	2.45e-08
12	364	36.4	231	2	D90806_11(D	E;coli genomic DNA, Ko	2.45e-08
13	360	36.0	243	6	RCRNFABCD_6	R;capsulatus rnfA, rnf	3.89e-08
14	360	36.0	243	2	RCRNFABCD_6	R;capsulatus rnfA, rnf	3.89e-08
15	354	35.4	441	6	RCRNFG_1(X7	R;capsulatus genes rnf	7.78e-08
16	354	35.4	441	2	RCRNFG_1(X7	R;capsulatus genes rnf	7.78e-08
17	345	34.5	235	6	HIU32841_11	Haemophilus influenzae	2.20e-07
18	345	34.5	235	2	HIU00086_50	Haemophilus influenzae	2.20e-07
19	263	26.3	84	4	C64003(C640	hypothetical protein H	2.23e-03
20	263	26.3	84	5	Y168_HAEIN	(P43958) HYPOTHETICAL	2.23e-03

Table 3.5. Sequence homology of NqrE polypeptide at PAM 250.

Statistics: Mean 56.290; Variance 469.241; scale 0.120

Pred. No. is the number of results predicted by chance to have a score greater than or equal to the score of the result being printed, and is derived by analysis of the total score distribution.

SUMMARIES

Result No.	Score	% Query Match	Length	DB	ID	Description	Pred. No.
1	910	94.5	198	1	VIBNQR36_3(	Vibrio alginolyticus n	2.59e-33
2	910	94.5	198	6	VIBNQR36_3(	Vibrio alginolyticus n	2.59e-33
3	826	85.8	198	6	HIU32702_8(	Haemophilus influenzae	3.55e-29
4	826	85.8	198	1	HIU32702_8	(U32702|gid:1573126)	3.55e-29
5	822	85.4	198	1	HIU32811_10	(U32811|gid:1222085)	5.58e-29
6	442	45.9	192	2	HIU32841_6	(U32841|gid:1574535)	1.04e-10
7	442	45.9	192	6	HIU32841_6(	Haemophilus influenzae	1.04e-10
8	440	45.7	94	1	S51019(S510	dehydrogenase (ubiquin	1.29e-10
9	437	45.4	93	2	VANQRBOL_6	(Z37111|gid:663274) V	1.77e-10
10	437	45.4	93	6	VANQRBOL_6(	V;alginolyticus bolA,	1.77e-10
11	431	44.8	193	2	HIU32788_1	(U32788|gid:1221834)	3.37e-10
12	422	43.8	193	6	ECAE000258_	Escherichia coli from	8.81e-10
13	393	40.8	193	6	RCAFDXC_2(D	R;capsulatus genes for	1.91e-08
14	393	40.8	193	2	RCAFDXC_2(D	R;capsulatus genes for	1.91e-08
15	393	40.8	193	6	RCRNFG_5(X7	R;capsulatus genes rnf	1.91e-08
16	393	40.8	193	6	RCRNFABCD_1	R;capsulatus rnfA, rnf	1.91e-08
17	217	22.5	441	6	RCRNFG_1(X7	R;capsulatus genes rnf	1.04e+00
18	217	22.5	243	6	RCRNFABCD_6	R;capsulatus rnfA, rnf	1.04e+00
19	217	22.5	441	2	RCRNFG_1(X7	R;capsulatus genes rnf	1.04e+00
20	217	22.5	243	2	RCRNFABCD_6	R;capsulatus rnfA, rnf	1.04e+00

This sequence homology was derived using the MPsrch programme with the SWISSPROT and Genpept database. A range of PAM values of 50-400 are usually used to compare the target sequence of interest with known sequences in the database to give a more accurate overview. A low PAM value search is usually more stringent and would require high identity of the target sequence to the known database sequence and allow less substitution of amino acids, therefore this comparison is normally over a short stretch of amino acid residues. Conversely, a search with a high PAM value is less stringent and allows more substitution of amino acids, requiring less identity and similarity of the target to the database sequence, hence this comparison would cover a longer stretch of amino acid sequence.
Predicted number is the number of results predicted by chance to have a score greater than or equal to the score of the result being printed, and is derived by analysis of the total score distribution. % Query match is not equivalent to % Match as it compares the match between the other search results with the result number one, which is most similar to the query sequence.

Significant or interesting alignments of these comparisons can be seen in the appendix. The alignmnts in the appendix will show the % Match which is the identity of the query sequence with sequences from the results of the database searches.
% Matches of less than 30% is deemed unsignificant identity or homology of query sequence with database sequence.

Only a flavin motif for FAD was obvious in the *nqr* operon sequence, located on NqrF. Although Hayashi and Unemoto have reported that they purified a FMN-containing NqrA, no GAG(A/R)Y motif indicative of a FMN binding site was detected on the sequence of NqrA or any other Nqr subunit.

From sequence analyses, it was concluded that Na^+-dependent NADH-ubiquinone oxidoredase is an evolutionarily distinct or distantly-related (unlike Na^+-ATPases and H^+-ATPases) functional alternative to the closely-related proton-translocating Complex I and NDH-1 present in all eukaryotes and most prokaryotes, respectively (Tan *et al.*, 1996).

3.3.4 Detailed sequence and motif analysis of NqrF

The gene for the catalytic NqrF or β subunit, *nqr*F, is located downstream of previously sequenced *nqr*A-*nqr*E genes and encodes a flavoprotein of 407 amino acids (Fig. 3.3). Sequence analysis of NqrF using the computer program MPsrch and a range of PAM values (40-350) revealed that the *N*-terminal region was similar to a electron transfer subunit of a number of monooxygenases and dioxygenases (e.g. xylene monooxygenase) and also with a number of ferredoxins, while the *C*-terminal region showed homology with several NAD(P)H-binding flavoproteins, including phenol hydroxylase P5 protein, phenol 2-monooxygenase and xylene monooxygenase (Karplus *et al.,* 1990; Correll *et al.*, 1992; Bruns *et al.*, 1994) (Table 3.6). The high homologies indicate that NqrF is likely an NADH-FAD reductase containing an iron-sulfur centre (Tan *et al.*, 1996). By comparison with the known crystal structure of FNR, F265 was identified as the border between the flavin domain (c.171-265) and the NAD^+-binding domain (266-407) (Fig. 3.3).

```
1    MDIILGVVMF TLIVLALVLV ILFAKSKLVP
31   TGDITISVND DPSLAIVTQP GGKLLSALAG
61   AGVFVSSACG GGGSCGQCRV KVKSGGGDIL
91   PTELDHITKG EAREGERLAC QVAMKTDMDI
121  ELPEEIFGVK KWECTVISND NKATFIKELK
151  LQIPDGESVP FRAGGYIQIE APAHHVKYAD
181  YDIPEEYRED WEKFNLFRYE SKVNEETIRA
211  YSMANYPEEH GIIMLNVRIA TPPPNNPDVP
241  PGIMSSYIWS LKEGDKCTIS GPFGEFFAKD
271  TDAEMVFVGG GAGMAPMRSH IFDQLKRLHS
301  KRKMSFWYGA RSKREMFYVE DFDMLQAEND
331  NFVWHCALSD PLPEDNWDGY TGFIHNVLYE
361  NYLRDHEAPE DCEYYMCGPP MMNAAVIGML
391  KDLGVEDENI LLDDFGG*
```

[2Fe-2S] binding site
FAD binding site
NAD binding site

Figure 3.3. Primary sequence of NqrF and putative binding sites.

Table 3.6. Sequence homology of NqrF polypeptide at PAM 180.

N-terminal

```
Statistics:      Mean 45.783;  Variance 113.439;  scale 0.404

      Pred. No. is the number of results predicted by chance to have a
      score greater than or equal to the score of the result being printed,
      and is derived by analysis of the total score distribution.

                                    SUMMARIES

Result          %
   No.  Score  Query  Length DB  ID          Description              Pred. No.
 ---------------------------------------------------------------------------
     1   1476  100.0     407  2  VIBNQR36_4( Vibrio alginolyticus n  2.44e-
220
     2   1476  100.0     407  6  VIBNQR36_4( Vibrio alginolyticus n  2.44e-
220
     3   1167   79.1     411  6  HIU32702_9( Haemophilus influenzae  5.88e-
168
     4   1167   79.1     411  2  D64052(D640 phenolhydroxylase comp  5.88e-
168
     5    173   11.7     342  4  TFU73041_4( Thiobacillus ferrooxid  4.11e-08
     6    173   11.7     342  6  TFU73041_4( Thiobacillus ferrooxid  4.11e-08
     7    169   11.4     350  6  D63341_5(D6 Pseudomonas putida TOL  1.38e-07
     8    169   11.4     350  5  XYLA_PSEPU  (P21394) XYLENE MONOOX  1.38e-07
     9    169   11.4     350  6  PSEXYLMA_2( TOL plasmid of P;putid  1.38e-07
    10    169   11.4     350  4  B37316(B373 xylene monooxygenase (  1.38e-07
    11    166   11.2     355  6  PSETBMAF_6( Pseudomonas sp; toluen  3.41e-07
    12    166   11.2     355  1  PSETBMAF_6  (L40033|gid:1008901 )  3.41e-07
    13    163   11.0     350  2  ACPHENOL_6( A;calcoaceticus genes   8.37e-07
    14    163   11.0     350  6  ACPHENOL_6( A;calcoaceticus genes   8.37e-07
    15    162   11.0     342  4  PPY12654_1( P;putida oxoR gene; 2-  1.13e-06
    16    162   11.0     342  6  PPY12654_1( P;putida oxoR gene; 2-  1.13e-06
    17    152   10.3     349  3  PAU86603_1( Pseudomonas aureofacie  2.14e-05
    18    152   10.3     349  6  PAU86603_1( Pseudomonas aureofacie  2.14e-05
    19    150   10.2     329  6  YEPASCD_1(L Yersinia pseudotubercu  3.83e-05
    20    150   10.2     329  6  YEPASCAF_2( Yersinia pseudotubercu  3.83e-05
```

```
RESULT    8
>XYLA_PSEPU
(P21394) XYLENE MONOOXYGENASE ELECTRON TRANSFER COMPONENT (CONTAINS

  DB  5;  Score     169;  Match 29.3%;  QryMatch 11.4%;  Pred. No. 1.38e-07;
  Matches    51;  Conservative   44;  Mismatches  63;  Indels  16;  Gaps
15;

           .* * * * **  . *.**  . .. .    *  .* ***  .  * .  *  * *** *
Db       4 FFKKISGLFVPPPESTVSVRGQ-GFQFKVPRGQTILESALHQGIAF-PHDCKVG-SCGTC 60
Qy      22 LFAK-SKL-VPTGDITISVNDDPSLAIVTQPGGKLL-SALAGAGVFVSSACGGGGSCGQC 78

           . *. **  . * .    ..    . * **.**   * *..*** . ..*  .   *  .
Db      61 KYKLISGRVNELTSSAMGLSGDLYQSGYRLGCQCIPKEDLEIEL-DTVLGQALVPIETSA 119
Qy      79 RVKVKSGGGDILPTELDHITKGEAREGERLACQVAMKTDMDIELPEEIFG--VKKWE-CT 135

           .**.... .  * *. . .** . ..* .* * ..* *    *. *. .  * .
Db     120 LISKQKRLAHDIVEMEV-VPDKQ-IAFYPGQYADVECAECSAVRSYS-FSAPPQ 170
Qy     136 VISNDNKATF-IKELKLQIPDGESVPFRAGGYIQIE-APAHHVK-YADYDIPEE 186
```

C-terminal

Statistics: Mean 49.175; Variance 119.302; scale 0.412

Pred. No. is the number of results predicted by chance to have a score greater than or equal to the score of the result being printed, and is derived by analysis of the total score distribution.

SUMMARIES

Result No.	Score	% Query Match	Length	DB	ID	Description	Pred. No.
1	2633	100.0	407	2	VIBNQR36_4(	Vibrio alginolyticus n	0.00e+00
2	2633	100.0	407	6	VIBNQR36_4(	Vibrio alginolyticus n	0.00e+00
3	2202	83.6	411	6	HIU32702_9(	Haemophilus influenzae	0.00e+00
4	2202	83.6	411	2	D64052(D640	phenolhydroxylase comp	0.00e+00
5	340	12.9	353	4	PPPHH_6(X79	P;putida genes for phe	7.29e-32
6	340	12.9	353	6	PPPHH_6(X79	P;putida genes for phe	7.29e-32
7	337	12.8	350	2	ACPHENOL_6(	A;calcoaceticus genes	2.12e-31
8	337	12.8	350	6	ACPHENOL_6(	A;calcoaceticus genes	2.12e-31
9	333	12.6	352	1	DMPP_PSEPU	(P19734) PHENOL HYDROX	8.77e-31
10	333	12.6	353	6	PSEPHHYD_6(	Pseudomonas putida phe	8.77e-31
11	333	12.6	353	1	F37831(F378	phenol 2-monooxygenase	8.77e-31
12	333	12.6	352	5	DMPP_PSEPU	(P19734) PHENOL HYDROX	8.77e-31
13	331	12.6	353	6	PSEPHEAA_6(	Pseudomonas putida phe	1.78e-30
14	331	12.6	353	3	PSEPHEAA_6	(D28864|gid:468471) P	1.78e-30
15	329	12.5	353	6	PPPHEHYD_6(	P;putida genes for phe	3.62e-30
16	329	12.5	353	2	PPPHEHYD_6(	P;putida genes for phe	3.62e-30
17	287	10.9	350	5	XYLA_PSEPU	(P21394) XYLENE MONOOX	8.81e-24
18	287	10.9	350	6	D63341_5(D6	Pseudomonas putida TOL	8.81e-24
19	287	10.9	350	6	PSEXYLMA_2(	TOL plasmid of P;putid	8.81e-24
20	287	10.9	350	4	B37316(B373	xylene monooxygenase (	8.81e-24

RESULT 5
>PPPHH_6(X79063|gid:483483)
P;putida genes for phenolhydroxylase and ferredoxi

DB 4; Score 340; Match 32.0%; QryMatch 12.9%; Pred. No. 7.29e-32;
Matches 54; Conservative 52; Mismatches 57; Indels 6; Gaps 6;

```
          *  *  .*.* . ** **   .***.*.** .*..* ...*..**.*... .* *** .
Db    170 VEGGAATSFIHRQLKVGDAVELSGPYGQFFVRDSQAGDLIFIAGGSGLSSPQSMIFDLFE 229
Qy    239 VPPGIMSSYI-WSLKEGDKCTISGPFGEFFAKDTDA-EMVFVGGGAGMAPMRSHIFDQLK 296

          *  . * ...  ***.. *..  * *. * * . **    **...  . .*.*. **.*.
Db    230 RGDT-RQITLFQGARNRAELYNRELFEELAARHSNFSYVPALNQAHDDPEWQGFKGFVHD 288
Qy    297 RLHSKRKMSFWYGARSKREMFYVEDFDMLQAENDNFVWHCALSDPLPEDNWDGYTGFIHN 356

              ..   . .     * .**** *  * *  *..  . . .*... *
Db    289 AAKAHF-DGRFSGHK-AY-LCGPPPMIDAAITTLMQGRLFERDIFMERF 334
Qy    357 VLYENYLRDHEAPEDCEYYMCGPPMMNAAVIGMLKDLGVEDENILLDDF 405
```

Analysis of each of the three domains, namely the ferredoxin domain, the NADH binding site and the flavin domain, was carried out independently using MPsrch. The ferredoxin domain was most similar to xylene monooxygenase ($1.38e^{-07}$), toluene/benzene-2-monooxygenase ($3.41e^{-07}$) and phenol hydroxylase ($8.37e^{-07}$) (Table 3.6 and appendix, Tan *et al.*, 1996). In all cases, there was high identity in the cysteine-rich region of the ferredoxin domain (Fig. 3.3) although the spacing was C-x_5-C-x_2-C as in putidaredoxin rather than the C-x_4-C-x_2-C motif of plant-type ferredoxins (Cammack, 1992).

Typical [2Fe-2S] binding motifs from plant type ferredoxin were used to identify the putative [2Fe-2S] binding site in NqrF below.

Motifs: C-x-x-x-x-x-C-x-x-C (another C would be located further downstream)

C-x-x-x -x-C-x-x-C

C-{C}-{C}-[GA]-{C}-C-[GAST}-{Cet}-C

NqrF: **C_{69}**-G-G-G-G-S-**C_{75}**-G-Q-**C_{78}**-R.....30 amino acids..... L_{108}-A-**C_{110}**-Q

The alignment and comparison of putative NqrF [2Fe-2S] site (Fig. 3.3) with known [2Fe-2S] sites in *Pseudomonas putida* ferredoxin and *Anabaena* ferredoxin is shown as follows:

```
P. putida Fd          CRGGG CGLCRVRVLSG
                      | ||| || ||| | ||
Vibrio NqrF           CGGGGSCGQCRVKVKSG
                      |  |  || ||||  ||
Anabaena Fd           CRAGA CGQCRVKLVSG
```

We propose that the ferredoxin domain is a [2Fe-2S] iron-sulphur centre, although a differing opinion by Rich *et al.* (1995) claims that it is a [4Fe-4S]centre instead.

Similarly, the FAD binding site and NADH binding site were identified using homologies to known consensus sequences and computer-predicted secondary structure analysis. By analogy with the broad family of FNR-related enzymes it is possible to identify regions that are likely to be involved in FAD binding. The flavin domain showed least homology with other proteins in the database but was similar to a number of NAD^+-dependent nitrate reductases, NADH-cytochrome b_5 reductases as well as lipoxygenase and benzoate 1,2 dioxygenase (a ferredoxin:ferredoxin-NAD^+ reductase) (Tan *et al.*, 1996). Using the crystal structure of FNR, residues **R_{209}AYS** from NqrF (Fig. 3.3) were equated with **Arg^{93}**, **Tyr^{95}** and **Ser^{96}** of FNR which forms part of its FAD-binding pocket (Rich *et al.*, 1995). The second putative FAD binding motif **G_{242}**IMSSYI of NqrF (Fig. 3.3) was identified and found to correspond to **G_{130}**VCSNFL of FNR and **G**RGG**S**ISF of PDR (Bruns and Kaplus, 1993), which anchors the pyrophosphate part of FAD.

Significantly, the NAD^+-binding domain showed high similarities with over 40 NAD^+-dependent enzymes including phenol hydroxylase, phenol 2-monooxygenase and xylene monooxygenase with predicted numbers of $7.29e^{-32}$, $8.77e^{-31}$ and $8.81e^{-24}$ (Table 3.6 and appendix, Tan *et al.*, 1996). The putative NAD^+ binding motif G_{279}G**G**A**G**MA**P**M (Fig. 3.3) shows good homology to the TGTGIA**P**F and G**G**I**G**IT**P**M and of FNR and PDR respectively (Bruns and Karplus, 1993). These conserved residues contain the type II' xGxG turn of a characteristic NADPH-binding loop that forms the βαβ fold for binding NADH. Likewise, the other NAD^+ binding residues Y_{375}MCGPP and L_{402}DDF were identified upon comparison with FNR and PDR.

As there are no firm consensus sequences for quinone binding sites, this could not be unambiguously identified in NqrF.

3.4 Hydropathy plots

Hydropathy plots indicate that NqrA, NqrC and NqrF are relatively hydrophilic subunits (Fig 3.4a). Conversely, hydropathy plots of NqrB, NqrD (Fig. 3.4) and NqrE (Fig. 3.5) indicate that they are integral membrane proteins that possess a number of defined putative transmembrane helices, predicted at 6-12, 4-6 and 6 respectively (Rich *et al.*, 1995).

Na^+-NQR is therefore provisionally expected to be composed of a relatively hydrophilic FP fragment of 3 subunits (NqrA, NqrC and NqrF) and containing 1 FAD and 1 [2Fe-2S] iron sulphur centre on the NADH-oxidising NqrF subunit, together with a hydrophobic HP fragment of 3 subunits (NqrB, NqrD and NqrE).

3.5 Proposed structure of NqrF

From hydropathy plots, NqrF is predicted to be a hydrophilic protein with a probable hydrophobic *N*-terminal transmembrane region (Fig. 3.6 and 3.7). A predicted folding model of NqrF and positions of prosthetic groups is shown in Fig. 3.8 (Rich *et al.*, 1995). The *N*-terminal region of NqrF is attached to the membrane or HP fragment via 2 membrane spanning α-helices while the proposed binding sites for FAD and NADH are cytoplasmic, consistent with expectations based on the orientations of other bacterial membrane proteins. The iron sulphur centre resides close to the interface between the hydrophobic region and the large globular head containing the FAD and NADH binding sites.

Fig. 3.4. Hydropathy plot of NqrD.

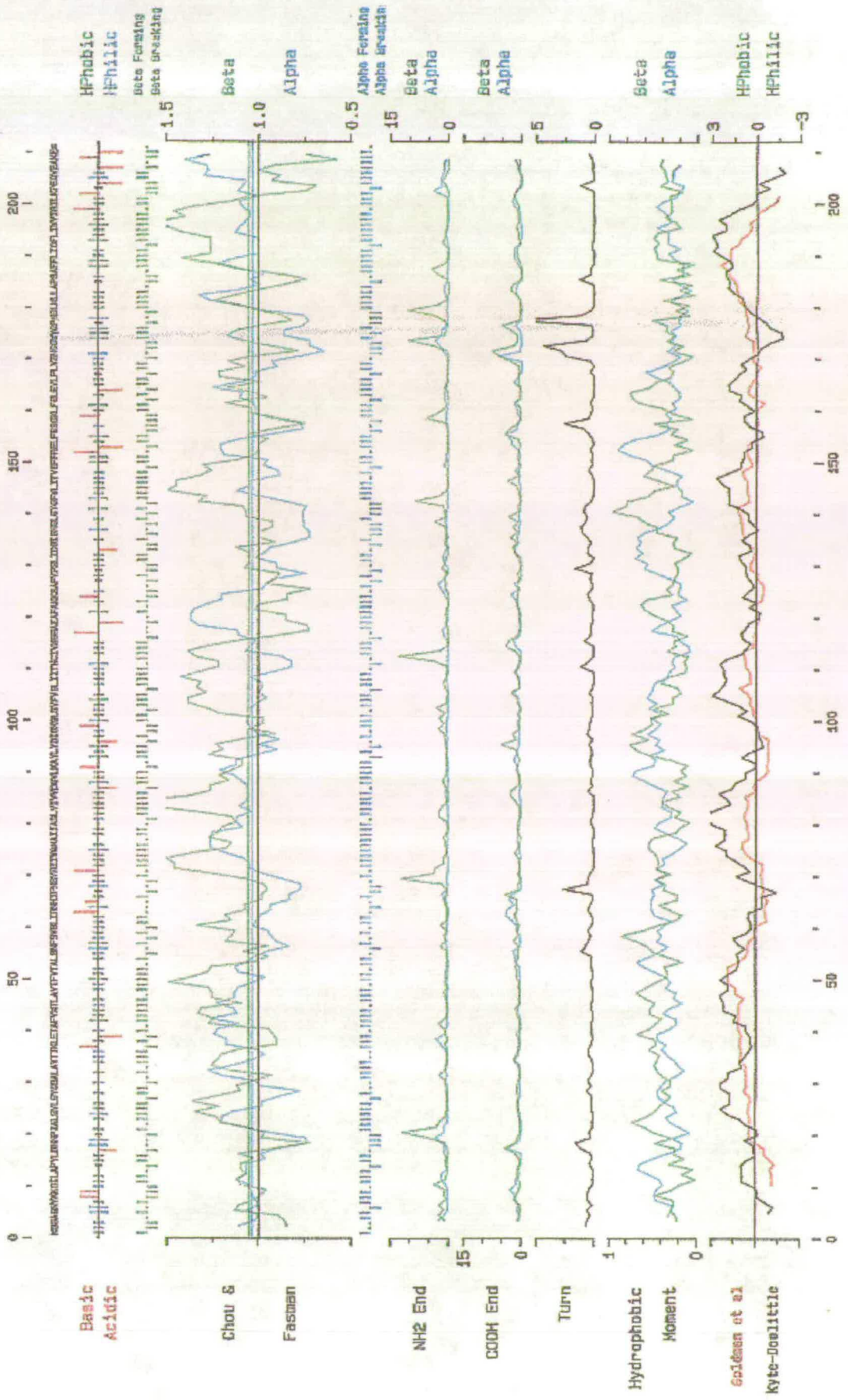

Legend for all hydropathy plots

All hydropathy plots were achieved using the PEPPLOT programme on the Wisconsin GCG8 package.

1. The sequence

The first part of the plot shows the amino acid sequence.

2. The residue schematic

The second part of the plot shows a schematic representation where each residue is represented by a line at the position it occurs in the sequence and the lengths and colours of the lines are used to indicate chemically similar groups of amino acids.

Green hydrophilic, charged
- down = acidic
- up = basic

Red hydrophilic, uncharged
- short = amides
- long = alcohols

Blue hydrophobic
- short = aliphatic
- long = aromatic

Black proline

Unmarked alanine, glycine, cysteine

3. Chou and Fasman beta-sheet forming and breaking residues

The third panel displays residues that are beta-sheet forming and breaking.

4. Chou and Fasman alpha and beta propensities

The fourth panel shows propensity measures for alpha-helix and beta-sheet. As each curve rises past the threshold for its colour, it satisfies one criterion for propagation of an alpha-helix or beta-sheet structure. If the curves drop below the black threshold and if there is at least one breaking residue in four, then the structure may terminate.

5. Chou and Fasman alpha-helix forming and breaking residues

The fifth panel shows the residues that are alpha-helix forming and breaking.

6. Chou and Fasman amino ends

The sixth panel shows regions of the sequence that resemble sequences typically found at the amino end of alpha-helices and beta-structures.

7. Chou and Fasman carboxyl ends

The seventh panel shows regions of the sequence that resemble sequences typically found at the carboxyl end of alpha-helices and beta-structures.

8. Chou and Fasman turns

The eighth panel shows regions of the sequence typically found in turns.

9. Hydrophobic moment

The ninth panel shows the helical hydrophobic moment at each position of the sequence. These curves rise when the molecule forms either an alpha-helix or a beta-sheet at the interface between the solvent and the interior of the molecule. The moment statistic is the probability that the sequence at each position is amphiphilic, that is, it appears to have hydrophobic residues on one side and hydrophilic residues on the other. In a typical alpha helix, each residue is oriented about 100 degrees from the preceding residue while in beta-strands, the rotation between adjacent residues is 160 degrees. Moment is a tool that makes a continuous contour plot of the helical hydrophobic moment for rotational angles between 0 and 180 degrees per residue.

10. Kyte and Doolittle hydropathy and Goldman, Engelman and Steitz transbilayer helices

The tenth panel has 2 curves based on the average hydrophobicity. The black Kyte and Doolittle curve is the average of a residue-specific hydrophobicity index over a window of nine residues. When the line is in the upper half of the frame, it indicates a hydrophobic region, and when it is in the lower half, a hydrophilic region. The green Goldman, Engelman and Steitz curve is the average of a residue-specific hydrophobicity scale (the GES scale) over a window of twenty residues. When the line is in the upper half of the frame, it indicates a hydrophobic region, and when it is in the lower half, a hydrophilic region.

Fig. 3.4a. Hydropathy plots of amino acid sequences of NqrA to NqrF. Plots were generated with a modified Chou-Fasman Secondary Structure Predictor program (version 1.00) supplied by A.R. Crofts (University of Illinois), using a modified Rao-Argos index with a span of 11 amino acids (Rich *et al*, 1995).

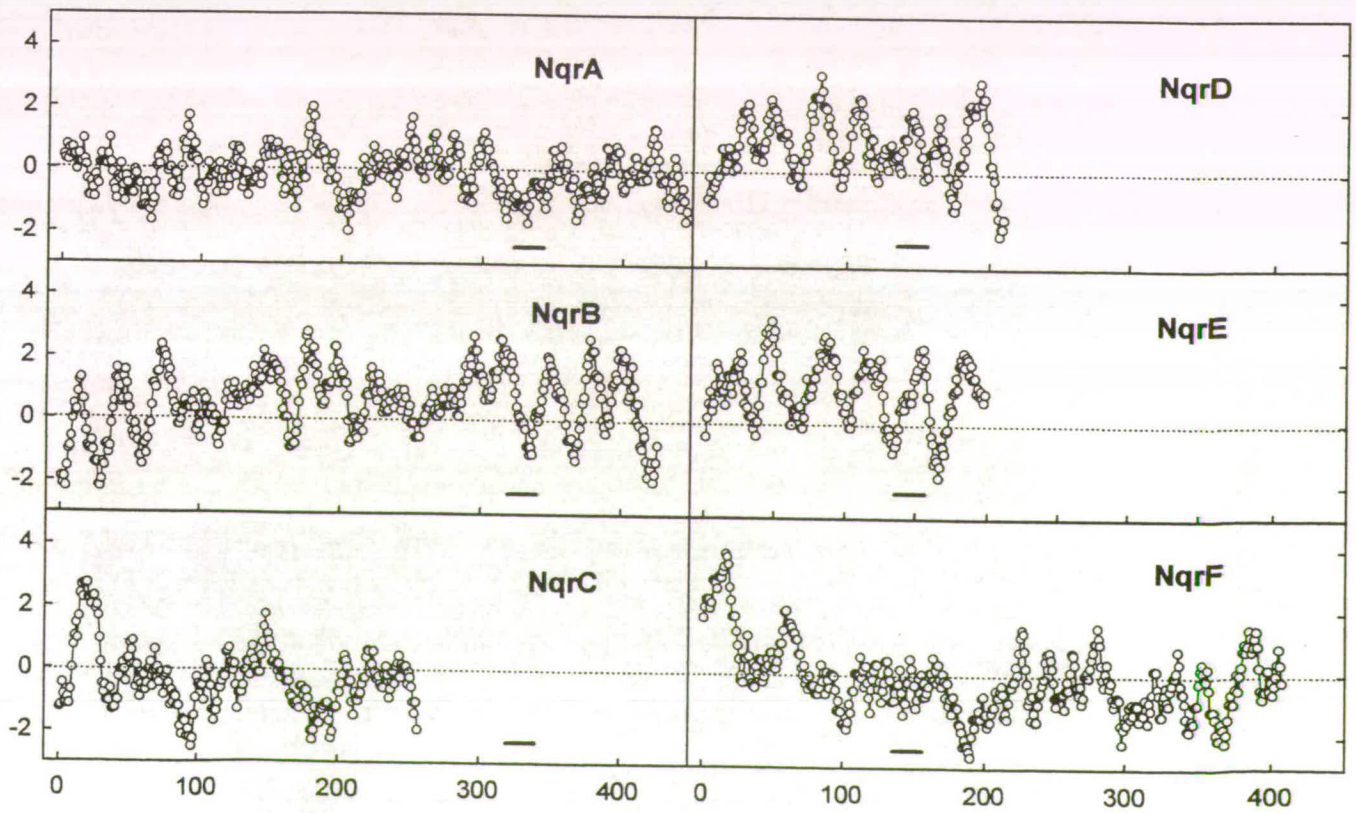

Fig. 3.5. Hydropathy plot of NqrE.
(See previous legend)

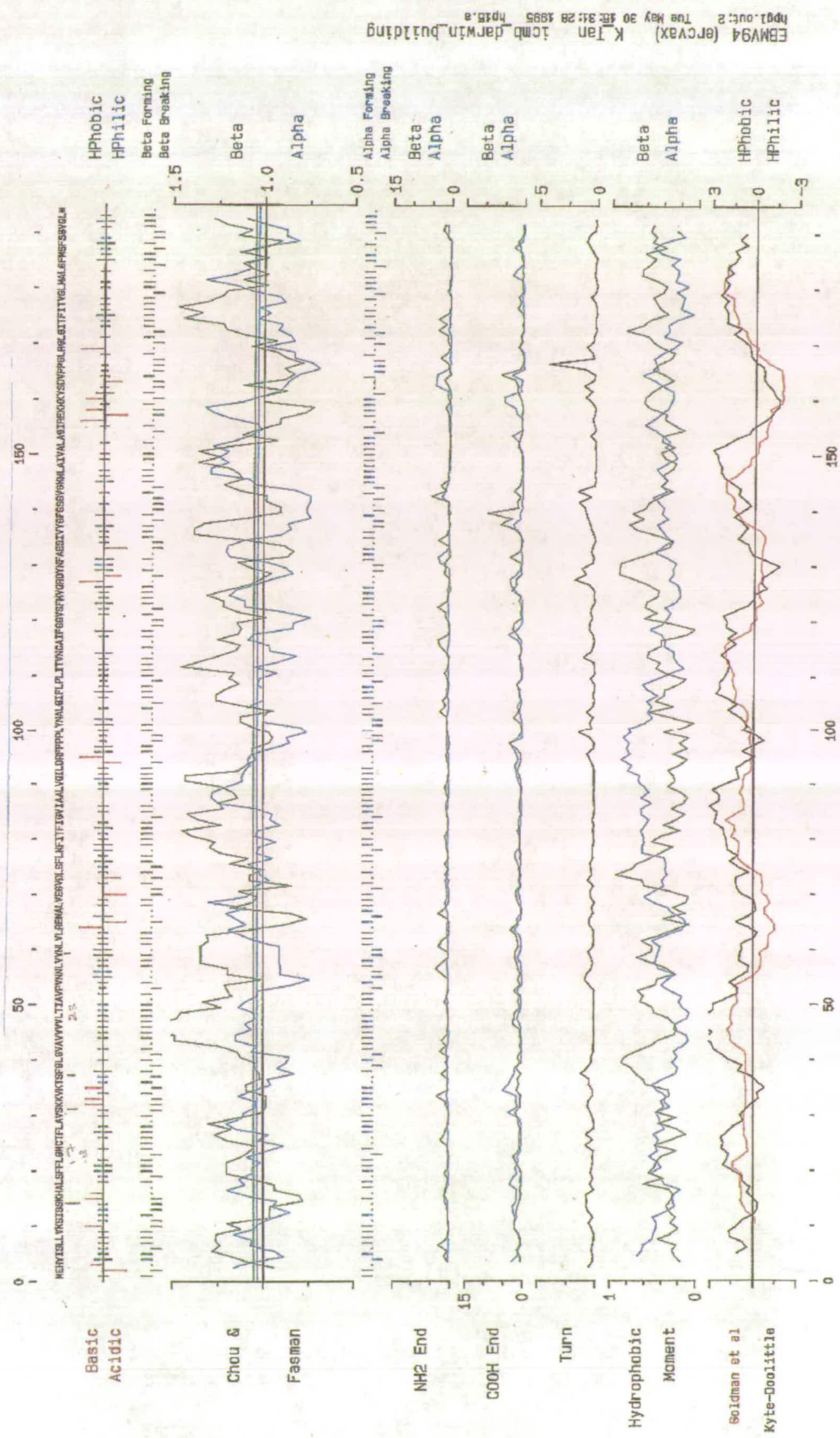

Fig. 3.6. Hydropathy plot of NqrF.
(See previous legend)

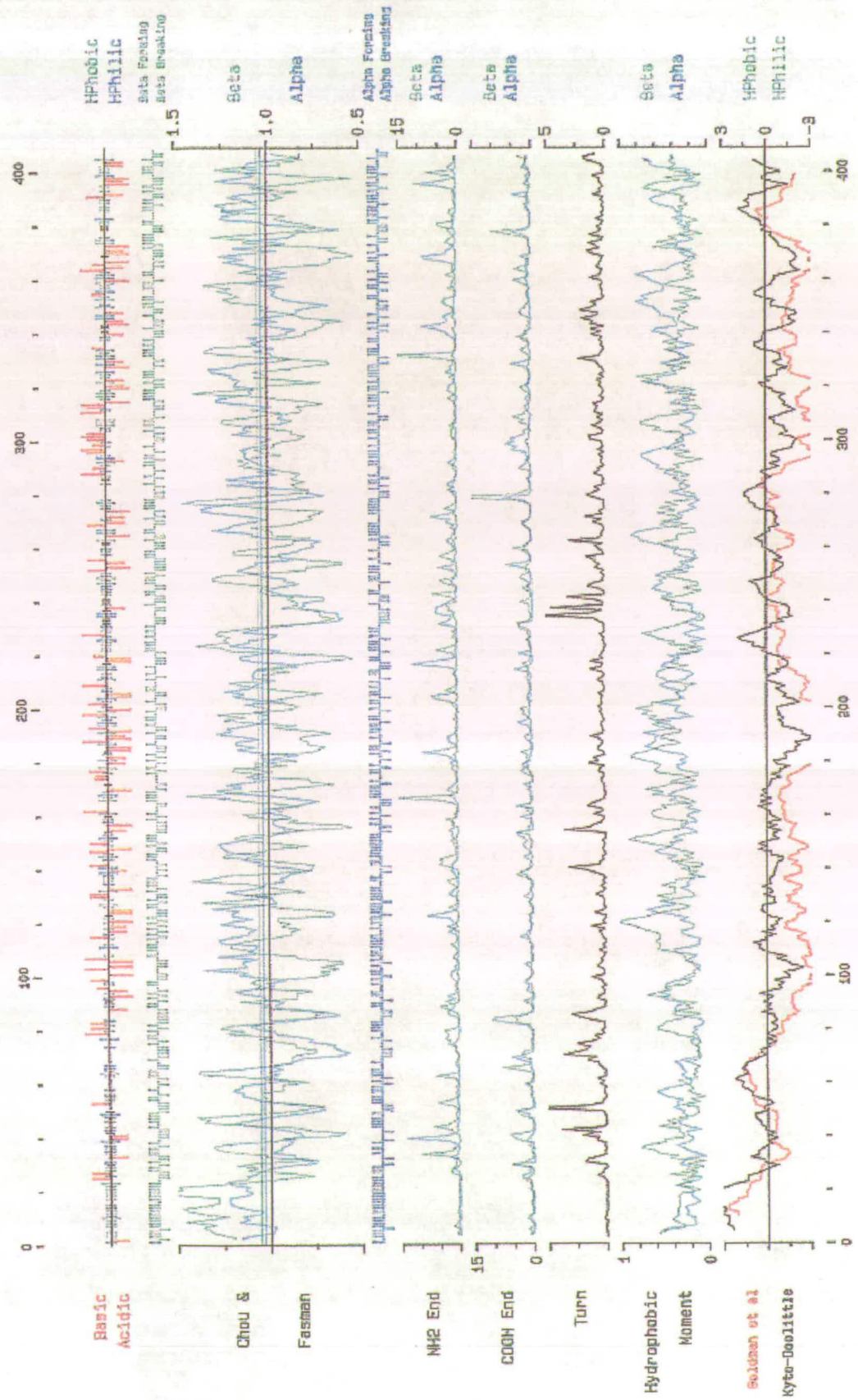

Fig. 3.7. Hydropathy plot of NqrF.
This plot was devised using the PLOTSTRUCTURE programme on the Wisconsin GCG8 package. The grey diamond regions indicate positions along the polypeptide where there is a area of predominantly hydrophobic amino acid residues while the blue octagon regions denote a zone of mainly hydrophilic amino acids.

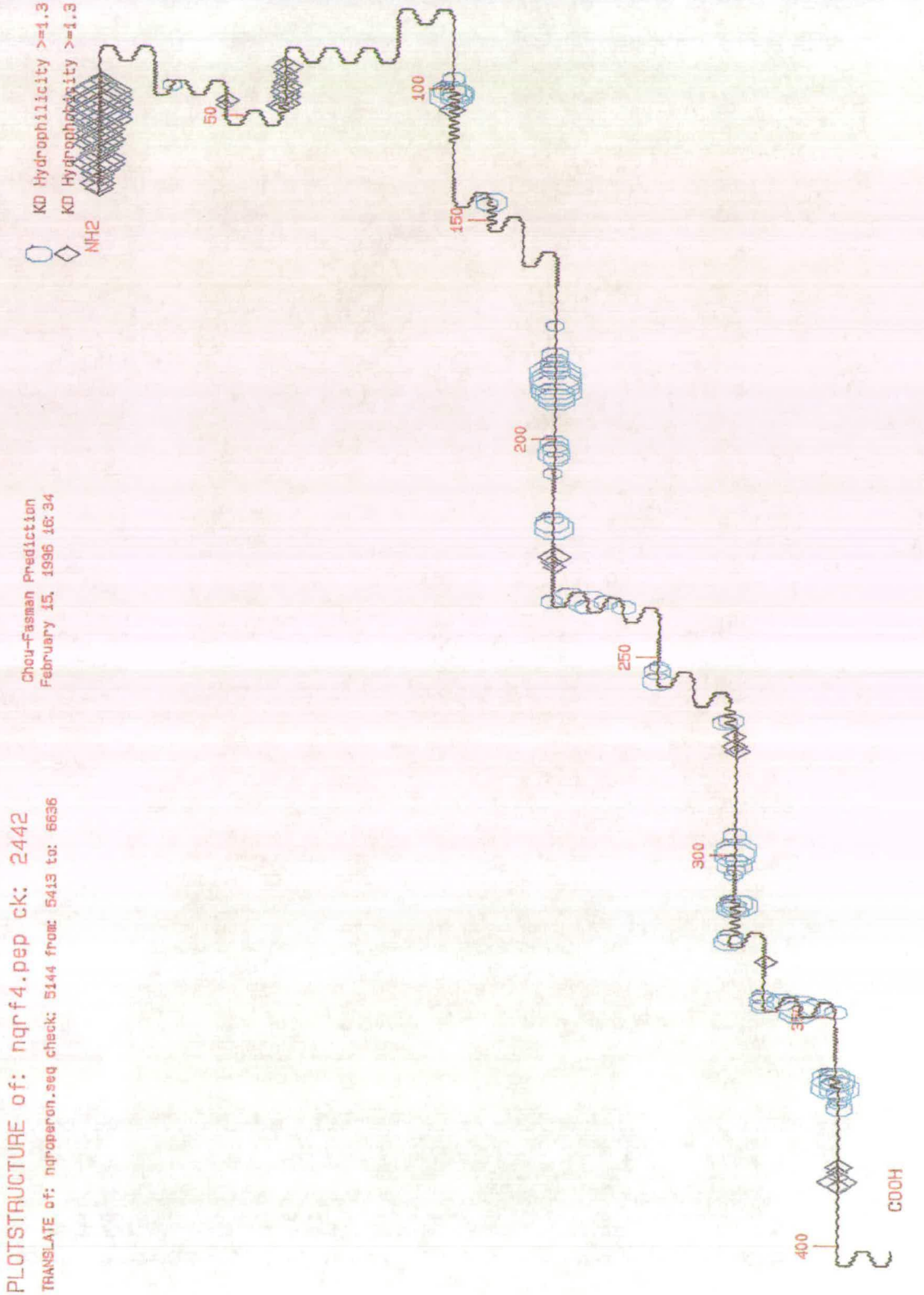

Fig. 3.8. A predicted folding model of NqrF and the positions of its prosthetic groups (Rich *et al*, 1995).

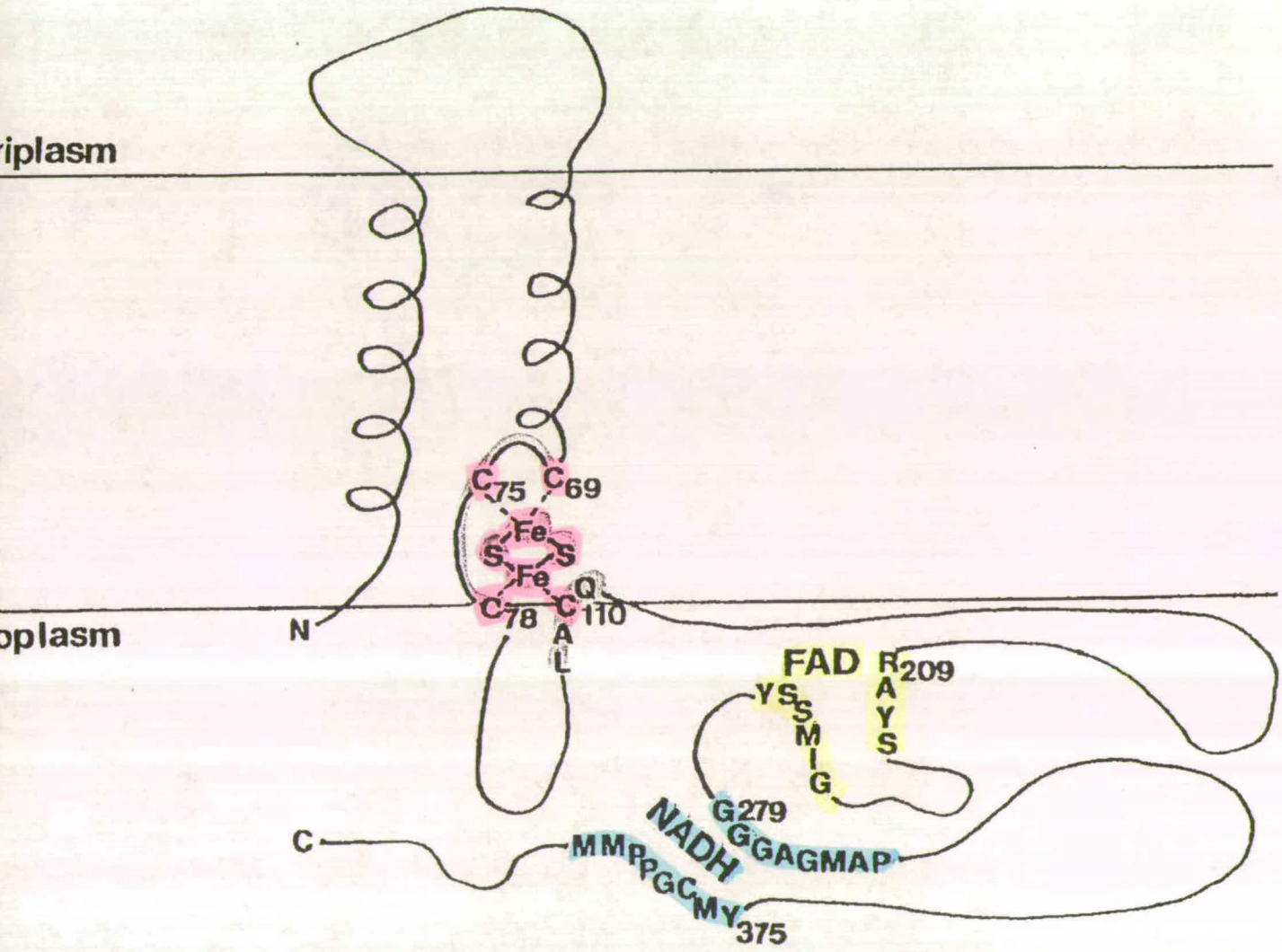

3.6 NqrF is the catalytic β subunit

On basis of three criteria, *nqr*F was deduced to be the structural gene for the NADH dehydrogenase catalytic subunit (β). Firstly, sequence comparisons using MPSRCH identifies significant homologies with the electron transfer subunit of a number of monooxygenases and dioxygenases (e.g. methane monooxygenase, phthalate dioxygenase (PDR) and xylene monooxygenase) and also with a number of ferredoxins. These electron transfer subunits are all flavoproteins consisting of a ferredoxin domain containing a [2Fe-2S] centre and a FAD-containing ferredoxin-NAD^+ reductase (FNR) domain. The homology is highly conserved around the ferredoxin motif although the spacing is C-X_5-C-X_2-C rather than C-X_4-C-X_2-C (Cammack, 1992; Matsubara and Saeki, 1992). Such high homologies (e.g. a predicted no. of 1.38* 10^{-07} at PAM 180 for XylA of xylene monooxygenase) indicate NqrF is very likely to be a NADH-FAD reductase containing an iron-sulphur centre. Secondly, NADH dehydrogenase activity was observed on native gels using solubilised extracts from *E. coli* cells containing a *Kpn*I-*Sal*I fragment cloned into expression vector pET16b (elaborated in later sections). Thirdly the deduced properties of NqrF, a polypeptide of 407 amino acids with an observed M_r of 46 kDa and an observed pI of 5.1 agree well with the properties previously observed or predicted for the NqrF subunit of NADH-ubiquinone oxidoreductase (Predicted M_r from primary sequence and M_r of previously-purified subunit is 46 kDa and the predicted pI is 4.54 from primary sequence) (elaborated in further detail in later sections).

Chapter 4

Results and Discussion

Expression of Nqr subunits

4.1 Expression

Expression of proteins allows purification, localisation and functional analysis of the proteins of interest. *E. coli* is normally chosen as the host for expression as there is a wide range of compatible expression vectors available for cloning and several very comprehensive, well-established expression systems exist. However, it is conceivable that *E. coli* has limited capacity to incorporate some membrane proteins into its cytoplasmic membrane and only simple membrane proteins are successfully overproduced because in nature, *E. coli* cytoplasmic membrane proteins, unlike its periplasmic and outer membrane proteins, are non-abundant. Two classes of membrane proteins are recognized, namely peripheral (extrinsic) and integral (intrinsic). Peripheral proteins are not readily distinguished from soluble polypeptides, since they are bound to the surface of the membrane only by electrostatic interactions, often via phospholipid headgroups, and are released in a water-soluble form by treatment at high ionic strength or alkaline pH without disrupting the lipid bilayer. In contrast, integral membrane proteins, have stretches of hydrophobic amino acid residues which interact with the non-aqueous phase within the confines of the lipid bilayer. For some proteins, this interaction is confined to a short stretch of polypeptide chain, often at their *N*- or *C*-termini, as in NqrF, cytochrome b_5 of the mitochondrial outer membrane, or the aminopeptidases of brush-border epithelia, which act as 'membrane anchors' inserting into the lipid bilayer while the catalytic domains of the enzymes are located without the confines of the membrane. Similarly, single membrane-spanning polypeptides, such as glycophorin of the red blood cell and the low-density lipoprotein (LDL) receptor, contain an easily identifiable hydrophobic region of approximately 20 amino acids in length corresponding to the transmembrane segment in an otherwise relatively hydrophilic structure. Overproduction of these

simple integral membrane proteins require their genes to be cloned into plasmids with a high copy number and/or downstream of strong promoters. The latter usually involves positioning the coding regions, devoid of their 5'-flanking sequences and if required, the 3'-coding sequences as well, downstream of strong, controllable promoters and ribosome-binding sites. This direct expression approach could alleviate problems whereby the structural features of the mRNA may prevent efficient ribosome binding, or target the message for rapid degradation (Gould, 1994). Complex multi-membrane spanning membrane proteins are markedly more hydrophobic in character and solubilization of these proteins necessitates the disruption of the lipid bilayer using detergents. These complex membrane proteins are often lethal when overproduced in *E. coli* due to sequestration of essential host components involved in membrane protein assembly or due to destabilisation of the permeability barrier afforded by the cytoplasmic membrane (Gould, 1994).

The ultimate aims of expressing *V. alginolyticus* Nqr subunits in *E. coli* were to allow purification of these polypeptides, their characterisation and to complement *nqr* null mutants in *V. alginolyticus* for biochemical analysis using the recombinant plasmids carrying the genes that code for these Nqr subunits. Reconstitution experiments in membrane vesicles then could be performed to determine the role of each polypeptide.

4.2 Cloning strategies for expression of *nqr* subunits

The vector pET16b (Figure 2.6) was chosen for the expression of *nqr* genes because it has the T7 *lac* promoter which tightly regulates expression. Expression of the target gene in pET16b is induced by providing a source of T7 RNA polymerase in the host cell BL21 which is a λDE3 lysogen. λDE3 carries the T7 RNA polymerase genes under *lacUV5* control with a *lac* operator and a *lac* repressor gene. These genes are inserted in the phage such that it disrupts its *int* gene so that λDE3 can only integrate and excise from BL21 with a helper phage. BL21 lacks *lon* protease and *ompT* protease and hence is favourable as an expression host for reducing protease

degradation of target proteins. This strain of BL21 also contains p*LysS* which makes a small amount of T7 lysozyme, a natural inhibitor of the T7 RNA polymerase. However, this should have no major effect on target gene expression, except for a short lag in appearance of the gene products. T7 RNA polymerase allows very selective and highly active expression of the target gene but is also able to maintain target genes transcriptionally silent in the uninduced state in the absence of IPTG as the T7 RNA polymerase gene is under *lacUV5* control in BL21. A *lac* operator sequence is located downstream of the T7 promoter in the vector pET16b and the plasmid also carries the natural promoter and coding sequence for the *lacI* repressor in the opposite orientation so that the *lacI* repressor acts on both the *lacUV5* promoter in BL21 to repress T7 RNA polymerase expression and at the T7*lac* promoter to block transcription of the target gene. This is important as pET vectors are present in high copy numbers and there is always background expression which must be silenced to avoid toxicity of gene expression. Possible cloning sites are *Nde*I, *Xho*I, *Bam*HI and *Nco*I; *Nco*I is at the translational start so that cloning into this site eliminates the leader sequence of His-tag of Factor Xa while cloning at *Nde*I incorporates the His-Tag at the *N*-terminal region of the protein of interest (Novagen pET system manual).

4.3 Cloning of *nqr*A

The promoter region of *nqr*A was excluded when ligating the DNA to the vector as there were problems trying to ligate the entire *nqr*A and the promoter to the vector and transform this to get a viable clone. Inclusion of *bol*A was avoided when trying to ligate *nqr*A to the vector as *bol*A is involved in cell division and this may interfere with cell expression. This NqrA polypeptide is so toxic that previous attempts to ligate its gene with its promoter region intact, into high copy number T7 promoter vectors (pBluescript KS-, pTZ18R, pT7 etc.) and then transforming into a expression host, or using *pcn*Δ host strains have failed and most clones obtained previously for sequencing have poor growth if *nqr*A is ligated in the correct orientation to T7 promoter for expression or are almost always found in the opposite

direction to the T7 promoter. Unfortunately, there are also no unique restriction sites just before the start of *nqr*A.

Hence, *nqr*A was ligated into pET16b using PCR to to generate a site at the translational start so as to exclude the promoter sequence just before it. Due to the sequence of *nqr*A, *Nco*I could not be used for creating the translational ATG start. *Nqr*A begins as ATGATTA... while the recognition site of *Nco*I is C^CATGG; therefore the base immediately after ATG must be G in order to clone precisely into *Nco*I at the translational start of the vector. Hence *Nde*I (CA^TATG) was selected as the 5'-terminal restriction site of *nqr*A. *Nde*I site was created at the 5'-terminal of *nqr*A by polymerase chain reaction using an oligonucleotide primer with the *Nde*I site and complementary bases of the start of *nqr*A and another primer (antisense) just downstream of the *Sph*I site. Using the Wisconsin GCG8 FOLDRNA programme, PCR primers were checked for the correct fold energy and that there is no hairpin loop formation as well as no likelihood of primer-dimer formation with each other. The PCR product was digested with *Nde*I and *Sph*I and ligated into pSL1180. The 3'-region of *nqr*A was to be cloned into pSL1180 vector containing the PCR-constructed 5'-terminal fragment. Finally, the entire *nqr*A gene was then to be ligated into pET16b using *Nde*I and *Sal*I (compatible ends with *Xho*I in pET16b).

The PCR-generated 5'-terminal *Nde*I/*Sph*I region of *nqr*A was successfully ligated into pET16b and transformed into a viable clone. Unfortunately, numerous subsequent attempts to clone the remaining gene or even operon have failed, perhaps because of the toxicity due to the basal expression of the Na^+-pump coded by *nqr*A in *E. coli.*

4.4 Cloning and expression of *nqr*B, *nqr*C and *nqr*D

4.4.1 Cloning and expression of *nqr*B, *nqr*C and *nqr*D

A 2.0 kb *Pst*I/*Cla*I insert containing the complete *nqr*C and *nqr*D genes and a 2.4 kb *Xba*I/*Hin*dIII insert containing the complete *nqr*B and *nqr*C genes, have been cloned into pBluescript KS- in *E. coli* DH5α-F'IQ and the inserts are positioned in the correct orientation with respect to the T7 promoter. These and a control plasmid pBluescript KS- were subsequently transformed into HMS174 or BL21(DE3)p*LysS*, strains which contain the genes encoding the T7 RNA polymerase. Target gene expression was induced in these λDE3 lysogens by adding IPTG and cells were collected at different time points after induction and together with uninduced controls loaded onto SDS-PAGE gels (BioRad Mini-Protean II Dual Slab Cell).

Only the overall protein profile can be obtained when the HMS174 host was used as this host was rifampicin-resistant and hence selective pulse-chase radiolabelling experiments could not be achieved. Due to the presence of major proteins in the *E. coli* host at about the same molecular weight as the target proteins, no clear overexpression could be seen upon IPTG induction.

With pulse-chase labelling experiments in the BL21(DE3)p*LysS* host, the predicted 32 kDa polypeptide of the hydrophilic NqrC was apparently expressed but the overexpression of highly hydrophobic NqrB (50 kDa) and NqrD (28 kDa) were not obvious (Fig. 4.1). It was noted that because the plasmid Bluescript KS- has the *lacZ* gene and is a multicopy plasmid that does not make its own *lac* repressor, the host *lacI* repressor is titrated out between the host *lacO* and the plasmid *lacO*, hence there was a high background of T7 RNA polymerase expression of toxic *nqr* genes in the absence of induction, i.e. NqrC was expressed in the absence of IPTG induction. Therefore it was eliminated as a candidate vector for expression.

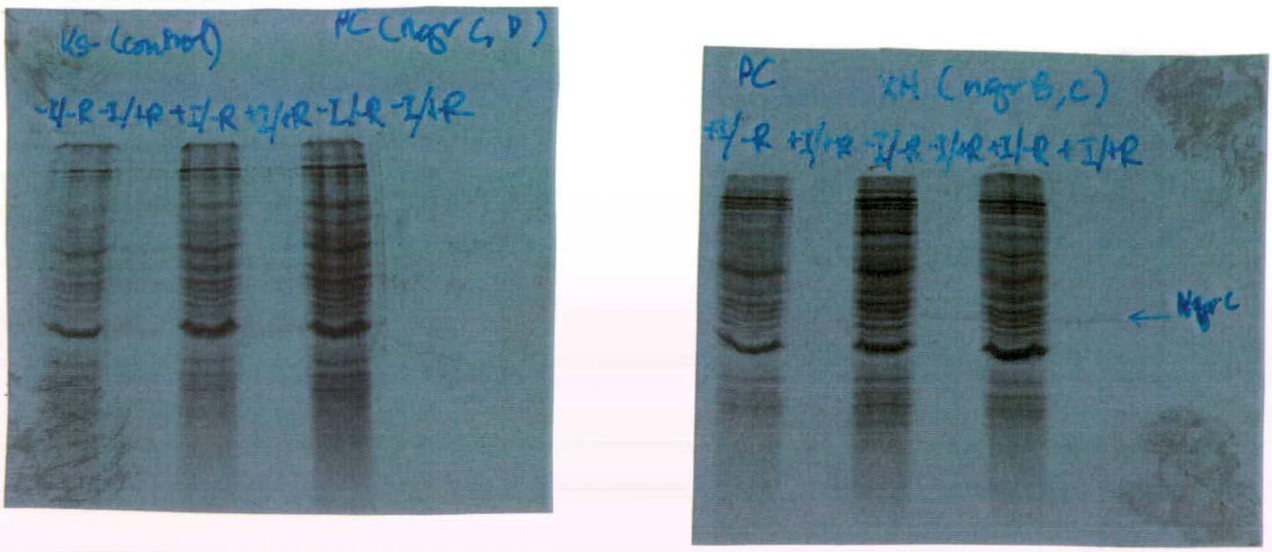

Fig. 4.1 Autoradiograph illustrating pulse-chase radiolabelling of NqrB, NqrC and NqrD expressed by BL21(DE3)p*LysS*.

-I/-R: no IPTG induction, no rifampicin inhibition of host protein synthesis, i.e. total protein expressed by the expression host.
-I/+R: no IPTG, with rifampicin, i.e. control showing the background of protein expression from the plasmid in the absence of induction and in the absence of host-synthesized proteins.
+I/-R: with IPTG, no rifampicin, i.e. total protein expressed by the host, including induced protein from the plasmid.
+I/+R: with IPTG, with rifampicin, i.e. protein expressed from the plasmid upon induction.

KS-: control BL21(DE3)p*LysS* strain with pBluescript KS- plasmid used for cloning gene(s) to be expressed.
PC: BL21(DE3)p*LysS* with *nqrC* and *nqrD* cloned into pBluescript KS-.
XH: BL21(DE3)p*LysS* with *nqrB* and *nqrC* cloned into pBluescript KS-.

4.4.2 Pulse-chase radiolabelling of expressed NqrB, NqrC and NqrD

A 2.9 kb *XbaI/ClaI* DNA fragment (comprising *nqr*B, *nqr*C and *nqr*D) was inserted into pET16b (pKT01, Fig. 4.2), transformed into BL21(DE3)p*LysS* and expressed upon IPTG induction. The radiolabelling of proteins expressed by this clone, shown in the autoradiographs (Fig. 4.3), indicate the presence of 3 proteins expressed from the cloned insert. A clear dark band at the correct molecular weight of 32 kDa was attributed to NqrC which is a relatively hydrophilic protein. NqrB (50 kDa) is indicated by the higher faint band while NqrD (28 kDa) is represented by the lower faint band. From previous hydrophobic plots of the primary sequences of NqrB, NqrC and NqrD, NqrB and NqrD were predicted to be highly hydrophobic transmembrane polypeptides while NqrC is more hydrophilic. Due to the extreme hydrophobic nature of NqrB and NqrD, they migrated as diffuse bands in denaturing polyacrylamide gels and their M_r appeared anomalous and smaller than expected. This is not an unusual phenomenon as this was also clearly the case for the mitochondrially-encoded ND1-ND6 subunits of the proton-translocating NADH-ubiquinone oxidoreductase of *Bovine taurus* (Walker, 1992).

As the genes in this clone were not cloned at the translational start of the vector, this could account for the poor repression by the T7*lac* promoter in the absence of IPTG inducer, therefore some expression of the proteins of interest occurred in the absence of induction.

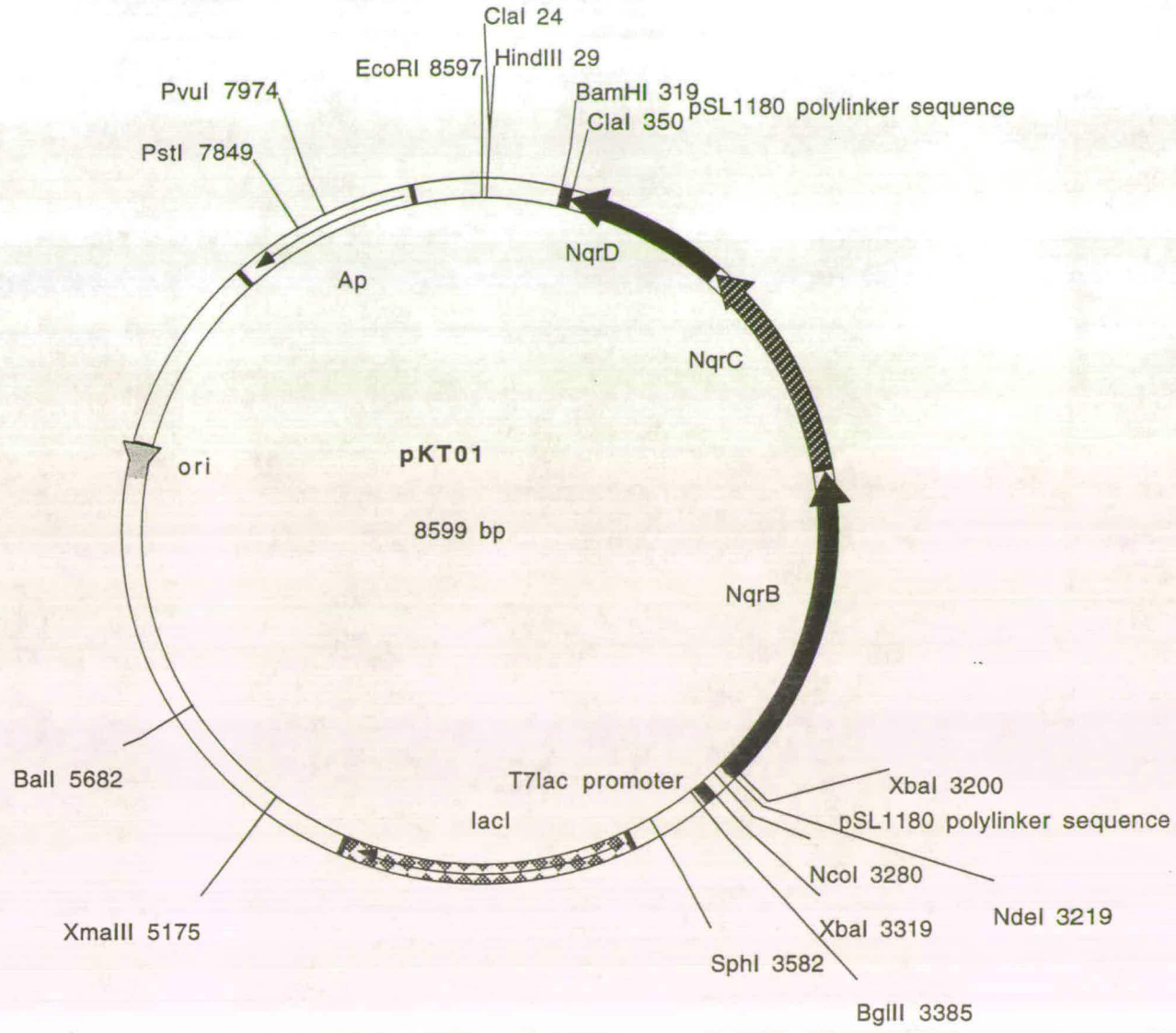

Plasmid name: pKT01
Plasmid size: 8599 bp
Constructed by: Karen Tan
Construction date: 1994
Comments/References: NqrB, NqrC and NqrD cloned into pET16-b using polylinker pSL1180.

Fig. 4.2 Plasmid map of pKT01. Contruction of pKT01 achieved by cloning *nqrB, nqrC* and *nqrD* into pET16b.

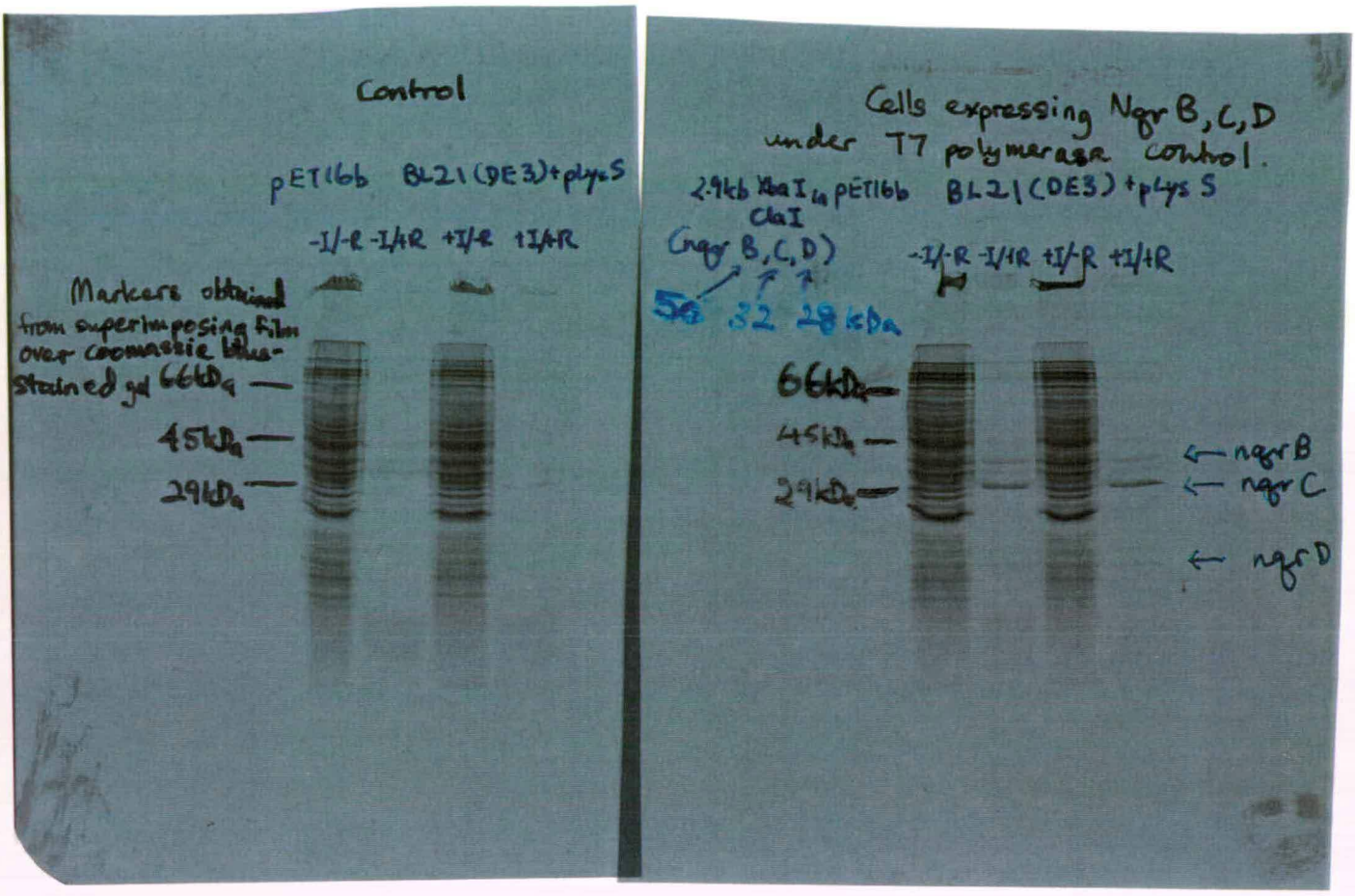

Fig. 4.3 Autoradiograph illustrating pulse-chase radiolabelling of NqrB, NqrC and NqrD expressed by BL21(DE3)p*LysS*.

-I/-R: no IPTG induction, no rifampicin inhibition of host protein synthesis, i.e. total protein expressed by the expression host.
-I/+R: no IPTG, with rifampicin, i.e. control showing the background of protein expression from the plasmid in the absence of induction and in the absence of host-synthesized proteins.
+I/-R: with IPTG, no rifampicin, i.e. total protein expressed by the host, including induced protein from the plasmid.
+I/+R: with IPTG, with rifampicin, i.e. protein expressed from the plasmid upon induction.

pET16b: control BL21(DE3)p*LysS* strain with pET16b plasmid used for cloning gene(s) to be expressed.
pKT01: BL21(DE3)p*LysS* with *nqrB, nqrC* and *nqrD* cloned into pET16b.

4.5 Cloning and expression of *nqr*E and *nqr*F

4.5.1 Cloning of *nqr*E and *nqr*F

With the discovery of λ clones comprising the 2.3 kb *Kpn*I/*Sal*I region expressing a product that was detected with NADH dehydrogenase activity staining and Western blotting with antibodies raised against the NqrF subunit (Hayashi *et al.*, 1994), a comparison of their restriction map with our map ensued. Consequently, we found a good indication that the catalytic subunit is present in our 10.7 kb λ clone and is downstream of *nqr*E. Hence, subcloning and sequencing had resumed to identify and analyse this catalytic subunit. The superlinker phagemids pSL1180 (Fig. 2.4) and pSL1190 (Fig. 2.5) which contain useful multiple cloning sites (superlinkers) were used. The 2.3 kb *Kpn*I/*Sal*I and 1.9 kb *Xba*I/*Sal*I fragments were ligated into pET16b with the help of superlinker sites *Nde*I and *Eco*RI in pSL1180 forming plasmid pKT02 (Fig. 4.4). These were first transformed into DH5αF'IQ and plasmids were purified and concentrated before being transformed into BL21(DE3)p*LysS* for expression.

In addition, *nqr*F was also cloned into pET16b using its translational start site *Nde*I. The *Nde*I site was engineered into *nqr*F using PCR, as with *nqr*A. The 5'-terminal region of *nqr*F was cut with *Nde*I and *Hin*dIII, and ligated into pKT02. Plasmid pKT02 comprised the *nqr*E and *nqr*F genes; cleavage with *Nde*I and *Hin*dIII removed the *nqr*E gene and ligation of the 5'-terminal PCR-generated DNA fragment of *nqr*F resulted in a complete *nqr*F gene (but no *nqr*E) ligated at the translational ATG start, tagged with Histidine residues at the 5'-terminal region (pKT03, Fig. 4.5). This construct gave the potential for the catalytic subunit to be expressed and purified easily in one step by His·Tag binding to a nickel chelation column.

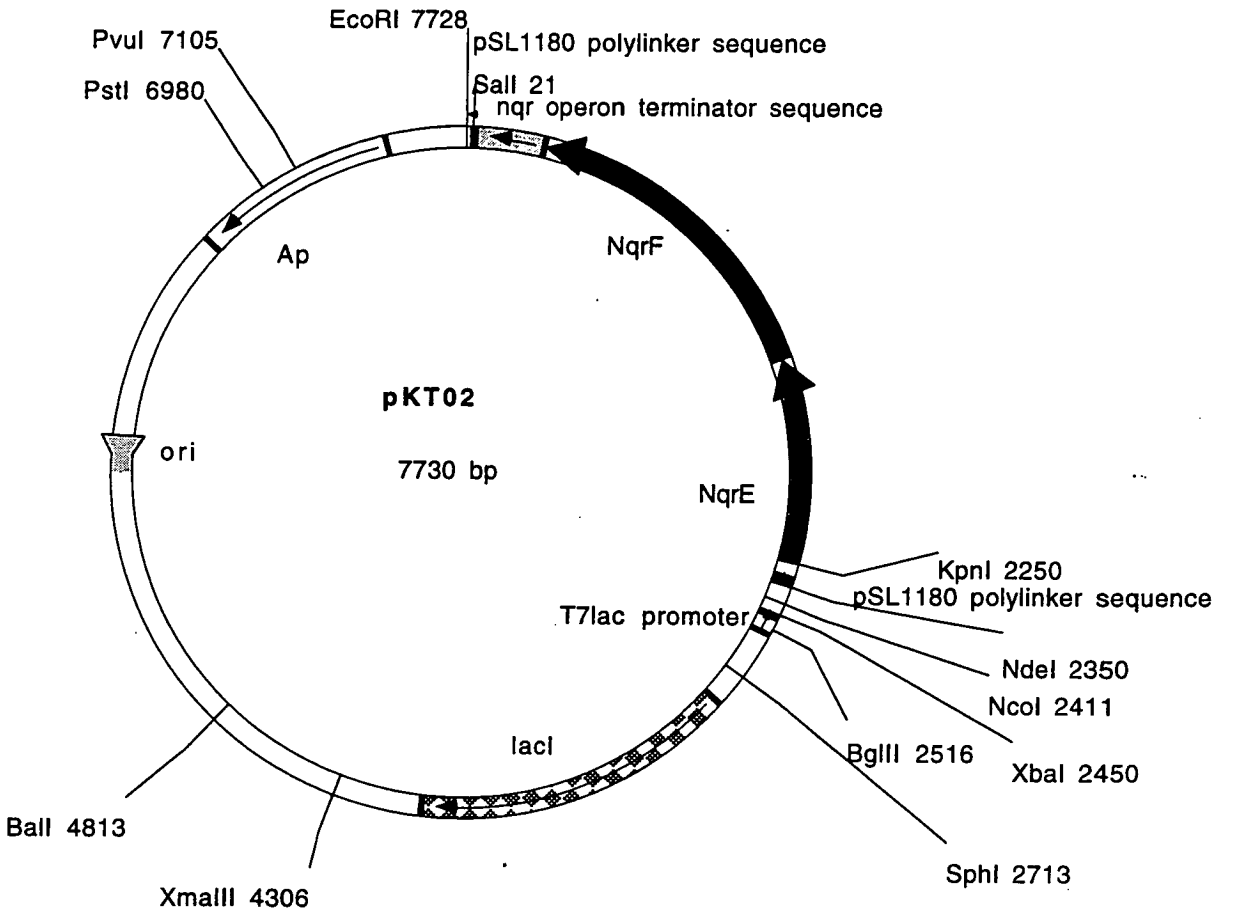

Plasmid name: pKT02
Plasmid size: 7730 bp
Constructed by: Karen Tan
Construction date: 1995
Comments/References: NqrE and NqrF cloned into pET16-b using polylinker pSL1180.

Fig. 4.4 Plasmid map of pKT02. pKT02 was constructed by cloning *nqrE* and *nqrF* into pET16b with the use of pSL1180 polylinker sequences.

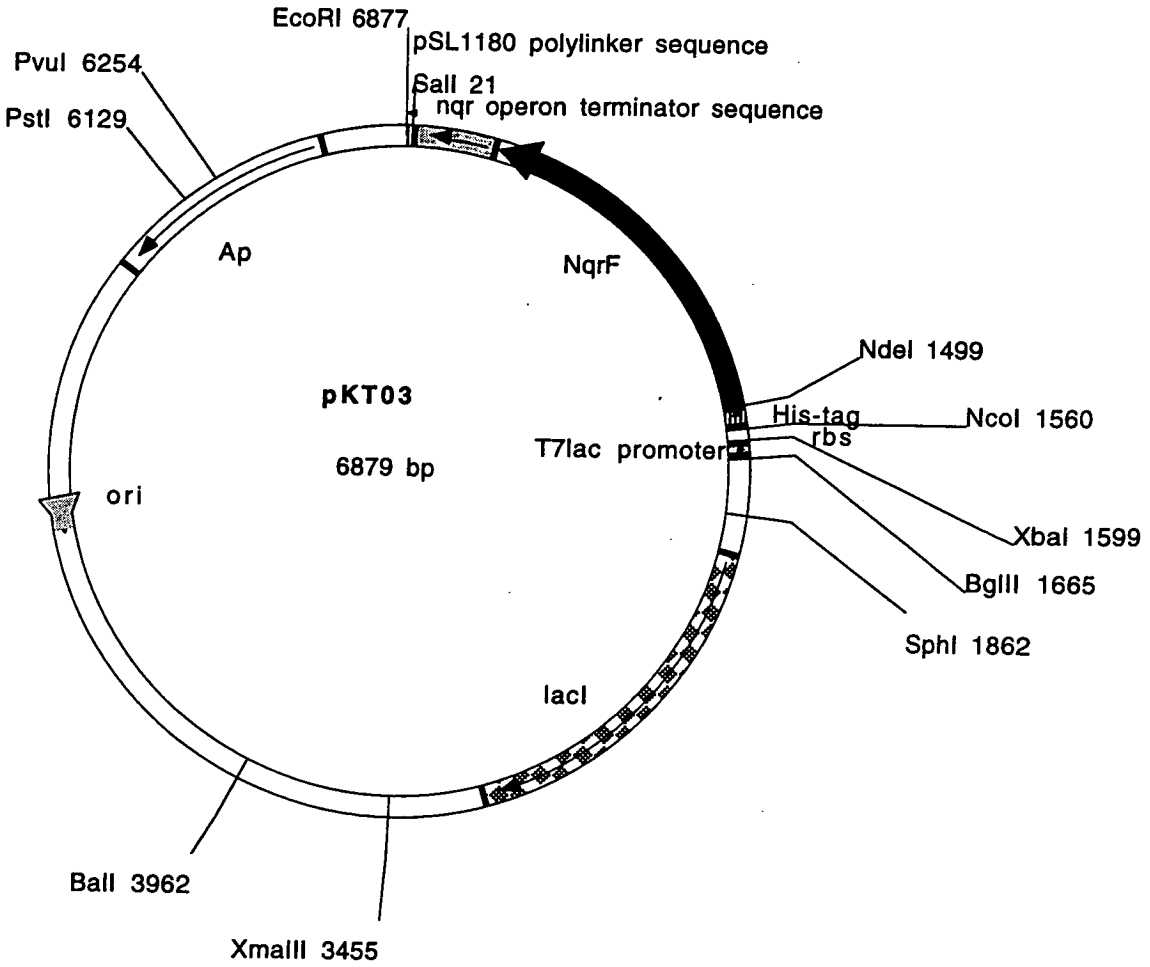

Plasmid name: pKT03
Plasmid size: 6879 bp
Constructed by: Karen Tan
Construction date: 1995
Comments/References: NqrF cloned into pET16-b at its translational start at NdeI using PCR so that expressed NqrF is His-tagged at N-terminal.

Fig. 4.5 Plasmid map of pKT03. *NqrF* was cloned into the translational start of pET16b at *Nde*I (using PCR to produce the N-terminal fragment), in order to generate pKT03. Expressed NqrF will be His-tagged at the N-terminal.

4.5.2 Pulse-chase radiolabelling of expressed NqrE, NqrF

NqrE and NqrF (46kDa) were expressed in BL21(DE3)p*LysS*, transformed with pKT02, derived from pET16b (Fig. 4.4). Using transformants kept refrigerated for a week as inoculants for expression studies, NqrE was strongly expressed by the T7 RNA polymerase but this seemed to be a constitutive expression even in the absence of IPTG (Fig. 4.6). This clone was slow to grow compared with other similar clones, probably due to the insertion of high amounts of recombinant membrane protein. However, NqrF does not seem to be overexpressed upon IPTG induction in this clone from this one-week old culture (Fig. 4.6) and this provides further evidence to support the concept that NqrF is toxic to the cells and therefore the cells stop expressing it after storage for just 1 week at 4°C. In fresh cultures of the same strain containing the same plasmid (pKT02), 46 kDa NqrF was clearly expressed as well as 28 kDa NqrE. NqrF was identified as the distinct 46 kDa protein band on the autoradiographs, overexpressed upon induction by IPTG. The more hydrophobic NqrE was represented by a faint weak band at about 28 kDa (Fig. 4.7 and Fig 4.8).

4.5.3 Pulse-chase radioloabelling of expressed His-tagged NqrF

Some His-tagged NqrF (from the clone comprising pKT03, Fig. 4.5) was expressed in the absence of IPTG, and much more was expressed when induced (Fig. 4.9 and 4.10). 2 bands were observed in each case, supporting and confirming later observations of SDS and native gels where 47 kDa His-tagged NqrF has degraded at a specific *N*-terminal point to form a 39 kDa protein. This established why binding to the His-Trap chelating column was poor as the *N*-terminal region containing the His-tag had been cleaved.

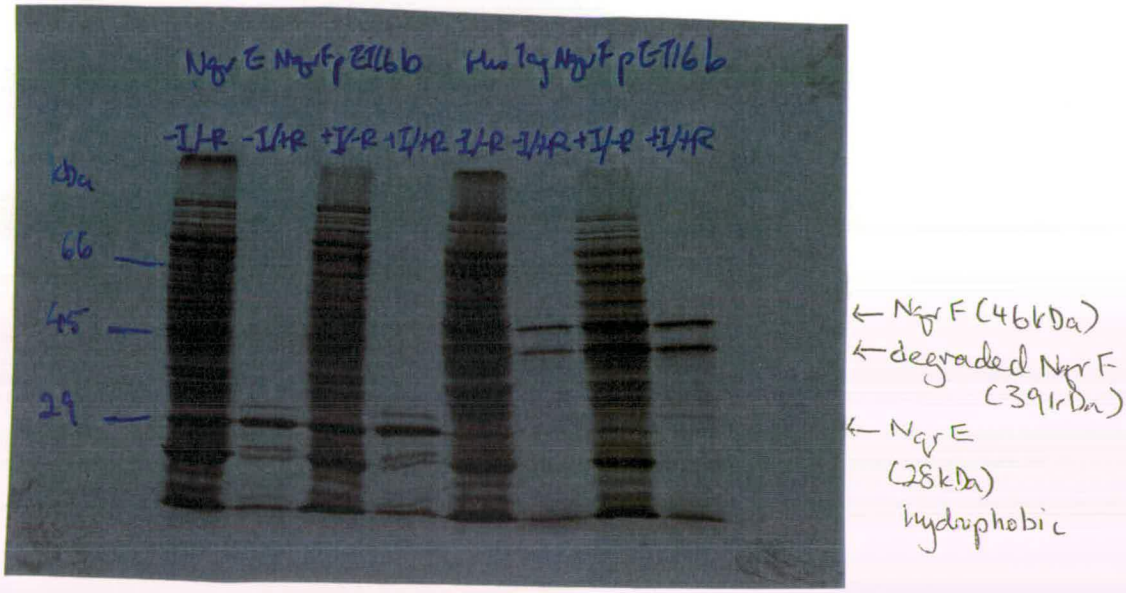

Fig. 4.6 Autoradiograph illustrating pulse-chase radiolabelling of NqrE and NqrF expressed by BL21(DE3)p*LysS* (old cultures).

-I/-R: no IPTG induction, no rifampicin inhibition of host protein synthesis, i.e. total protein expressed by the expression host.
-I/+R: no IPTG, with rifampicin, i.e. control showing the background of protein expression from the plasmid in the absence of induction and in the absence of host-synthesized proteins.
+I/-R: with IPTG, no rifampicin, i.e. total protein expressed by the host, including induced protein from the plasmid.
+I/+R: with IPTG, with rifampicin, i.e. protein expressed from the plasmid upon induction.

pET16b: control BL21(DE3)p*LysS* strain with pET16b plasmid used for cloning gene(s) to be expressed.
pKT02: BL21(DE3)p*LysS* with *nqrE* and *nqrF* cloned into pET16b.

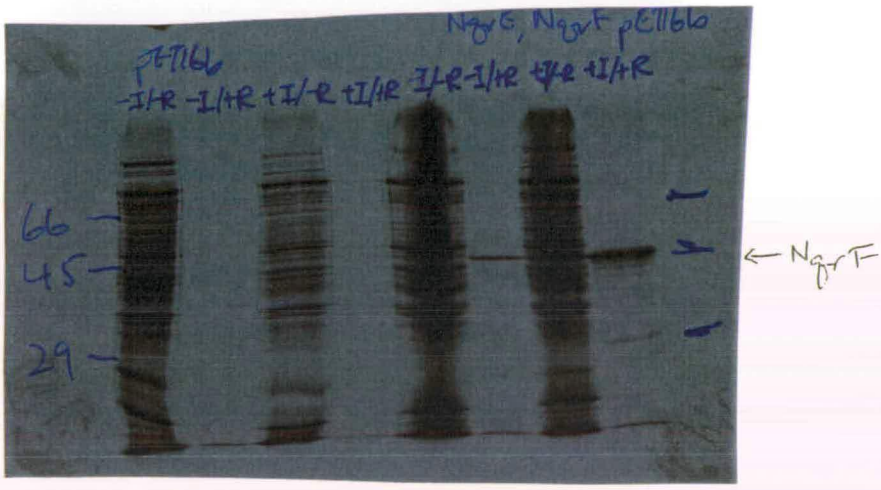

Fig. 4.7 Autoradiograph illustrating pulse-chase radiolabelling of NqrE and NqrF expressed by BL21(DE3)p*LysS* (new cultures).

-I/-R: no IPTG induction, no rifampicin inhibition of host protein synthesis, i.e. total protein expressed by the expression host.
-I/+R: no IPTG, with rifampicin, i.e. control showing the background of protein expression from the plasmid in the absence of induction and in the absence of host-synthesized proteins.
+I/-R: with IPTG, no rifampicin, i.e. total protein expressed by the host, including induced protein from the plasmid.
+I/+R: with IPTG, with rifampicin, i.e. protein expressed from the plasmid upon induction.

pET16b: control BL21(DE3)p*LysS* strain with pET16b plasmid used for cloning gene(s) to be expressed.
pKT02: BL21(DE3)p*LysS* with *nqrE* and *nqrF* cloned into pET16b.

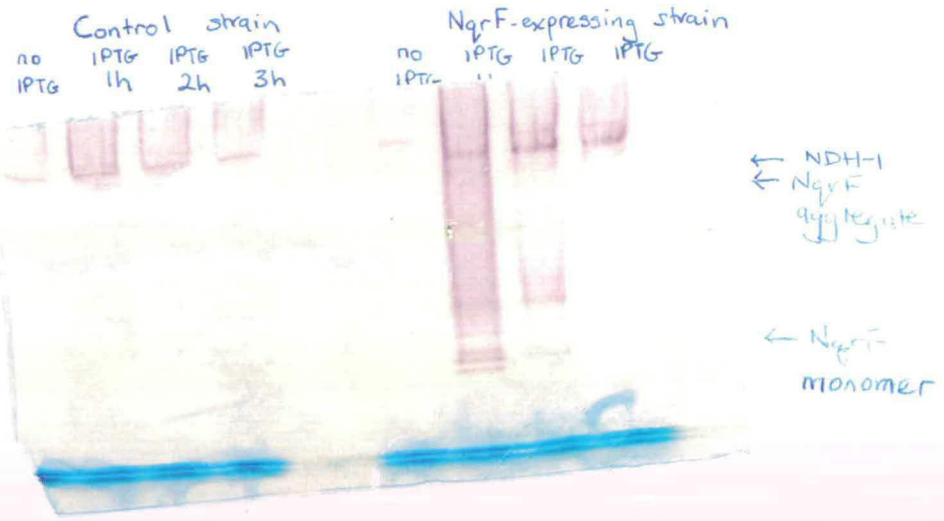

Fig. 4.8 Zymogram stain of 10% native PAGE gel demonstrating NADH dehydrogenase activity in BL21(DE3)p*LysS* cells expressing NqrF. Control strain contains only pET16b without cloned insert.
no IPTG: uninduced cells.
IPTG 1h: cells after 1h induction with IPTG.
IPTG 2h: cells after 2h induction with IPTG.
IPTG 3h: cells after 3h induction with IPTG.

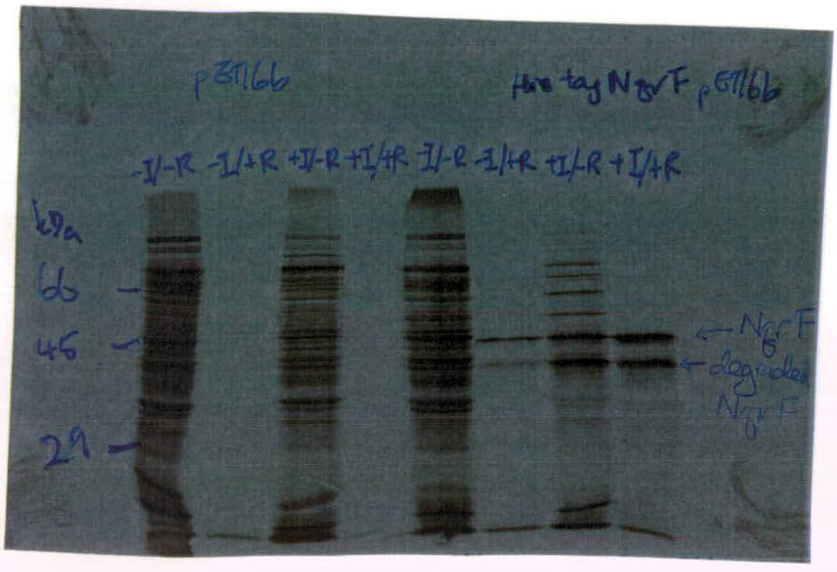

Fig. 4.9 Autoradiograph illustrating pulse-chase radiolabelling of His-tagged NqrF expressed by BL21(DE3)p*LysS*.

-I/-R: no IPTG induction, no rifampicin inhibition of host protein synthesis, i.e. total protein expressed by the expression host.
-I/+R: no IPTG, with rifampicin, i.e. control showing the background of protein expression from the plasmid in the absence of induction and in the absence of host-synthesized proteins.
+I/-R: with IPTG, no rifampicin, i.e. total protein expressed by the host, including induced protein from the plasmid.
+I/+R: with IPTG, with rifampicin, i.e. protein expressed from the plasmid upon induction.

pET16b: control BL21(DE3)p*LysS* strain with pET16b plasmid used for cloning gene(s) to be expressed.
pKT03: BL21(DE3)p*LysS* with *nqrF* cloned into pET16b at the translational start to allow tagging with His residues at the N-terminal.

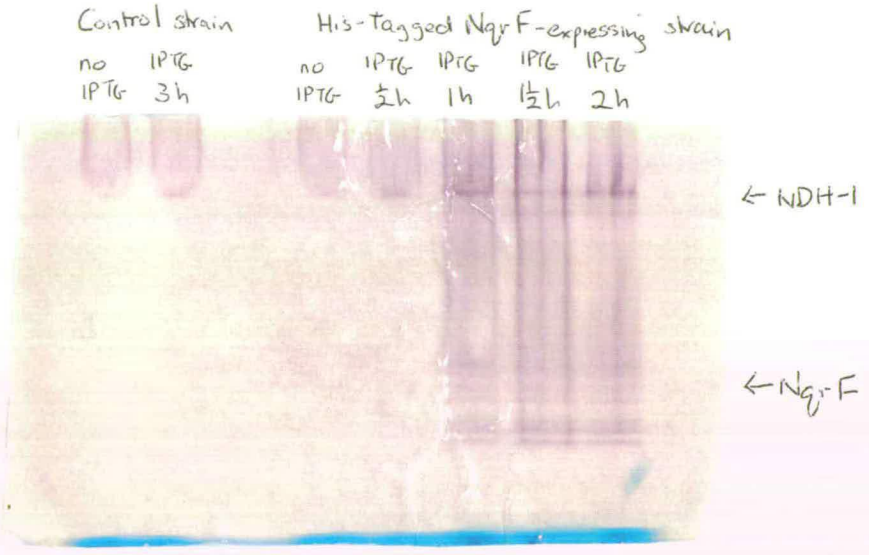

Fig. 4.10 Zymogram stain of 10% native PAGE gel demonstrating NADH dehydrogenase activity in BL21(DE3)p*LysS* cells expressing His-tagged NqrF. Control strain contains only pET16b without cloned insert.
no IPTG: uninduced cells.
IPTG 1/2h: cells after 1/2h induction with IPTG.
IPTG 1h: cells after 1h induction with IPTG.
IPTG 1 1/2h: cells after 1 1/2h induction with IPTG.
IPTG 2h: cells after 2h induction with IPTG.
IPTG 3h: cells after 3h induction with IPTG.

4.5.4 Pulse-chase radiolabelling of expressed NqrF cloned into pT7-7

BL21(DE3)p*LysS* containing pKT04 (Fig. 4.11) expressed NqrF when induced by IPTG. Plasmid pKT04, a derivative of pT7-7 (Fig. 2.7), expressed native NqrF at the right molecular weight of 46 kDa when IPTG was added (Fig. 4.12). However, there was a high basal level expression of NqrF in the absence of inducer IPTG due to poor repression in the absence of a *lac* operator and *lacI* in pT7-7 (but present in pET16-b). This had a very undesired effect on the *E .coli* cells as they grew poorly and as much as five times slower compared with the other clones previously mentioned, due to the high amounts of toxic NqrF expressed and inserted into their cell membranes, even in the absence of inducer, IPTG.

In all controls, the parental plasmid-containing strains showed the absence of proteins expression when induced by IPTG, in the presence of rifampicin.

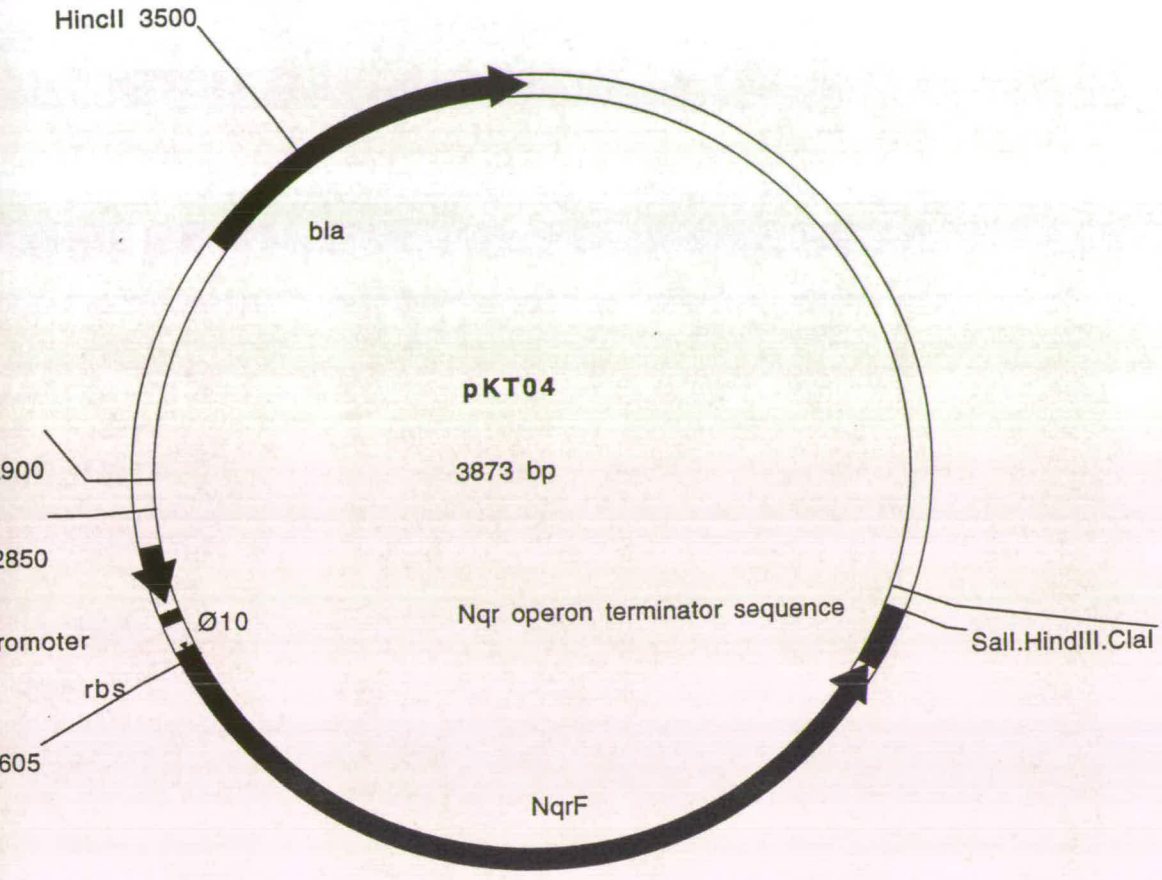

lasmid name: pKT04
lasmid size: 3873 bp
Constructed by: Karen Tan
Construction date: 1996
Comments/References: NqrF cloned into pT7-7.

Fig. 4.11 Plasmid map of pKT04. This was constructed by cloning *nqrF* into the translational start of pT7-7 at *Nde*I.

Fig. 4.12 Autoradiograph illustrating pulse-chase radiolabelling of NqrF expressed by BL21(DE3)p*LysS*.

-I/-R: no IPTG induction, no rifampicin inhibition of host protein synthesis, i.e. total protein expressed by the expression host.
-I/+R: no IPTG, with rifampicin, i.e. control showing the background of protein expression from the plasmid in the absence of induction and in the absence of host-synthesized proteins.
+I/-R: with IPTG, no rifampicin, i.e. total protein expressed by the host, including induced protein from the plasmid.
+I/+R: with IPTG, with rifampicin, i.e. protein expressed from the plasmid upon induction.

pT7-7: control BL21(DE3)p*LysS* strain with pT7-7 plasmid used for cloning gene(s) to be expressed.
pKT04: BL21(DE3)p*LysS* with *nqrF* cloned into pT7-7 at the translational start to allow tagging with His residues at the N-terminal.

4.6 Difficulties with expression and troubleshooting

Problems encountered in the expression studies and techniques to counteract the problems, are outlined below:

- **Protein toxicity**

Due to protein toxicity, transformants kept over 3 days even at 4°C, lost expression abilities. No transformants of the complete *nqr*A gene could be obtained despite using tightly-regulated promoters. Fresh transformants were always used within 1-2 days and IPTG solutions were freshly made. Protein toxicity causes the over-expresssing cells to grow slowly or die. Minimal medium was used to grow cells to exponential phase and not beyond to avoid protein toxicity. Carbenicillin was used instead of ampicillin so that plasmid-bearing strains are selected. When genes produce toxic proteins, β-lactamase which is produced in high amounts and secreted into the medium, can afford other cells protection from ampicillin (not carbenicillin) even though they have lost the plasmid and have stopped producing β-lactamase (Novagen pET system manual).

Plasmids, such as pBluescript KS- and pT7-7, that are not tightly regulated for expression could not be used as small amounts of toxic Nqr protein are expressed while cells are starting to grow, even in the absence of inducer. The use of pBluescript KS- vector was avoided as this system produces cells that are very leaky, which is undesirable for membrane proteins. Cells were induced only when necessary. Phage mGP1-2, an M13 derivative that carries T7 RNA polymerase genes, to infect at induction point, could be used. Other vectors such as pT7 or pET with T7 polymerase system and in the latter case, with a *lacI* gene and *lac* operator just before ribosome binding sites, were used to clone genes at the ATG translational start site. These T7 vectors are expressed in the host BL21(DE3)p*LysS*. PCR was used to create restriction sites to allow cloning at ATG translational initiation codon of T7*lac* vectors to allow tighter regulation of expression to prevent high background expression of toxic proteins.

- **BL21(DE3)p*LysS* has a very low transformation frequency unless competent cells are purchased from the supplier Novagen.**

Ligation mixes were transformed into DH5αF'IQ (contains no T7 RNA polymerase genes), plasmid DNA was then purified from transformants and subsequently transformed at high concentration into BL21(DE3)pLysS.

- **Aeration**

Na^+-NQR is an aerobic respiratory chain enzyme, therefore cells were shaken in flasks of capacity 10 times volume of culture liquid, kept shaking continuously and prevented from stopping for longer than 1 min, or vigorously aerated in a 50 ℓ fermenter vessel.

- **Inclusion bodies**

Membrane proteins tend to form inclusion bodies so cells were grown at 25°C to minimise this (Gould, 1994). Inclusion bodies could be separated from cell preparations by mechanical techniques, sonication or lysozyme and detergents, then pelleted by centrifugation. The protein is then solubilized and refolded. Alternatively, 10% (w/v) SDS and β–mercaptoethanol from sample buffer were added directly to samples and vortexed, in order to get proper migration of protein on SDS-PAGE gels.

- **Degradation of proteins**

Pulse-chase radiolabelling of expressed protein could be done when all that was required is a visual confirmation by detection of expression of the target protein. Serine protease inhibitors such as PMSF and metalloprotease inhibitors such as EDTA were added to cultures to prevent degradation. Cell fractions and proteins were stored or processed at 4°C.

4.7 Large scale NqrF expression and purification

From results obtained from previous small scale expression and radiolabelling studies, the pET16b T7*lac*-BL21(DE3)p*LysS* system was chosen as the expression system, and scaled up to large volume to produce enough protein for purification and subsequent characterisation.

4.7.1 Qualitative and quantitative sample measurements

All samples from cell fractions and purification column fractions were measured quantitatively for magnitude of NADH dehydrogenase activity using NADH menadione oxidase assays, run on Coomassie brilliant blue-stained SDS polyacrylamide gels to check purity of sample and also run on native polyacrylamide gels with 1% (v/v) Triton X-100, which were stained for NADH dehydrogenase activity. Protein concentrations of samples were determined using the Peterson's Lowry-derived method. Using all these values, specific activities, purification factors, yields were calculated and tabulated.

4.7.2 Expression, sonication and membrane extraction

Preliminary expression results

Results in Fig. 4.13 and 4.14 showed that there was NADH dehydrogenase activity in a protein represented by a high M_r band (greater than 100 kDa) in all membrane samples (pET16b, pKT01 and pKT02). This was attributed to the presence of the H^+-translocating NADH-ubiquinone oxidoreductase present in the membranes of the host BL21(DE3)p*LysS*. There also appeared to be a slightly higher M_r activity-stained band for clones overexpressing NqrF (pKT02) and this can be attributed to the NqrF subunit binding to the H^+ NDH-1 complex in the host or other *E. coli* proteins, or the formation of NqrF aggregates. A band demonstrating NADH dehydrogenase activity at about the correct M_r (46 kDa) for NqrF emerged only in the pKT02 clones. Several slightly lower M_r bands below the broad 46 kDa band may indicate degradation of NqrF or while the faint higher M_r bands suggest there may be a

possible equilibrium of NqrF between monomers, dimers and trimers. There were activity-stained bands at different molecular weights in all cytoplasmic samples probably due to cytoplasmic NADH oxidases and a small amount of NqrF dislodged from the membrane from over-sonication and hence accumulating in the cytoplasm. The predominant presence of NqrF in the membranes was slightly surprising as it was predicted to be mainly hydrophilic from hydropathy plots. Nevertheless, its hydrophobic *N*-terminal region could be responsible for its attachment to the membrane (see predicted membrane model, Fig. 3.7).

The membrane samples were then run on 10% (w/v) and 12% (w/v) SDS-PAGE gels and stained with Coomassie brilliant blue. Control pET16b showed a few faint bands but no protein obviously over-produced. pKT02 clones produced a very distinct thick band at about 46 kDa, showing that NqrF was being overproduced. This 46 kDa protein was the major band in the membrane fraction. The pKT01 clones produced bands at 44 kDa, 35 kDa and 30 kDa indicating the expression of NqrB, NqrC and NqrD. When run on native gels, all pKT02 preparations showed varying degrees of degradation patterns for NqrF even with the addition of PMSF during expression and sonication (Fig. 4.14).

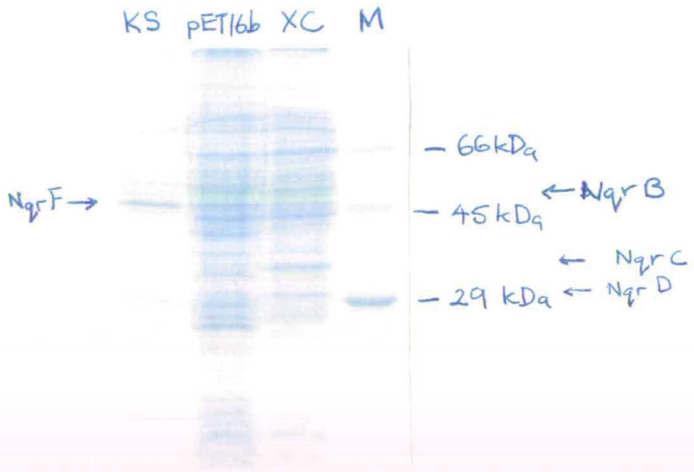

Fig 4.13 Coomassie Blue-stained 10% SDS PAGE gel demonstrating expression of NqrF upon IPTG induction.

M: Markers: Bovine serum albumin, 66 kDa; Chicken egg ovalbumin, 45 kDa; Carbonic anhydrase, 29 kDa.

pET16b: control BL21(DE3)p*LysS* cells with only pET16b.
KS: cells with *nqrE* and *nqrF* cloned into pET16b.
XC: cells with *nqr B, nqrC* and *nqrD* cloned into pET16b.

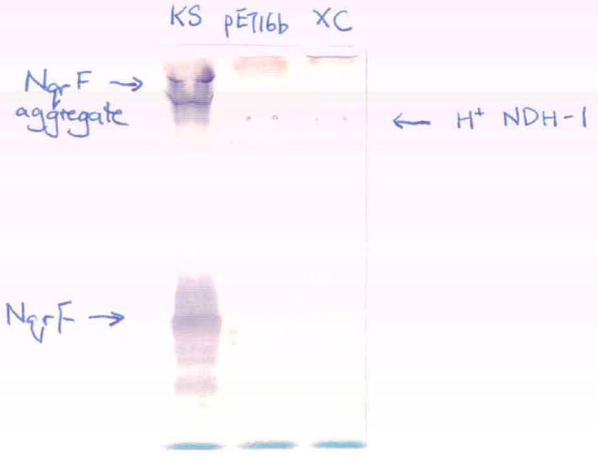

Fig. 4.14 Zymogram stain of 10% native PAGE gel demonstrating NADH dehydrogenase activity in cells expressing NqrF.

pET16b: control BL21(DE3)p*LysS* cells with only pET16b.
KS: cells with *nqrE* and *nqrF* cloned into pET16b.
XC: cells with *nqr B, nqrC* and *nqrD* cloned into pET16b.

4.8 Cell fractionation/spheroplasting

SDS and native zymogram gels of the various fractions have confirmed that native NqrF is a membrane protein. NqrF is only present in the membrane fraction of the cells expressing it. Activity assays have concurred with the above conclusion; although there is much NADH dehydrogenase activity in the cytoplasmic fraction, this activity is not Ag^{+}-sensitive, a well-documented (Bourne and Rich, 1992) characteristic of NqrF, unlike the Ag^{+}-sensitive NqrF NADH dehydrogenase activity present in the membrane (Fig. 4.15). As this cytoplasmic NADH dehydrogenase activity was not Ag^{+}-sensitive, it was concluded that it originates from NDH-2 not Na^{+}-NQR. Inhibitor sensitivity of NADH dehydrogenase activity in the various cell fractions is further discussed in Chapter 6.

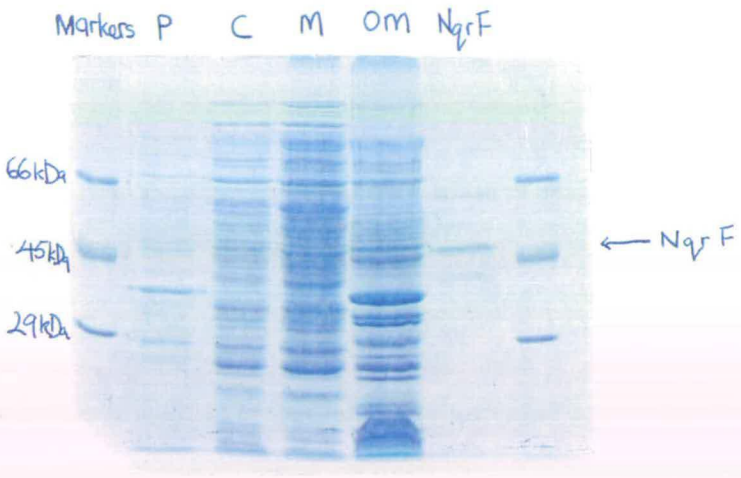

Fig. 4.15 Coomassie Blue-stained 10% SDS PAGE gel illustrating the distribution of proteins in various cell fractions of BL21(DE3)pLysS expressing NqrF from pET16b (pKT02).

Markers: Bovine serum albumin, 66 kDa; Chicken egg ovalbumin, 45 kDa; Carbonic anhydrase, 29 kDa.
P: periplasmic fraction
C: cytoplasmic fraction
M: inner membrane detergent-extract
OM: outer membrane pellet
NqrF: purified NqrF

Chapter 5

Results and Discussion

Protein purification

5.1 3-step purification procedure

5.1.1 First column

5.1.1.1 Ion exchange chromatography DEAE sepharose CL6B (Pharmacia)

Proteins carry both positively and negatively charged groups on their surface due to acidic negative chains (aspartic, glutamic acids, *C*-terminal-carboxyl groups, cysteine residues) and basic positive side chains (histidine, lysine, arginine, and *N*-terminal amines). The relative charge on a protein depends on the relative number of positive and negative groups and this varies with pH. The pH where a protein has equal number of positively and negatively charged groups is termed its isoelectric point. Above their pI, proteins have net negative charge while below its pI, proteins have a net positive charge. An increasing linear gradient of NaCl provides anionic counter-ions of Cl^- which 'screen' exchanger groups and prevent their binding with protein, consequently eluting the proteins.

DEAE sepharose was chosen as the matrix for the first column as it has a very high loading and binding capacity, and a fast flow rate that did not compromise resolution. This anionic-exchange column was selected as the predicted pI of NqrF was 4.54 and the protein complex appears to be stable at high pHs. Using a Tris-HCl buffer at pH 8.0 would give rise to a negatively-charged NqrF subunit which would bind to the anionic column and be eluted with an increasing salt gradient. All chromatography columns were run at 4°C.

Preliminary observations

Membrane fractions containing NqrF, obtained from large-scale expression cultures, were loaded onto the DEAE sepharose column. Fractions eluting at 0.15 M NaCl were orange/brown, indicating perhaps a cytochrome or Fe-S protein was

present, while fractions at 0.2 M NaCl were bright yellow, suggesting the presence of a flavoprotein. Using NADH/dNADH-menadione oxidase assays to analyse every fifth fraction, there appeared to be a distinct peak of NADH dehydrogenase activity eluting at 0.19 M NaCl, within the yellow fractions. Fractions with the highest specific activities were pooled and used for the next purification step.

Protein concentration was measured using Peterson's modified Lowry method (Peterson, 1977) because conventional spectrophotometry methods relied on absorbance at 280 nm, which was the absorbance maximum of Triton X-100 present in the buffers. Results indicate that proteins in the initial membrane preparation were well separated, with a protein peak at initial wash fractions (unbound protein) and a large major protein peak at 0.15 M NaCl, tapering at 0.2 M NaCl. There seemed to be good purification as the activity peak emerges just after the major protein profile peak (Fig. 5.1).

On running fractions distributed over the entire elution profile on 10% native PAGE gels, zymogram stains detected NADH dehydrogenase activity increasing progressively from samples eluting at about 0.2 M NaCl (Fig. 5.2 and 5.3). Zymogram-stained bands at the correct M_r (46 kDa) in these fractions were similar to ones observed in recombinant membrane fractions but not present in control membrane fractions (i.e., this 46 kDa band was verified as protein expressed from cloned DNA and not a native protein of *E. coli* or a product coded by the pET16b plasmid). The degradation pattern of the 46 kDa band that was conspicuous in crude membrane extracts, was not as prominent here, perhaps due to purification of the protein of interest from some proteases present in the crude membrane fraction (Fig. 5.3). Just one very high M_r band was observed as opposed to two high M_r bands previously seen in crude membrane extracts. The slightly lower M_r band which was seen in all samples including control samples, was attributed to the native H^+-translocating NADH-ubiquinone oxidoreductase in *E. coli*. This was not present in the DEAE sepharose column-purified membrane samples, a good indication that the expressed NqrF had now been purified from the native H^+-translocating NDH-1

complex. The other high M_r band present in the samples expressing NqrF could be explained by the possibility that the catalytic NqrF subunit bound to another *E. coli* protein, or that the hydrophobic NqrF subunits formed aggregates, the latter reason being most likely. Coomassie brilliant blue-stained SDS polyacrylamide gels indicated good purification from major proteins present in crude membrane extractions (Fig. 5.4). Please note that the fraction numbers do not match up between the elution profiles and the gels because different volumes of the NaCl gradient were applied due to using different bed volumes of DEAE matrix to get the profile results (Fig. 5.1) and the gel results (Fig. 5.2-5.4), i.e. different runs.

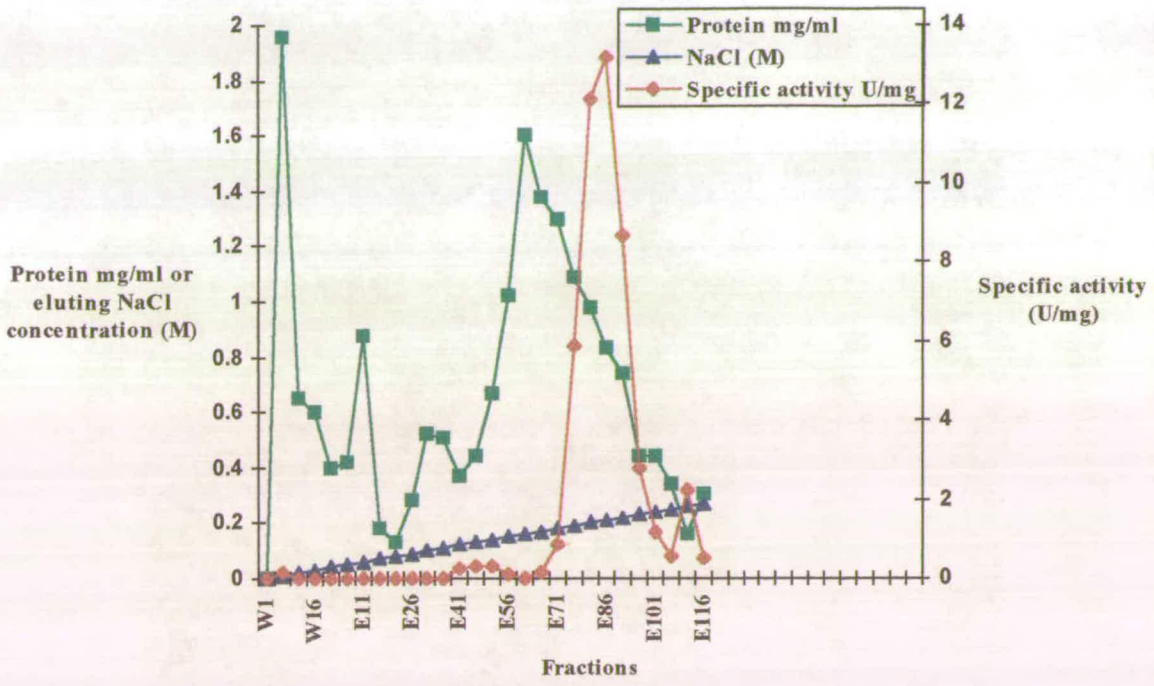

Fig. 5.1 DEAE Sepharose CL-6B ion exchange chromatography protein elution profile.

Ion exchange chromatography

DEAE sepharose CL6B (Pharmacia)

Membrane preparations were loaded onto a DEAE sepharose fast flow column in a 21 cm x 2.5 cm bed volume, equilibrated with 50 mM Tris-HCl, pH 8.0, 5 mM EDTA, 10% (v/v) glycerol, 0.1 mM PMSF, 1 mM DTT and 0.1% (w/v) Triton-X-100. Elution of proteins at 80 ml/h from the DEAE sepharose column was employed with the creation of 4 bed volumes of an increasing linear gradient from 0 to 0.5 M NaCl.

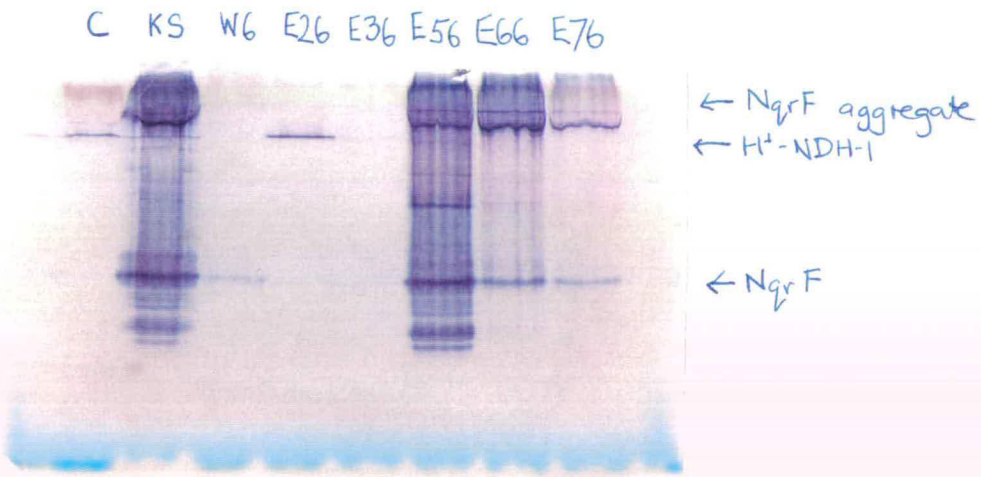

Fig. 5.2 Zymogram stain of 10% native PAGE gel illustrating NADH dehydrogenase activity in various DEAE Sepharose fractions.

C: membrane extract of control BL21(DE3)p*LysS* cells with pET16b.
KS: membrane extract of BL21(DE3)p*LysS* cells expressing NqrF from pET16b (pKT02).
W6: Wash fraction 6 from the DEAE Sepharose column.
E26: Elution fraction 26 from the DEAE Sepharose column.
E36: Elution fraction 36 from the DEAE Sepharose column.
E56: Elution fraction 56 from the DEAE Sepharose column.
E66: Elution fraction 66 from the DEAE Sepharose column.
E76: Elution fraction 76 from the DEAE Sepharose column.

Fig. 5.3 Zymogram stain of 10% native PAGE gel illustrating NADH dehydrogenase activity in various DEAE Sepharose fractions. The apparent removal of proteases by the DEAE Sepharose chromatography procedure has led to the stability of NqrF with less evident degradation in the DEAE Sepharose fractions compared with the membrane extract.

C: membrane extract of control BL21(DE3)p*LysS* cells with pET16b.
KS: membrane extract of BL21(DE3)p*LysS* cells expressing NqrF from pET16b (pKT02).
E26: Elution fraction 26 from the DEAE Sepharose column.
E51: Elution fraction 51 from the DEAE Sepharose column.
E66: Elution fraction 66 from the DEAE Sepharose column.
E76: Elution fraction 76 from the DEAE Sepharose column.

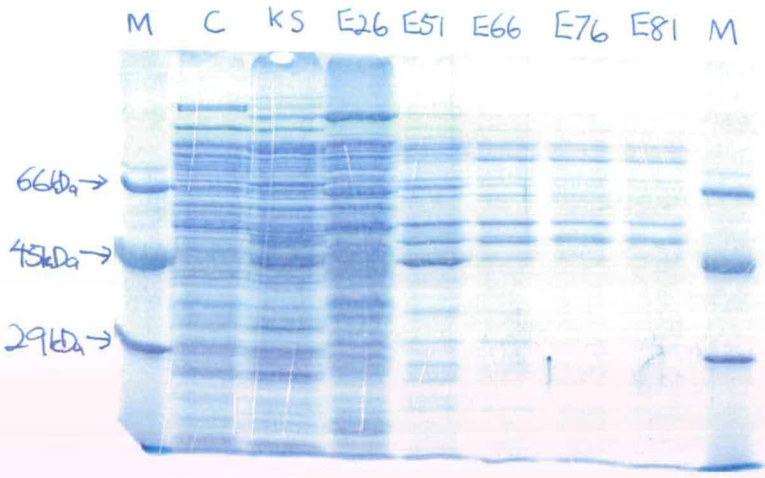

Fig. 5.4 Coomassie Blue-stained 10% SDS PAGE gel displaying the total protein profile in various DEAE Sepharose fractions.

M: Markers. Bovine serum albumin, 66 kDa; Chicken egg ovalbulmin, 45 kDa; Carbonic anhydrase, 29 kDa.
C: membrane extract of control BL21(DE3)p*LysS* cells with pET16b.
KS: membrane extract of BL21(DE3)p*LysS* cells expressing NqrF from pET16b (pKT02).
E26: Elution fraction 26 from the DEAE Sepharose column.
E51: Elution fraction 51 from the DEAE Sepharose column.
E66: Elution fraction 66 from the DEAE Sepharose column.
E76: Elution fraction 76 from the DEAE Sepharose column.
E81: Elution fraction 81 from the DEAE Sepharose column.

5.1.2 Second columns

5.1.2.1 Hydrophobic interaction chromatography (HIC)

Phenyl sepharose chromatography (Pharmacia)

A simplistic model of protein tertiary structure envisages an essentially hydrophilic outer shell surrounding a hydrophobic core. But surface hydrophobicity occurs due to the presence at the surface of side chains of non-polar amino acids such as alanine, methionine, tryptophan and phenylalanine. In HIC, substances are separated on basis of their varying hydrophobic interactions with an uncharged bed material containing hydrophobic groups. HIC columns are filled with gel matrices and equilibrated under conditions which favour hydrophobic binding, e.g. high ionic strength. Elution is achieved by applying one or more of the following: (1) descending salt gradient, (2) ascending linear detergent gradient, (3) increasing concentration of chaotropic ions in a positive gradient, (4) raising pH, (5) reducing temperature, (6) ethylene glycol.

NADH menadione-oxidase activity assays indicated signs of weak NADH dehydrogenase activity eluting in fractions 9, 10, 11, 12 and 13 when an ascending detergent (Tween 80) gradient was applied to the phenyl sepharose column. On running these fractions on 10% (w/v) native PAGE gels with 0.1% (v/v) Triton X-100 and stained for activity, a single distinct low M_r band of NADH dehydrogenase activity was apparent, with no high M_r bands seen this time (Fig. 5.5). This indicated that the protein of interest was eluting very early and improvements were made by reducing the detergent concentration gradient to get better separation.

Fig. 5.5 Zymogram stain of 10% native PAGE gel illustrating NADH dehydrogenase activity in various Phenyl Sepharose fractions.

E9: Elution fraction 9 from the Phenyl Sepharose column.
E10: Elution fraction 10 from the Phenyl Sepharose column.
E11: Elution fraction 11 from the Phenyl Sepharose column.
E12: Elution fraction 12 from the Phenyl Sepharose column.
E13: Elution fraction 13 from the Phenyl Sepharose column.

Pooled DEAE sepharose fractions were also run through the phenyl sepharose column, eluting from 2 M NaCl (to promote binding to hydrophobic column) to 0 M NaCl in 0.1% (w/v) Tween 80, 50 mM Tris-HCl, pH 7.5, 5 mM EDTA buffer. NqrF appeared to elute at 0 M NaCl but there was only a little activity detected in the eluted fractions and hence the column was eluted with an increasing Triton X-100 gradient from 0 to 1% (v/v). NADH dehydrogenase activity was also apparent in the final fractions at 1% (v/v) Triton X-100. On running these fractions on a native gel and staining it, the fractions eluted in Tween 80, 0 M NaCl, showed a single 46 kDa band but the Triton X-100-eluted fractions displayed the presence of high M_r NqrF aggregates (Fig. 5.6, 5.7, 5.8). This may indicate that Tween 80 may be a better detergent to use than Triton X-100, which seems to promote the forming of NqrF aggregates. A protein maximum peak unfortunately coincided with the 1% (v/v) Triton X-100 active fractions, hence only a small factor of purification was achieved through this column, i.e. non-selective.

5.1.2.2 Mono Q HR 5/5 (Pharmacia)

Mono Q is an ion exchange FPLC column used successfully in the final stage of purification of *V. harveyi* Na^+-NQR complex by Stevenson (1994). However, when used for NqrF, very little no activity could be found in the wash or elution fractions of Mono Q HR 5/5. NqrF seemed to bind very strongly and possibly irreversibly to the column. Another possibility was that as the FPLC equipment was housed at room temperature and proved difficult to relocate to the cold room, the unstable NqrF was degrading even when left only for 1 hour at this temperature.

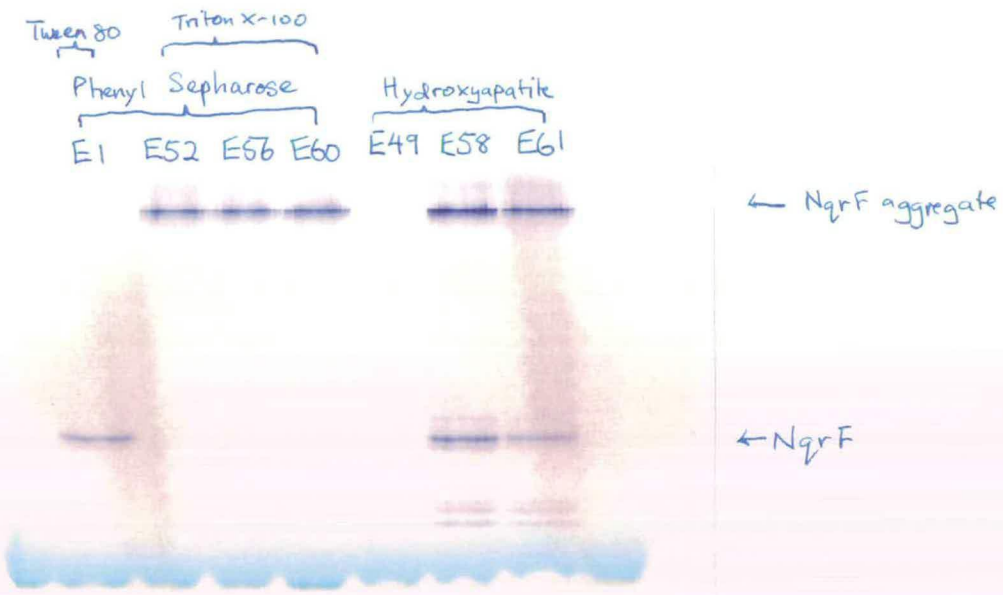

Fig. 5.6 Zymogram stain of 10% native PAGE gel illustrating NADH dehydrogenase activity in various Phenyl Sepharose and Hydroxyapatite fractions.

E1: Elution fraction 1 from the Phenyl Sepharose column (0 M NaCl, 0% Triton X-100, 0.1% Tween 80).
E52: Elution fraction 52 from the Phenyl Sepharose column (0.1% Triton X-100 gradient).
E56: Elution fraction 56 from the Phenyl Sepharose column (0.1% Triton X-100 gradient).
E60: Elution fraction 60 from the Phenyl Sepharose column (0.1% Triton X-100 gradient).
E49: Elution fraction 49 from the Hydroxyapatite column.
E58: Elution fraction 58 from the Hydroxyapatite column.
E61: Elution fraction 61 from the Hydroxyapatite column.

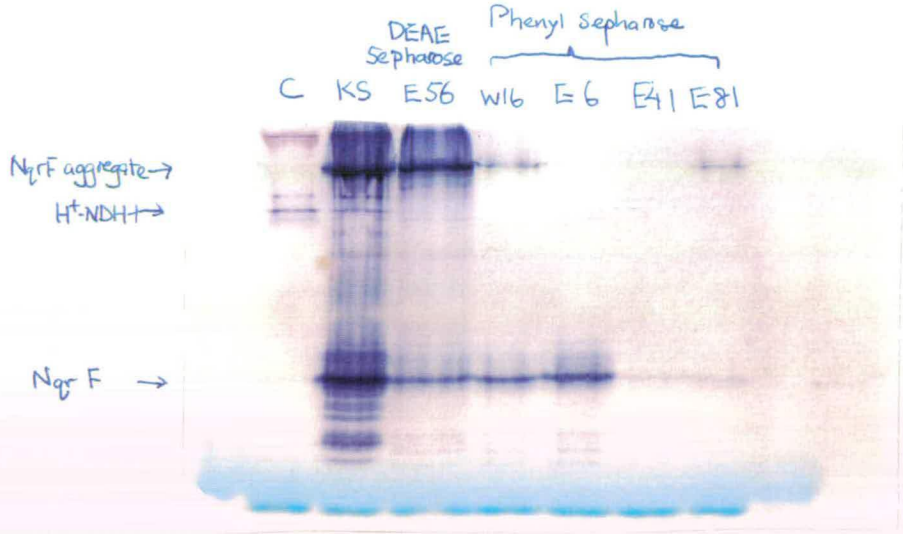

Fig. 5.7 Zymogram stain of 10% native PAGE gel illustrating NADH dehydrogenase activity in various Phenyl Sepharose and Hydroxyapatite fractions.

C: membrane extract of control BL21(DE3)p*LysS* cells with pET16b.
KS: membrane extract of BL21(DE3)p*LysS* cells expressing NqrF from pET16b (pKT02).
DEAE E56: Elution fraction 56 from the DEAE Sepharose column.
W16: Wash fraction 16 from the Phenyl Sepharose column.
E6: Elution fraction 6 from the Phenyl Sepharose column.
E41: Elution fraction 41 from the Phenyl Sepharose column.
E81: Elution fraction 81 from the Phenyl Sepharose column.

Fig. 5.8 Coomassie Blue-stained 10% SDS PAGE gel displaying the total protein profile in membrane extract, pooled DEAE Sepharose fractions, pooled Hydroxyapatite fractions and various Phenyl Sepharose fractions.

M: Markers. Bovine serum albumin, 66 kDa; Chicken egg ovalbulmin, 45 kDa; Carbonic anhydrase, 29 kDa.
KS: membrane extract of BL21(DE3)p*LysS* cells expressing NqrF from pET16b (pKT02).
DEAE: Pooled DEAE Sepharose fractions.
HA: Pooled Hydroxyapatite fractions.
PS11: Elution fraction 11 of Phenyl Sepharose column.
PS20: Elution fraction 20 of Phenyl Sepharose column.

5.1.2.3 Hydroxyapatite chromatography (Pharmacia)

Amino groups allow the adsorption of proteins to hydroxyapatite as a result primarily of non-specific electrostatic interactions between their positive charges and the general negative charge on the hydroxyapatite column when the column is equilibrated with phosphate buffer. Carboxyl groups are repelled electrostatically from the negative charge of the column. Proteins can also bind specifically by complexation to calcium sites on the column. Elution of basic proteins occur as a result of normal Debye-Hueckel charge screening, which operates in the elution by F^-, Cl^-, ClO_4^-, SCN^-, and phosphate, or by specific displacement by Ca^{2+} and Mg^{2+} ions which complex with column phosphates and neutralize their negative charges. Acidic proteins are eluted by displacement of their carboxyls from hydroxyapatite calcium sites by ions which form stronger complexes with calcium than do carboxyls, e.g., fluoride or phosphate. Testing indicates that the activity of NqrF was not significantly inhibited by azide and this was subsequently used in the hydroxyapatite column to prevent contamination as the hydroxyapatite column matrix constitutes a rich medium susceptible to microbial growth.

Preliminary observations

Pooled fractions from the DEAE sepharose column were applied to the hydroxyapatite column. Although the activity peak coincided with a protein peak, there was some purification as other protein peaks elsewhere in the purification profile were observed. A broad protein peak with no NADH dehydrogenase activity eluted with the 1 M NaCl wash, a smaller peak eluted at about 0.1 M phosphate, and a large peak eluting at 0.2 M (elution fractions 11-22, which were visibly yellow), contained large amounts of NADH dehydrogenase activity (Fig. 5.6). When samples in the region of the activity maxima were run on a 10% (w/v) SDS gel, NqrF appeared to be purified from a few low molecular weight proteins present in the pooled DEAE sepharose fractions and calculations of specific activities indicated that an adequate factor of purification was attained (Fig. 5.9 and 5.10).

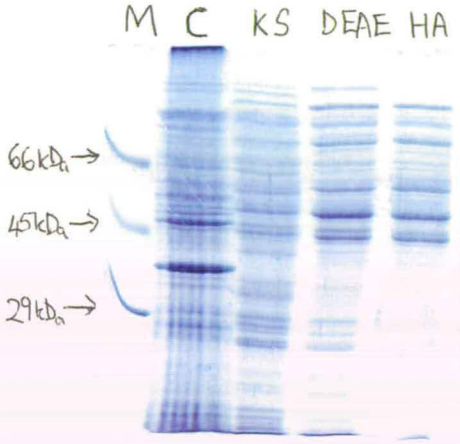

Fig. 5.9 Coomassie Blue-stained 10% SDS PAGE gel displaying the total protein profile in membrane extract, pooled DEAE Sepharose fractions and pooled Hydroxyapatite fractions.

M: Markers. Bovine serum albumin, 66 kDa; Chicken egg ovalbulmin, 45 kDa; Carbonic anhydrase, 29 kDa.
C: membrane extract of control BL21(DE3)p*LysS* cells with pET16b.
KS: membrane extract of BL21(DE3)p*LysS* cells expressing NqrF from pET16b (pKT02).
DEAE: Pooled DEAE Sepharose fractions.
HA: Pooled Hydroxyapatite fractions.

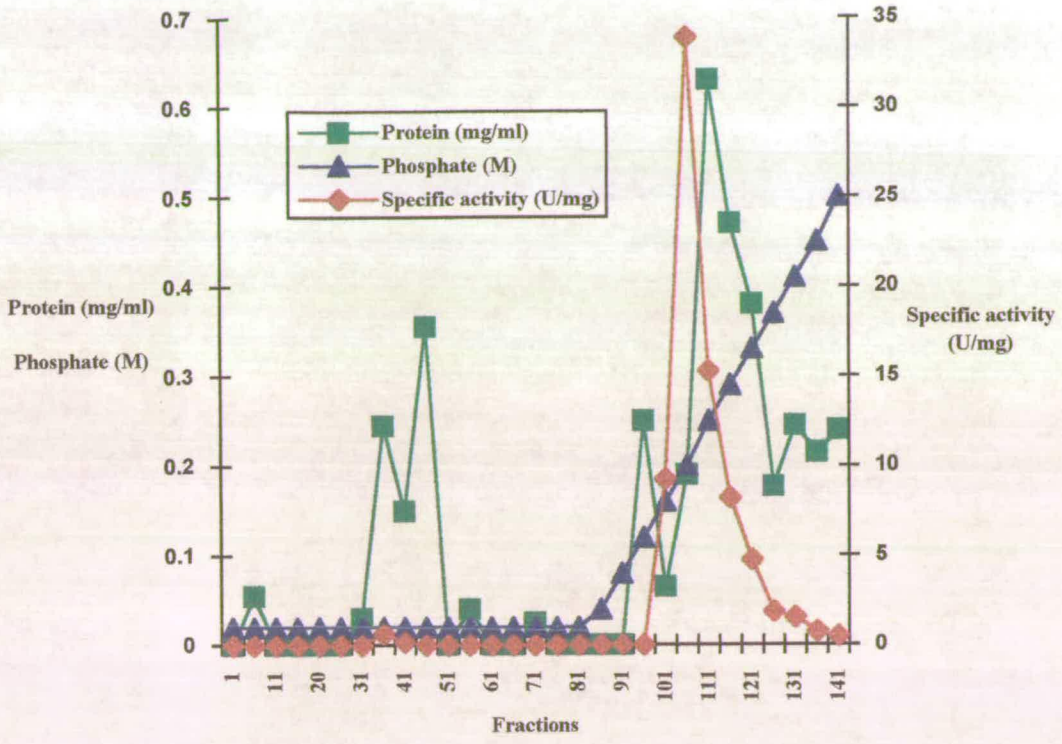

Fig. 5.10 Hydroxyapatite chromatography protein elution profile.

Hydroxyapatite chromatography (Pharmacia)

Pooled fractions from the DEAE sepharose column were run through a 15 cm x 2.5 cm hydroxyapatite column equilibrated with 10 mM potassium phosphate buffer, pH 6.5, 100 mM NaCl, 10% (w/v) ethylene glycol, 1% (w/v) Triton X-100, 3 mM sodium azide (0.02%). After a wash to remove unbound proteins with the equilibration buffer, a 1.0 M NaCl wash was incorporated to elute neutral but not acidic proteins. Elution was achieved with a phosphate gradient increasing from 0.02 M to 0.5 M at 50 ml/h (Fig. 5.10).

5.1.3 Final columns

5.1.3.1 Dye Affinity chromatography

Mimetic Blue-2 (0100-0025) and Mimetic Green-1 (0080-0025) (Affinity Chromatography Ltd)

MIMETIC Affinity Ligands are especially well suited for the purification of enzymes and proteins which interact strongly with nucleotides and cofactors. The initial dye affinity products offered by Affinity Chromatography Ltd. have proven promising in the purification of blood proteins, dehydrogenases, kinases, oxidases, nucleases, proteases, transferases and ligases. These triazine dyes form a biospecific ligand that is covalently attached to a chromatographic bed material, to which proteins bind. Desorption and elution is achieved by applying an increasing linear NaCl gradient.

Initial observations

Initially, a MIMETIC screening kit (PIKSI) containing 12 1-ml dye affinity test columns was used to assess the ability of the 12 different columns to bind NqrF. Active hydroxyapatite fractions were loaded onto the test columns. NqrF bound strongly and eluted easily from Mimetic Blue 2, Green 1, Yellow 1, but Orange 3, Red 2, Mimetic Blue 1 and Cibacron blue either did not bind NqrF or bound to it too strongly to be eluted. Mimetic Blue-2 and Mimetic Green-1 were eventually chosen for a scaled-up purification of NqrF.

In both the green and blue dye columns, a large protein peak with no NADH dehydrogenase activity was observed in the wash fractions. In the blue column, a small protein peak was observed to coincide with the broad activity peak in elution fractions 26-36 (0.5 M NaCl). No obvious protein peak was found in the elution fractions of the green column even though there was a large activity peak eluting at about 20 - 35.

From activity gels from the green dye column (Fig. 5.11 and 5.12), monomeric NqrF and NqrF aggregates seem to be eluting at several different points of the purification process, hence the absence of a distinct protein peak whereby NqrF was eluted. A major contaminating protein, about 66 kDa, also seemed to be present. Hence this column was not employed further. Instead, the Mimetic Blue-2 dye affinity column was used.

On analysis with SDS-PAGE and zymogram-stained native PAGE, NqrF was purified to homogeneity (from membrane extracts to DEAE sepharose to hydroxyapatite to Mimetic Blue-2 dye affinity chromatography) and only 1 band at 46 kDa was found on both gels (Fig 5.13, 5.14). No NqrF aggregates like those observed in previous chromatographic fractions were seen when laurylsulphobetaine (LSB) was used as a detergent in the buffers of the final dye affinity column (Fig. 5.14). However, NqrF lost activity in LSB and not Triton X-100, when Triton X-100 substituted LSB in the buffers, recovery improved significantly but the NqrF aggregates reappeared in activity-stained native gels (Fig. 5.15). CHAPS later substituted Triton X-100 as it was found to resolve the aggregates giving only monomeric NqrF although it did not affect the NADH dehydrogenase activity of NqrF adversely (Fig. 5.16, 5.17. 5.18). CHAPS was only used for buffers in the dye affinity column, as it is more expensive compared to Triton X-100. The overall purification profile of this last column is seen in Fig. 5.19.

Fig. 5.11 Coomassie Blue-stained 10% SDS PAGE gel presenting the total protein profile in Mimetic Green-1 dye affinity chromatography fractions.

M: Markers. Bovine serum albumin, 66 kDa; Chicken egg ovalbulmin, 45 kDa; Carbonic anhydrase, 29 kDa.

L6: Load fraction 6 in Mimetic Green-1 dye column.
L8: Load fraction 8 in Mimetic Green-1 dye column.
L16: Load fraction 16 in Mimetic Green-1 dye column.
W6: Wash fraction 6 in Mimetic Green-1 dye column.
E11: Elution fraction 11 in Mimetic Green-1 dye column.

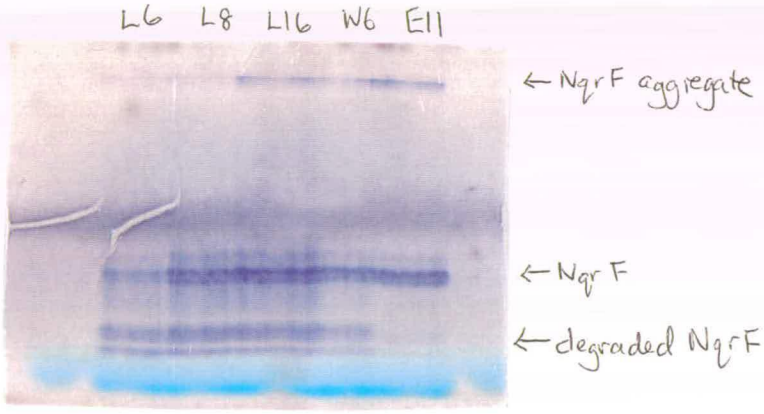

Fig. 5.12 Zymogram stain of 10% native PAGE gel displaying NADH dehydrogenase activity in Mimetic Green-1 dye affinity chromatography fractions.

L6: Load fraction 6 in Mimetic Green-1 dye column.
L8: Load fraction 8 in Mimetic Green-1 dye column.
L16: Load fraction 16 in Mimetic Green-1 dye column.
W6: Wash fraction 6 in Mimetic Green-1 dye column.
E11: Elution fraction 11 in Mimetic Green-1 dye column.

Fig. 5.13 Coomassie Blue-stained 10% SDS PAGE gel displaying the total protein profile in various stages of purification.

M: Markers. Bovine serum albumin, 66 kDa; Chicken egg ovalbulmin, 45 kDa; Carbonic anhydrase, 29 kDa.
C: membrane extract of control BL21(DE3)p*LysS* cells with pET16b.
KS: membrane extract of BL21(DE3)p*LysS* cells expressing NqrF from pET16b (pKT02).
DEAE: Pooled DEAE Sepharose fractions with activity.
HA: Pooled Hydroxyapatite fractions with activity.
OS: Pooled Octyl Sepharose fractions with activity.
GD: Pooled Mimetic Green-1 Dye affinity fractions with activity.
BD: Pooled Mimetic Blue-2 Dye affinity fractions with activity.

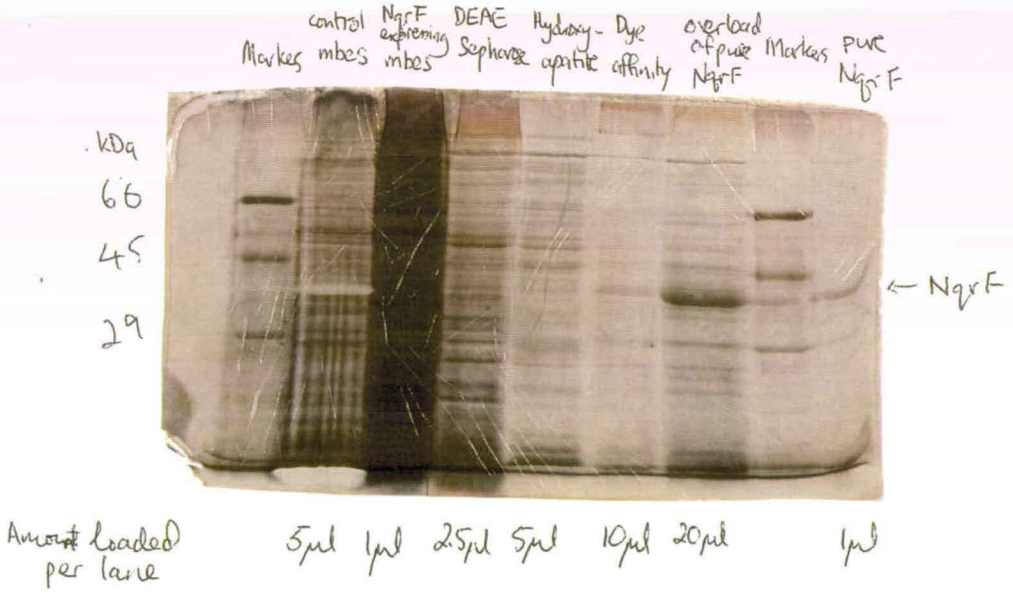

Silver stain of 10% (w/v) SDS polyacrylamide gel of various fractions previously demonstrated in Fig. 5.13, Coomassie Blue-stained. This silver stained gel shows the purified NqrF sample in the very last lane.

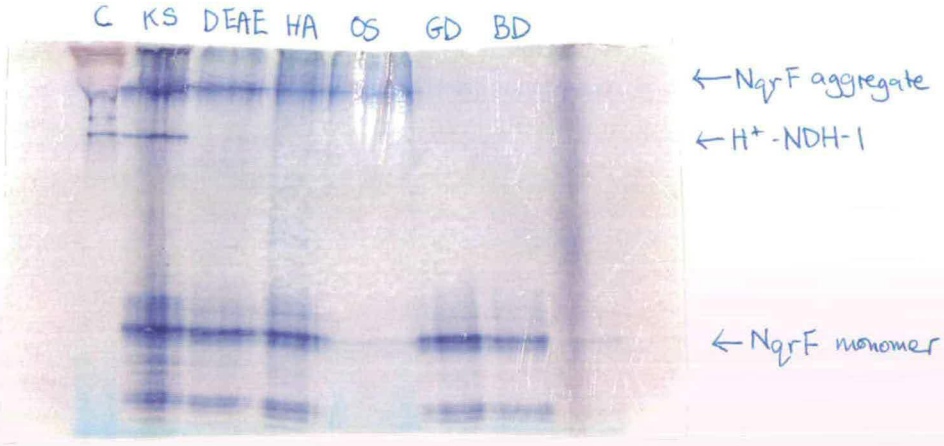

Fig. 5.14 Zymogram stain of 10% native PAGE gel run with samples from various stages of purification. This shows that with laurylsulphobetaine, the final purified NqrF is resolved into monomers.

C: membrane extract of control BL21(DE3)p*LysS* cells with pET16b.
KS: membrane extract of BL21(DE3)p*LysS* cells expressing NqrF from pET16b (pKT02).
DEAE: Pooled DEAE Sepharose fractions with activity.
HA: Pooled Hydroxyapatite fractions with activity.
OS: Pooled Octyl Sepharose fractions with activity.
GD: Pooled Mimetic Green-1 Dye affinity fractions with activity (LSB).
BD: Pooled Mimetic Blue-2 Dye affinity fractions with activity (LSB).

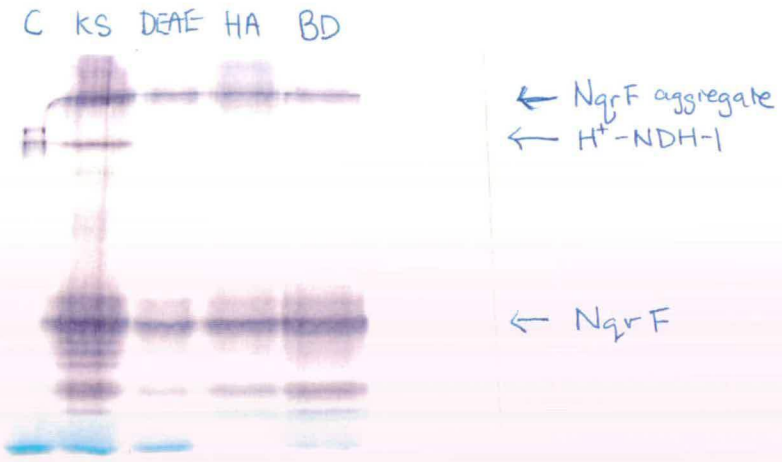

Fig. 5.15 Zymogram stain of 10% native PAGE gel run with samples from various stages of purification. This shows that with Triton X-100, the final purified NqrF forms aggregates.

C: membrane extract of control BL21(DE3)p*LysS* cells with pET16b.
KS: membrane extract of BL21(DE3)p*LysS* cells expressing NqrF from pET16b (pKT02).
DEAE: Pooled DEAE Sepharose fractions with activity.
HA: Pooled Hydroxyapatite fractions with activity.
BD: Pooled Mimetic Blue-2 Dye affinity fractions with activity (Triton X-100).

Fig. 5.16 Coomassie Blue-stained 10% SDS PAGE gel displaying the total protein profile in various stages of purification. This demonstrates the CHAPS resolves NqrF into a single band (monomer).

M: Markers. Bovine serum albumin, 66 kDa; Chicken egg ovalbulmin, 45 kDa; Carbonic anhydrase, 29 kDa.
C: membrane extract of control BL21(DE3)p*LysS* cells with pET16b.
KSC: cytoplasmic fraction of BL21(DE3)p*LysS* cells expressing NqrF from pET16b (pKT02).
KSM: membrane extract of BL21(DE3)p*LysS* cells expressing NqrF from pET16b (pKT02).
DEAE: Pooled DEAE Sepharose fractions with activity.
HA: Pooled Hydroxyapatite fractions with activity.
BD: Pooled Mimetic Blue-2 Dye affinity fractions with activity (Triton X-100).
HA: Pooled Hydroxyapatite fractions with activity.
CBD: Pooled Mimetic Blue-2 Dye affinity fractions with activity (CHAPS).

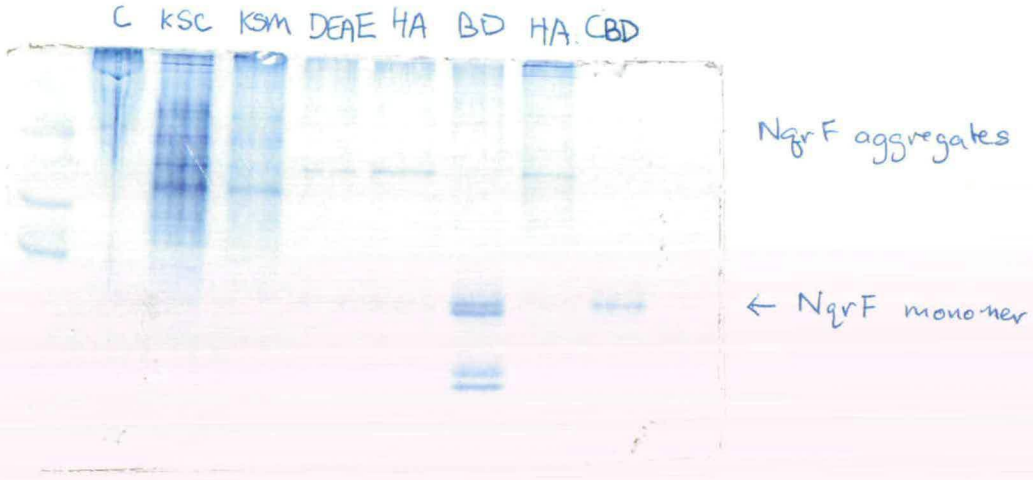

Fig. 5.17 Zymogram stain of 10% native PAGE gel demonstrating NADH dehydrogenase activity in various stages of purification. This demonstrates that CHAPS resollves NqrF into a single band (monomer).

C: membrane extract of control BL21(DE3)p*LysS* cells with pET16b.
KSC: cytoplasmic fraction of BL21(DE3)p*LysS* cells expressing NqrF from pET16b (pKT02).
KSM: membrane extract of BL21(DE3)p*LysS* cells expressing NqrF from pET16b (pKT02).
DEAE: Pooled DEAE Sepharose fractions with activity.
HA: Pooled Hydroxyapatite fractions with activity.
BD: Pooled Mimetic Blue-2 Dye affinity fractions with activity (Triton X-100).
HA: Pooled Hydroxyapatite fractions with activity.
CBD: Pooled Mimetic Blue-2 Dye affinity fractions with activity (CHAPS).

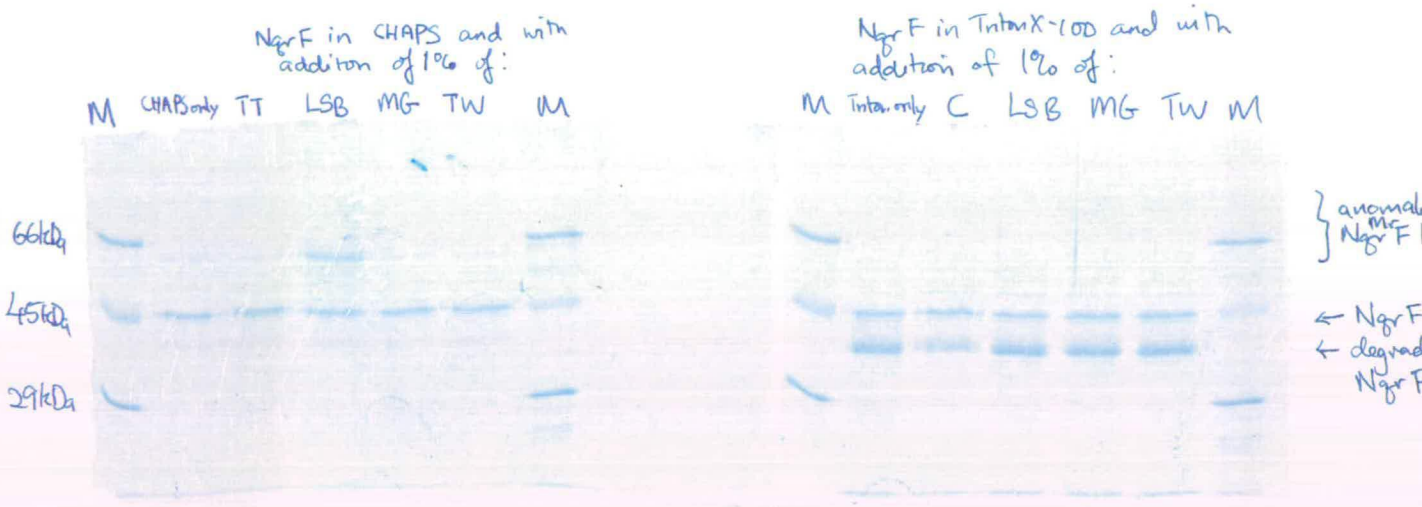

Fig. 5.18 Coomassie Blue-stained 10% SDS PAGE gel displaying the use of various detergents and their effect on NqrF, encouraging degradation or aggregate formation or resolving them into monomers.

M: Markers. Bovine serum albumin, 66 kDa; Chicken egg ovalbulmin, 45 kDa; Carbonic anhydrase, 29 kDa.
Detergents:
C: CHAPS
TT: Triton X-100
LSB: Laurylsulphobetaine
MG: Mega 10
TW: Tween 80

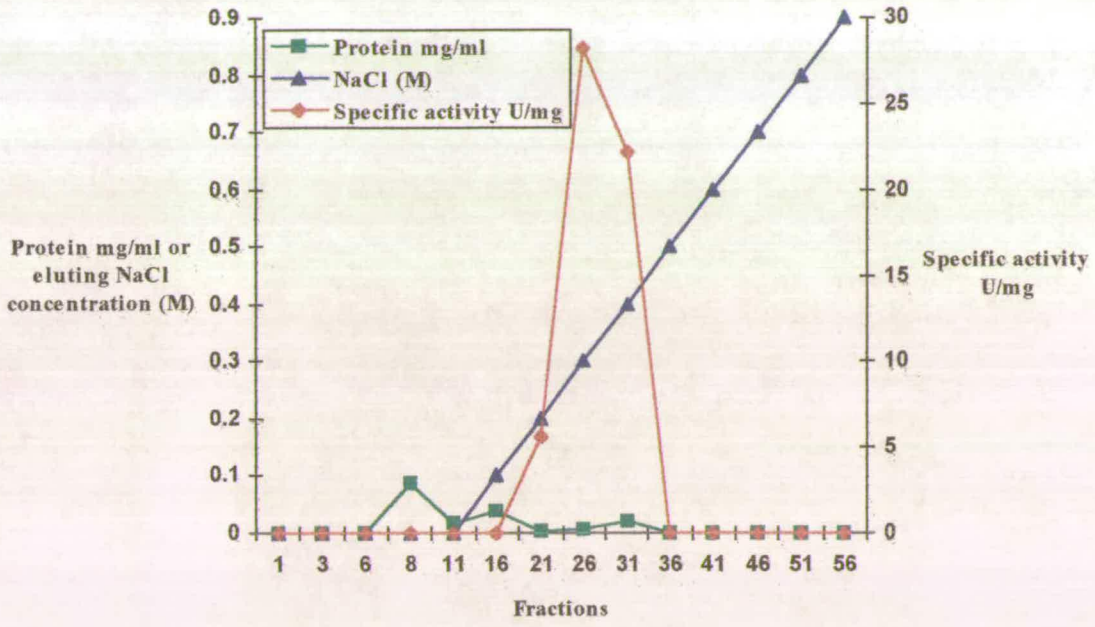

Fig. 5.19 Mimetic Blue 2 dye affinity chromatography protein elution profile.

Dye Affinity chromatography (Dye Affinity Chromatography Ltd)

Mimetic Blue 2 (0100-0025)

A MIMETIC screening kit (PIKSI) was used to test the suitability of mimetic triazine dyes for chromatography. Samples purified from the hydroxypatite column were loaded onto the 12.5 cm x 1.6 cm Mimetic Blue-2 dye column (which demonstrated binding to NqrF in the screening kit) equilibrated with 20 mM potassium phosphate buffer, pH 6.5 (or pH 8.0), 10% (v/v) glycerol, 0.1% (w/v) CHAPS, (0.1% (v/v) Triton X-100 or 0.1% LSB) and proteins were eluted with 4 bed volumes of 0 to 1.0 M NaCl at 25 ml/h (Fig. 5.19).

5.1.3.2 Octyl sepharose (Pharmacia)

Pooled active fractions of the hydroxyapatite column were loaded onto the octyl sepharose column. This hydrophobic interaction chromatography column gave good recovery with high activity yields but upon SDS-PAGE analysis of eluted fractions with NADH dehydrogenase activity, other bands of protein were evident and the purification factor calculated was deemed unsatisfactory (Fig. 5.13 and 5.14). Eluted fractions from the octyl sepharose column which demonstrated NADH dehydrogenase activity contained almost as many different number of bands of protein as the loaded hydroxyapatite fractions, as observed on a Coomassie brilliant blue-stained SDS-PAGE gel in Fig. 5.13. As with the phenyl sepharose hydrophobic column, chromatography on this column also yielded exclusively NqrF aggregates. This is clearly indicated in the activity stain of the native PAGE gel in Fig. 5.14.

5.1.3.3 Gel permeation chromatography

Sephadex column (Pharmacia)

Sephadex columns separate molecules by virtue of size. Small molecules are eluted later as they are trapped in the pores of the gel matrix and retarded, while larger polypeptides pass through the column relatively quickly. In addition to its use in desalting NqrF samples, this column was also used to separate unbound FAD from NqrF that had been re-constituted with excess FAD. Two month-old purified NqrF samples, which had lost some activity and some yellow colouration as well, were reconstituted with FAD by pre-incubating pooled active fractions from the dye columns with 1 mM FAD for 1 hour at 4^{o}C and putting these samples through a 30 ml bed volume Sephadex column which was equilibrated with 20 mM Tris-HCl, pH 7.5, 0.1% lauryl sulphobetaine, 0.1 M NaCl. The same buffer was used to wash proteins out at 60 ml/h after samples were loaded. It was just possible to see evidence that NqrF had bound the FAD and hence give rise to 2 groups of fractions that are yellow: one large group of golden yellow fractions with NqrF bound to FAD (eluting early) and one small group of pale yellow fractions containing excess unbound FAD

(eluting later). However, these two groups of fractions were not very distinct from each other and could easily be mistaken for one large group of yellow fractions.

5.2 1-step purification procedure

Histrap column

Expressed NqrF should be readily purified in 1 step as the pET16b vector carries a stretch of histidine residues (His·Tag) that may be expressed at the *N*-terminal region of the target protein. The His·Tag sequence should bind to divalent Ni^{2+} immobilized on the metal chelation resin. After washing away unbound proteins, target proteins may be recovered by elution with imidazole. The His·Tag may then be removed by cleaving with Factor Xa.

When NqrF was His-tagged at the *N*-terminal, it dramatically altered from being a membrane protein to a cytoplasmic one (Fig. 5.20). Ag^{+}-sensitive NADH dehydrogenase activity was now detected in the cytoplasm rather than the membrane. This is likely due to the His-tag interfering with the hydrophobic *N*-terminal region's ability to span the membrane. The strain expressing His-tagged NqrF also grew better than the strain producing native membrane-bound NqrE and NqrF as it was no longer leaky due to multiple insertions of overexpressed recombinant proteins in the membrane.

Purification by the HisTrap column proved to be inefficient. Binding of the His-tagged NqrF to the nickel-chelation column was only 5% and was improved to only 25% even after buffers were altered (changing from Tris to Phosphate buffer, and using CHAPS rather than Trition X-100) and incorporating a half hour standing time after sample loading to improve binding (Table 5.1). Binding to the column was poor because of the degradation and removal of the *N*-terminal region of NqrF (see earlier section on pulse-chase labelling) which contained the His-tag. Purity of the final eluted sample was also suspect from the SDS gel pictures (Fig. 5.21 and 5.22).

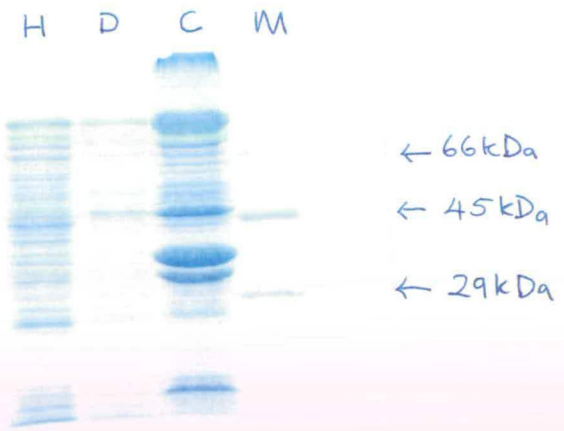

Fig. 5.20 Coomassie Blue-stained 10% SDS PAGE gel exhibiting the total protein profile and distribution of His-tagged NqrF expressed by BL21(DE3)p*LysS* during purification.

H: His-Trap column elution fractions.
D: Pooled DEAE Sepharose fractions with activity.
C: Cytoplasmic fraction with NqrF activity.
M: Markers. Bovine serum albumin, 66 kDa; Chicken egg ovalbulmin, 45 kDa; Carbonic anhydrase, 29 kDa.

Table 5.1. Results for activities for HisTrap column (comparing use of different buffers)

HisTrap - Tris buffer, no detergent	volume (ml)	Total activity µmol NADH/min	% recovery	Improved HisTrap - PO4 buffer, standing time and CHAPS	volume (ml)	Total activity µmol NADH/min	% recovery
sample loaded	1.0	7.39	-	sample loaded	1.0	4.10	-
loading fraction	1.2	2.89	37%	loading fraction	1.0	0.32	0
wash fraction	4.9	4.59	60%	wash fraction	5.5	3.18	75%
elute fraction	1.1	0.15	3%	elute fraction	2.0	1.16	25%

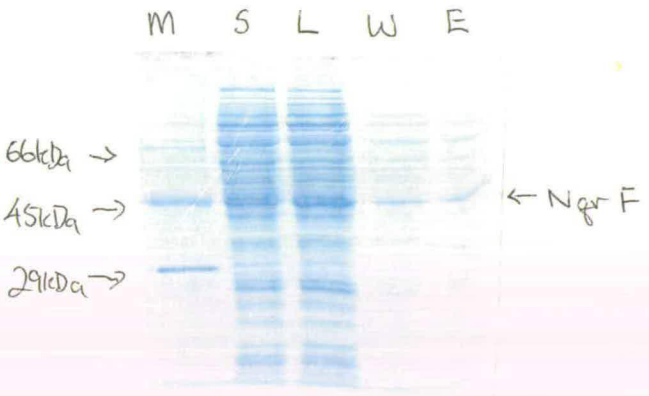

Fig. 5.21 Coomassie Blue-stained 10% SDS PAGE gel exhibiting the total protein profile and distribution of His-tagged NqrF expressed by BL21(DE3)p*LysS* at various stages in His-Trap column purification.

M: Markers. Bovine serum albumin, 66 kDa; Chicken egg ovalbulmin, 45 kDa; Carbonic anhydrase, 29 kDa.
S: Pooled DEAE Sepharose sample.
L: Load fraction of the His-trap column.
W: Wash fraction of the His-Trap column.
E: Elute fraction of the His-Trap column.

Fig. 5.22 Coomassie Blue-stained 10% SDS PAGE gel exhibiting the total protein profile and distribution of His-tagged NqrF expressed by BL21(DE3)p*LysS* at various stages in the improved His-Trap column purification.

M: Markers. Bovine serum albumin, 66 kDa; Chicken egg ovalbulmin, 45 kDa; Carbonic anhydrase, 29 kDa.
E: Elute fraction of the His-Trap column.
W: Wash fraction of the His-Trap column.
L: Load fraction of the His-trap column.
S: Pooled DEAE Sepharose sample.

The His-tagged NqrF purified well with conventional purification columns like DEAE sepharose, hydroxyapatite and Mimetic dye affinity with high recovery yields (Table 5.2) but it was rather unstable or susceptible to proteases (other than serine proteases) despite the addition of serine-protease inhibitor, PMSF, and the activity figures were half that compared to purification of native NqrF (Table 5.3). His-tagged NqrF, in crude cytoplasmic extract, lost 67% activity over 1 week at 4°C storage. The peaks of His-tagged NqrF purified also appeared at different points of the eluting gradients on the various columns, compared with native NqrF. The His-tag has altered the biochemical properties of NqrF. Moreover, there was the additional inconvenience of having to use Factor Xa to cleave off the His·Tag from the *N*-terminal region of NqrF after purification. There was also significant lost of activity of NqrF over time and due to the significant cleavage of the *N*-terminal His·Tag leading to poor binding to the nickel column, this method was not used.

Table 5.2. Purification table for His-tagged NqrF

His-tagged NqrF conventional purification	Total activity µmol NADH/min	% recovery (yield)
Cytoplasmic fraction	382	-
DEAE Sepharose pool	295	100%
Hydroxyapatite pool	217	75%
Dye affinity pool	220	75%

Table 5.3. Comparison of His-tagged NqrF purification and native NqrF purification

values from 15 l culture	Total activity µmol NADH/min	Ag+-sensitive activity µmol NADH/min	% Ag+-sensitive activity
His-tagged NqrF cytoplasmic fraction	2355	1849	78%
Native NqrF cytoplasmic fraction	427	30	7%
His-tagged NqrF membrane fraction	48	0	0%
Native NqrF membrane fraction	4226	3169 (1043 is rotenone-sensitive, approx. 25%!)	75%

5.3 Concentration of sample with a step gradient on DEAE Sepharose and/or with Centriplus concentrators (Amicon)

The pooled fractions from the final chromatography column were concentrated by a step gradient elution with 0.5 M NaCl from the DEAE sepharose column (optional) and then spun in an Amicon Centriplus Concentrator 30 at 3000 x g, 75 min, 4°C. Samples were collected with a 4 min reversed spin at 2 000 g, 4°C. The latter technique allowed up to 10X concentration of sample per run.

5.4 Final choice of columns and scheme of purification

With consideration of effectiveness, efficiency and preservation of activity of NqrF, the following columns were selected in this order for the purification of NqrF:

1. Expression was achieved using the pKT02 clone that expressed NqrE and NqrF without His-tag.
2. The membrane fraction was loaded onto DEAE sepharose column
3. DEAE sepharose pooled samples containing Ag^{+}-sensitive NADH dehydrogenase activity were loaded onto the hydroxyapatite column
4. Hydroxyapatite samples were pooled after determination of activity peak from assay, and loaded onto Mimetic Blue-2 dye affinity chromatography column
5. Dye affinity pool at the activity peak, was concentrated using Amicon concentrators
6. Samples from various pools from different stages of purification were loaded onto polyacrylamide gels and stained with Coomassie brilliant blue. Protein determination assays were performed on samples

5.5 Results summation

Although NADH dehydrogenase activity was observed in the cytoplasmic fraction, this activity was not Ag^+-sensitive unlike the majority of the activity in the membrane fraction.

Fig. 5.13 shows a Coomassie brilliant blue-stained SDS gel showing the overall protein profile of the samples at each stage of purification, and a zymogram stain of a native gel in Fig. 5.14, illustrating the proteins that exhibit NADH dehydrogenase activity at each stage of purification.

The results showed that there was some NADH activity in a high M_r protein (greater than 100 kDa) in all crude membrane samples of both the control and the NqrF-expressing transformants. This was due to the presence of the native H^+-translocating NADH-ubiquinone oxidoreductase present in the membranes of BL21(DE3)p*LysS*. This protein was removed by the first purification step on the DEAE sepharose column. There also seemed to be a thick and very much higher M_r protein band present for clones overexpressing NqrF and this can be attributed to the NqrF subunit binding to the H^+ complex in the host or other *E. coli* proteins or forming NqrF aggregates. A major activity band and protein band at about 46 kDa for NqrF emerged only in the NqrF-expressing strain and not in the controls. Some degradation of NqrF was evident in the zymogram-stained native gels.

14 mg of NqrF was obtained from the membranes of 40 g (7 ℓ) of cells overexpressing NqrF and a good yield of 50% and purification factor of 12 was achieved (Table 5.4a and 5.4b). NqrF was purified by ion exchange chromatography, hydroxyapatite chromatography and affinity chromatography. On DEAE sepharose CL6B, NADH dehydrogenase activity was eluted at about 0.2 M NaCl. Fractions from the DEAE sepharose column was then applied to a hydroxyapatite column. A 1 M NaCl wash, designed to remove neutral proteins did not elute NqrF but NqrF was detected in the fractions of acidic protein eluting at about 0.2 M in the 0.02 M to 0.5 M linear phosphate gradient. A number of 1 ml dye affinity test columns were assessed for their ability to bind NqrF. It bound strongly and eluted easily from

Mimetic Blue 2, Green 1, Yellow 1, but Orange 3, Red 2, Mimetic Blue 1 and Cibacron blue either did not bind NqrF or bound to it too strongly to be eluted. Mimetic Blue 2 was finally chosen as the final purification column and NqrF was eluted in a single peak at 0.5 M NaCl.

Table 5.4a. Purification table

Before improvements (small scale 1*l*, 5 g wet cells)

	Volume (ml)	Conc. (mg/ml)	Total protein (mg)	Total activity (μmole NADH/min)	Specific activity (μmole NADH/min/mg protein)	Purification	Yield (%)
KS membrane fraction	5.3	7.6	40.28	144	3.57	-	-
DEAE Sepharose pool	57	0.25	14.25	88	6.175	1.73	61
Hydroxyapatite pool	62	0.116	7.192	43.26	6.015	1.68	30.5
Mimetic Blue 2 Dye affinity pool	44	0.033	1.452	31.13	21.44	6.01	22

Table 5.4b Purification table.

After improvements (large scale 7*l* run, 40 g wet cells).

	Volume (ml)	Conc. (mg/ml)	Total protein (mg)	Total activity (μmole NADH/min)	Specific activity (μmole NADH/min/mg protein)	Purification	Yield (%)
KS membrane fraction	40.5	8.20	3332.1	1872	5.6	-	-
DEAE Sepharose pool	80.5	1.66	133.6	2239	16.8	3.0	120
Hydroxyapatite pool	105	0.75	78.8	2904	36.9	6.54	155
Mimetic Blue 2 Dye affinity pool	116	0.12	13.9	933	67.0	11.9	50

Chapter 6

Results and Discussion

Characterization of purified NqrF

6.1 Detergents

Upon inspection of Coomassie brilliant blue-stained SDS polyacrylamide gels and zymogram-stained native polyacrylamide gels run with purified NqrF, only 1 band at 46 kDa was visualized on both gels when LSB was included in the buffers used in the final chromatography step (Fig. 5.13 and 5.14). NqrF lost activity in LSB and not Triton X-100; therefore Triton X-100 was substituted for LSB in the Mimetic Blue-2 chromatography buffers instead. Recovery improved significantly when Triton X-100 was used, but the NqrF aggregates reappeared in activity-stained native gels and even in Coomassie brilliant blue-stained SDS gels where samples containing SDS, were boiled prior to loading. This aggregate-forming in Triton X-100 is a reversible process because if a small amount of Triton X-100-solubilized pure NqrF was incubated in a 1% (w/v) LSB buffer at 4°C overnight, only 1 band at 46 kDa was seen when this sample was subsequently run on SDS gels. On the other hand, activity was permanently lost when LSB buffers were used. CHAPS was finally selected as it produced only the 46 kDa band of NqrF (Fig 5.16 and 5.17), did not affect the activity of the enzyme and allowed conventional spectrophotometric protein assays at A_{280}. A wide range of other detergents were also tested on NqrF to determine their suitability for inclusion in sample buffers (Fig. 6.1). Although predicted to be mainly hydrophilic from hydropathy plots, NqrF required the inclusion of detergents for solubilization. There was obvious precipitation of this protein in concentrated solutions (approximately 1 mg/ml) of this protein in Tris-HCl buffer + 0.1% (v/v) Triton X-100 or CHAPS, after 1 week's storage at 4°C.

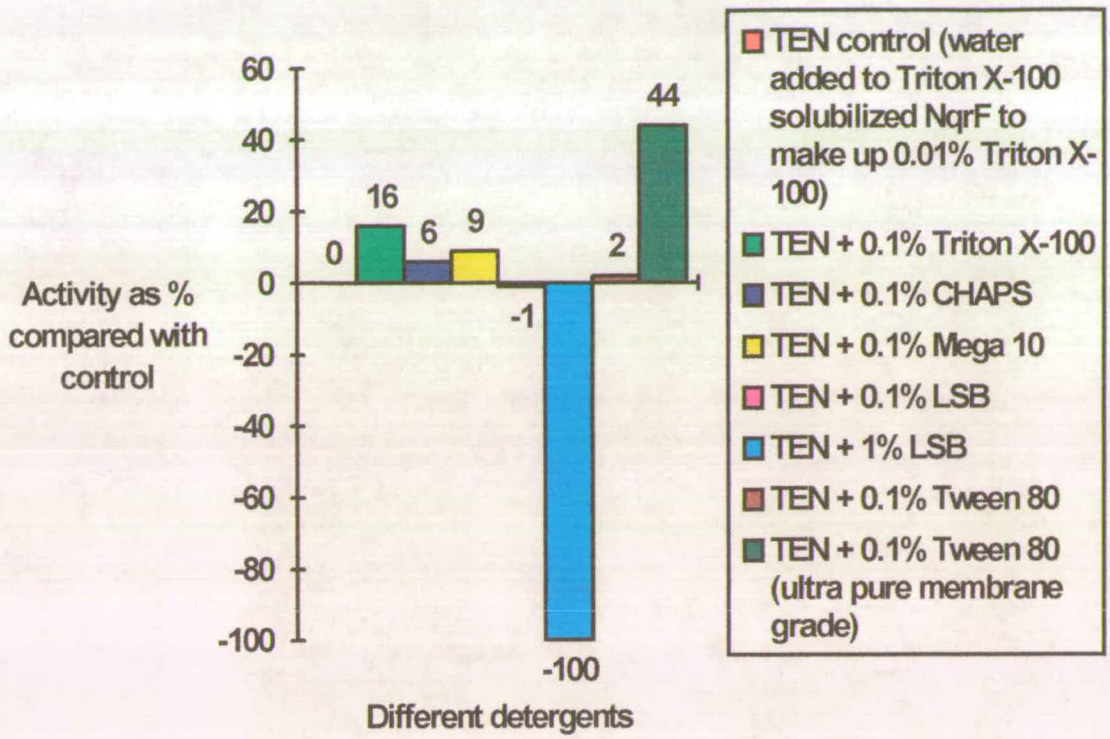

Fig. 6.1 Chart comparing the inclusion of some commonly-used detergents in NqrF chromatography buffers. Samples were incubated at 4°C for 16 hours before being assayed for NADH dehydrogenase activity. Each sample was assayed thrice and an average value obtained.

Legend

TEN: 50 mM Tris-HCl (pH 7.5), 5 mM EDTA, 0.4 M NaCl.

TENT: 50 mM Tris-HCl (pH 7.5), 5 mM EDTA, 0.4 M NaCl, 0.1% Triton X-100.

6.2 Degradation

After purification and storage at 4°C for weeks, NqrF seemed to be specifically degrading as evidenced by the emergence of a 39 kDa protein replacing the 46 kDa protein as the major product (Fig. 6.2). This lower molecular weight band retained NADH dehydrogenase activity when the zymogram stain was applied. This may imply that NqrF was degrading, probably at a specific point on its hydrophobic *N*-terminal region rather than the *C*-terminal region where the NADH-binding site is located. Alternatively, it could also imply that in the absence of its native lipid environment when purified, it was folding into a conformation which made it run anomalously on gels.

Calculations of the precise molecular weight of this apparently degraded product indicates that it was 39 kDa. If this resulted from degradation of the *N*-terminal hydrophobic region of NqrF, this would mean that approximately 62 amino acid residues (which constitute the hydrophobic *N*-terminal region of NqrF) just upstream of the [2Fe-2S] binding site have been deleted. Since this deletion is very close to the iron-sulfur cluster site, this could explain the absence of iron-sulfur clusters in EPR analysis as this deletion could affect the conformation of this site. This degradation may ironically prove favourable as it could provide the key to purification of a soluble protein for crystallization studies.

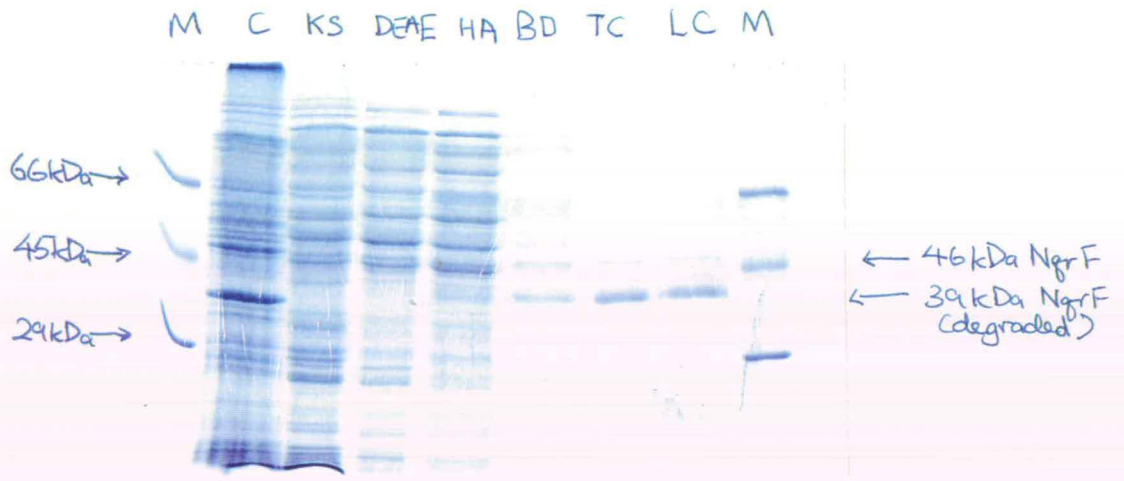

Fig. 6.2 Coomassie Blue-stained 10% SDS PAGE gel displaying the total protein profile in various stages of purification. This shows the degradation of 46 kDa NqrF to a 39 kDa polypeptide in TC and LC.

M: Markers. Bovine serum albumin, 66 kDa; Chicken egg ovalbulmin, 45 kDa; Carbonic anhydrase, 29 kDa.
C: membrane extract of control BL21(DE3)p*LysS* cells with pET16b.
KS: membrane extract of BL21(DE3)p*LysS* cells expressing NqrF from pET16b (pKT02).
DEAE: Pooled DEAE Sepharose fractions with activity.
HA: Pooled Hydroxyapatite fractions with activity.
BD: Pooled Mimetic Blue-2 Dye affinity fractions with activity (Triton X-100).
TC: Concentrated purified NqrF (Triton X-100).
LC: Concentrated purified NqrF (LSB).

6.3 Stability of NqrF under different conditions

Experimental results tabulated in Table 6.1 indicate that there was a minute loss of activity when stored at 4°C rather than frozen. A 30% loss in activity was observed when left at room temperature for 2 hours as compared with storage in ice. Very low temperatures prevent degradation (Fig. 6.3). Crude membrane fractions containing the NqrF subunit tended to retain activity for weeks when stored at -20°C, in 10% (v/v) glycerol and 1 mM PMSF which may imply that the NqrF catalytic subunit requires lipids in the crude membrane extracts or interaction with other Nqr subunits for stability under normal physiological conditions and temperatures. Fig. 6.4 demonstrates that NqrF is most stable at pH 8.0 and 7.0.

Solubilization in Triton X-100 rather than Tween-80 or LSB, was preferred as inferred from incubation of NqrF in various detergents and previous solubilization results of the Na^+-NQR complex (Stevenson, 1994). Although the zwitterionic detergent, lauryl sulphobetaine, resolves the NqrF subunit from aggregates to monomers, it possibly affected NqrF's catalytic activity adversely by disrupting its natural conformation (Fig. 6.1). Ethylene glycol and high concentrations of Triton X-100 aided chromatography in hydroxyapatite columns but not in DEAE sepharose columns.

There was a small loss of activity when NqrF was incubated with azide or PMSF (Fig. 6.5 and Table 6.1). 10% (v/v) glycerol added to buffers appeared to prevent proteolysis and loss of activity, as is the case with EDTA which inhibits metalloproteases at the initial stages of purification. Dithiothreitol reduces the [2Fe-2S] cluster which in its reduced state is slightly oxygen-sensitive but stable otherwise. It also protects the -SH groups ion in the catalytic NADH dehydrogenase site and prevent its inactivitation.

Table 6.1. Activity of NqrF with respect to different storage buffer conditions.

Conditions	Average total activity μmol NADH/min (assayed twice)	% compared with control
Control: Tris, EDTA, NaCl, Triton X-100, (TENT), pH 7.5, fridge	0.069	100% (This is the control)
TENT, pH 7.5, room temperature	0.012	17%
TENT, pH 7.5, freezer	0.075	109%
PO_4, LSB, pH 6.0	0.051	74%
PO_4, LSB, pH 6.5	0.057	83%
TENT, pH 7.0	0.068	99%
TENT, pH 7.5	0.069	100%
TENT, pH 8.0	0.069	100%
TEN, Tween 80, pH 7.5	0.047	68%
TENT, pH 7.5, 10% glycerol	0.079	114%
TENT, pH 7.5, 1% ethylene glycol	0.062	90%
TENT, pH 7.5, 1 mM PMSF	0.054	79%
TENT, pH 7.5, 1 mM DTT	0.073	105%
TENT, pH 7.5, 0.1 mM FAD	0.072	104%
TEN, pH 7.5	0.067	97%
TNT, pH 7.5	0.047	68%
TENT, pH 7.5, 0.02% azide	0.050	72%

TNT: buffer with 50 mM Tris-HCl, 0.5 M NaCl and 0.1% (v/v) Triton X-100.
TEN: buffer with 50 mM Tris-HCl, 5 mM EDTA, 0.5 M NaCl.
TENT: buffer with 50 mM Tris-HCl, 5 mM EDTA, 0.5 M NaCl and 0.1% (v/v) Triton X-100.
PO_4: buffer with 20 mM potassium phosphate.

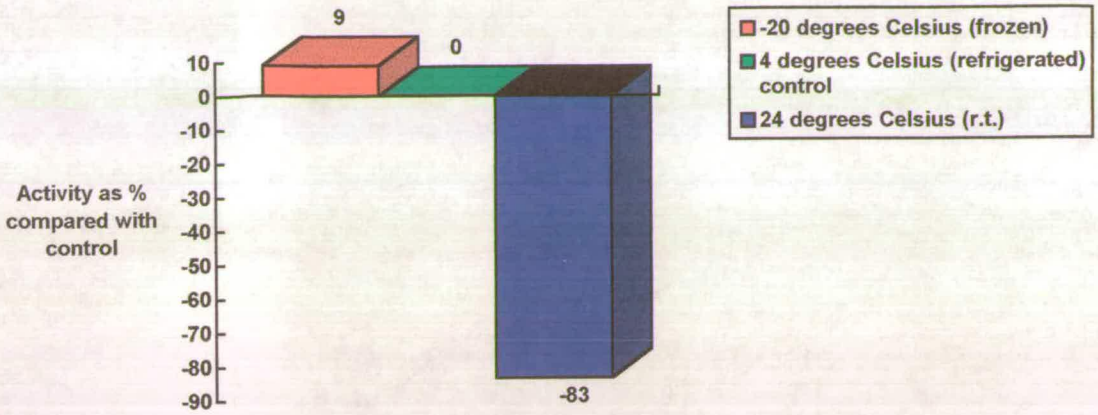

Fig. 6.3 Effect of different storage temperatures on the activity of NqrF. Purified NqrF was stored at the above temperatures for 16 hours and tested for NADH dehydrogenase activity. Each sample was assayed thrice and an average value obtained.

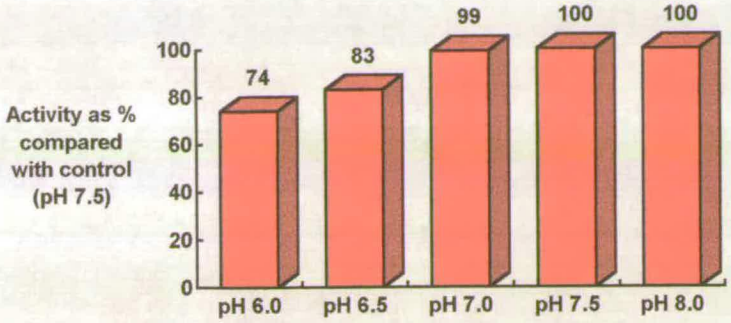

Fig. 6.4 Chart comparing the stability of NqrF at different pHs. Purified NqrF was incubated in the buffers of various pHs at 4^{o}C, 16 hours and then tested for NADH dehydrogenase activity. Each sample was assayed thrice and an average value obtained.

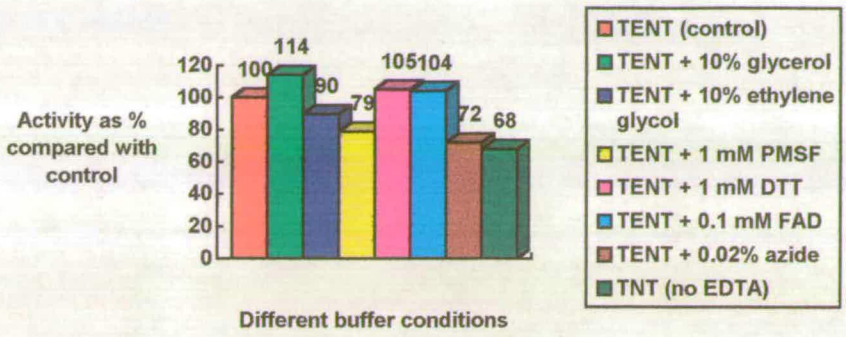

Fig. 6.5 Chart comparing the stability of NqrF stored in the presence of different additives to its storage buffer. Incubation proceeded at 4°C for 16 hours before samples were tested for NADH dehydrogenase activity. Each sample was assayed thrice and an average value obtained.

Legend

TNT: buffer with 50 mM Tris-HCl, 0.5 M NaCl and 0.1% (v/v) Triton X-100.

TEN: buffer with 50 mM Tris-HCl, 5 mM EDTA, 0.5 M NaCl.

TENT: buffer with 50 mM Tris-HCl, 5 mM EDTA, 0.5 M NaCl and 0.1% (v/v) Triton X-100.

According to the predicted model (Fig. 3.8), the [2Fe-2S] cluster is found near the membrane and it may hence need a hydrophobic environment and interactions to maintain its structure. Alternatively, these iron sulphur clusters may have been damaged when the polypeptide was extracted from the membranes during sonication and solubilization.

Table 6.2 also indicates that the cells should be processed past the sonication stage, unbroken cells spun down and the supernantant frozen in storage awaiting further fractionation by centrifugation the next day. Loss of activity when cells are just frozen upon harvesting without proceeding to the sonication stage, is attributed to lysis of BL21(DE3)p*LysS* (this strain lyses upon thawing) allowing cytoplasmic proteases to attack the membrane proteins and cause harmful oxidative stress to these proteins as well. The lysis of BL21(DE3)p*LysS* also seems to dislodge some membrane-bound NqrF into the cytoplasmic fraction. The addition of DTT and protease-inhibitors to sonication buffers helped reduce degradation of overexpressed membrane proteins. PMSF added at the point of induction also seemed to preserve NqrF activity to some degree from serine-protease degradation.

6.4 Isoelectric focussing (Moredun Research Institute)

An SDS protein gel profile obtained from running isoelectrically focussed samples, suggested that the pI of NqrF was about 5.1 to 5.44, although the predicted pI from sequence data was 4.54, but the inherent instability of NqrF at low pH may have caused denaturation at lower pH (Fig. 6.6).

Table 6.2. Results for activities of small scale preparations processed under different conditions.

Fractionation conditions	Fractiion	Total activity µmol NADH/min	Total Ag^{+}-insensitive activity µmol NADH/min	Total Ag^{+}-sensitive activity µmol NADH/min	% Ag^{+}-sensitive activity
old DNA IPTG PMSF Spin Process	cytoplasmic	2.60	2.49	0.11	1.6%
	membrane	0.31	0.22	0.09	30%
	outer membrane	0	0	0	0
old DNA IPTG PMSF Spin/stop Process	cytoplasmic	2.17	1.55	0.62	28.6%
	membrane	0.07	0.08	0	0
	outer membrane	0	0	0	0
old DNA IPTG+PMSF Spin Process	cytoplasmic	2.19	2.06	0.13	5.9%
	membrane	0.68	0.23	0.45	66.2%
	outer membrane	0	0	0	0
new DNA IPTG PMSF Spin Process	cytoplasmic	1.81	1.83	0	0
	membrane	0.15	0.14	0.013	8.1%
	outer membrane	0	0	0	0
new DNA IPTG PMSF Spin/stop Process	cytoplasmic	2.61	2.49	0.12	4.6%
	membrane	0.19	0.12	0.067	35.0%
	outer membrane	0	0	0	0
new DNA IPTG+PMSF Spin Process	cytoplasmic	3.17	2.62	0.55	17%
	membrane	0.70	0.13	0.57	82%
	outer membrane	0	0	0	0
control IPTG PMSF Spin Process	cytoplasmic	1.59	1.52	0.07	4.4%
	membrane	0.137	0.14	0	0
	outer membrane	0	0	0	0

The usual scheme of growth, purification and fractionation involves transforming the expression host with pKT02 DNA to obtain fresh transformants, growing the cells, inducing with IPTG and adding serine-protease PMSF and then harvesting the cells by spinning then down in a centrifuge. Disrupted cells are then sonicated and centrifuged at high speed to obtain a soluble cytoplasmic fraction and a membrane pellet. The membrane pellet is finally solubilized with detergent and another high speed centrifugation speed yields the outer membrane pellet and cytoplasmic membrane fraction.

New DNA and old DNA illustrates the age of the DNA used to transform into the expression host. The control does not express NqrF as it has not been transformed with pKT02 which contains the *nqr*F gene. IPTG + PMSF meant that IPTG and PMSF were added at the same time while IPTG followed by PMSF written below it, referred to PMSF being added 1 hour after induction by IPTG. Spin/stop referred to unsonicated/undisrupted cells being spun down and frozen after harvesting while Spin followed by Process beneath it, indicated that cells are sonicated before being frozen in a solution containing glycerol and PMSF.

Fig. 6.6 Coomassie Blue-stained 10% SDS PAGE gel run with samples from isoelectric focussing.

6.5 Metallic cation inhibition

One important aspect of NqrF inhibitor specificity is that it is irreversibly and significantly inhibited by low concentrations of Ag^{+}. This was demonstrated in Fig. 6.7 whereby Ag^{+} inhibited the purified NqrF drastically after 1 min incubation at room temperature (K_i 1 μM). However, the addition of Cu^{2+}, Cd^{2+}, Pb^{2+} and Zn^{2+}, which are strong inhibitors of the Na^{+}-NQR complex (Bourne *et al*, 1992), gave only weak non-specific inhibition (<20%) of NqrF; increasing the concentration of these cations in the range 2.5 - 10 μM caused little further change. Moreover, the addition of EDTA did not reverse inhibition in all cases.

The Ag^{+}-sensitivity of native NqrF and His-tagged NqrF and their distribution in cytoplasmic, membrane and outermembrane pellet fractions were also examined, and the results are illustrated in Fig. 6.8, 6.9 and 6.10. NADH dehydrogenase activity that was Ag^{+}-sensitive and rotenone-insensitive (i.e. NqrF activity) was found mainly in the inner membrane fraction for native NqrF-expressing clones and in the cytoplasm in the His-tagged NqrF-expressing clones. Rotenone-sensitive NADH dehydrogenase activity in the membrane and cytoplasmic fractions are attributed to the activity of subunits of the H^{+}-translocating NDH-1. Much of the cytoplasmic NADH dehydrogenase activity was rotenone-insensitive and Ag^{+}-insensitive and this is characteristic of NDH-2 which is resistant to most inhibitors.

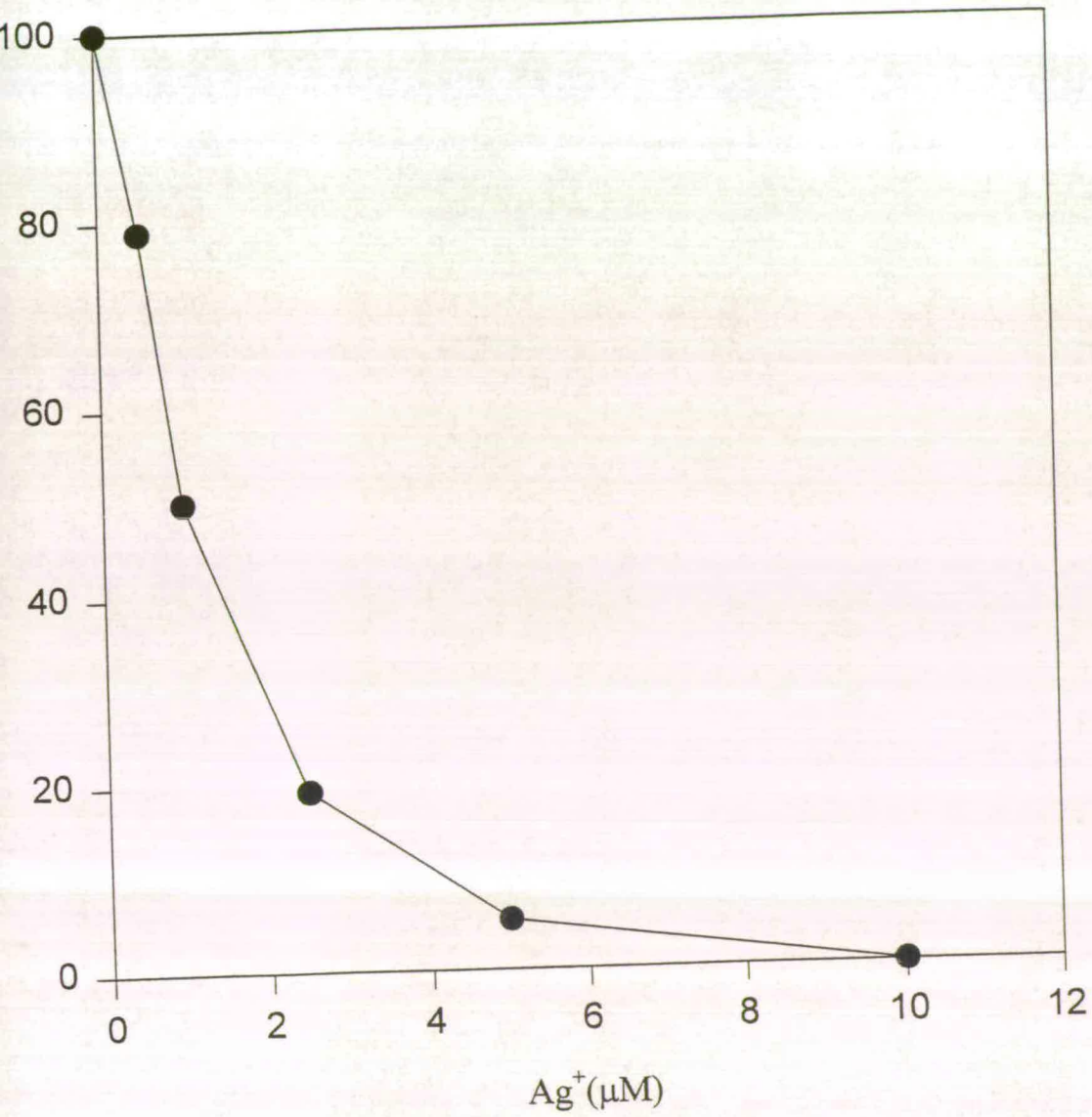

Fig. 6.7 Inhibition of NADH dehydrogenase activity by addition of Ag^+.
0.8 μg of NqrF was incubated with various concentrations of Ag^+ for 1 min at room temperature before being subjected to NADH menadione oxidase assays. 100% activity = 39 U/mg. K_i = 1 μM.

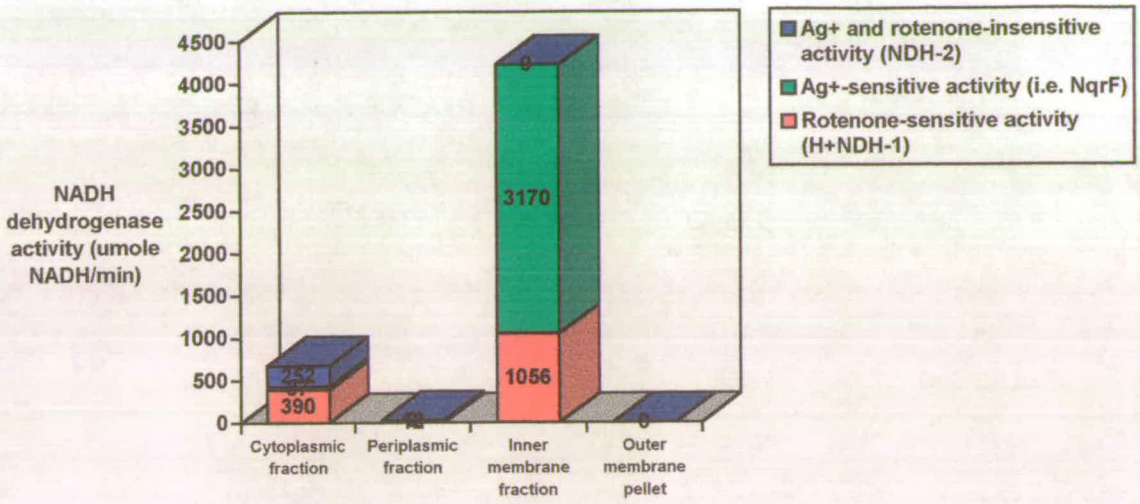

Fig. 6.8 Chart illustrating the distribution of native NqrF activity in the various cell fractions. Ag^+-sensitive activity is attributed to NqrF, rotenone-sensitivity is ascribed to H^+-NDH-1, while Ag^+- and rotenone-insensitive NADH dehydrogenase activity is characteristic of NDH-2. Triplicate samples were incubated with 10 μM Ag^+ or rotenone before being tested for NADH dehydrogenase activity using the NADH menadione oxidase assay.

In both the outer membrane pellet and periplasmic fraction, there was no or negligible NADH dehydrogenase activity detected, as expected. 58% of the NADH dehydrogenase activity in the cytoplasmic fraction was rotenone-sensitive and attributed to the native H^+-translocating NADH ubiquinone oxidoreductase (NDH-1) of the *E. coli* host while 37% of the activity in this fraction was rotenone- and silver-insensitive and ascribed to the non-energy coupled NADH dehydrogenase (NDH-2) of *E. coli* with negligible NqrF activity. About 25% of the activity in the cytoplasmic membrane was rotenone-sensitive and hence identified as that of NDH-1 while 75% of the NADH dehydrogenase activity in the inner membrane was silver-sensitive and hence linked to NqrF.

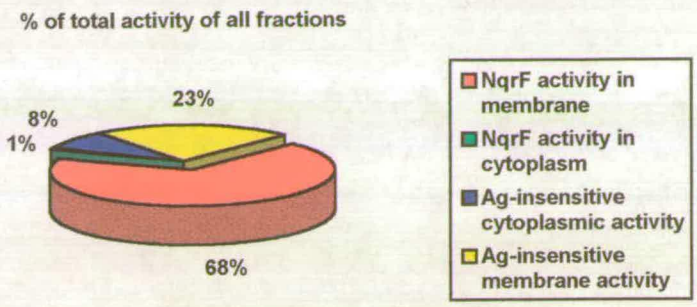

Fig. 6.9 Pie-chart showing the distribution of NADH dehydrogenase activity in various cell fractions. Each sample was assayed thrice for NADH dehydrogenase activity after 1 min incubation with 10 μM Ag^{+} and an average value obtained.

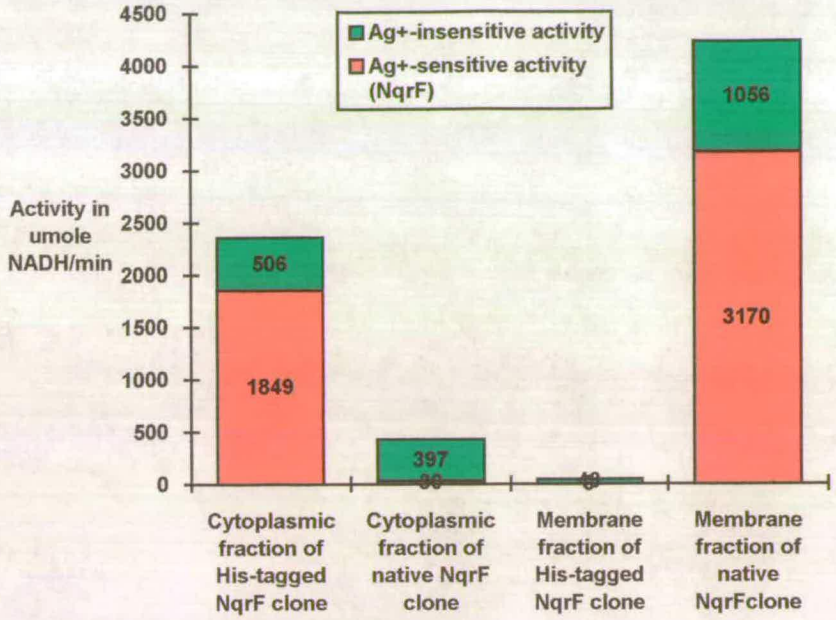

Fig. 6.10 Chart comparing the distribution of NqrF and His-tagged NqrF in the different cell fractions. Each sample was assayed thrice for NADH dehydrogenase activity after 1 min incubation with 10 μM Ag^{+} and an average value obtained.

75% of the NADH dehydrogenase activity was silver-sensitive (i.e. attributed to NqrF and not NDH-1 nor NDH-2) in the membrane fraction of the native NqrF clone, while about 75% of the NADH dehydrogenase activity was silver-sensitive in the cytoplasmic fraction of the His-tagged NqrF clone. The histidine residues had tagged onto the *N*-terminus of NqrF, affecting the hydrophobic domain's ability to span the cytoplasmic membrane, resulting in its location in the cytoplasmic fraction rather than in the membrane fraction.

6.6 Cysteinyl (sulphydryl) inhibitors

Cysteinyl inhibitors such as iodoacetic acid and *N*-ethylmaleimide, were tested for the inhibition of catalytic activity of NqrF from concentrations ranging from 1 μm to 500 μM. No significant decrease in activity of NqrF was observed when these substances were incubated with NqrF for 1 min at room temperature before assays were commenced. This concludes that the cysteine residues found in NqrF, especially C-377 at the NADH-binding site, do not have direct interaction with the substrate, NADH via disulphide bonds. This also suggests that the [2Fe-2S] cluster (coordinated by 4 cysteine residues) was already disrupted during the sonication stages, cleaved off or not formed at all as there is no noticeable decrease in activity when these cysteinyl inhibitors were applied to NqrF.

6.7 Inhibition by classical NADPH oxidoreductase and nitroreductase inhibitors

It was determined that dicoumarol is not an inhibitor and there is less than 20% inhibition even at a high concentration of 100 μM. 4-nitrobenzoic acid is also not an inhibitor. Nitrofurantoin is an irreversible inhibitor at high concentration (0.5 mM) whereas nitrofurazone is not an inhibitor but appears to be a poor substrate at high concentrations (1 mM), giving 40% of the rate observed with menadione but only 0.6% of this rate at 0.1 mM.

6.8 Substrate specificity

NqrF utilizes the NADH analogue dNADH as a substrate (K_m 50 μM, Fig. 6.11) but has much poorer affinity for it as compared with NADH (K_m 10 μM, Fig. 6.12). Ferricyanide has a poor affinity for NqrF (K_m 1.7 mM) but is a good electron acceptor for NqrF at high concentrations (V_{max} 530 U, Fig. 6.13), compared with menadione (Fig. 6.14) while cytochrome *c* is not able to act as an electron acceptor for NqrF.

The K_m of 10 μM obtained for NADH, is similar to figures obtained by other groups but the K_m for menadione (143 μM) was much higher than previously reported for the complex. NqrA, NqrC and another hydrophobic subunit was reported to be essential for quinone reductase activity (Hayashi and Unemoto, 1984, 1986); this supports the proposal that binding and reduction of the physiological electron donor, ubiquinone, a hydrophobic molecule, requires NqrA and NqrC, in addition to NqrF (Rich *et al.*, 1995).

Although all points for graphical plots were obtained by repeating the experiment at least 3 to even 6 times per value and the figures averaged (for sections 6.5-6.8), it is noted that it would be more useful in future to create graphical plots with standard deviations for each point for more meaningful results.

6.9 Sodium ion dependence

The catalytic activity of NqrF was not dependent on Na^+ or affected by NaCl concentrations. It is not the Na^+-translocating subunit of the Nqr complex.

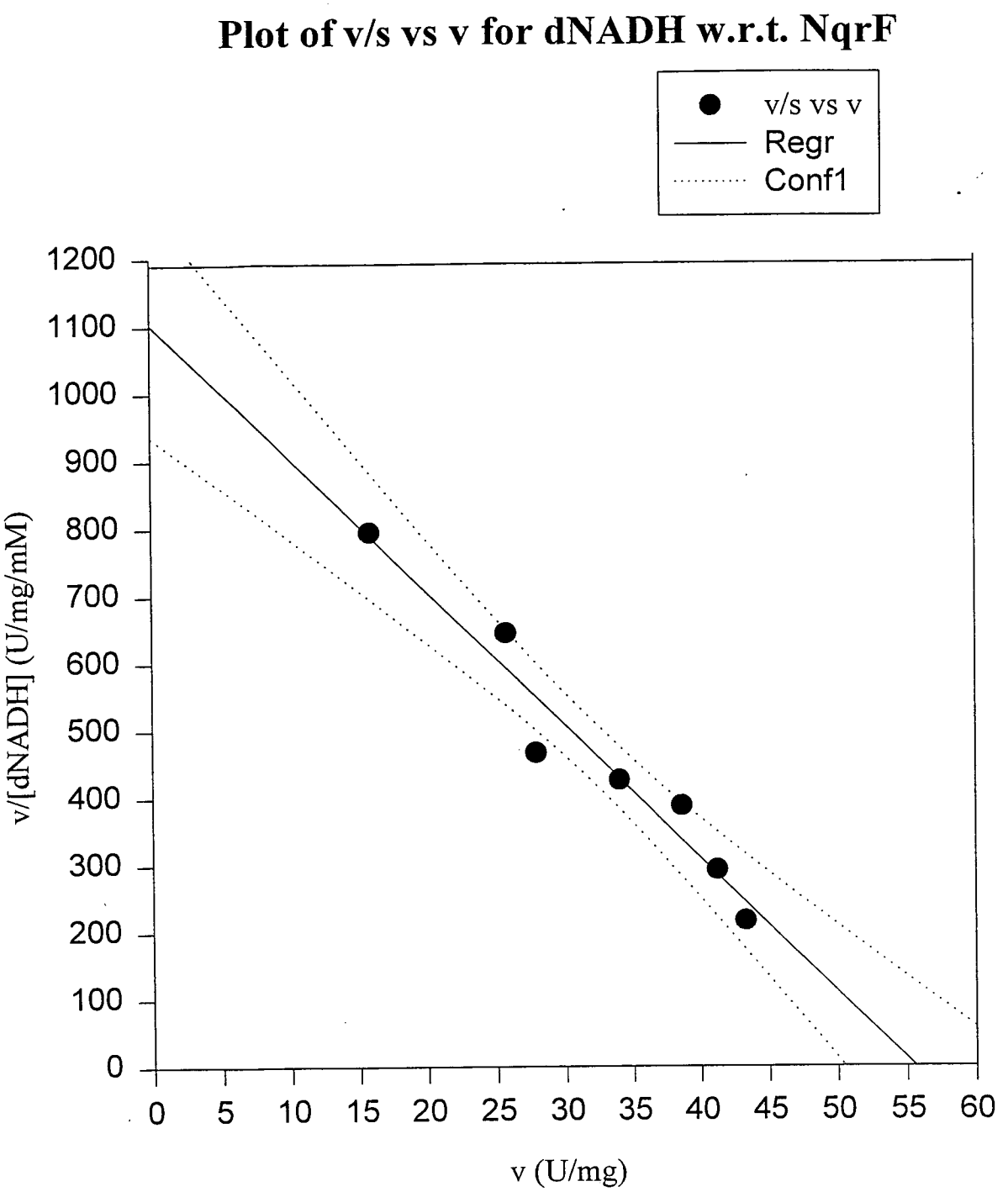

g. 6.11 Plot of v/s vs v to determine K_m and V_{max} values for dNADH.

$_m$ for dNADH = 50 μM, V_{max} = 55.7 U/mg

6 μg of NqrF was added to assay mixture containing 20 mM Tris-HCl, pH 7.5, 0.4 M NaCl.

)0 μM menadione was used as electron acceptor.

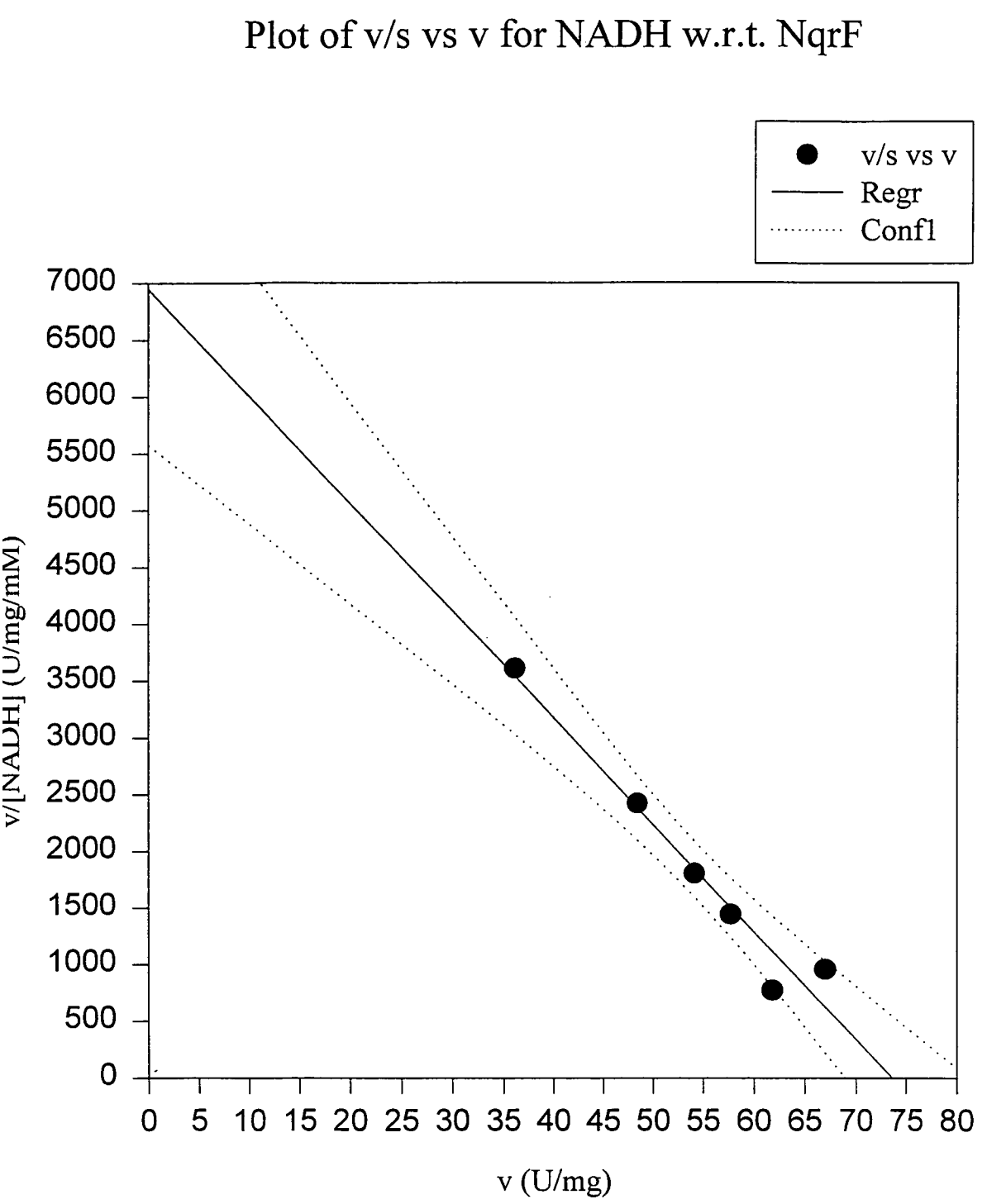

Fig. 6.12 Graph of v/s vs v for determination of K_m of NADH.
K_m of NADH = 10.5 μM and V_{max} = 73 U/mg
1.6 μg NqrF was incubated with assay mixture containing 20 mM Tris-HCl, pH 7.5, 0.4 M NaCl and various [NADH], using 0.1mM menadione as electron acceptor.

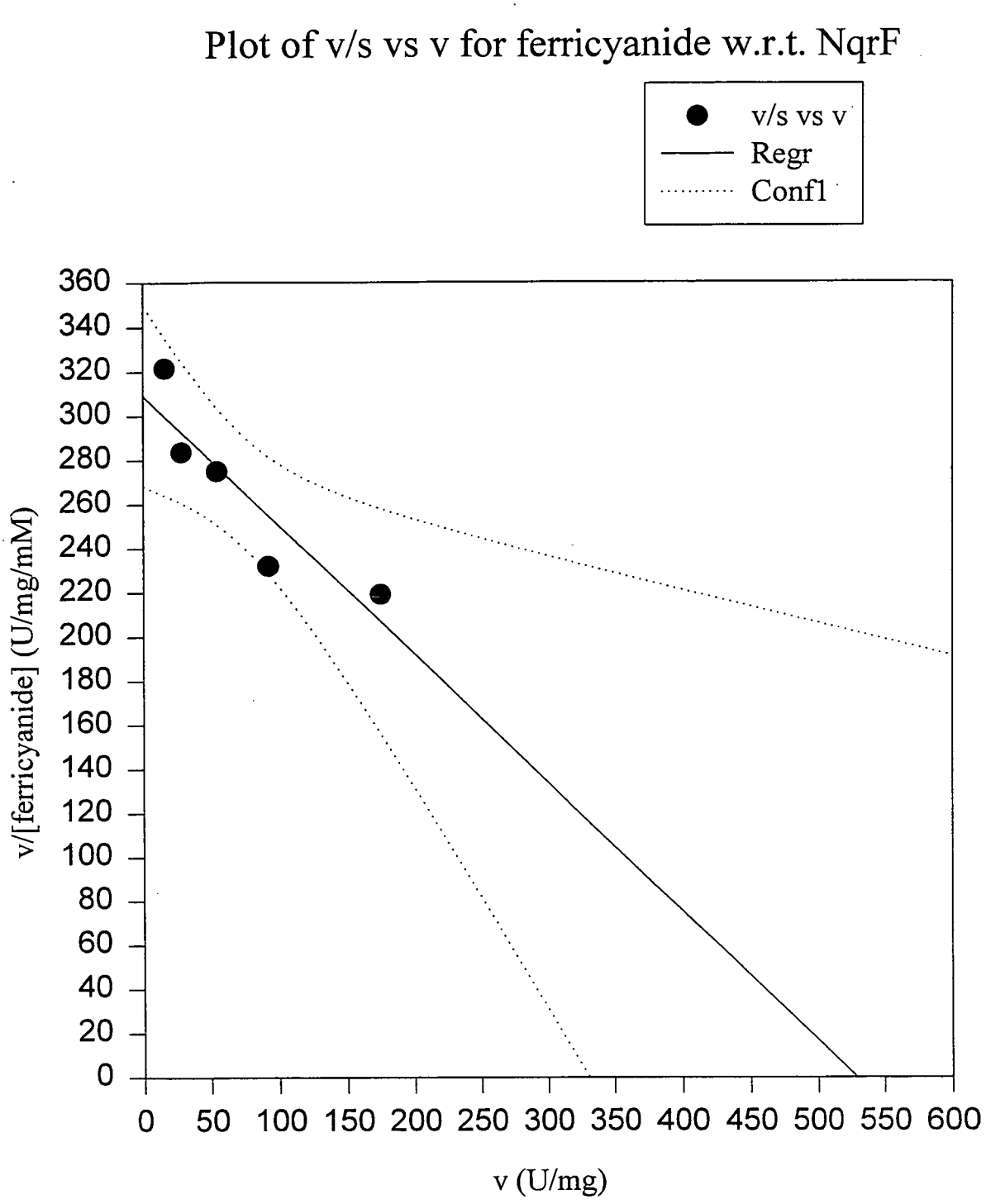

Fig. 6.13 Plot of v/s vs v to determine K_m and V_{max} values for ferricyanide
K_m of ferricyanide = 1.7 mM, V_{max} = 525.6 U/mg
1.6 µg of NqrF was added to assay mixture containing 20 mM Tris-HCl, pH 7.5, 0.4 M NaCl, 0.2 mM NADH.

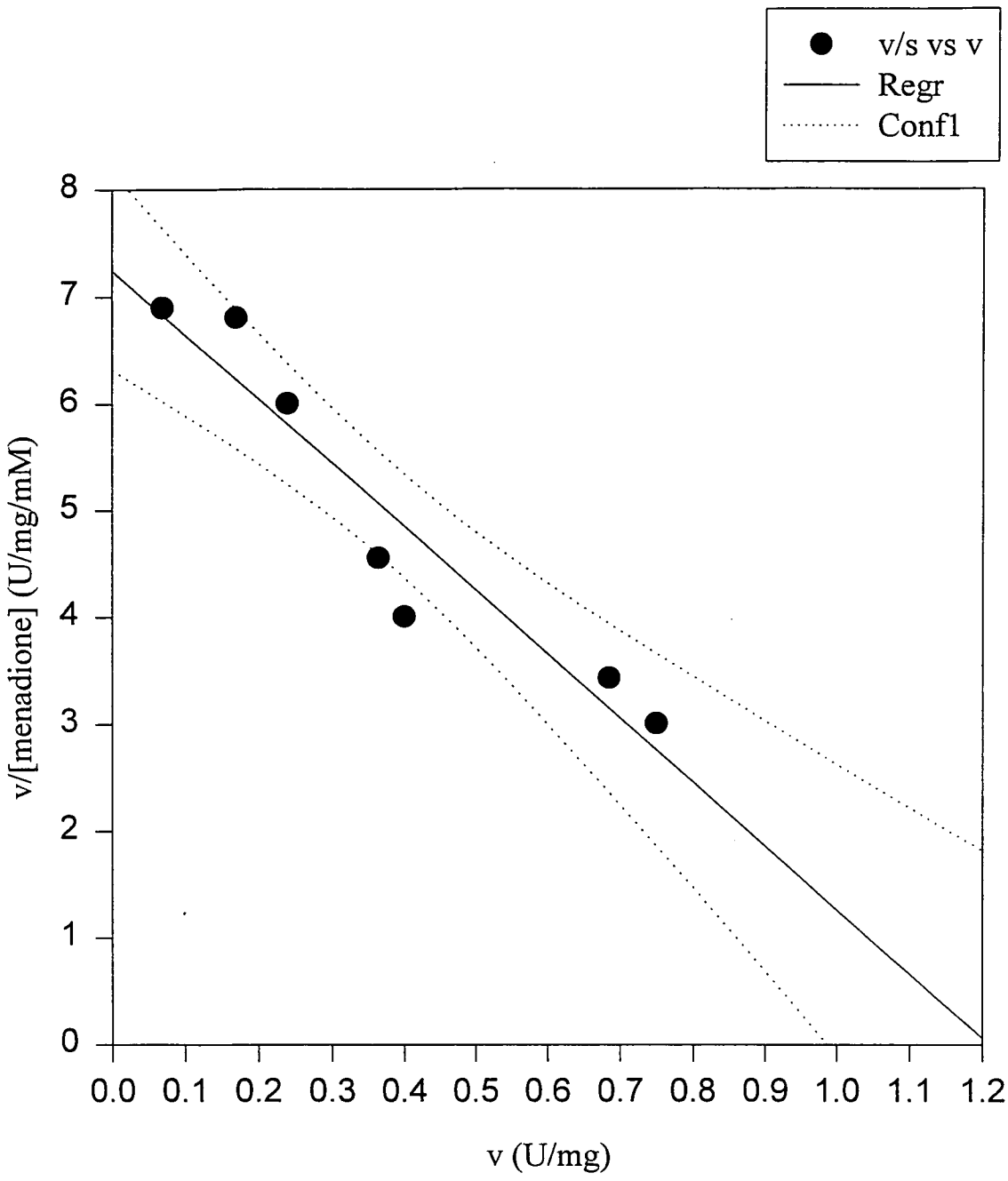

Fig. 6.14 Plot of v/s vs v to determine K_m and V_{max} values for menadione
K_m for menadione = 143 μM
V_{max} for menadione = 106 U/mg
1.6 μg of NqrF was added to assay mixture containing 20 mM Tris-HCl, pH 7.5, 0.4 M NaCl, 0.2 mM NADH

6.10 Absorbance spectrum of NqrF

The oxidised spectrum of NqrF produced maximum at 475 nm and 405 nm which is a characteristic absorbance of a flavin. An interesting feature of the spectrum of partially reduced NqrF, was a maximum at 525 nm, a possible indication of the formation of a relatively stable flavin semiquinone anion. When NqrF was fully reduced anaerobically by NADH, there was a general decrease in absorbance between 420 nm to 510 nm indicating the flavin is fully reduced to quinol and the absence of the semiquinone (Fig. 6.15). This absorbance spectrum of NqrF is quite similar to that of phthalate dioxygenase reductase which has a plant Fd type [2Fe-2S] centre and FMN on a 34 kDa protein (Corell *et al.*, 1992). Using the molar extinction coefficient of FAD at 450 nm (11.3 mM^{-1}) and the spectral absorbance values of a known concentration of NqrF sample at 450 nm, the ratio of the number of moles of FAD per mole of NqrF was calculated to be 0.8. Hence it was concluded that there is 1 mole of FAD per mole of NqrF.

6.11 Flavin determination and reconstitution

There was only a modest increase in NADH dehydrogenase activity (20%) when NqrF was reconstituted with FAD while there was no increase and probably a minute decrease in activity (-5%) when NqrF was incubated with FMN.

Comparisons of paper chromatography R_f values obtained from NqrF, FAD and FMN, the latter two being used as commercial standards, suggests that NqrF contains FAD, not FMN. Overall, no significant loss of FAD was observed to occur with NqrF when stored at 4°C over time.

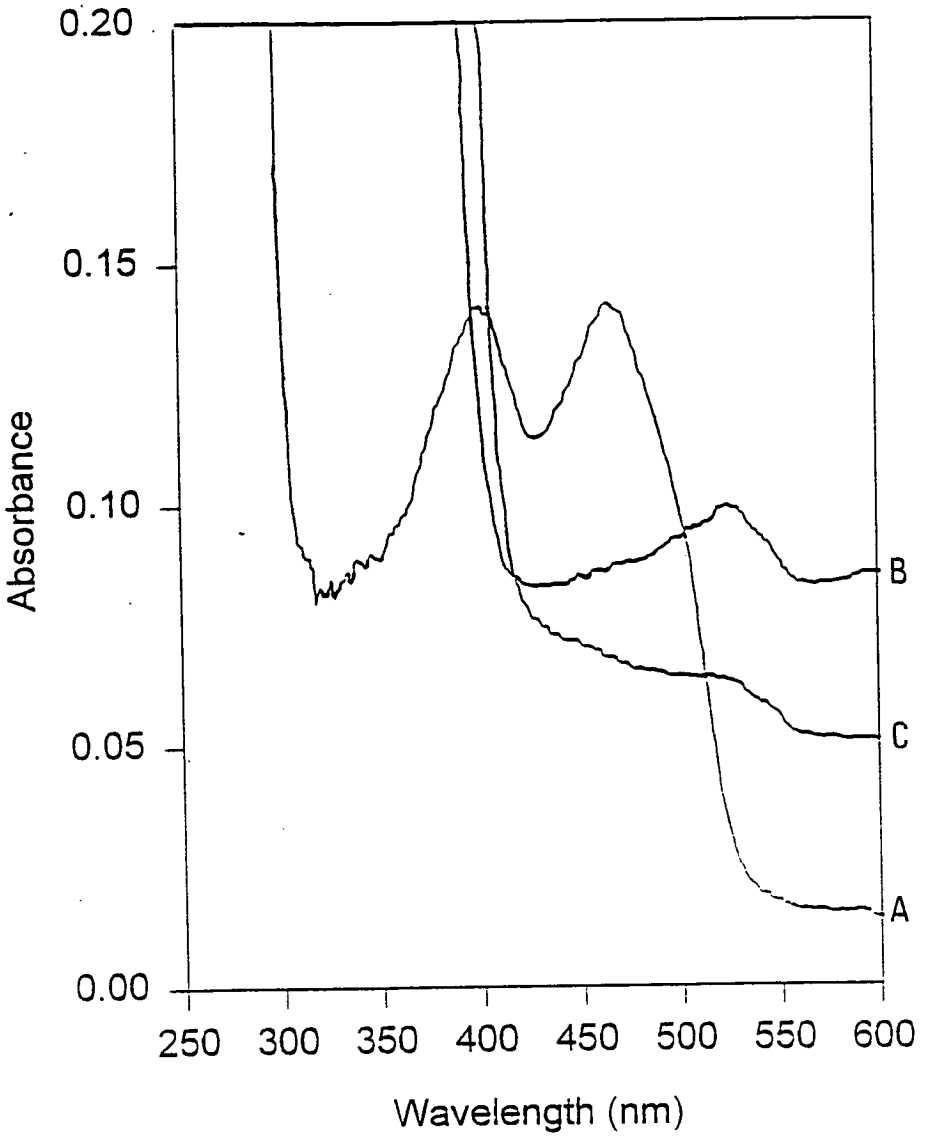

Fig. 6.15 Absorption spectra of NqrF.
Curve A is the spectrum of oxidised NqrF. B is the spectrum recorded 10 seconds after NqrF was mixed anaerobically with excess NADH, while C is the spectrum recorded 20 min later.

6.12 Electron paramagnetic resonance studies (R. Cammack, King's College)

Samples were sent to Prof. Cammack at King's College for EPR analysis. The EPR spectra did not show any signals other than a small radical signal at g=2.00. This was partly in the quartz and there were no significant signals at g=1.94 which would have been expected for a [2Fe-2S] cluster. The increase in the radical in dithionite-reduced sample is probably due to SO_2^- radicals. The samples were hence either too dilute or they had lost their Fe-S clusters due to sonication. The latter may be due to the fact that the predicted [2Fe-2S] site is very close to the membrane-spanning hydrophobic *N*-terminal and hence the conformation of the protein may have altered in this region when the membrane was sonicated and solubilized, such that it no longer binds the iron-sulphur cluster. The specific degradation to the 39 kDa protein may also contribute to this loss of conformation. Pfenninger-Li *et al.* (1996) purified the Na+-NQR complex and have reported that although clear EPR signals indicating [2Fe-2S] in the purified Nqr complex, these signals were lost when NqrF was fractionated from the rest of the complex. From their results, they suggested that NqrF required possibly 1 or more of the hydrophobic subunits for maintaining the [2Fe-2S] site. In addition, the incoporation of such centres into the apoprotein in overexpressed systems may not be keeping in pace with the rapid synthesis of the protein. Ferric citrate and sodium sulphite were added to the culture medium to enhance [2Fe-2S] incorporation. The absence of Fe-S EPR signals was also not surprising as previous expression of the H^+-NDH-1 flavoprotein subcomplex composed of 50 kDa (NQO1) and 25 kDa (NQO2) subunits of *P. denitrificans* in *E. coli* achieved for EPR studies by Yano *et al.* (1996), required reconstitution of the Fe-S clusters. Incorporation of FMN and [4Fe-4S] was postulated to require some specific *P. denitrificans* genes/ gene products or interaction with neighbouring NQO subunits as overexpressed subunits had to be reconstituted for EPR studies.

6.13 Blotting and *N*-terminal sequencing

Purified samples of NqrF containing both the 46 kDa native protein and its 39 kDa *N*-terminally degraded derivative, were run using a modified SDS-PAGE procedure optimized for efficient *N*-terminal sequencing. The protein from these gels were electroblotted onto PVDF membranes and frozen, awaiting *N*-terminal sequencing.

6.14 *nqr*F::*bla*M translational fusions

The *nqr*E and *nqr*F genes were cloned into pJBS633 (pKT05) using *Eco*RV (blunt-ended site on pJBS633)/ *Pvu* I (blunt-ended site on pKT02) and *Sal*I site (on pJBS633 and pKT02), as shown in Fig. 6.16. A *Sph*I site close to the *C*-terminal of *nqrF*, produces a 4-base 3' extension which is not susceptible to exonuclease III digest, while a *Bfr*I site just upstream of the *Sph*I site produces a 3-base 5' extension which can be digested by exonuclease III.

From an agarose gel picture of DNA obtained at different time courses of exonuclease III digestion, the deletion experiment has been successful (Fig. 6.17). In excess of 200 in-frame *bla*M fusion mutants were identified when they were streaked on ampicillin (200 μg/ml). However when screened subsequently for single colony-resistance to ampicillin, none were found, indicating that all 200+ fusions were cytoplasmic. Two of these cytoplasmic fusions which grew best when patched on ampicillin, were sequenced and confirmed to be fused at a predicted cytoplasmic region of NqrF or exonuclease III-undigested parental pKT05. Hence, there were no fusions of periplasmic/membrane regions of NqrF to β-lactamase. This leads to the conclusion that either all periplasmic/membrane fusions of NqrF with β-lactamase led to unviable mutants or the previously observed degradation of NqrF at a specific *N*-terminal point has removed its hydrophobic *N*-terminal region, resulting in a soluble recombinant fusion protein that remains in the cytoplasm and does not insert into the membrane of the host cell.

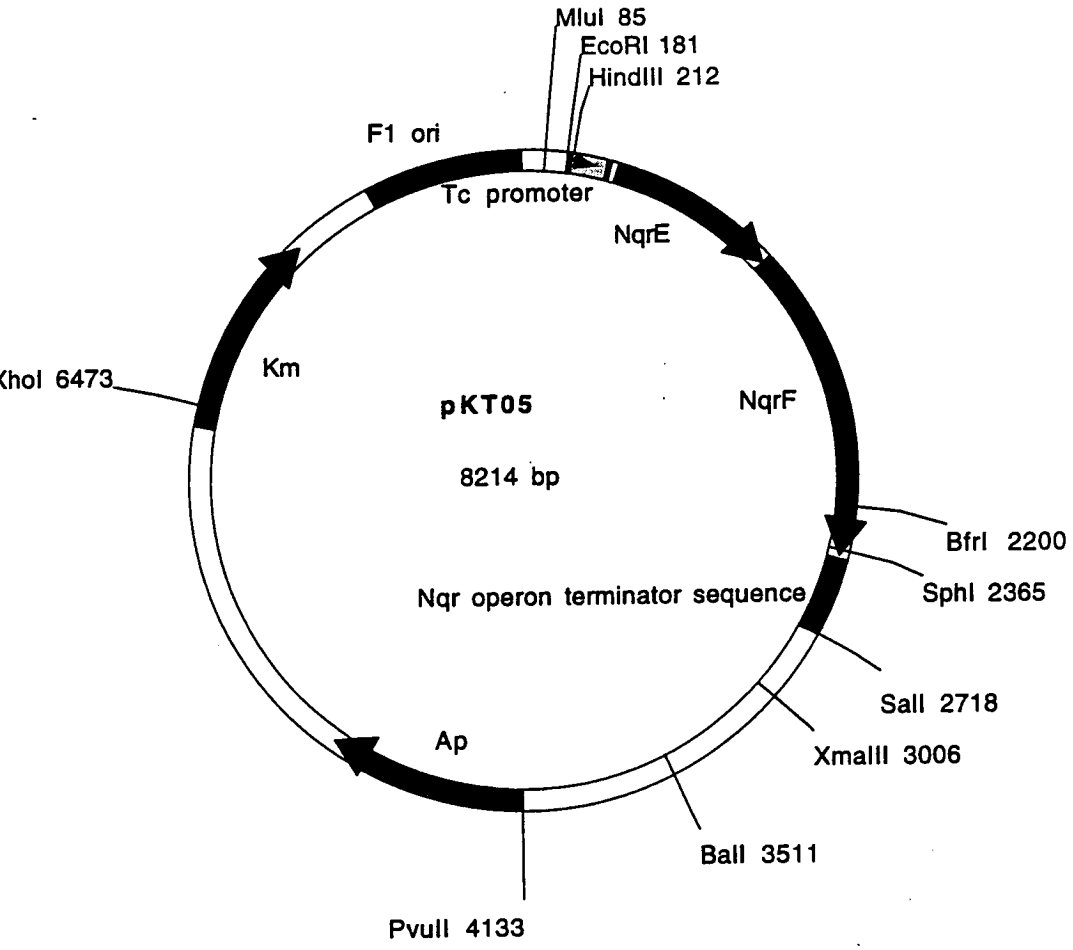

Plasmid name: pKT05
Plasmid size: 8214 bp
Constructed by: Karen Tan
Construction date: 1996
Comments/References: NqrE and NqrF cloned into pJBS633, using polylinker pSL1180.

Fig. 6.16 Plasmid map of pKT05. This plasmid was constructed by cloning *nqrE* and *nqrF* into pJBS633.

Fig. 6.17 Photograph of UV-illuminated DNA bands from exonuclease III digests, in ethidium bromide-stained 0.8% agarose gel. Samples 1, 4, 7, 10, 13, 16, 19 from progressive time-frames in exonuclease III digestion, demonstrate successful deletion. Marker, λ*Bst*EII, gives sizes in kb, 8.454, 7.242, 6.369, 5.686, 4.822, 4.324, 3.675, 2.323, 1.929, 1.371, 1.264, 0.702, 0.224.

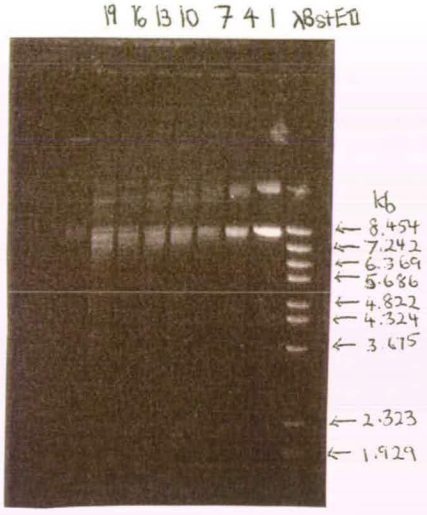

Chapter 7

Conclusions, discussion and future prospects

From sequence data and analysis, it is deduced that Na^+-NQR comprises 6 putative subunits that are co-transcribed from the same operon, using the same promoter. The Nqr proteins are encoded by chromosomal DNA, agreeing with results from Nakamura *et al.* and proving that the proposal from Tokuda and co-workers (1987) that Na+ pump genes are located on a plasmid, is erroneous. Hydropathy plots predicted that NqrA, NqrC and NqrF were the more hydrophilic polypeptides whereas NqrB, NqrD and NqrE were postulated to be highly hydrophobic transmembrane proteins. This accounts why previous purifications or partial purifications of the Na^+-NQR complex from *V. alginolyticus* by Hayashi and Unemoto (1987), Bourne and Rich (1992), Pfenninger-Li *et al.* (1996) and Beattie *et al.* (1994), only indicated the presence of 3 or 4 of the more hydrophilic subunits, as very hydrophobic polypeptides are easily lost in the purification process. Therefore, Na^+-NQR is provisionally anticipated to be composed of a relatively hydrophilic FP fragment of 3 subunits (NqrA, NqrC and NqrF) and containing 1 FAD and 1 [2Fe-2S] iron sulphur centre on the NADH-oxidising NqrF subunit, together with a hydrophobic HP fragment of 3 subunits (NqrB, NqrD and NqrE). Rich *et al.* (1995) proposed that the HP does not possess any obvious additional cofactor motifs, but may act as a transmembrane anchor which incorporates the ubiquinone binding site and possible sodium/proton channels between the iron sulphur centre and the membrane surface. This would be in agreement with our sequence analysis data that hydrophobic subunits NqrB and NqrD were 20-30% homologous to sodium channel transporters. Moreover, the experimental data that showed NqrF had the same K_m for NADH but a lower K_m for menadione compared to values obtained for the entire Na^+-NQR complex, would suggest that the binding site for hydrophobic ubiquinone (or other electron acceptor) may be formed by NqrF and another Nqr subunit(s). From comparison of sequences in

the SwissProt database, Nqr proteins have no obvious homology to any known protein in the database.

The Na^+-NQR complex not only lacked homology to the H^+-NDH1 or Complex I subunits, but also consists of a different number of subunits, with different cofactors and prosthetic groups. Hence it was concluded that Na^+-NQR was an evolutionarily distinct functional alternative to its H^+-translocating counterparts unlike the closely related Na^+-F type ATPases and H^+-F type ATPases. The theory of modular evolution proposed for H^+-translocating NADH ubiquinone oxidoreductases, seems also to be a likely explanation for the evolution for Na^+-NQR whereby a sodium pump which regulates pH homeostasis, and an NADH dehydrogenase entity evolved as separate structural modules but came together to form the present Na^+-NQR enzyme. This hypothesis is more plausible than the view that Na^+-NQR evolved from its H^+-translocating counterpart.

Hayashi *et al.* (1987) had purified a 52 kDa FMN-containing polypeptide which displayed Na^+-translocation in membrane vesicles. From the molecular weight of the protein, this was inferred to be NqrA or perhaps NqrB, although we could not detect an FMN-binding motif in the entire Nqr operon sequence. Our finding agreed with experimental data from Pfenninger-Li *et al.* (1995), who performed flavin analyses on their purified Nqr complex, and only detected the presence of FAD but no FMN in the purified enzyme and in *V. alginolyticus* membranes. A lack of a second flavin group motif was consistent with the previous inability of Bourne *et al.* (1992) to identify 2 different redox potentials of the flavin complement of the enzyme. Pfenninger-Li *et al.* (1995) suggested that Hayashi *et al.* (1987) may have detected the presence of FMN in their 'purified' sample due to contamination with other FMN-containing proteins in the membranes of *V. alginolyticus*.

An FAD motif was located on the NqrF sequence. The identification of the FAD binding site in the sequence of NqrF by comparison with known motifs, was substantiated by the evidence presented by Pfenninger-Li *et al.* (1995) that FAD co-purified with the NADH dehydrogenase. Their purified enzyme also exhibited an

absorption spectrum similar to ours, with a maximum at 450 nm that is typical for a flavoprotein. Upon incubation with NADH this absorption disappeared indicating reduction of the enzyme-bound FAD.

Comparison of the NqrF sequence using MPsrch with known sequences in the database, revealed that its *N*-terminal region was similar to the electron transfer subunit of a number of monooxygenases and dioxygenases and some ferredoxins while its *C*-terminal region was homologous to NAD(P)H-binding flavoproteins. From such homologies, a [2Fe-2S] binding site, an FAD binding site and a NADH binding site were identified. A predicted folding model of NqrF was then proposed (Rich *et al.*, 1995), whereby it was envisaged that the hydrophobic *N*-terminal region is attached to the membrane with the [2Fe-2S] centre close to the interface between the hydrophobic region and the large globular head in the cytoplasmic phase, containing the FAD and NADH binding sites.

To verify that the putative products encoded by the *nqr* sequences were transcribed and translated *in vivo*, *nqr* genes were cloned and the proteins they coded for were overproduced using an *E. coli* expression system. A wide range of expression vectors in *E. coli* are readily available. Some of these serve as direct expression vectors for constructing region- and site-directed mutations, and so for membrane proteins that are functionally expressed, mutant alleles may be constructed, and their phenotypes analysed without recourse to any subcloning/transfer of genes into other hosts. For example, plasmid pYZ4 and its recent derivatives, pEH1 and pEH2, allow direct expression of eukaryotic and prokaryotic proteins in *E. coli* by the construction of translational fusions of the mature β-lactamase to pYZ4-cloned genes and for the site-directed mutagenesis of the cloned genes and expression of the resultant mutant alleles in *E. coli* (Gould, 1994). Recombinant fusion vectors are also available for expression where target proteins are translationally fused to β-lactamase, β-galactosidase (e.g. pGEM series) and alkaline phosphatase and the resultant recombinant proteins are therefore large in molecular weight and can be easily purified as such or by specific antisera binding to the β-lactamase, β-galactosidase and

alkaline phosphatase region of the protein. However, *N*-terminal fusion of NqrF to β-lactamase had proven problematic due to the specific cleavage of the *N*-terminal hydrophobic region of NqrF. Other vectors such as mGP-1, that utilise the λ P_L temperature-inducible promoter, were avoided as heat induction may create inclusion bodies of the hydrophobic NqrF. The recent pET expression vectors (Novagen pET system technical manual) proved useful for the expression of NqrF. Some of these pET vectors contain the T7 promoter upstream of the *lac*UV5 promoter. The *lac*UV5 promoter is a moderate-strength but tightly-controllable promoter which is normally repressed by the binding of host and plasmid-encoded lac repressor to the operator with very low basal level of transcription and is easily induced by IPTG. The chief advantage of this system is that it is simpler to reproduce induction conditions using chemical rather than heat induction. With the pET system, the expression host will encode the T7 RNA polymerase under *lac*UV5 promoter control, again allowing the tight control of expression, which is very useful when expressing toxic membrane proteins.

Therefore, various *nqr* genes were cloned into pET16-b and overexpressed in host BL21(DE3)p*LysS*. Upon IPTG induction, NqrB, NqrC and NqrD were expressed and radiolabelled with ^{35}S-Met. Autoradiographs indicated the expression of hydrophilic NqrC at the correct molecular weight of 32 kDa while NqrB and NqrD were observed as diffuse bands migrating to anomalous molecular weights due to their extreme hydrophobic nature. Using the same T7 polymerase radiolabelling system, NqrE and NqrF were also clearly expressed. A faint diffuse band represented NqrE while a distinct band at 46 kDa was observed for NqrF, which corresponds to the size of the NADH dehydrogenase catalytic subunit of Na^+-NQR described by Bourne *et al.* (1992) and Hayashi *et al.* (1987). NqrA was especially toxic to *E. coli* as no viable clones of this complete gene could be cloned in the correct orientation with respect to an inducible promoter, even when a tightly regulated promoter was used.

Due to the toxicity of NqrF and other Nqr subunits, a tightly-regulated T7*lac* expression system had to be used. Moreover, NqrF was a membrane protein, hence

cultures were grown at 25°C to avoid inclusion bodies. To promote cell viability and optimal expression, fresh transformants were used and induced with freshly-prepared IPTG. Ferric citrate and sodium sulphide were included as supplements to the growth media, to encourage iron-sulphur cluster formation in overexpressing cells.

Having established the expression system for NqrF, a large scale fermentor run proceeded and harvested cells were fractionated into cytoplasmic, inner membrane and outer membrane fractions. As there are 3 different NADH dehydrogenases, a crucial and useful property of NqrF was its Ag^{+}-sensitivity (the other 2 NADH dehydrogenases are Ag^{+}-insensitive) and this was exploited in localising the NqrF activity in the various cell fractions. Ag^{+}-sensitive NADH dehydrogenase activity of NqrF was detected predominantly (75%) in the inner cell membrane fraction, supporting the predicted folding model that NqrF is attached to the cell membrane via its hydrophobic *N*-terminus.

Purification of NqrF from the cell membrane fraction progressed. Ion exchange chromatography with DEAE Sepharose was chosen as the initial step of purification. An anionic column was selected rather than a cationic one because the predicted pI of NqrF was 4.54 and the protein was apparently stable at alkaline pH. NqrF was eluted at 0.2 M NaCl. A 3-fold purification was accomplished with an excellent 120% yield (NqrF preferred resuspension in the DEAE sepharose elution buffers compared with the membrane solubilization buffer), 16.8 U/mg specific activity and a total activity of 2239 U (1 U = 1 μmole NADH/min).

Pooled DEAE sepharose fractions containing NqrF were applied to a hydroxyapatite column in the second stage of purification. This separated NqrF from some low molecular weight proteins using an increasing linear phosphate gradient, eluting NqrF at 0.15 M phosphate. A 155% yield (explanation as before) with 36.9 U/mg specific activity and 6.5 fold purification was attained. Total NADH dehydrogenase activity was high at 2904 U.

Finally, pooled active fractions of this second column was then run through a Mimetic Blue-2 dye affinity column. NqrF was purified, eluting in a broad peak at

about 0.5 M NaCl. 13.9 mg of NqrF was recovered from 7 ℓ (40 g, wet weight) of cells with a final yield of 50%, 12 fold purification and a specific activity of 67 U/mg. The total activity was 933 U.

As NqrF tended to precipitate, detergents had to be included in all buffers. Various detergents were tested for their suitability for inclusion in buffers, taking cost into consideration as well as other properties. Ionic detergents were avoided as they have charged heads that are useful for disrupting protein-protein interactions but interfer with ion exchange chromatography and isoelectric focussing. These detergents, such as SDS, also tend to denature proteins and hence were not used as it was crucial to preserve NqrF conformation and activity.

From previous studies on solubilizing the Na^+-NQR complex in *V. harveyi,* (Stevenson, 1994), taking into account of the critical micelle concentration of the detergent and preserving the activity of the enzyme, non-ionic detergent Triton X-100 was found to be the most economical and efficient detergent for extracting NqrF. Triton X-100, a non-ionic detergent with an uncharged head group, was less denaturing compared with ionic detergents and could be used in ion exchange chromatography. However, at concentrations ranging from 0.1-1.0% (v/v), solubilization with Triton X-100 gave rise to persistent NqrF aggregates which sometimes gave multiple high molecular weight bands on electrophoresis in native and SDS polyacrylamide gels, even after boiling SDS samples before loading on gels. This is not an unusual trait of integral membrane proteins such as NqrF, as all integral membrane proteins exhibit a marked tendency to form aggregates; even the presence of a short hydrophobic segment is sufficient to promote lateral aggregation as a means of sequestering these segments away from the aqueous environment (Gould, 1994). Another inconvenience arising from the inclusion of Triton X-100 in buffers was that it hindered easy protein concentration determination via spectrophotometric measurements at A_{280} which is around the absorption maximum of Triton X-100.

Zwitterionic detergents have head groups with positive and negative charges and are more effective than non-ionic detergents at disrupting the protein-protein

interactions prevalent in the aggregates, while less denaturing compared with ionic detergents. Lauryl sulphobetaine, resolved the aggregates into monomers when added at 1% (w/v) to Triton X-100 solubilized NqrF, but it possibly adversely affected NqrF conformation, prosthetic group or substrate binding sites, which invariably led to a 100% loss in activity after 10 hours. CHAPS was eventually chosen as the detergent for inclusion to buffers in the final purification column as it resolved NqrF into monomers without detrimental effects to its activity and it does not interfere with ion exchange chromatography or isoelectric focussing.

It was immediately apparent that after a week's storage at 4°C, purified 46 kDa NqrF was specifically degrading to a 39 kDa polypeptide, which replaced the 46 kDa protein as the major product. This 39 kDa protein retains NADH dehydrogenase activity, signifying that NqrF was degrading at its *N*-terminal region, losing its hydrophobic domain, rather than degrading at the *C*-terminal region where the NADH-binding site is located. Since this deletion was close to the predicted [2Fe-2S] cluster, this could explain the absence of [2Fe-2S] signals in EPR analysis. NqrF may also require lipids, absent in the final purified fraction, to stabilise and maintain its conformation, prosthetic groups and catalytic centre.

NqrF was susceptible to proteases which were inhibited by using a cocktail of inhibitors such as 5 mM EDTA (metalloprotease inhibitor) and 1 mM PMSF (serine protease inhibitor). The presence of glycerol and ethylene glycol in buffers also improved chromatography and minimized ice damage to the protein when freezing and thawing. The rationale for including reducing agent, dithiothreitol in sonication buffers was to assist proteins in counteracting adverse effects due to increased contact with oxygen and dilution of naturally occurring reducing agents like glutathione, when cells are disrupted. Nevertheless, DTT was discriminately used only in the sonication buffer as continual use in later stages of purification leads to the reduction of the FAD moiety to a semiquinone or $FADH_2$ and a subsequent lost in the yellow colouration of the protein.

The catalytic polypeptide was thermolabile; both loss of activity and degradation were observed at room temperature with a 30% loss in 2 h, and to a lesser degree with refrigeration or freezing. To minimize loss of activity, all samples were frozen or stored at 4°C; cell fractionation, centrifugation and chromatography were achieved at 4°C. NqrF activity was pH-sensitive, most stable between pH 6.0 to pH 8.0, but particularly unstable at low pH. The observed pI of 5.2 from isoelectric focussing was higher than the theoretical value of 4.5 possibly due to denaturation at lower pH. Hence the use of buffers in the range of pH 6.5 to pH 8.0 was adopted.

NADH dehydrogenase activity of the NqrF subunit is independent of Na^+, and this subunit is hence deduced not to be involved in sodium translocation. NqrF was shown to contain FAD from its absorption spectrum and paper chromatography, and it exhibited properties akin to those reported by other groups, for example, it is severely and irreversibly inhibited by Ag^+, and insensitive to rotenone which is a Complex I and H^+-NDH1 inhibitor. However, it is only very slightly inhibited by Cu^{2+}, Cd^{2+}, Pb^{2+} and Zn^{2+} (<20% inhibition), which are severe inhibitors of the Na^+-NQR complex. These metal cation inhibitors possibly affect other subunits of the complex which in turn inhibits NADH dehydrogenase activity, while the direct site of inhibition of Ag^+ is in NqrF. The presence of Ag^+-sensitive NADH dehydrogenase activity is a good indication that the NqrF subunit purified originated from the Na^+-NQR complex, as all other known NADH dehydrogenases are insensitive to Ag^+ inhibition. Although EDTA was able to reverse inhibition of Zn^{2+} and Pb^{2+} on Na^+-NQR, it was ineffective in reversing inhibition of NqrF by all of these metallic cations. This weak irreversible non-specific inhibition by Cu^{2+}, Cd^{2+}, Pb^{2+} and Zn^{2+} reinforces to the conclusion that these cations do not act directly on NqrF. Cysteinyl inhibitors had no effect on the activity of NqrF, which meant that the cysteine residue in the NADH binding site does not participate in binding or interactions with the substrate moiety in the catalytic process and that there was cleavage of the *N*-terminal region of NqrF which contained the crucial cysteine residues for the formation of a [2Fe-2S] centre. However, it was pointed out that NqrF

may be incubated with suboptimal concentrations of cysteinyl inhibitors for effective inhibition and that the incubation period should have been extended to 20 mins for the effect of these inhibitors to be apparent.

Although the K_m of 10 μM for NADH, is virtually identical to figures obtained by other groups, the K_m for menadione (143 μM) is much higher than previously reported for the complex (10 μM). NqrA, NqrC and another hydrophobic subunit were reported to be essential for quinone reductase activity (Hayashi and Unemoto, 1984, 1986). This supports the proposal that binding and reduction of the physiological electron donor, ubiquinone, a hydrophobic molecule, requires NqrA and NqrC. The overall NADH dehydrogenase specific activity calculated for this purified NqrF subunit of 67 U/mg was in the range of reported figures (120 U/mg (only NqrF); 88 U/mg (entire complex) for Pfenninger *et al.*, 1996; 390 U/mg (only NqrF); 181 U/mg (entire complex) for Unemoto and Hayashi, 1989; 22 U/mg (entire complex in *V. harveyi*), Stevenson, 1994).

This specific activity of NqrF is 2-6 fold lower than some figures previously quoted for purified NqrF from *V. alginolyticus*, probably relating to the apparent degradation of the N-terminal region of NqrF, perhaps leading to the loss of the [2Fe-2S] cluster and a subsequent lost of activity due to an arrest of electron transfer from the FAD to the [2Fe-2S]. Other subunits such as the sodium translocating subunit and perhaps some of the more hydrophobic subunits are required for optimum catalytic activity by coupling the sodium motive force to NADH dehydrogenase activity and aiding in the transfer of electrons and reduction of ubiquinone. Another possibility was that NqrF was not folding to its natural configuration for optimum catalytic activity when expressed in a foreign host such as *E. coli* or that it being a membrane protein, requires lipids added to maintain its conformation.

Very recently, a model for coupled sodium ion translocation has been proposed based upon a newly outlined model for proton translocation in the coupled iron/copper terminal oxidases, which incorporates a general consideration of a rule of local electroneutrality of stable catalytic intermediates (Michell *et al.*, 1992; Rich,

1995). When these intermediates are produced in a region of low dielectric strength, such charge neutralisation occurs by counterion uptake. This consideration has been combined with the above structural considerations and a previous finding of a lack of sodium ion dependency of the midpoint potential of FAD (Bourne and Rich, 1992) to produce a new proposal for the essential features of coupling electron transfer and sodium ion translocation in NqrF.

In this model (Fig. 7.1), the iron sulphur centre is proposed to be in a relatively low dielectric environment so that electron transfer to it requires counterion uptake. It is suggested that the other subunits of this enzyme provide ion selectivity so that sodium (or lithium) ions can produce such charge counterbalance (step 2). Binding of a quinone then results in electron transfer from iron sulphur centre to quinone. The final quinol product of quinone reduction must, inevitably, become protonated (whether the quinol is formed by a dismutation of two semiquinones, or whether there are two sequential electron transfers to the same bound quinone, remains an open point). Indeed, there will be a very strong driving force for such protonation, analogous to the driving force provided by oxide protonation to form water in the protonmotive oxidases (Rich, 1992). Two possible ways in which this drives net sodium ion translocation may be envisaged. In one of these (steps 3A, 4A), the spatial orientation of the reactants results in electrostatic repulsion by the proton of the sodium ion into the positive aqueous phase, resulting in a net balance overall of both sodium and proton translocation across the membrane. In the second possibility (steps 3B, 4B), protonation is achieved by a sodium/proton antiport channel in the protein structure, resulting in the net translocation of sodium ions only. It might be noted that the type of model outlined in steps 3A, 4A might also be considered as a basis of proton translocation in complex I, by substituition of an electronation-linked protonation of centre N-2 for the sodium -dependent steps (Rich *et al.*, 1995).

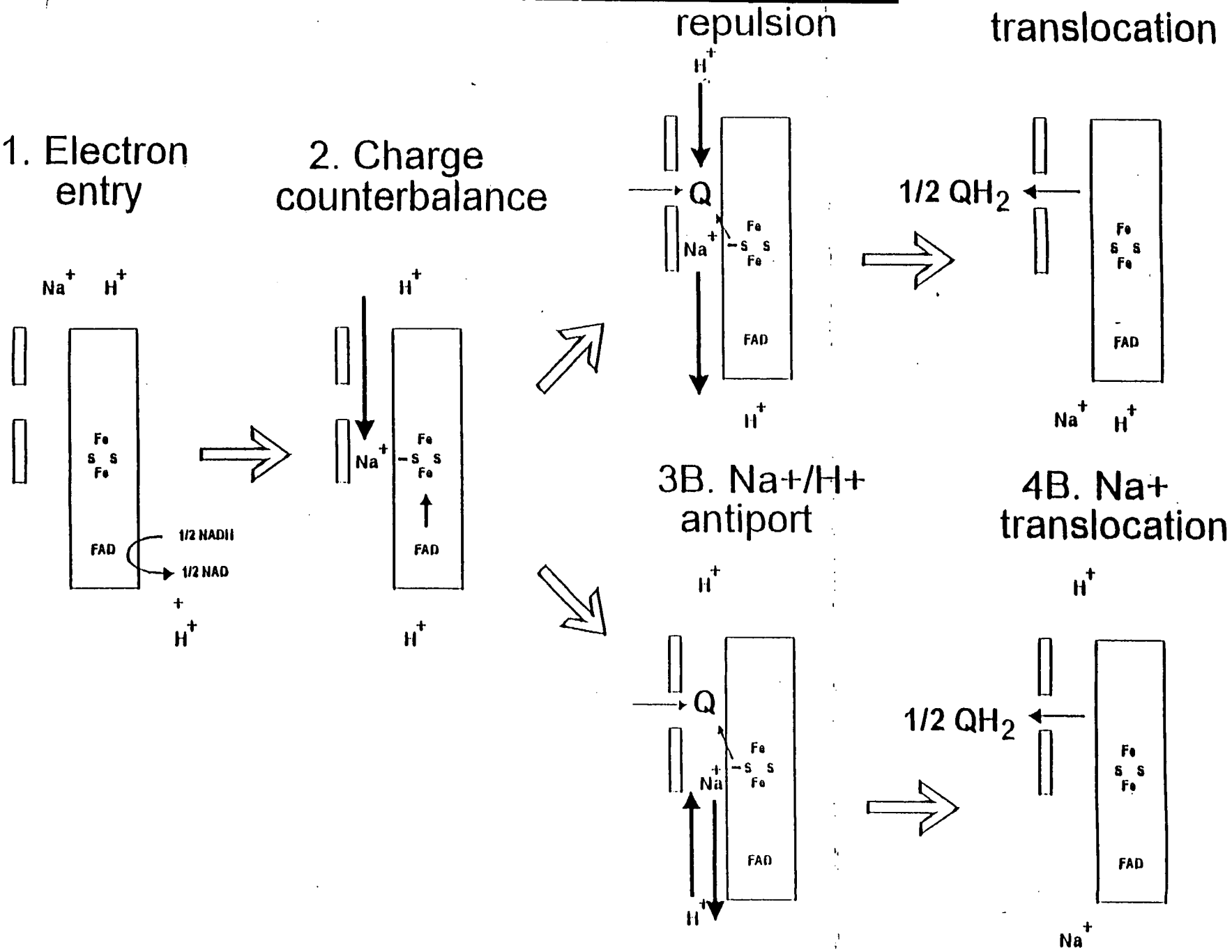

Fig. 7.1. Sodium translocation model (Rich *et al.*, 1995).

More experiments on Na^+-NQR could proceed in the future, involving the identification of the elements regulating the *nqr* operon. Initial work involving the cloning of the *nqr* promoter region into a *lac*Z transcriptional fusion vector, pHRP309, and transforming into an appropriate *E. coli* or *Vibrio alginolyticus* strain (Parales and Harwood, 1993) has commenced in our laboratory. This two-step cloning procedure uses a set of 'cohort' vectors that allowed direct cloning of fragments downstream from the Ω streptomycin/spectinomycin-resistance cassette while maintaining multiple flanking restriction sites. The fusion vector carries a gentamycin-resistance-encoding gene as the selectable marker and can hence be used in Tn*5* (kanamycin-resistant) and Tn*10* (tetracycline-resistant) mutant strains. Since pHRP309 is a member of the IncQ incompatibility group, it is compatible with IncP cloning vectors and can be used in strains carrying cloned regulatory genes, The cloning of the *nqr* promoter just upstream of the *lac*Z gene allows the control of β-galactosidase expression by the *nqr* promoter. Hence, the measurement of β-galactosidase activity would shed light on the regulation by the *nqr* promoter. To confirm that it is a true promoter region it could be cloned in both orientations and checked for activity by β–galactosidase (Miller, 1972 Cold Spring Harbour). Levels of metallic and divalent ions, pH, temperature, iron and other supplements in the growth media could be altered and the β-galactosidase activity is measured to determine if there is autoregulation by these components. Alternatively, *nqr*::*lac*Z transcriptional fusion inserted in λ phage cloning vector capable of lysogeny can be used. The λ lysogen of *E. coli* is then used as a host for screening recombinant plasmids to identify those with genes regulating *nqr* expression.

Characterization of the different domains in NqrF has also been initiated recently in the lab, using carefully-designed primers in PCR to introduce specific restriction sites and start and stop codons in *nqr*F and amplify this altered *nqr*F gene so that soluble NqrF fragments comprising combinations of the [2Fe-2S] cluster and/or the FAD domain and/or the NADH-binding domain could all be expressed individually from pET16-b or pT7-7 in BL21(DE3)p*Lys*S. These domains will be

expressed and purified for the purpose of further structural analysis by X-ray crystallography, EPR or NMR.

Future work to characterise the Na^+-NQR complex further could involve the generation of null mutants. To generate null mutants *in vitro*, the sole *Sph*I site that is located early in the *nqr*A gene, can be converted to a *Bam*HI site and then a Ω transposon cassette containing a spectinomycin resistance gene (Fellay *et al.*, 1987) is inserted to disrupt the *nqr*A gene and create a strongly polar mutation. The mutation would then be introduced into the wild type *V. alginolyticus* chromosome by recombination due to the homology of flanking *nqr* sequence on a suicide vector. The enzyme activities of the mutants would be determined by a simple colorimetric assay that can be used on both PAGE gels and in cell membranes. Expression of *nqr* genes on plasmids to complement *nqr* null mutations in *V. alginolyticus* created above and 2 Nap (Na^+-NQR) mutants obtained previously from Unemoto, would provide further evidence that these genes code for the structural components of the Na^+ pump.

Once a few Nqr subunits have been purified, antibodies could be raised from purified subunits or partially purified subunits electro-eluted from a zymogram-stained band in a native gel. These Nqr-specific antibodies can be subsequently used to screen expression libraries or identify protein subunits in SDS polyacrylamide gels by Western blotting. Since the entire Na^+-NQR complex of *V. alginolyticus* has never been successfully purified due to the inherent instability and apparent dissociation of the subunits on further purification (Pfenninger-Li *et al.*, 1996), these antibodies could also be useful for purifying the entire complex, including the hydrophobic components, by affinity chromatography. Routinely, between 1000 to 10 000 fold purifications have been achieved using this technique with a suitable antibody as an affinity ligand (Harlow and Lane, 1988).

A number of powerful tools could be applied to dissect the structure and functions of individual subunits. As fusion of *nqr*F with *bla*M proved problematic, epitope mapping or fusion with other reporter genes such as *phoA* or *lacZ*, could alternatively proceed to elucidate the arrangement of subunits of Na^+-NQR on the

membrane. Reactivity of antibodies to regions of protein outwith the membrane and enzyme activity of reporter gene products fused to a known region on the Nqr proteins would confirm the positions and numbers of transmembrane helices proposed by predicted models designed from sequence data. An illustration to clarify this point is that a *pho*A fusion would only exhibit alkaline phosphatase activity if fused to a periplasmic region of the target protein while a *lac*Z fusion exhibits β-galactosidase activity if fused to a cytoplasmic portion of the protein of interest. In addition, site-directed mutagenesis of specific residues in the NADH, FAD and [2Fe-2S] binding sites would identify important amino acid residues for binding substrate and prosthetic groups, conferring inhibitor specificity, and maintaining overall structural integrity.

Furthermore, primer extension could be performed to verify the transcription initiation start. Total RNA can be extracted from exponential cultures using QIAGEN columns. Antisense oligonucleotide corresponding to nucleotides 29 to 58 downstream of transcriptional start is 5' labelled with [γ-^{32}P] ATP (10^5 counts/min), and hybridised to 20 µl RNA (total) at temperatures between 35°C and 50°C at 5°C intervals before primer extension proceeds with reverse transcriptase. The largest transcript would reflect transcription initiation site.

As the bioenergetics of sodium metabolism and primary Na^+ pumps were only recently elucidated in the last 15 years (Lanyi, 1979; Skulachev, 1985 and 1987; Dibrov *et al.*, 1986a and 1986b), studies of Na^+-NQR would provide a useful tool to further analyse the structure and functioning of the Na^+ pump and compare its properties to that of the H^+ pump. Although the function of Na^+ as a secondary coupling ion in antiport, proton gradient buffering, regulation of cytoplasmic pH and solute, has long been recognized, its mechanism as a primary coupling ion was not well understood with the exception of its role in the animal plasma membrane. The first discovery of a primary Na^+ pump generating a sodium motive force with no proton motive force involved was in 1980, where a decarboxylase from anaerobically grown *K. aerogenes* was found to convert oxaloacetate to pyruvate and CO_2 only if Na^+ is present and pumps Na^+ from the cytoplasm against the Na^+ electrochemical

gradient (Dimroth, 1980). Later, the first indication that an ion other than H^+ energizes the bacteria under alkaline conditions was obtained by Tokuda and Unemoto (1982) when studying the alkalotolerant *V. alginolyticus*. The Na^+-translocating NADH-ubiquinone oxidoreductase was thus identified. This bacterial sodium pump provides a good model for studying and understanding Na^+-translocation which occurs in numerous primary and secondary transport systems and in sodium channel neurotransmission.

Moreover, the molecular characterisation of Na^+-NQR would provide information about the complex which could be applied in the design of herbicides and pesticides based on quinone inhibitors. The quinone-binding site of respiratory photosynthetic electron transfer enzymes, such as Q_b site photosystem II in plant photosynthesis and Q sites of the mitochondrial bc_1 and on complex I, are major target sites for inhibitors in commercially available herbicides, fungicides and acaricides. Three dimensional information on the Q site in the Na^+-dependent NADH ubiquinone oxidoreductase will contribute to improved understanding of general features of Q site structure, while studies of inhibitor specificity of this site may lead to the design of chemicals as specialised and unique bactericidal agents.

In antibody-directed enzyme prodrug therapy (ADEPT), an antibody or antibody fragment is conjugated to an enzyme, such as nitroreductases and NADPH-quinone oxidoreductases, and used to localise the enzyme at the site of solid tumours. Once localised, this enzyme activates a noncytotoxic prodrug to an active cytotoxic form. The NADH ubiquinone oxidoreductase of *Vibrio alginolyticus* is a possible enzyme candidate as it is similar (40% similarity) but distinct in cofactor binding binding sites and substrate specificities from the nitroreductase from *Escherichia coli* B which has potential applications in this field. Further investigations into quinone and nitrocompound binding sites and substrate specificities using a range of potential prodrugs, could produce alternative drugs to those currently under examination.

Detoxification of trace aromatic pollutants in waters and industrial effluents is another field of application if NqrF::dioxygenase chimeras can be successfully

produced. Hybrid dioxygenase chimeras have enhanced rates of degradation of particular substrates and some can be altered to provide new substrate specificity, e.g. chimaeric biphenyl/benzene dioxygenase produces indigo from indole. These chimeras can be expressed in heterologous Gram-negative hosts. Expressing dioxygenase chimeras in a host such as *V. alginolyticus*, avoids problems encountered when relying on *Pseudomonas* species to produce the native dioxygenases for detoxification, such as multiplicity of pathways of metabolism, toxicity of products and viability. The advantages of the *V. alginolyticus* Na^+-NQR system are that the Na^+-NQR enzyme complex is a major stable cell component, which is inducible under conditions simply applied in industrial situations, the microbial species is viable under a wide variety of osmotic, temperature and nutrient conditions, substrate specificity can be defined by modifications to the second enzyme complex, and NADH is generated *in situ* from simple carbon substrates and in which energy is derived from the associated Na^+-translocation.

The catalytic NqrF is a flavoprotein reductase that belongs to the FNR (spinach ferredoxin-$NADP^+$ reductase) family of enzymes, which comprise many enzymes that are important in biotechnology and medicine and display an amazing diversity in catalytic specificity but share great similarities in the pattern of protein folding and conservation of core secondary structural elements. Three characteristics of the FNR family favour the prospect of designing novel enzymes:

1) the catalytic segments are organised into a number of distinct domains which are potentially exchangeable for creating new enzymes.
2) the redox potentials of the prosthetic groups involved in catalysis can be considerably altered by their bonding to neighbouring amino acid residues.
3) the catalytic subunits can be associated with a number of additional subunits to form enzymes of very different substrate specificity.

Mutagenesis to increase the efficiency of the dioxygenase::NqrF chimeras can be achieved by alteration of the length of the linker region between the ferredoxin and flavin domains, mutation of the residues affecting the relative specificity for FAD and

FMN or mutation of residues surrounding the iron sulphur cluster site. These may affect both the interface between the domains and the redox potential of the [2Fe-2S] centre.

By tailoring gene induction systems to provide the required metabolic capacity and using immobilized cell technology to optimize metabolic capacity, complex stability and bacterial survival rates in long-term trials, successfully-produced chimaeric flavoprotein reductase:dioxygenase complexes could be utilized to degrade specific industrial effluent components, e.g. azocompounds in the dye industry or toluene derivatives in chemical industries.

Further development of these chimaeras would generate stable enzymes for specific bioconversions using whole cells. This requires the elucidation of the three dimensional structure of the complex and in particular the catalytic domain to enable design of second generation of chimaeric enzymes in which a series of enzymes with common regulation and induction mechanisms and each with a well-defined pyridine nucleotide and flavin domain are interfaced to a variety of oxygenase/hydroxylase/azoreductase complexes through a one-electron carrier domain so that geometrical requirements for efficient electron transfer are less stringent.

Bibliography

Anraku, Y. 1988. Bacterial electron transport chains. *Annual Reviews of Biochemistry* **57**: 101-132.

Arizmendi, J.M., Runswick, M.J., Skehel, J.M., Walker, J.E. 1992. NADH:ubiquinone oxidoreductase from bovine heart mitochondria: a fourth nuclear encoded subunit with a homologue encoded in chloroplasts. *FEBS Letters* **301**: 237-242.

Atsumi, T., Maekawa, Y., Yamada, T., Kawagishi, I., Imae, Y., Homma, M. 1996. Effect of viscosity on swimming by the lateral and polar flagella of *Vibrio alginolyticus. Journal of Bacteriology* **178**: 5024-5026.

Avetisyan, A.V., Dibrov, P.A., Skulachev, V.P. and Sokolov, M.V. 1989. The Na^+-motive respiration in *Escherichia coli. FEBS Letters* **254**: 17-21.

Batie, C.J., Ballou, D.P., Correll, C.C. 1991. Phthalate dioxygenase reductase and related flavin-iron-sulfurncontaining electron transferases. Chemistry and Biochemistry of Flavoenzymes. Vol. III, pp 543-556.

Batie, C.J., Ballou, D.P. 1990. Phthalate dioxygenase. *Methods in Enzymology* 188: 61-70.

Beattie, P., Tan, K., Bourne, R., Leach, D., Rich, P.R., and Ward, F.B. 1994. Poster and oral presentation (B. Ward) *Proc.Soc.Gen.Microbiol, Noordwijkerhout, Netherlands*

Beattie, P., Tan, K., Bourne, R.M., Leach, D., Rich, P.R., Ward, F.B. 1994. Cloning and sequencing of four structural genes for the Na^+-translocating NADH-ubiquinone oxidoreductase of *Vibrio alginolyticus. FEBS letters* **356**: 333-338.

Bebbington, K.J., Williams, H.D. 1993. Investigation of the role of cydD gene product in the production of a functional cytochrome *d* oxidase in *Escherichia coli. FEMS Microbiology letters* **112**:19-24.

Belogrudov, G., Hatefi, Y. 1994. Catalytic sector of complex-I (NADH-ubiquinone oxidoreductase) - subunit stoichiometry and substrate-induced conformational changes. *Biochemistry* **33**: 4571-4576.

Van Belzen, R., De-Jong, A.M.P., Albracht, S.P.J. 1992. On the stoichiometry of the iron-sulfur clusters in mitochondrial NADH-ubiquinone oxidoreductase. *European Journal of Biochemistry* **209**: 1019-1022.

Bhaskar, N., Setty, T.M.R. 1994. Incidence of vibrios of public health significance in the farming phase of tiger shrimp (*Penaeus monodon). Journal of the Science of Food and Agriculture* **66**: 225-231.

Birdsell, D.C., Cota-Robles, E.H. 1967. Production and ultrastructure of lysozyme and ethylenediaminetetraacetate-lysozyme spheroplasts of *Escherichia coli. Journal of Bacteriology* **93**: 427-437.

Birkmayer, J.G.D. 1995. Nicotinamide adenine-dinucleotide (NADH) - a new therapeutic approach - preliminary-results with cancer-patients and patients with dementia of the Alzheimer-type. *Journal of Tumor Marker Oncology* **10**: 71-78

Botstein, D. 1980. A theory for molecular evolution of bacteriophages. *Ann. N.Y. Acad. Sci.* **354**: 484-491.

Bourne, R.M., Rich, P.R. 1992. Characterization of a sodium motive NADH: ubiquinone oxidoreductase. *Biochemical Society Transactions* **20**: 577-582.

Boyer, P.D. 1975. A model for conformational coupling of membrane potential and proton translocation to ATP synthesis and to active transport. *FEBS Letters* **58**: 1-6.

Bragg, P.D. and Hou, C. 1967. Reduced nicotinamide adenine dinucleotide oxidation in *Escherichia coli* particles. II. NADH dehydrogenases. *Arch. Biochem. Biophys.* **119**: 202-208.

Broome-Smith, J.K., Spratt, B.G. 1986. A vector for the construction of translational fusions to TEM β-lactamase and the analysis of protein export signals and membrane topology. *Gene* **49**: 341-349.

Bruns, C.M., Karplus, P.A. 1993. Flavins and Flavoproteins. Walter de Gruyter & Co., Berlin. New York, 1994.

Brunt, C.E., Cox, M.C., Thurgood, A.G.P., Moore, G.R., Reid, G.A., Chapman, S.K. 1992. Isolation and characterization of the cytochrome domain of flavocytochrome b_2 expressed independently in *Escherichia coli. Biochemical Journal* **283**: 87-90.

Buchanan, S.K., Walker, J.E. 1996. Large-scale chromatographic purification of F_1F_0-ATPase and complex I from bovine heart mitochondria. *Biochemical Journal* **318**: 343-349.

Burbaev, D., Moroz, S.H., Kotlyar, I.A., Sled, V.D., Vinogradov, A.D. 1989. Ubisemiquinone in the NADH-ubiquinone reductase region of the mitochondrial respiratory chain. *FEBS Letters* **254**: 47-51.

Cammack, R. 1992. Iron-sulphur clusters in enzymes - themes and variations. *Advances in Inorganic Chemistry* **38**: 281-322.

Capozza, G., Dmitriev, O.Y., Krasnoselskaya, I.A., Papa, S., Skulachev, V.P. 1991. The effect of F_0 inhibitors on the *Vibrio alginolyticus* membrane ATPase. *FEBS Letters* **280**: 274-276.

Chung, C.T., Niemela, S.L., Miller, R.H. 1989. One-step preparation of competent *Escherichia coli*: Transformation and storage of bacterial cells in the same solution. *Proceedings of the National Academy of Science, U.S.A.* **86**: 2172-2175.

Clark, J. 1994. ATPases of *V. harveyi*. Honours project. University of Edinburgh.

Clarkson, A.B., Bienen, E.J., Pollakis, G., Grady, R.W. 1989. Respiration of blood-stream forms of the parasite *Trypanosoma brucei* is dependent on a plant-like alternative oxidase. *Journal of Biological Chemistry* **264**: 17770-17776.

Correll, C.C., Ludwig, M.L., Bruns, C.M., Karplus, P.A. 1993. Structural prototypes for an extended family of flavoprotein reductases: Comparison of phthalate dioxygenase reductase with ferredoxin reductase and ferredoxin. *Protein Science* **2**: 2112-2133.

Correll, C.C., Batie, C.J., Ballou, D.P., Ludwig, M.L. 1992. Phthalate dioxygenase reductase: A modular structure for electron transfer from pyridine nucleotides to [2Fe-2S]. *Science* **258**: 1604-1610.

Crouse, B.R., Yano, T., Finnegan, M.G., Yagi, T., Johnson, M.K. 1994. Properties of the iron-sulfur center in the 25-kilodalton subunit of proton-translocating NADH-quinone oxidoreductase of *Paracoccus denitrificans*. *Journal of Biological Chemistry* **269**: 21030-21036.

Degli-Esposti, M., Ghelli, A., Ratta, M., Cortes, D., Estornel, E. 1994. Natural substances (acetogenins) from the family *Annonaceae* are powerful inhibitors of mitochondrial NADH dehydrogenase (Complex I). *Biochemical Journal* **301**:161-167

De-Jong, A.M.P., Albracht, S.P.J. 1994. Ubisemiquinones as obligatory intermediates in the electron transfer from NADH to ubiquinone. *European Journal of Biochemistry* **222**: 975-982.

De-Jong, A.M.P., Kotlyar, A.B., Albracht, S.P.J. 1994. Energy-induced structural changes in NADH:Q oxidoreductase of the mitochondrial respiratory chain. *Biochimica et Biophysica Acta* **1186**: 163-171.

Dibrov, P.A., Lazarova, R.L., Skulachev, V.P., Verkhovskaya, M.L. 1986a. The sodium cycle. I. Na+-dependent motility and modes of membrane energization in the marine alkalotolerant *Vibrio alginolyticus*. *Biochimica et Biophysica Acta* **850**: 449-457.

DeVries, S., Marres, C.A.M. 1987. The mitochondrial respiratory chain of yeast-Structure and biosynthesis and the role in cellular metabolism. *Biochimica et Biophysica Acta* **895**: 205-239.

Dibrov, P.A., Lazarova, R.L., Skulachev, V.P., Verkhovskaya, M.L. 1986b. The sodium cycle. II. Na+-coupled oxidative phosphorylation in *Vibrio alginolyticus* cells. *Biochimica et Biophysica Acta* **850**: 458-465.

Dibrov, P.A., Lazarova, R.L., Skulachev, V.P., Verkhovskaya, M.L. 1989. A study on sodium-coupled oxidative phosphorylation: ATP formation supported by artificially imposed delta-pNa and delta-pK in *Vibrio alginolyticus* cells. *Journal of Bioenergetics and Biomembranes* **21**: 347-358.

Dimroth, P. 1980. A new sodium-transport system energized by the decarboxylation of oxaloacetate. *FEBS Letters* **122**: 234-236.

Dimroth, P. 1982a. Purification of the sodium transport enzyme oxalacetate decarboxylase by affinity chromatography on avidin-Sepharose. *FEBS Letters* **141**: 59-62.

Dimroth, P. 1982b. The generation of an electrochemical gradient of sodium ions upon decarboxylation of oxaloacetate by the membrane-bound and Na^+-activated oxaloacetate decarboxylase from *Klebsiella aerogenes*. *European Journal of Biochemistry* **121**: 435-441.

Dimroth, P. 1987. Sodium ion transport decarboxylases and other aspects of sodium ion cycling in bacteria. *Microbiological Reviews* **51**: 320-340.

Dimroth, P. 1990. Mechanisms of sodium transport in bacteria. *Philosophical Transactions of the Royal Society, London* **326**: 465-477.

Dimroth, P., Thomer, A. 1989. A primary respiratory sodium pump of an anaerobic bacterium: The sodium-dependent NADH: quinone oxidoreductase of *Klebsiella pneumoniae*. *Archives of Microbiology* **151**: 439-444.

Dmitriev, O.Y., Chernyak, B.V. 1988. Study of membrane ATPase of marine alkali-tolerant bacterium *Vibrio alginolyticus*. *Biokhimiya* **53**: 1380-1388.

Dmitriev, O.Y., Krasnoselskaya, I.A., Papa, S., Skulachev, V.N. 1991. F_0F_1-ATPase from *Vibrio alginolyticus* - subunit composition and proton pumping activity. *FEBS Letters* **284**: 273-276.

Dmitriev, O.Y., Dann, S., Krasnoselskaya, I.A., Papa, S., Skulachev, V.N. 1992. Membrane ATPase of *Vibrio alginolyticus*: Ion transport activity and homology to *Escherichia coli* F_0F_1 ATPase. *Biokhimiya* **57**: 1499-1507.

Do, H.K., Kouure, K., Sinudu, U. 1990. Identification of deep-sea sediment bacteria which produce tetrodotoxin. *Applied and Environmental Microbiology* **50**: 1162-1163.

Dupuis, A., Skehel, J.M. and Walker, J.E. 1991a. Plant chloroplast genomes encode a homologue of a nuclear coded iron-sulfur protien subunit of bovine mitochondrial complex I. *Biochemistry* **30**: 2954-2960.

Dupuis, A., Skehel, J.M. and Walker, J.E. 1991b. NADH:ubiquinone reductase from bovine mitochondria: complementary DNA sequence of a 19 kDa cysteine-rich subunit. *Biochemical Journal* **277**: 11-15.

Earley, F.G.P., Ragan, C.I. 1984. Photoaffinity labelling of mitochondrial NADH dehydrogenase with arylazidomorphigenin, an analogue of rotenone. *Biochemical Journal* **224**: 525-534.

Earley, F.G.P., Patel, S.D., Ragan, C.I. and Attardi, G. 1987. Photoaffinity labelling of mitochondrially encoded subunit of NADH dehydrogenase with [^{3}H]dihydrorotenone. *FEBS Letters* **219**: 108-113.

Easter, M.C. 1982. Trimethylamine-N-oxide reduction by *Alteromonas* spp. PhD thesis. University of Edinburgh.

Easter, M.C., Gibson, D.M., Ward, F.B. 1983. The induction and location of Trimethylamine-N-oxide Reductase in *Alteromonas* sp. NCMB 400. *Journal of General Microbiology* **129**: 3689-3696.

Fearnley, I.M., Runswick, M.J., Walker, J.E. 1989. A homologue of the nuclear encoded 49 kDa subunit of bovine mitochondrial NADH-ubiquinone reductase encoded in chloroplast DNA. *EMBO Journal* **8**: 665-672.

Fearnley, I.M., Finel, M., Skehel, J.M., Walker, J.E. 1991. NADH:ubiquinone oxidoreductase from bovine heart mitochondria; cDNA sequences of the important precursors of the nuclear coded 39-kDa and 42-kDa subunits. *Biochemical Journal* **278**: 821-829.

Fearnley, I.M., Walker, J.E. 1992. Conservation of sequences of subunits of mitochondrial complex I and their relationships with other proteins. *Biochimica et Biophysica Acta* **1140:** 105-134.

Fecke, W., Sled, V.D., Ohnishi, T., Weiss, H. 1994. Disruption of the gene encoding the NADH-binding subunit of NADH-ubiquinone oxidoreductase in *Neurospora crassa*: Formation of a partially assembled enzyme without FMN and the iron-sulfur cluster N-3. *European Journal of Biochemistry* **220**: 551-558.

Fellay, R., Frey, J. and Krisch, H. 1987. Interposon mutagenesis of soil and water bacteria- a family of DNA fragments designed for *in vitro* insertional mutagenesis of Gram-negative bacteria. *Gene* **52**: 147-154.

Finel, M., Majander, A.S., Tyynela, J., DeJong, A.M.P., Albracht, S.P.J., Wikstrom, M. 1994. Isolation and characterization of subcomplexes of the mitochondrial NADH-ubiquinone oxidoreductase (complex-I). *European Journal of Biochemistry* **226**: 237-242.

Finel, M., Skehel, J.M., Albracht, S.P.J., Fearnley, I.M., Walker, J.E. 1992. Resolution of NADH-ubiquinone oxidoreductase from bovine heart mitochondria into two subcomplexes, one of which contains the redox centers of the enzyme. *Biochemistry* **31**: 11425-11434.

Fleischmann, R.D., Adams, M.D., White, O., Clayton, R.A., Kirkness, E.F., Kerlavage, A.R., Bult, C.J., Tomb, J.F., Dougherty, B.A., Merrick, J.M., McKenney, K., Sutton, G., FitzHugh, W., Fields, C., Gocayne, J.D., Scott, J., Shirley, R., Liu, L.I., Glodek, A., Kelley, J.M., Weidman, J.F., Phillips, C.A., Spriggs, T., Hedblom, E., Cotton, M.D., Utterback, T.R., Hanna, M.C., Nguyen, D.T., Saudek, D.M., Brandon, R.C., Fine, L.D., Fritchman, J.L., Fuhrmann, J.L., Geoghagen, N.S.M., Gnehm, C.L., McDonald, L.A., Small, K.V., Fraser, C.M., Smith, H.O. and Venter, J.C. 1995. Whole genome random sequencing and assembly of *Haemophilus influenzae* RD. *Science* **269**: 496-512.

Friedrich, T., Strohdeicher, M., Hofhaus, G., Preis, D., Sahm, H., Weis, H. 1990. The same domain motif for ubiquinone reduction in mitochondrial or chloroplast NADH dehydrogenase and bacterial glucose dehydrogenase. *FEBS Letters* **265**: 37-40.

Friedrich, T., Vanheek, P., Leif, H., Ohnishi, T., Forche, E., Kunze, B., Jansen, R., Trowitzschkienast, W., Hofle, G., Reichenbach, H., Weiss, H. 1994. 2 binding-sites of inhibitors in NADH-ubiquinone oxidoreductase (complex I) - Relationship of one-site with the ubiquinone-binding site of a bacterial glucose-ubiquinone oxidoreductase. *European Journal of Biochemistry* **219**: 691-698.

Friedrich, T., Weidner, U., Nehls, U., Fecke, W., Schneider, R., Weiss, H. 1993. Attempts to define distinct parts of NADH-ubiquinone oxidoreductase (complex I). *Journal of Bioenergetics and Biomembranes* **25**: 331-337.

Gibb, G.M., Ragan, C.I. 1990. Identification of the subunits of bovine NADH dehydrogenase which are encoded in the mitochondrial genome. *Biochemical Journal* **265**: 903-906.

Gould, G.W. 1994. Membrane proteins expression systems. Portland Press, London.

Guffanti, A.A., Blanco, R., Benenson, R.A., Krulwich, T.A. 1980. Bioenergetic properties of alkali-tolerant and alkalophilic strains of *Bacillus firmus. Journal of General Microbiology* **119**: 79-86.

Guffanti, A.A., Cohn, D.E., Kaback, H.R., Krulwich, T.A. 1981. Relationship between the Na+/H+ antiporter and Na+/substrate symport in *Bacillus alcalophilus. Proceedings of the National Academy of Science, U.S.A.* **78**: 1481-1484.

Guzman, L.M., Belin, D., Carson, M.J., Beckwith, J. 1995. Tight regulation, modulation and high-level expression by vectors containing the Arabinose P_{BAD} promoter. *Journal of Bacteriology* **177**: 4121-4130.

Harlow, E., Lane D. 1988. Antibodies: A laboratory manual. Cold Spring Harbor Press.

Harvey, W.R. 1992. Physiology of V-ATPases. *Journal of Experimental Biology* **172**: 1-17.

Hatefi, Y., Haavik, A.G., Griffiths, D.E. 1962. Studies on the electron transfer system. XL. Preparation and properties of mitochondrial DPNH-coenzyme Q reductase. *Journal of Biological Chemistry* **237**: 1676-1680.

Hatefi, Y. 1985. The mitochondrial electron transport and oxidative phosphorylation system. *Annual reviews of Biochemistry* **54**: 1015-1069.

Hayashi, M., Hirai, K., Unemoto, T. 1994. Cloning of the Na^+-translocating NADH-quinone reductase gene from the marine bacterium *Vibrio alginolyticus* and the expression of the β-subunit in *Escherichia coli. FEBS letters* **356**: 330-332.

Hayashi, M., Hirai, K., Unemoto, T. 1995. Sequencing and the alignment of structural genes in the *nqr* operon encoding the Na^+-translocating NADH-quinone reductase from *Vibrio alginolyticus. FEBS letters* **363**: 75-77.

Hayashi, M., Miyoshi, T., Sato, M., Unemoto, T. 1992. Properties of respiratory chain-linked Na^+-independent NADH-quinone reductase in marine *Vibrio alginolyticus. Biochimica et Biophysica Acta* **1099**: 145-151.

Hayashi, M., Nakayama, Y., Unemoto, T. 1996. Existence of Na^+-translocating NADH-quinone reductase in *Haemophilus influenzae. FEBS Letters* **381**: 174-176.

Hayashi, M., Unemoto, T., Kozuka, Y., Hayashi, M. 1970. Anion-activated 5'-nucleotidase in cell envelopes of a slightly halophilic *Vibrio alginolyticus. Biochimica et Biophysica Acta* **220**: 244-255.

Hayashi, M., Unemoto, T. 1986. FAD and FMN flavoproteins participate in the sodium-transport respiratory chain NADH: quinone reductase of a marine bacterium, *Vibrio alginolyticus. FEBS Letters* **202**: 327-330.

Hayashi, M., Unemoto, T. 1987. Characterization of the Na^+-dependent respiratory chain NADH: quinone oxidoreductase of the marine bacterium, *Vibrio alginolyticus*, in relation to the primary Na^+ pump. *Biochimica et Biophysica Acta* **767**: 470-478.

von Heijne, G. 1986a. A new method for predicting signal sequence cleavage sites. *Nucleic Acids Research* **14**: 4683-4690.

von Heijne, G. 1986b. The distribution of positively-charged residues in bacterial inner membrane proteins correlates with transmembrane topology. *The EMBO Journal* **5**: 3021-3027.

Hofhaus, G., Attardi, G. 1995. Efficient selection and characterization of mutants of a human cell-line which are defective in mitochondrial DNA-encoded subunits of respiratory NADH dehydrogenase. *Molecular and Cellular Biology* **15**: 964-974.

Hofhaus, G., Weiss, H., Leonard, K. 1991. Electron microscopic analysis of the peripheral and membrane parts of mitochondrial NADH dehydrogenase (Complex I). *Journal of molecular biology* **221**: 1027-1043.

Homma, M., Oota, H., Kojima, S., Kawagishi, I, Imae, Y. 1996. Chemotactic responses to an attractant and a repellent by the polar and lateral flagellar systems of *Vibrio alginolyticus. Microbiology-U.K.* **142**: 2777-2783.

Hornstrup, M.K., Gahrnhansen, G. 1993. Extraintestinal infections caused by *Vibrio parahaemolyticus* and *Vibrio alginolyticus* in a Danish county. *Scandivanian Journal of Infectious Diseases* **25**: 735-740.

Ji, S.P. *et al.* 1989. The first isolation of *Vibrio alginolyticus* from samples which caused food poisoning. *Chinese Journal of Preventive Medicine* **23**: 71-73.

Kaback, H.R. 1988. Site-directed mutagenesis and ion-gradient driven active transport. *Annual Reviews of Physiology* **50**: 234-256.

Kakinuma, Y., Unemoto, T. 1985. Sucrose uptake is driven by the Na^+ electrochemical potential in the marine bacterium *Vibrio alginolyticus. Journal of Bacteriology* **163**: 1293-1295.

Karplus, P.A., Daniels, M.J., Herriott, J.R. 1990. Atomic structure of Ferredoxin NADP Reductase: prototype for a structurally novel flavoprotein family. *Science* **251**: 60-66.

Kawagishi, I., Maekawa, Y., Atsumi, T., Homma, M., Imae, Y. 1995. Isolation of the polar and lateral flagellum-defective mutants in *Vibrio alginolyticus* and identification of their flagellar driving energy sources. *Journal of Bacteriology* **177**: 5158-5160.

Kawagishi, I., Imagawa, M., Imae, Y., McCarter, L., Homma, M. 1996. The sodium-driven polar flagellar motor of marine vibrio as the mechanosensor that regulates lateral flagellar expression. *Molecular Microbiology* **20**: 693-699.

Kotlyar, A.B., Sled, V.D., Burbaev, D. Moroz, I.A., Vinogradov, A.D. 1990. Coupling site I and the rotenone-sensitive ubisemiquinone is tightly coupled in submitochondrial particles. *FEBS Letters* **264**: 17-20.

Kotlyar, A.B., Sled, V.D., Vinogradov, A.D. 1992 Effect of calcium ions on the slow active/inactive transition of the mitochondrial NADH-ubiquinone reductase. *Biochimica et Biophysica Acta* **1098**: 144-150.

Koyama, N., Ishikawa, Y., Nosoh, Y. 1980. Dependence of the growth of pH-sensitive mutants of a facultatively alkalophilic *Bacillus* on the regulation of cytoplasmic pH. *FEMS Microbiological Letters* **72**: 77-78.

Krulwich, T.A. 1983. Na^+/H^+ antiporters. *Biochimica et Biophysica Acta* **726**: 245-264.

Krulwich, T.A. 1986. Bioenergetics of alkalophilic bacteria. *Journal of Membrane Biology* **89**: 113-125.

Krulwich, T.A., Federbush, J.G., Guffanti, A.A. 1984. Presence of a non-metabolizable solute that is translocated with Na^+ enhances Na^+-dependent pH homeostasis in an alkalophilic *Bacillus*. *Journal of Biological Chemistry* **260**: 4055-4058.

Krulwich, T.A., Guffanti, A.A. 1986. Regulation of internal pH in acidophilic and alkalophilic bacteria. *Methods in Enzymology* **125**: 352-365.

Krulwich, T.A., Guffanti, A.A., Fong, M.Y., Falk, L., Hicks, D.B. 1986. Alkalophilic *Bacillus firmus* RAB generates variants which can grow at lower Na^+ concentrations than the parental strain. *Journal of Bacteriology* **165**: 884-889.

Krulwich, T.A., Guffanti, A.A. 1989. Alkalophilic bacteria. *Annual Review of Microbiology* **43**: 435-463.

Krulwich, T.A., Guffanti, A.A., Seto-Young, D. 1990. pH homeostasis and bioenergetic work in alkalophiles. *FEMS Microbiological Reviews* **75**: 271-278.

Krulwich, T.A., Mandel, K.G., Bornstein, R.F., Guffanti, A.A. 1979. A non-alkalophilic mutant of *Bacillus alcalophilus* lacks the Na^+/H^+ antiporter. *Biochemical and Biophysical Research Communications* **91**: 58-62.

Krumholz, L.R., Esser, U., Simoni, R.D. 1990. Characterisation of the proton pumping F_1F_0 ATPase of *Vibrio alginolyticus*. *Journal of Bacteriology* **172**: 6809-6817.

Laemmli, U.K. 1970. Cleavage of structural proteins during the assembly of the head bacteriophage T4. *Nature* **227**: 680-685.

Lanyi, J.K. 1979. The role of Na^+ in transport processes of bacterial membranes. *Biochemica et Biophysica Acta* **559**: 377-397.

Lee, S.H., Cohen, N.S., Jacobs, A.J., Brodie, A.F. 1979. Isolation, purification and reconstitution of a proline carrier protein from *Mycobacterium phlei*. *Biochemistry* **18**: 2232-2238.

Leonard, K., Haiker, H., Weiss, H. 1987. Three-dimensional structure of NADH:ubiquinone reductase (Complex I) from *Neurospora* mitochondria determined by electron microscopy of membrane crystals. *Journal of Molecular Biology* **194**: 277-286.

Lewis, R.J., Kabak, E., Krulwich, T.A. 1982. Pleiotropic properties of mutations to non-alkalophily in *Bacillus alcalophilus*. *Journal of General Microbiology* **128**: 427-430.

Lim, L.W., Shamala, N., Mathews, F.S., Steenkamp, D.J., Hamlin, R., Xuong, N.H. 1986. Three-dimensional structure of the iron-sulfur flavoprotein trimethylamine dehydrogenase at 2.4 A resolution. *Journal of Biological Chemistry* **261**: 15140-15146.

Lin, T.I., Sled, V.D., Ohnishi, T., Brennicke, A., Grohmann, L. 1995. Analysis of iron-sulfur clusters within the complex I (NADH:ubiquinone oxidoreductase) isolated from potato tuber mitochondria. *European Journal of Biochemistry* **230**: 1032-1036.

Lindqvist, Y. 1989. Refined structure of spinach glycolate oxidase at 2 A resolution. *Journal of Molecular Biology* **209**: 151-166.

Litwin, C.M., Calderwood, S.B. 1993. Cloning and genetic analysis of the *Vibrio vulnificus fur* gene and construction of a *fur* mutant by *in vivo* marker exchange. *Journal of Bacteriology* **175**: 706-715.

Liu, J.Z., Dapice, M., Khan, S. 1990. Ion selectivity of the *Vibrio alginolyticus* flagellar motor. *Journal of Bacteriology* **172**: 5236-5244.

Ludwig, W., Kaim, G., Laubinger, W., Dimroth, P., Hoppe, J., Schleifer, K.H. 1990. Sequence of subunit c of the sodium ion translocating ATP synthase of *Propionigenium modestum*. *European Journal of Biochemistry* **193**: 395-400.

Majander, A., Finel, M., Wikstrom, M. 1994. Diphenyleneiodonium inhibits reduction of iron-sulfur clusters in the mitochondrial NADH-ubiquinone oxidoreductase (complex I). *Journal of Biological Chemistry* **269**: 21037-21042.

Mariottini, P., Chomyn, A. 1995. Immunoprecipitation of human NADH:ubiquinone oxidoreductase and cytochrome-*c* oxidase with single subunit-specific antibodies. *Methods in Enzymology* **260**: 202-210.

Matsubara, H., Saeki, K. 1992. Evolutionary aspects of iron-sulfur proteins in photosynthetic apparatus. *Advances in Inorganic Chemistry* **38**: 223-280.

Matsubayashi, T., Wakasugi, T., Shinozaki, K., Yamaguchi-Shinozaki, K., Zaita, N., Hidaka, T., Meng, B.Y., Ohto, C., Tanaka, A, Maruyama, T., Sugiura, M. 1987. Six chloroplast genes (*ndh A-F*) homologous to human respiratory chain NADH dehydrogenase are actively expressed. *Molecular General Genetics* **210**: 385-393.

Matsushita, K., Ohnishi, T., Kaback, H.R. 1987. NADH-ubiquinone oxidoreductases of *Escherichia coli* aerobic respiratory chain. *Biochemistry* **26**: 7732-7737.

Matte, G.R., Matte, M.H., Sato, M.I.Z., Sanchez, P.S., Rivera, I.G., Martins, M.T. 1994a. Potentially pathogenic vibrios associated with mussels from a tropical region on the Atlantic coast of Brazil. *Journal of Applied Bacteriology* **77**: 281-287.

Matte, G.R., Matte, M.H., Rivera, I.G., Martins, M.T. 1994b. Distribution of potentially pathogenic vibrios in oysters from a tropical region. *Journal of Food Protection* **57**: 870-873.

Mayhew, S.G., Ludwig, M. 1975. Flavodoxins and electron-transferring flavoproteins, In *The Enzymes* (ed P.D. Boyer), pp. 57-118. New York: Academic Press.

McCarter, L.L. 1994. MotY, a component of the sodium-type flagellar motor. *Journal of Bacteriology* **176**: 4219-4225.

McCarter, L.L. 1995. Genetic and molecular characterization of the polar flagellum of *Vibrio parahaemolyticus. Journal of Bacteriology* **177**: 1595-1609.

McLaggan, D., Selwyn, M.J., Dawson, A.P. 1984. Dependence on Na^+ of control of cytoplasmic pH in a facultative alkalophile. *FEBS Letters* **165**: 254-258.

Miller, V.L., Mekalanos, J.J. 1988. A novel suicide vector and its use in construction of insertion mutations: Osmoregulation of outer membrane proteins and virulence determinants in *Vibrio cholerae* requires *toxR. Journal of Bacteriology* **170**: 2575-2583.

Miller, V.L., DiRita, V.J., Mekalanos, J.J. 1989. Identification of *toxS*, a regulatory gene whose product enhances ToxR-mediated activation of the cholera toxin promoter. *Journal of Bacteriology* **171**: 1288-1293.

Mitchell, P. 1966. Chemiosmotic coupling in oxidative and photosynthetic phosphorylation. *Biological Reviews* **41**: 455-502.

Moss, J., Lane, M.D. 1971. The biotin-dependent enzymes. *Advanced Enzymology* **35**: 321-442.

Muramoto, K., Kawagishi, I., Kudo, S., Magariyama, Y., Imae, Y., Homma, M. 1995a. High-speed rotation and speed stability of the sodium-driven flagellar motor in *Vibrio alginolyticus. Journal of Molecular Biology* **251**: 50-58.

Muramoto, K., Magariyama, Y., Homma, M., Kawagishi, I., Sugiyama, S., Imae, Y., Kudo, S. 1995b. Rotational fluctuation of the sodium-driven flagellar motor in *Vibrio alginolyticus* induced by binding of inhibitors. *Journal of Molecular Biology* **259**: 687-695.

Nakamura, T., Hayashi, S., Yamanaka, R., Hamashima, H., Arai, T., Unemoto, T. 1993. Respiration-driven Na^+ pump of the marine Vibrio is encoded by chromosomal DNA. *Biological & Pharmaceutical Bulletin* **16**: 751-753.

Nakamura, T., Kawasaki, S., Unemoto, T. 1992. Roles of potassium and sodium in pH homeostasis and growth of the marine bacterium *Vibrio alginolyticus. Journal of General Microbiology* **138**: 1271-1276.

Nakamura, T., Komano, Y., Itaya, E., Tsukamoto, K., Tsichiya, T., Unemoto, T. 1994a. Cloning and sequencing of an Na^+/H^+ antiporter gene from marine bacterium *Vibrio alginolyticus. Biochimica et Biophysica Acta - Biomembranes* **1190**: 465-468.

Nakamura, T., Suzuki, F., Abe, M., Matsuba, Y., Unemoto, T. 1994b. K^+ transport in *Vibrio alginolyticus*- Isolation of a mutant defective in an inducible K^+ transport system. *Microbiology UK* **140**: 1781-1785.

Nakamura, Matsuba, Y., Yamamuro, N., Booth, I.R., Unemoto, T. 1994c. Cloning and sequencing of a K^+ transport gene (*trkA*) from the marine bacterium *Vibrio alginolyticus. Biochimica et Biophysica Acta- Gene Structure and Expression* **1219**: 701-705.

Nakamura, T., Komano, Y., Unemoto, T. 1995. 3 Aspartic residues in membrane-spanning regions of Na^+/H^+ antiporter from *Vibrio alginolyticus* play a role in the activity of the carrier. *Biochimica et Biophysica Acta - Bioenergetics* **1230**: 170-176.

Nakamura, T., Enomoto, H., Unemoto, T. 1996. Cloning and sequenciong of the *nhaB* gene encoding an Na^+/H^+ antiporter from *Vibrio alginolyticus. Biochimica et Biophysica Acta - Bioenergetics* **1275**: 157-160.

Nehls, U., Friedrich, T., Schmeide, A., Ohnishi, T, Weiss, H. 1992. Characterization of assembly intermediates of NADH:ubiquinone oxidoreductase (complex I) accumulated in *Neurospora* mitochondria by gene disruption. *Journal of Molecular Biology* **227**: 1032-1042.

Nelson, N. 1992. The vacuolar H^+-ATPase- one of the most fundamental ion pumps in nature. *Journal of Experimental Biology* **172**: 19-27.

Nicholls, D.G., Ferguson, S.J. 1992. Bioenergetics 2. Academic Press.

Niiya, S., Yamasaki, K., Wilson, T.H., Tsuchiya, T. 1982. Altered cation coupling to melibiose transport in mutants of *Escherichia coli. Journal of Biological Chemistry* **257**: 8902-8906.

Novagen pET system manual- technical bulletin.

Ogierman, M.A., Zabihi, S., Mourtzios, L., Manning, P.A. 1993. Genetic organization and sequence of the promoter-distal region of the *tcp* gene cluster of *Vibrio cholerae. Gene* **126**: 51-60.

Okunishi, I., Kawagishi, I., Homma, M. 1996. Cloning and characterisation of *motY*, a gene coding for a component of the sodium-driven flagellar motor in *Vibrio alginolyticus. Journal of Bacteriology* **178**: 2409-2415.

Oliver, D. 1985. Protein secretion in *Escherichia coli. Annual Reviews of Microbiology* **39**: 615-648.

Ohnishi, T. 1993. NADH-quinone oxidoreductase, the most complex complex. *Journal of Bioenergetics and Biomembranes* **25**: 325-329.

Ottemann, K.M., DiRita, V.J., Mekalanos, J.J. 1992. ToxR proteins with substitutions in residues conserved with OmpR fail to activate transcription from the cholera toxin promoter. *Journal of Bacteriology* **174**: 6807-6814.

Padan, E., Maisler, N., Taglicht, D., Karpel, R., Schuldiner, S. 1989. Deletion of *ant* in *Escherichia coli* reveals its function in adaptation to high salinity and an alternative Na^+/ H^+ antiporter system(s). *Journal of Biological Chemistry* **264**: 20297-20302.

Parales, R.E., Harwood, C.S. 1993. Construction and use of a broad-host-range *lacZ* transcriptional fusion vector, pHRP309, for $Gram^-$ bacteria. *Gene* **133**: 23-30.

Parsot, C., Mekalanos, J.J. 1991. Expression of the *Vibrio cholerae* gene encoding aldehyde dehydrogenase is under control of ToxR, the cholera toxin transcriptional activator. *Journal of Bacteriology* **173**: 2842-2851.

Parsot, C., Mekalanos, J.J. 1992. Structural analysis of the *acfA* and *acfD* genes of *Vibrio cholerae*: Effects of DNA topology and transcriptional activators on expression. *Journal of Bacteriology* **174**: 5211-5218.

Pelczar, M.J., Chan, E.C.S., Krieg, N.R. 1986. Microbiology. 5th Edition. McGraw-Hill Book Company.

Peltier, G., Ravenel, J., Vermeglio, A. 1987. Inhibition of a respiratory activity by short saturating flashes in *Chlamydomonas*: evidence for a chlororespiration. *Biochimica et Biophysica Acta* **893**: 83-90.

Peterson, G.L. 1977. A simplification of the protein assay method of Lowry *et al* which is more generally applicable. *Analytical Biochemistry* **83**: 346-356.

Pfenninger-Li, X.D., Dimroth, P. 1995. The Na^+-translocating NADH:ubiquinone oxidoreductase from the marine bacterium *Vibrio alginolyticus* contains FAD but not FMN. *FEBS Letters* **369**: 173-176.

Pfenninger-Li, X.D., Albracht, S.P.J., van Belzen, R., Dimroth, P. 1996. NADH:ubiquinone oxidoreductase of *Vibrio alginolyticus*: Purification, Properties, and Reconstitution of the Na^+ pump. *Biovhemistry* **35**: 6233-6242.

Pilkington, S.J., Walker, J.E. 1989. Mitochondrial NADH-ubiquinone reductase: complementary DNA sequences of import precursors of the bovine and human 24 kDa subunit. *Biochemistry* **28**: 3257-3264.

Pilkington, S.J., Skehel, J.M., Gennis, R.B., Walker, J.E. 1991a. Relationship between mitochondrial NADH-ubiquinone reductase and a bacterial NAD-reducing hydrogenase. *Biochemistry* **30**: 2166-2175.

Pilkington, S.J., Skehel, J.M., Walker, J.E. 1991b. Plant chloroplast genomes encode a homologue of the nuclear encoded 30 kDa subunit of the bovine mitochondrial Complex I. *Biochemistry* **30**: 1901-1908.

Pinner, E., Padan, E., Schuldiner, S. 1992. Cloning, sequencing and expression of the *nhaB* gene, encoding a Na^+/H^+ antiporter in *Escherichia coli. Journal of Biochemistry* **267**: 11064-11068.

Pourcher, T., Bassilana, M., Sarkar, H.K., Kabak, H.R., Leblanc, G. 1990. The melibiose/Na^+ symporter of *Escherichia coli:* kinetic and molecular properties. Philosophical Transactions of the Royal Society of London B series- Biological Sciences **326**: 411-423.

Preis, D., van des Pas, J.C., Nehls, U., Roehlen, D., Sackmann, U., Jahnke, U., Weiss, H. 1990. The 49 kDa subunit of NADH:ubiquinone reductase (complex I) from *Neurospora crassa* mitochondria: primary structure of the gene and the protein. *Current Genetics* **18**: 59-64.

Preis, D., Weidner, U., Conzen, C., Azevedo, J.E., Nehls, U., Roehlen, D., van der Pas, J., Sackmann, U., Schneider, R., Werner, S., Weiss, H. 1991. Primary structure of two subunits of NADH:ubiquinone reductase (complex I) from *Neurospora crassa* mitochondria: relationship to a soluble NAD-reducing hydrogenase from *Alcaligenes eutrophus. Biochimica et Biophysica Acta* **1090**: 133-138.

Prince, R.C. 1988. Tetrodotoxin. *TIBS* **13**: 76-77.

Promper, C., Schneider, R., Weiss, H. (1993) The role of the proton-pumping and alternative respiratory-chain NADH-ubiquinone oxidoreductases in overflow catabolism of *Aspergillus niger. European Journal of Biochemistry* **216**: 223-230.

Rahav-Manor, O., Carmel, O., Karpel, R., Taglicht, D., Glaser, G., Schuldiner, S., Padan, E. 1992. *Nha* R, a protein homologous to a family of bacterial regulatory proteins (*lys* R), regulates *nha* A, the sodium proton antiporter gene in *Escherichia coli. Journal of Biological Chemistry* **267**: 10433-10438.

Raine, A.R.C., Scrutton, N.S., Mathews, F.S. 1994. On the evolution of alternate core packing in eightfold β/α-barrels. *Protein Science* **3**: 1889-1892.

Ragan, C.I. 1987. Structure of NADH-ubiquinone reductase (complex I). *Current Topics in Bioenergetics* **15**: 1-36.

Rasmusson, A.G. and Mϕller, I.M. 1991. Effect of calcium ions and inhibitors on internal NAD(P)H dehydrogenases in plant mitochondria. *European Journal of Biochemistry* **202**: 617-623.

Reid, G.A., White, S., Black, M.T., Lederer, F., Matthews, F.S., Chapman, S.K. 1988. Probing the active site of flavocytochrome b_2 by site-directed mutagenesis. *European Journal of Biochemistry* **178**: 329-333.

Reeves, H.C., Rabin, R., Wegner, W.S., Ajl, S.J. 1971. Assays of enzymes of the tricarboxylic acid and glyoxylate cycles. *Methods in Microbiology* **6A**: 435-436.

Rich, P.R., Meunier, B., Ward, F.B. 1995. Predicted structure and possible ionmotive mechanism of the sodium-linked NADH-ubiquinone oxidoreductase of *Vibrio alginolyticus*. *FEBS Letters* **375**: 5-10.

Rimler, R.B., Shotts Jr., E.B., Brown, J., and Davis, R.B. 1977. The effect of sodium chloride and NADH on the growth of six strains of haemophilus species pathogenic to chickens. *Journal of General Microbiology* **98**: 349-354.

Roehlen, D.A., Hoffmann, J., van der Pas, J.C., Nehls, U., Preis, D., Sackman, U., Weiss, H. 1991. Relationship between a subunit of NADH dehydrogenase (complex I) and a protein family including subunits of cytochrome reductase and processing protease from mitochondria. *FEBS Letters* **278**: 75-78.

Rosen, B.P. 1986. Recent advances in bacterial ion transport. *Annual reviews in Microbiology* **40**: 263-286.

Runswick, M.J., Gennis, R.B., Fearnley, I.M., Walker, J.E. 1989. Mitochondrial NADH:ubiquinone reductase: complementary DNA sequence of the import precursor of the bovine 75 kDa subunit. *Biochemistry* **28**: 9452-9459.

Runswick, M.J., Fearnley, I.M., Skehel, J., Walker, J.E. 1991. Presence of an acyl carrier in NADH:ubiquinone oxidoreductase from bovine heart mitochondria. *FEBS Letters* **286**: 121-124.

Sakai-Tomita, Y., Moritani, C., Kanazawa, H., Tsuda, M., Tsuchiya, T. 1992. Catabolite repression of the H^+-translocating ATPase in *Vibrio parahaemolyticus*. *Journal of Bacteriology* **174**: 6743-6751.

Sambrook, J., Fritsch, E.F., Maniatis, T. 1989. Molecular cloning: a laboratory manual. Second edition, Cold Spring Harbor Laboratory Press, Cold Spring Harbor, New York.

Schlegel, H.G. 1990. General Microbiology. 6th Edition. Cambridge University Press.

Schmidt, M., Friedrich, T., Wallrath, J., Ohnishi, T., Weiss, H. 1992. Accumulation of the preassembled membrane arm of NADH-ubiquinone oxidoreductase in mitochondria of manganese-limited grown *Neurospora crassa. FEBS Letters* **313**: 8-11.

Schneider, K., Cammack, R., Schlegel, H.G. 1984. Content and localization of FMN, Fe-S cluster and nickel in the NAD-linked hydrogenase of *Nocardia opaca* 1B. *European Journal of Biochemistry* **142**: 75-84.

Singer, T.P., Ramsay, R.R. 1994. The reaction sites of rotenone and ubiquinone with mitochondrial NADH dehydrogenase. *Biochimica et Biophysica Acta* **1187**: 198-202.

Skehel, J.M., Pilkington, S.J., Runswick, M.J., Fearnley, I.M., Walker, J.E. 1991. NADH:ubiquinone oxidoreductase from bovine heart mitochondria. Complementary DNA sequence of the import precursor of the 10 kDa subunit of the flavoprotein fragment. *FEBS Letters* **282**: 135-138.

Skulachev, V.P. 1987. Bacterial sodium transport: Bioenergetic functions of sodium ions. *Ion transport in prokaryotes*: 131- 164. Academic Press.

Skulachev, V.P. 1985. Membrane-linked energy transductions. Bioenergetic functions of sodium: H^+ is not unique as a coupling ion. *European Journal of Biochemstry* **151**: 199-208.

Sled, V.D., Rudnitzky, N.I., Hatefi, Y., Ohnishi, T. 1994. Thermodynamic analysis of flavin in mitochondrial NADH-ubiquinone oxidoreductase (complex I). *Biochemistry* **33**: 10069-10075.

Smirnova, I.A., Kostyrko, V.A. 1988. Proton transmembrane potential generation by the respiratory chain of the marine bacterium *Vibrio alginolyticus. Biokhimiya* **53**: 1939-1949.

Smirnova, I.A., Vagina, M.L., Kostyrko, V.A. 1990. Delta-psi and delta-pH generation by the proton pumps of the respiratory chain and ATPase in subcellular vesicles from marine bacterium *Vibrio alginolyticus. Biochimica et Biophysica Acta* **1016**: 385-391.

Smith, W.W., Pattridge, K.A., Ludwig, M.L. 1983. Structure of oxidised flavodoxin from *Anacystis nidulans. Journal of Molecular Biology* **165**: 737-755.

Sokolov, M.V., Dibrov, P.A., Skulachev, V.P. 1988. An ATP-dependent sodium pump is found in the membrane of an aerobic bacterium. *Biologicheskie Membrany* **5**: 878-880.

Stanier, R.Y., Ingraham, J.L., Wheelis, M.L., Painter, P.R. 1987. General Microbiology. 5th Edition. Macmillan Education Ltd.

Stevenson, A. 1991. Molecular characterisation of the Na^+ pump in *Vibrio alginolyticus.* Week 8 report. ICMB, University of Edinburgh.

Stevenson, A. 1991. Molecular characterisation of the respiratory dependent sodium pump in *Vibrio alginolyticus.* First year report. ICMB, University of Edinburgh.

Stevenson, A. 1994. Molecular characterisation of the respiratory dependent sodium pump in *Vibrio alginolyticus.* MPhil. Thesis. ICMB, University of Edinburgh.

Studier, F.W., Rosenberg, A.H., Dunn, J.J., Dubendorff, J.W. 1990. Use of T7 RNA polymerase to direct expression of cloned genes. *Methods in Enzymology* **185**: 60-89.

Stryer, L. 1988. Biochemistry. 3rd Edition. W.H. Freeman and Company.

Sumegi, B. and Srere, P.A. 1984. Complex I binds several mitochondrial NAD-coupled dehydrogenases. *Journal of Biological Chemistry* **259**: 15040-15045.

Suzuki, H., Ozawa, T. 1986. An ubiquinone-binding protein in the mitochondrial NADH-ubiquinone reductase of the mitochondrial respiratory chain. *Journal of Biological Chemistry* **258**: 352-358.

Tabor, S., Richardson, C.C. 1985. A bacteriophage T7 RNA polymerase promoter system for controlled exclusive expression of specific genes. *Proceedings of National Academy of Science, U.S.A.* **81**: 1074.

Taglicht, D., Padan, E., Schuldiner, S. 1991. Overproduction and purification of a functional Na^+/H^+ antiporter coded by *nhaA* (*ant*) from *Escherichia coli. Journal of Biological Chemistry* **266**: 11289-11294.

Tan, K., Beattie, P., Leach, D.R.F., Rich, P.R., Coulson, A.F.W., Ward, F.B. 1996. Expression and analysis of the gene for the catalytic β subunit of the sodium-translocating NADH-ubiquinone oxidoreductase of *Vibrio alginolyticus. Biochemical Society Transactions* **24**: 12S.

Taylor, R.K., Miller, V.L., Furlong, D.B., Mekalanos, J.J. 1987. Use of *phoA* gene fusions to identify a pilus colonization factor coordinately regulated with cholera toxin. *Proceedings of the National Academy of Science U.S.A.* **84**: 2833-2837.

Thompson, L.M.M., MacLeod, R.A. 1974. Factors affecting the activity and stability of alkaline phosphatase in a marine pseudomonad. *Journal of Bacteriology* **117**: 813-818.

Tokuda, H. 1983. Isolation of *Vibrio alginolyticus* mutants defective in the respiration-coupled Na^+ pump. *Biochemical and Biophysical Research Communications* **114**: 113-118.

Tokuda, H. 1986. Sodium translocation by NADH oxidase of *Vibrio alginolyticus*: Isolation and characterisation of the sodium pump-defective mutants. *Methods in Enzymology* **125**: 520-530.

Tokuda, H., Udagawa, T., Unemoto, T. 1985. Generation of the electrochemical potential of Na^+ by the Na^+-motive NADH oxidase in inverted membrane vesicles of *Vibrio alginolyticus. FEBS Letters* **183**: 95-98.

Tokuda, H., Kogure, K. 1989. Generalized distribution and common properties of sodium-dependent NADH: quinone oxidoreductases in gram-negative marine bacteria. *Journal of General Microbiology* **135**: 703-710.

Tokuda, H., Sugasawa, M., Unemoto, T. 1982. Roles of Na^+ and K^+ in A-aminoisobutyric acid transport by the marine bacterium *Vibrio alginolyticus. Journal of Biological Chemistry* **257**: 788-794.

Tokuda, H., Unemoto, T. 1981. A respiration-dependent primary sodium extrusion system functioning at alkaline pH in the marine bacterium *Vibrio alginolyticus. Biochemical and Biophysical Research Communications* **102**: 265-271.

Tokuda, H., Unemoto, T. 1982. Characterisation of the respiration-dependent Na^+ pump in the marine bacterium *Vibrio alginolyticus. Journal of Biological Chemistry* **257**: 10007-10014.

Tokuda, H., Unemoto, T. 1983. Growth of a marine bacterium *Vibrio alginolyticus* and moderately halophilic *Vibrio costicola* becomes uncoupler resistant when the respiration-dependent Na^+ pump functions. *Journal of Bacteriology* **156**: 636-643.

Tokuda, H., Unemoto, T. 1984. Na^+ is translocated at NADH:quinone oxidoreductase segment in the respiratory chain of *Vibrio alginolyticus. Journal of Biological Chemistry* **259**: 7785-7790.

Towler, D.A., Adams, S.P., Eubanks, S.R., Towery, D.S., Jackson-Machelski, E., Glaser, L., Gordon, J.I. 1988. Myristoyl CoA: protein N-myristoyl transferase activities from rat liver and yeast possess overlapping yet distinct peptide substrate specificities. *Journal of Biological Chemistry* **263**: 1784-1790.

Trumpower, B.L. 1990. The proton-motive Q-cycle. *Journal of Biological Chemistry* **265**: 11409-11412.

Tuschen, G., Sackmann, U., Nehls, U., Haiker, H., Buse, G., Weiss, H. 1990. Assembly of NADH:ubiquinone reductase (complex I) in *Neurospora* mitochondria: independent pathways of nuclear encoded and mitochondrially encoded subunits. *Journal of Molecular Biology* **213**: 845-857.

Unemoto, T., Akagawa, A., Mizugaki, M., Hayashi, M. 1992. Distribution of sodium dependent respiration and a respiration-driven electrogenic sodium pump in moderately halophilic bacteria. *Journal of General Microbiology* **138**: 1999-2005.

Unemoto, T., Akagawa, A., Hayashi, M. 1993. Correlation between the respiration-driven Na+ pump and Na+-dependent amino acid transport in moderately halophilic bacteria. *Journal of General Microbiology* **139**: 2779-2782.

Unemoto, T., Hayashi, M. 1977. Na^+-dependent activation of NADH oxidase in membrane fractions from halophilic *Vibrio alginolyticus* and *V. costicolus. Journal of Biochemistry* **82**: 1389-1395.

Unemoto, T., Hayashi, M. 1979a. Regulation of internal solute concentrations of marine *Vibrio alginolyticus* in response to external NaCl concentrations. *Canadian Journal of Microbiology* **25**: 922-926.

Unemoto, T., Hayashi, M. 1979b. NADH:quinone oxidoreductase as a site of Na^+-dependent activation in the respiratory chain of marine *Vibrio alginolyticus. Journal of Biochemistry* **85**: 1461-1467.

Unemoto, T., Hayashi, M. 1989. Sodium transport NADH-quinone reductase of a marine *Vibrio alginolyticus. Journal of Bioenergetics and Biomembranes* **21**: 649-662.

Unemoto, T., Miyoshi, T., Hayashi, M. 1992. Characteristic differences in the mode of quinone reduction and stability between energy-coupled and -uncoupled NADH-quinone reductases from bacterial respiratory chain. *FEBS Letters* **306**: 51-53.

Unemoto, T., Nakamura, T., Hayashi, M. 1991. The role of membranes in the microbial adaptations to environmental changes. *Membrane* **16**: 3-14.

Unemoto, T., Ogura, T., Hayashi, M. 1993. Modifications by Na^+ and K^+, and the site of Ag^+ inhibition in the Na^+-translocating NADH-quinone reductase from a marine *Vibrio alginolyticus. Biochimica et Biophysica Acta* **1183**: 201-205.

Unemoto, T., Tsuruoka, T, Hayashi, M. 1973. Role of Na^+ and K^+ in preventing lysis of a slightly halophilic *Vibrio alginolyticus. Canadian Journal of Microbiology* **19**: 563-571.

Vagina, M.L., Kostyrko, V.A. 1989. Protonophore-resistant alkalinization inside subcellular vesicles, accompanying the oxidation of NADH by the respiratory chain of the marine bacterium *Vibrio alginolyticus*. Recording according to the change in the fluorescence of pyranine. *Biokhimiya* **54**: 1557-1564.

Vagina, M.L., Kostyrko, V.A. 1989. The delta-pH generation by the respiratory chain and ATPase from the subcellular vesicles of the marine bacterium *Vibrio alginolyticus. Biokhimiya* **54**: 1337-1343.

Veeger, C., DerVartanian, D.V., Zeylemaker, W.P. 1969. Succinate dehydrogenase. *Methods in Enzymology* **XIII**: 81-90.

Videira, A., Tropschueg, M., Werner, S. 1990. Primary structure and expression of a nuclear-encoded subunit of complex I homologous to proteins specified by the chloroplast genome. *Biochemical and Biophysical Research Communications* **171**: 1168-1174.

Walker, J.E. 1992. The NADH:ubiquinone oxidoreductase (complex I) of respiratory chains. *Quarterly Reviews of Biophysics* **25**: 253-324.

Walker, J.E., Arizmendi, J.M., Dupuis, A., Fearnley, I.M., Finel, M., Medd, S.M., Pilkington, S.J., Runswick, M.J., Skehel, J.M. 1992. Sequences of twenty subunits of NADH:ubiquinone oxidoreductase from bovine heart mitochondria. Application of a novel strategy for sequencing proteins using the polymerase chain reaction. *Journal of Molecular Biology* **226**: 1051-1072.

Walker, J.E., Cozens, A.L. 1986. Evolution of ATP synthase. *Chemica Scripta* **26B**: 263-272.

Walker, J.E., Saraste, M., Gay, N.J. 1984. The *unc* operon: nucleotide sequence, regulation and structure of ATP synthase. *Biochimica et Biophysica Acta* **768**: 164-200.

Walker, J.E., Skehel, M., Buchanan, S.K. 1995. Structural analysis of NADH:ubiquinone oxidoreductase from bovine heart mitochondria. *Methods in Enzymology* **260**: 14-34.

Weidner, U., Geier, S., Ptock, A., Friedrich, T., Leif, H., Weiss, H. 1993. The gene locus of the proton-translocating NADH:ubiquinone oxidoreductase in *Escherichia coli*. *Journal of Molecular Biology* **233**: 109-122.

Weinstock, G.M. 1987. Use of open reading frame expression vectors. *Methods in Enzymology*. Wu, R. and Grossman, L. (Editors), Academic Press **154**: 156-163

Wierenga, R.K., Terpstra, P., Hol, W.G.J. 1986. Prediction of the occurrence of the ADP-binding βαβ-fold in proteins, using an amino acid sequence fingerprint. *Journal of Molecular Biology* **187**: 101-107.

Weiss, H., Friedrich, T., Hofhaus, G., Pries, D. 1991. The respiratory chain NADH dehydrogenase (complex I) of mitochondria. *European Journal of Biochemistry* **197**: 563-576.

Willeford, K.O., Gomobos, Z., Gibbs, M. 1989. Evidence for chloroplastic succinate dehydrogenase participating in the chloroplastic respiratory and photosynthetic electron transport chains of *Chlamydomonas reinhardtii*. *Plant Physiology* **90**: 1084-1087.

Xia, Z.N., Mathews, F.S. 1990. Molecular structure of flavocytochrome b_2 at 2.4 A resolution. *Journal of Molecular Biology* **212**: 837-863.

Xu, X., Matsuno-Yagi, A., Yagi, T. 1991a. The NADH-binding subunit of the energy-transducing NADH-ubiquinone oxidoreductase of *Paracoccus denitrificans*: Gene cloning and deduced primary structure. *Biochemistry* **30**: 6422-6428.

Xu, X., Matsuno-Yagi, A., Yagi, T. 1991b. Characterization of the 25-kilodalton subunit of the energy-transducing NADH-ubiquinone oxidoreductase of *Paracoccus denitrificans*: Sequence similarity to the 24-kilodalton subunit of the flavoprotein fraction of mammalian Complex I. *Biochemistry* **30**: 8678-8684.

Xu, X., Matsuno-Yagi, A., Yagi, T. 1992a. Structural features of the 66 kDa subunit of the energy transducing NADH ubiquinone oxidoreductase (NDH-1) of *Paracoccus denitrificans*. *Arch. Biochem. Biophys.* **296**: 40-48.

Xu, X., Matsuno-Yagi, A., Yagi, T. 1992b. Gene cluster of the energy-transducing NADH-quinone oxidoreductase of *Paracoccus denitrificans*: Characterization of four structural gene products. *Biochemistry* **31**: 6925-6932.

Xu, X., Matsuno-Yagi, A., Yagi, T. 1993. DNA sequencing of the seven remaining structural genes of the gene cluster encoding the energy-transducing NADH-quinone oxidoreductase of *Paracoccus denitrificans*. *Biochemistry* **32**: 968-981.

Yagi, T. 1993. The bacterial energy-transducing NADH-quinone oxidoreductases. *Biochimica et Biophysica Acta* **1141**: 1-17.

Yagi, T. 1991. Bacterial NADH-quinone oxidoreductases. *Journal of Bioenergetics and Biomembranes* **23**: 211-225.

Yagi, T. 1989. Structure and function of NADH quinone oxidoreductases in respiratory chain. *Prot. nucleic acid and enzyme (Japanese journal: Taripaku shitsu kakusai koso)* **34**: 351-363.

Yagi, T. 1987. Inhibition of NADH ubiquinone reductase activity by N, N'-dicyclohexylcarbodiimide and correlation of this inhibition with the occurence of energy coupling site 1 in various organisms. *Biochemistry* **26**: 2822-2828.

Yagi, T. 1986. Purification and characterization of NADH dehydrogenase complex from *Paracoccus denitrificans*. *Arch. Biochem. Biophys.* **250**: 302-311.

Yagi, T. and Dinh, T.M. 1990. Identification of the NADH binding subunit of NADH-ubiquinone oxidoreductase of *Paracoccus denitrificans*. *Biochemistry* **29**: 5515-5520.

Yagi, T., Hon-nami, K. and Ohnishi, T. 1988. Purification and characterization of 2 types of NADH-quinone reductases from *Thermus thermophilus*. *Biochemistry* **27**: 2008-2013.

Yagi, T., Yano, T., Matsunoyagi, A. 1993. Characteristics of the energy-transducing NADH-quinone oxidoreductase of *Paracoccus denitrificans* as revealed by biochemical, biophysical and molecular biological approaches. *Journal of Bioenergetics and Biomembranes* **25**: 339-345.

Yamaguchi, M., Hatefi, Y. 1993. Mitochondrial NADH-ubiquinone oxidoreductase (complex I)- Proximity of the subunits of the flavoprotein and the iron-sulfur protein subcomplexes. *Biochemstry* **32**: 1935-1939.

Yano, T., Sled, V.D., Ohnishi, T., Yagi, T. 1994. Expression of the 25-kilodalton iron-sulfur subunit of the energy-transducing NADH-ubiquinone oxidoreductase of *Paracoccus denitrificans*. *Biochemistry* **33**: 494-499.

Yano, T., Sled, V.D., Ohnishi, T., Yagi, T. 1994 Identification of amino acid residues associated with the [2Fe-2S] cluster of the 25 kDa (NQO2) subunit of the proton-translocating NADH-quinone oxidoreductase of *Paracoccus denitrificans*. *FEBS Letters* **354**: 160-164.

Yano, T., Sled, V.D., Ohnishi, T., Yagi, T. 1996. Expression and characterization of the flavoprotein subcomplex composed of the 50-kDa (NQO1) and 25-kDa (NQO2) subunits of the proton-translocating NADH-quinone oxidoreductase of *Paracoccus denitrificans*. *Journal of Biological Chemistry* **271**: 5907-5913.

Yano, T., Yagi, T., Sled, V.D., Ohnishi, T. 1995. Expression and characterization of the 66-kilodalton (NQO3) iron-sulfur subunit of the proton-translocating NADH-quinone oxidoreductase of *Paracoccus denitrificans*. *Journal of Biological Chemistry* **270**: 18264-18270.

Yoshida, S., Sugiyama, S., Hojo, Y., Tokuda, H., Imae, Y. 1990. Intracellular sodium ion kinetically interferes with the rotation of the sodium ion-driven flagellar motors of *Vibrio alginolyticus*. *Journal of Biological Chemistry* **265:** 20346-20350.

Zilberstein, D., Ophir, I.J., Padan, E., Schuldiner, S. 1982. Na^+ gradient-coupled porters of *Escherichia coli* share a common subunit. *Journal of Biological Chemistry* **257**: 3692-3696.

Appendix

```
**************************************************************************
```

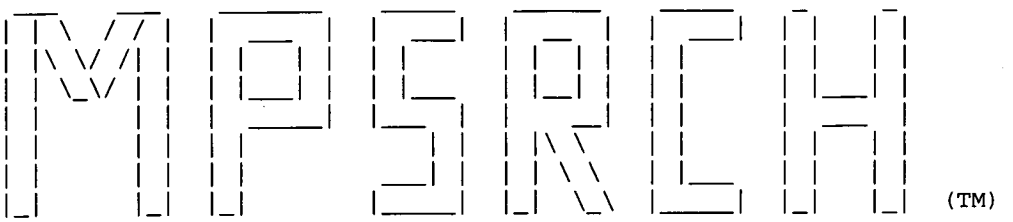


```
**************************************************************************

          Release 2.1D John F. Collins, Biocomputing Research Unit.
          Copyright (c) 1993, 1994, 1995  University of Edinburgh, U.K.
                  Distribution rights by IntelliGenetics, Inc.

MPsrch_pp   protein - protein database search, using Smith-Waterman
algorithm

NqrA

Title:          >NqrA
Description:    No description found
Perfect Score:  2118
Sequence:       1 MITIKKGLDLPIAGTPSQVI.........GKYEYGTLLRECLDTIEKEG 446

Scoring table:  PAM 250
                Gap 7

Searched:       540814 seqs, 168260508 residues

                                ALIGNMENTS

RESULT    1
>S51015(S51015)
NADH dehydrogenase (ubiquinone) (EC 1.6.5.3) alpha chain - Vibr

  DB  3;  Score    2118;  Match 100.0%;  QryMatch 100.0%;  Pred. No. 2.48e-
74;
  Matches   446;  Conservative    0;  Mismatches   0;  Indels   0;  Gaps
0;

          ************************************************************
Db      1 MITIKKGLDLPIAGTPSQVINDGKTIKKVALLGEEYVGMRPTMHVRVGDEVKKAQVLFED 60
Qy      1 MITIKKGLDLPIAGTPSQVINDGKTIKKVALLGEEYVGMRPTMHVRVGDEVKKAQVLFED 60

          ************************************************************
Db     61 KKNPGVKFTAPAAGKVIEVNRGAKRVLQSVVIEVAGEEQVTFDKFEAAQLSGLDREVIKT 120
Qy     61 KKNPGVKFTAPAAGKVIEVNRGAKRVLQSVVIEVAGEEQVTFDKFEAAQLSGLDREVIKT 120

          ************************************************************
Db    121 QLVDSGLWTALRTRPFSKVPAIESSTKAIFVTAMDTNPLAAKPELIINEQQEAFIAGLDI 180
Qy    121 QLVDSGLWTALRTRPFSKVPAIESSTKAIFVTAMDTNPLAAKPELIINEQQEAFIAGLDI 180

          ************************************************************
Db    181 LSALTEGKVYVCKSGTSLPRSSQSNVEEHVFDGPHPAGLAGTHMHFLYPVNAENVAWSIN 240
Qy    181 LSALTEGKVYVCKSGTSLPRSSQSNVEEHVFDGPHPAGLAGTHMHFLYPVNAENVAWSIN 240

          ************************************************************
Db    241 YQDVIAFGKLFLTGELYTDRVVSLAGPVVNNPRLVRTVIGASLDDLTDNELMPGEVRVIS 300
```

```
Qy    241 YQDVIAFGKLFLTGELYTDRVVSLAGPVVNNPRLVRTVIGASLDDLTDNELMPGEVRVIS 300

          ************************************************************
Db    301 GSVLTGTHATGPHAYLGRYHQQVSVLREGREKELFGWAMPGKNKFSVTRSFLGHVFKGQL 360
Qy    301 GSVLTGTHATGPHAYLGRYHQQVSVLREGREKELFGWAMPGKNKFSVTRSFLGHVFKGQL 360

          ************************************************************
Db    361 FNMTTTTNGSDRSMVPIGNYERVMPLDMEPTLLLRDLCAGDTDSAQALGALELDEEDLAL 420
Qy    361 FNMTTTTNGSDRSMVPIGNYERVMPLDMEPTLLLRDLCAGDTDSAQALGALELDEEDLAL 420

          **************************
Db    421 CTFVCPGKYEYGTLLRECLDTIEKEG 446
Qy    421 CTFVCPGKYEYGTLLRECLDTIEKEG 446



RESULT    3
>APU24492_1(U24492|gid:1185395)
Actinobacillus pleuropneumoniae 48 kDa outer me

  DB  6;  Score    1550;  Match 66.0%;  QryMatch 73.2%;  Pred. No. 5.52e-51;
  Matches   297;  Conservative   74;  Mismatches  74;  Indels   5;  Gaps
5;

          ****************.***..*.*.. **.**********.* ** ** ***.******
Db      1 MITIKKGLDLPIAGTPAQVIHNGNTVNEVAMLGEEYVGMRPSMKVREGDVVKKGQVLFED 60
Qy      1 MITIKKGLDLPIAGTPSQVINDGKTIKKVALLGEEYVGMRPTMHVRVGDEVKKAQVLFED 60

          ****** *****.* *. .*** ********* * *.**.** ..*****..*  * .*
Db     61 KKNPGVVFTAPASGTVVTINRGEKRVLQSVVIKVEGDEQITFTRYEAAQLASLSAEQVKQ 120
Qy     61 KKNPGVKFTAPAAGKVIEVNRGAKRVLQSVVIEVAGEEQVTFDKFEAAQLSGLDREVIKT 120

          .*..******.**********...   .*** ********* **....* .  *  ** .
Db    121 NLIESGLWTAFRTRPFSKVPALDAIPSSIFVNAMDTNPLAADPEVVLKEYETDFKDGLTV 180
Qy    121 QLVDSGLWTALRTRPFSKVPAIESSTKAIFVTAMDTNPLAAKPELIINEQQEAFIAGLDI 180

          *. * .* * **.** .....* *.  . .    * * ***** ***.**. ** * .
Db    181 LTRLFNGQKPVYLCKDADSNIPLSPAIEGITIKSFSGVHPAGLVGTHIHFVDPVGATKQV 240
Qy    181 LSALTEG-K-VYVCK-SGTSLPRSSQSN-VEEHVFDGPHPAGLAGTHMHFLYPVNAENVA 236

          * .*******.**** ****.***..***** *.******* .**.* .** *** .**
Db    241 WHLNYQDVIAIGKLFTTGELFTDRIISLAGPQVKNPRLVRTRLGANLSQLTANELNAGEN 300
Qy    237 WSINYQDVIAFGKLFLTGELYTDRVVSLAGPVVNNPRLVRTVIGASLDDLTDNELMPGEV 296

          ********.*. *.**  *****  ***** ********** *** .***.**. *** *
Db    301 RVISGSVLSGATAAGPVDYLGRYALQVSVLAEGREKELFGWIMPGSDKFSITRTVLGH-F 359
Qy    297 RVISGSVLTGTHATGPHAYLGRYHQQVSVLREGREKELFGWAMPGKNKFSVTRSFLGHVF 356

            .*** **. .*..*.***** ********. ******** ******** ** ******
Db    360 GKKLFNFTTAVHGGERAMVPIGAYERVMPLDIIPTLLLRDLAAGDTDSAQNLGCLELDEE 419
Qy    357 KGQLFNMTTTTNGSDRSMVPIGNYERVMPLDMEPTLLLRDLCAGDTDSAQALGALELDEE 416

          ******.***** .** .**  *. *****
Db    420 DLALCTYVCPGKNNYGPMLRAALEKIEKEG 449
Qy    417 DLALCTFVCPGKYEYGTLLRECLDTIEKEG 446



RESULT    5
>HIU32702_4(U32702|gid:1573122)
Haemophilus influenzae from bases 176044 to 189

  DB  6;  Score    1534;  Match 65.0%;  QryMatch 72.4%;  Pred. No. 2.49e-50;
```

```
  Matches   291;  Conservative   72;  Mismatches  82;  Indels   3;  Gaps
3;

          ************** *.***. *.....**.**********.* ** ** ***.******
Db       1 MITIKKGLDLPIAGKPAQVIHSGNAVNQVAILGEEYVGMRPSMKVREGDVVKKGQVLFED 60
Qy       1 MITIKKGLDLPIAGTPSQVINDGKTIKKVALLGEEYVGMRPTMHVRVGDEVKKAQVLFED 60

          ****** *****.* .  .*** *********.* *.*..** *. . **. *  * .*
Db      61 KKNPGVIFTAPASGTITAINRGEKRVLQSVVINVEGDEKITFAKYSTEQLNTLSSEQVKQ 120
Qy      61 KKNPGVKFTAPAAGKVIEVNRGAKRVLQSVVIEVAGEEQVTFDKFEAAQLSGLDREVIKT 120

          .*..****************.*** . .*** ********* * ....*  . *  ** .
Db     121 NLIESGLWTALRTRPFSKVPSIESEASSIFVNAMDTNPLAADPSVVLKEYSQDFTNGLTV 180
Qy     121 QLVDSGLWTALRTRPFSKVPAIESSTKAIFVTAMDTNPLAAKPELIINEQQEAFIAGLDI 180

          ** *  .* . .**.* * .* .   *.. * * * ***** ***.**. **  ..  *
Db     181 LSRLFPSKPLHLCKAGDSNIPTADLENLQIHDFTGVHPAGLVGTHIHFIDPVGIQKTVWH 240
Qy     181 LSALTEGK-VYVCKSGTS-LPRSSQSNVEEHVFDGPHPAGLAGTHMHFLYPVNAENVAWS 238

          ******** **** *****..**.***** *..****** ***.* .**.*** .*  **
Db     241 INYQDVIAVGKLFTTGELYSERVISLAGPQVKEPRLVRTTIGANLSQLTQNELSAGKNRV 300
Qy     239 INYQDVIAFGKLFLTGELYTDRVVSLAGPVVNNPRLVRTVIGASLDDLTDNELMPGEVRV 298

          ****** *  * ..* *****  ****. ** ***.*** **  **.****. *** *
Db     301 ISGSVLCGQIAKDSHDYLGRYALQVSVIAEGNEKEFFGWIMPQANKYSVTRTVLGH-FSK 359
Qy     299 ISGSVLTGTHATGPHAYLGRYHQQVSVLREGREKELFGWAMPGKNKFSVTRSFLGHVFKG 358

          .*** **. **..*.*****.********. ********  ****.** ** ********
Db     360 KLFNFTTSENGGERAMVPIGSYERVMPLDILPTLLLRDLIVGDTDGAQELGCLELDEEDL 419
Qy     359 QLFNMTTTTNGSDRSMVPIGNYERVMPLDMEPTLLLRDLCAGDTDSAQALGALELDEEDL 418

          ***.**********..**. ** *****
Db     420 ALCSFVCPGKYEYGSILRQVLDKIEKEG 447
Qy     419 ALCTFVCPGKYEYGTLLRECLDTIEKEG 446


RESULT   13
>RPOB_THEMA
(P29398) DNA-DIRECTED RNA POLYMERASE BETA CHAIN (EC 2.7.7.6) (TRANS

  DB  5;  Score     231;  Match 14.9%;  QryMatch 10.9%;  Pred. No. 1.38e+01;
  Matches    67;  Conservative  143;  Mismatches 214;  Indels  27;  Gaps
22;

          ** . . .**    *  * .   ***  . .*  *   ...   .*.   ..  .... .
Db     632 TPYRKVVNGKVTDEVVYLRANEEEEYKIIPATTPVDEEGNIIPERVV--ARMGEDIRLVP 689
Qy      15 TPSQVINDGKTIKKVALL-G---EEYVGMRPTMHVRVGDEVKKAQVLFEDKKNPGVKFTA 70

                ..*.      . . .*    ... .   . ....      ..**.  **..*.
Db     690 KEEVDFMDVSTKQPFSVSASLIPFLEHDDAS-RALMGSNMQRQAVPLLKTEAPLVGTGME 748
Qy      71 PAAGKVIEVNRGAKRVLQSVVIEVAGEEQVTFDKFEAAQLSGLDREVIKTQ--LVDSGL- 127

          * * .   .  ..  ..  * . . .  .   . .*. ... .. .   .*  .
Db     749 WEAAKNSGYVILAEHDGIVKEVDAARVVVHRTDENGNLMYDDKGNPVVDEYRLLKFVRSN 808
Qy     128 WTALRTRPFSKVPAIESSTKAIFVTAMDTNPLAAKPELIINEQQEAFIAGLDILSALTEG 187

          .  . .   .  .  .  . . *** .... * .. .   .    ..* . **.* *
Db     809 QDTMINQKPIVNEGDFVKKGDPIADGP-ATDM-G-ELALGRNILVAFMPWEGYNYEDAIL 865
Qy     188 KVYVCKSGTSLPRSSQSNVEEHVFDGPHPAGLAGTHMHFLYPVNAENVAW-SINYQDVIA 246

           .. .*  ...*   . .       . **    * * . ... . *.  .*  .*  *. .
Db     866 VSQELLEEDVFTSIHIEVYETQARETRLGPEEITADIPNVSKELLKNLDENGIIRVGAYV 925
Qy     247 FGKLFLTGELYTDRVVSLAGPVVNNPRLVRTVIGASLDDLTDNELMP-GEVRVIS-GSVL 304
```

```
            . . *..* * *.   . .     * .  . .** ..   *.  . . . .  *.*..
Db    926 VSDYGVGSQAILVGKVTPKGEGDTTPEEKIIRSVFGERGRDVKDTSLRLPHGVEGRVIRV 985
Qy    305 TGTHATGPHAYL-GRY-HQ-QVSVLREGRE-KELFG-WAMPGKNK-FSVTRSFLGHVFKG 358

            ....    .. .   .  .  *    . **.   *  *.   *   .  .   . * *
Db    986 DVYDQNDIAELGAGVLKLVRVYVASRKTLDIGDKLAGRHGNKGVVSNILPKEDMPFLPDG 1045
Qy    359 QLFNMTTTTNGSDRSMVPIGNY-ERVMPLDMEPTLLLRDLCAGDTDSAQALGALE-L-DE 415

               .. *   .  *.. . * .*   *. . *
Db   1046 TPVQMVLNPLGIPSRMNVGQILETHLGWLAK 1076
Qy    416 E--DLALCTFVCPGKYEYGTLLRECLDTIEK 444
```

NqrB

```
Title:           >NqrB
Description:     No description found
Perfect Score:   2237
Sequence:        1 MPRYYREGRVIFMALKKFLE.........LFDHVVIEKNIKRRLARYGK 426

Scoring table:   PAM 250
                 Gap 7

Searched:        540814 seqs, 168260508 residues
```

ALIGNMENTS

```
RESULT    1
>S51016(S51016)
NADH dehydrogenase (ubiquinone) (EC 1.6.5.3) nqrB protein - Vib

  DB  3;  Score    2237;  Match 100.0%;  QryMatch 100.0%;  Pred. No. 1.22e-
88;
  Matches   426;  Conservative    0;  Mismatches   0;  Indels   0;  Gaps
0;

            ************************************************************
Db      1 MPRYYREGRVIFMALKKFLEDIEHHFEPGGKHEKWFALYEAVATVFYTPGIVTNKSSHVR 60
Qy      1 MPRYYREGRVIFMALKKFLEDIEHHFEPGGKHEKWFALYEAVATVFYTPGIVTNKSSHVR 60

            ************************************************************
Db     61 DSVDLKRIMIMVWFAVFPAMFWGMYNAGGQAIAALNHMYAGDQLATVISGNWHYWLTEML 120
Qy     61 DSVDLKRIMIMVWFAVFPAMFWGMYNAGGQAIAALNHMYAGDQLATVISGNWHYWLTEML 120

            ************************************************************
Db    121 GGTIAADAGVGSKMLLGATYFLPIYATVFLVGGFWEVLFCMVRKHEVNEGFFVTSILFAL 180
Qy    121 GGTIAADAGVGSKMLLGATYFLPIYATVFLVGGFWEVLFCMVRKHEVNEGFFVTSILFAL 180

            ************************************************************
Db    181 IVPPTLPLWQAALGITFGVVVAKEIFGGTGRNFLNPALAGRAFLFFAYPAQISGDVVWTA 240
Qy    181 IVPPTLPLWQAALGITFGVVVAKEIFGGTGRNFLNPALAGRAFLFFAYPAQISGDVVWTA 240

            ************************************************************
Db    241 VDGFSGATALSQWAQGGNGALVNTVTGSPITWMDAFIGNIPGSIGEVSTLALMIGAAMIV 300
Qy    241 VDGFSGATALSQWAQGGNGALVNTVTGSPITWMDAFIGNIPGSIGEVSTLALMIGAAMIV 300

            ************************************************************
Db    301 YMRIASGRIIAGVMIGMIAVSTLFNVIGSDTNPMFNMPWHWHLVLGGFAFGMFFMATDPV 360
Qy    301 YMRIASGRIIAGVMIGMIAVSTLFNVIGSDTNPMFNMPWHWHLVLGGFAFGMFFMATDPV 360

            ************************************************************
```

```
Db    361 SASFTNKGKWWYGILIGAMCVMIRVVNPAYPEGMMLAILFANLFAPLFDHVVIEKNIKRR 420
Qy    361 SASFTNKGKWWYGILIGAMCVMIRVVNPAYPEGMMLAILFANLFAPLFDHVVIEKNIKRR 420

          ******
Db    421 LARYGK 426
Qy    421 LARYGK 426


RESULT    3
>HIU32702_5(U32702|gid:1573123)
Haemophilus influenzae from bases 176044 to 189

  DB  6;  Score    1594;  Match 71.0%;  QryMatch 71.3%;  Pred. No. 2.09e-59;
  Matches   292;  Conservative   67;  Mismatches  49;  Indels   3;  Gaps
2;

          *.**...* .*  * ****  * ....*.. *..**** **.*..****..* **.** *
Db      1 MGLKNLFEKMEPAFLPGGKYSKLYPIFESIYTLLYTPGTVTHKNTHVRDALDSKRMMITV 60
Qy     13 MALKKFLEDIEHHFEPGGKHEKWFALYEAVATVFYTPGIVTNKSSHVRDSVDLKRIMIMV 72

          ..*.***.*.**** * ***.***..  *. *  .*. .*** *.  **  ..*.*  **
Db     61 FLALFPAIFYGMYNVGNQAIPALNQL--GN-LDQLIANDWHYALASSLGLDLTANATWGS 117
Qy     73 WFAVFPAMFWGMYNAGGQAIAALNHMYAGDQLATVISGNWHYWLTEMLGGTIAADAGVGS 132

          ** *** .*****  ** *  .**.** .** ****** **..*****************
Db    118 KMALGAIFFLPIYLVVFTVCTIWELLFSVVRGHEVNEGMFVSTILFALIVPPTLPLWQAA 177
Qy    133 KMLLGATYFLPIYATVFLVGGFWEVLFCMVRKHEVNEGFFVTSILFALIVPPTLPLWQAA 192

          ******..******** ****.********************** **** ***********
Db    178 LGITFGIIVAKEIFGGVGRNFMNPALAGRAFLFFAYPAQISGDTVWTAADGFSGATALSQ 237
Qy    193 LGITFGVVVAKEIFGGTGRNFLNPALAGRAFLFFAYPAQISGDVVWTAVDGFSGATALSQ 252

          *.***.*** .****.********.**.***.*******..**.*.**. ***. *****
Db    238 WSQGGQGALQHTVTGAPITWMDAFVGNLPGSMGEVSTLAILIGGAVIVFTRIAAWRIIAG 297
Qy    253 WAQGGNGALVNTVTGSPITWMDAFIGNIPGSIGEVSTLALMIGAAMIVYMRIASGRIIAG 312

          ******* *****.***.*****.******.******.** ************* *****
Db    298 VMIGMIATSTLFNLIGSETNPMFSMPWHWHFVLGGFALGMVFMATDPVSASFTNTGKWWY 357
Qy    313 VMIGMIAVSTLFNVIGSDTNPMFNMPWHWHLVLGGFAFGMFFMATDPVSASFTNKGKWWY 372

          * *** * *.** **********************.** .*.. ***** **
Db    358 GALIGVMAVLIRTVNPAYPEGMMLAILFANLFAPIFDYIVVQANIKRRRAR 408
Qy    373 GILIGAMCVMIRVVNPAYPEGMMLAILFANLFAPLFDHVVIEKNIKRRLAR 423


RESULT    4
>C64052(C64052)
nitrogen fixation protein (rnfE) homolog - Haemophilus influenz

  DB  3;  Score    1594;  Match 71.0%;  QryMatch 71.3%;  Pred. No. 2.09e-59;
  Matches   292;  Conservative   67;  Mismatches  49;  Indels   3;  Gaps
2;

          *.**...* .*  * ****  * ....*.. *..**** **.*..****..* **.** *
Db      1 MGLKNLFEKMEPAFLPGGKYSKLYPIFESIYTLLYTPGTVTHKNTHVRDALDSKRMMITV 60
Qy     13 MALKKFLEDIEHHFEPGGKHEKWFALYEAVATVFYTPGIVTNKSSHVRDSVDLKRIMIMV 72

          ..*.***.*.**** * ***.***..  *. *  .*. .*** *.  **  ..*.*  **
Db     61 FLALFPAIFYGMYNVGNQAIPALNQL--GN-LDQLIANDWHYALASSLGLDLTANATWGS 117
Qy     73 WFAVFPAMFWGMYNAGGQAIAALNHMYAGDQLATVISGNWHYWLTEMLGGTIAADAGVGS 132

          ** *** .*****  ** *  .**.** .** ****** **..*****************
Db    118 KMALGAIFFLPIYLVVFTVCTIWELLFSVVRGHEVNEGMFVSTILFALIVPPTLPLWQAA 177
```

```
Qy    133 KMLLGATYFLPIYATVFLVGGFWEVLFCMVRKHEVNEGFFVTSILFALIVPPTLPLWQAA 192

          ******..******** ****.********************** **** ***********
Db    178 LGITFGIIVAKEIFGGVGRNFMNPALAGRAFLFFAYPAQISGDTVWTAADGFSGATALSQ 237
Qy    193 LGITFGVVVAKEIFGGTGRNFLNPALAGRAFLFFAYPAQISGDVVWTAVDGFSGATALSQ 252

          *.***.*** .****.********.**.***.*******..**.*.**. ***. *****
Db    238 WSQGGQGALQHTVTGAPITWMDAFVGNLPGSMGEVSTLAILIGGAVIVFTRIAAWRIIAG 297
Qy    253 WAQGGNGALVNTVTGSPITWMDAFIGNIPGSIGEVSTLALMIGAAMIVYMRIASGRIIAG 312

          ******* ******.***.******.******.******.** ************* *****
Db    298 VMIGMIATSTLFNLIGSETNPMFSMPWHWHFVLGGFALGMVFMATDPVSASFTNTGKWWY 357
Qy    313 VMIGMIAVSTLFNVIGSDTNPMFNMPWHWHLVLGGFAFGMFFMATDPVSASFTNKGKWWY 372

          * *** * *.** **********************.** .*.. ***** **
Db    358 GALIGVMAVLIRTVNPAYPEGMMLAILFANLFAPIFDYIVVQANIKRRRAR 408
Qy    373 GILIGAMCVMIRVVNPAYPEGMMLAILFANLFAPLFDHVVIEKNIKRRLAR 423


RESULT    5
>ECAE000258_10(AE000258|gid:1787917)
Escherichia coli from bases 1697303 to 171

  DB  6;  Score     267;  Match 27.9%;  QryMatch 11.9%;  Pred. No. 1.08e-01;
  Matches    93;  Conservative  101;  Mismatches 105;  Indels  34;  Gaps
24;

          **   .** .*..... ..*   .. *  .  . . . * *  ..**. *   .     .
Db     21 MLLVLLAAVPGIAAQLWFFGWGTLVQILLAS-VSALLAEALVLKLRKQSVAATLKDNSAL 79
Qy    119 MLGGTIAADAGVGSKM-LLGATYFLPIYATVFLVGGFWEVLFCMVRKHEVNEGF-----F 172

          .*..*.*. .**  * *   **  *.*..**...** *.* .***. *   *....* *.
Db     80 LTGLLLAVSIPPLAPWWMVVLGTVFAVIIAKQLYGGLGQNPFNPAMIGYVVLLISFPVQM 139
Qy    173 VTSILFALIVPPTLPLWQAALGITFGVVVAKEIFGGTGRNFLNPALAGRAFLFFAYPAQI 232

          ..    . .   . ** .*  .  * . * **.  .*   . * *  * .*.*  .. .*
Db    140 TSWLPPHEIAVNIPGFIDAIQVIFSGHTASGGDMNTLRLGIDGISQATPLDTFKTSVRAG 199
Qy    233 SG----DVVWTAVDGFSGATAL--S-QWAQGGN-GALVNTVTG-SPITWMDAFIGNI-PG 282

           *. ..    .  ... **.   * . ..*.* ...   ..   * .  . ** .  ..*
Db    200 HSVEQIMQYPIYSGILAGAGWQWVNLAWLAGGVWLLWQKAIRWHIPLSFLVTLALCAMLG 259
Qy    283 -SIGEV-S-TL--ALMIGAAMI-VYM-RIASG-RII-A-GVM--IGMIAVSTL-F-NVIG 328

             .*  .  * . **. *.  .* **. ****.** **.*.  .* * * .  .**
Db    260 WLFSPETLAAP-QIHLLSGATMLGAFFILTDPVTASTTNRGRLIFGALAGLLVWLIRSFG 318
Qy    329 SDTNP-MFNMPWHWHLVLGGFAFGMFFMATDPVSASFTNKGKWWYGILIGAMCVMIRVVN 387

           .**.*. .*.*.**.  **.*     .  .*
Db    319 -GYPDGVAFAVLLANITVPLIDYYTRPRVYGHR 350
Qy    388 PAYPEGMMLAILFANLFAPLFDHVVIEKNIKRR 420


RESULT    6
>RCRNFG_2(X72888|gid:435524)
R;capsulatus genes rnfA - rnfF, fdxC, fdxN, Orf14

  DB  6;  Score     234;  Match 26.5%;  QryMatch 10.5%;  Pred. No. 1.84e+00;
  Matches    82;  Conservative   81;  Mismatches 122;  Indels  24;  Gaps
21;

          **  ** .  *... ..   ** . . * *.  *.       * . **  . .. ** *.
Db      2 HMPVAGPHTHTLFTVSRTM-LTVVAAVTPATLFGL-WEFGWPAIFLFLTTVVSAWVFEVA 59
Qy     97 HM-YAGDQLATVISGNWHYWLTEMLGGTIAADAGVGSKMLLGATY-FLP-IYAT-VFLVG 152
```

```
          .  .    .*    . . .... * *. .**  * * . .*  ...*.**..*** *.*
Db     60 CL-KIAHKPIRPFPTDGSAILSGWLVAMTLPPYAPWWVGVIGSFIAIVIAKHLFGGLGQN 118
Qy    153 GFWEVLFCMVRKHEVNEGFFVTSILFALIVPPTLPLWQAALGITFGVVVAKEIFGGTGRN 212

          ..***. .** *  * * *..    * *  *. *. .. ..    . * .    *  **
Db    119 LFNPAMVARAMLVVALPVQMTT---WIAPVGLLEAS-ITLFGSHVPAQLAHQEQISRATW 174
Qy    213 FLNPALAGRAFLFFAYPAQISGDVVWTAVDGFSGATALSQWAQGGNGALVNTVTGSPITW 272

          . .. *   .  .*       *    *..   . ..   ***.  . .*... .*
Db    175 QILPSWRIWKAVFWASCPAAWRDLDRASGTGR-GF-WLLVTRIITPTIPLGLLGTLSRCR 232
Qy    273 --MDAF-I-GNIP-GSIGEV-STLALMIGAAMIVYMRIASGRIIAGVM-IGMIA-VSTLF 324

          ..  .   *  *   **  *.  .  **.*** *... *  *** *** **..  *.
Db    233 RSVSFLAPDPFAPP-ILHLTSGSTMLCAFFIATDYVTSPVTTAGKWVYGIGIGTLVFVIP 291
Qy    325 NVIGSDTNPMFNMPWHWHLVLGGFAFGMFFMATDPVSASFTNKGKWWYGILIGAMC-VM- 382

          .* .  *.*
Db    292 LRRLPRAWP 300
Qy    383 IRVVNPAYP 391
```

NqrC

```
Title:          >NqrC
Description:    No description found
Perfect Score:  1168
Sequence:       1 MASNNDSIKKTLGVVIGLSL.........WLGDKGFGPFLAKVRDGELN 256

Scoring table:  PAM 250
                Gap 7

Searched:       540814 seqs, 168260508 residues

                                ALIGNMENTS

RESULT    1
>S51017(S51017)
NADH dehydrogenase (ubiquinone) (EC 1.6.5.3) gamma2 chain - Vib

  DB  3;  Score    1168;  Match 100.0%;  QryMatch 100.0%;  Pred. No. 2.11e-
74;
  Matches   256;  Conservative    0;  Mismatches   0;  Indels   0;  Gaps
0;

          ************************************************************
Db      1 MASNNDSIKKTLGVVIGLSLVCSIIVSTAAVGLRDKQKANAVLDKQSKIVEVAGIDANGK 60
Qy      1 MASNNDSIKKTLGVVIGLSLVCSIIVSTAAVGLRDKQKANAVLDKQSKIVEVAGIDANGK 60

          ************************************************************
Db     61 KVPELFAEYIEPRLVDLETGNFTEGNASTYDQREASKDAERSIALTPEEDVADIRRRANT 120
Qy     61 KVPELFAEYIEPRLVDLETGNFTEGNASTYDQREASKDAERSIALTPEEDVADIRRRANT 120

          ************************************************************
Db    121 AVVYLVKDQDEVQKVILPMHGKGLWSMMYAFVAVETDGNTVSAITYYEQGETPGLGGEVE 180
Qy    121 AVVYLVKDQDEVQKVILPMHGKGLWSMMYAFVAVETDGNTVSAITYYEQGETPGLGGEVE 180

          ************************************************************
Db    181 NPSRRDQFIGKKLYNEDHQPAIKVVKGGAPQGSEHGVDGLSGATLTSNGVQHTFDFWLGD 240
Qy    181 NPSRRDQFIGKKLYNEDHQPAIKVVKGGAPQGSEHGVDGLSGATLTSNGVQHTFDFWLGD 240

          ****************
Db    241 KGFGPFLAKVRDGELN 256
```

```
Qy    241 KGFGPFLAKVRDGELN 256


RESULT    6
>Y167_HAEIN
(P43957) HYPOTHETICAL PROTEIN HI0167.

  DB  5;  Score     649;  Match 53.3%;  QryMatch 55.6%;  Pred. No. 1.78e-34;
  Matches   136;  Conservative   62;  Mismatches  42;  Indels  15;  Gaps
8;

          **  *.**.  *. **. *********. .** *.  *  . .**** .*..***.  .
Db      1 MAKFNKDSVGGTILVVLLLSLVCSIIVAGSAVMLKPAQEEQKLLDKQKNILNVAGLLQEN 60
Qy      1 MAS-NNDSIKKTLGVVIGLSLVCSIIVSTAAVGLRDKQKANAVLDKQSKIVEVAGIDANG 59

           .* * .* .****.*** **   *     * * .*  *....*.  .. * * ** *..
Db     61 TNVKETYAKFIEPRFVDLATG---E-----YTQ-QAD-DSQQAIP--ADADKARIRSRSK 108
Qy     60 KKVPELFAEYIEPRLVDLETGNFTEGNASTYDQREASKDAERSIALTPEEDVADIRRRAN 119

          *. ****** *.. *.****. * ****.**..*.*. ****...****..*********
Db    109 TTEVYLVKDEQGQTQQVILPIYGTGLWSVMYGLVSVQPDGNTINGITYYQHGETPGLGGE 168
Qy    120 TAVVYLVKD-QDEVQKVILPMHGKGLWSMMYAFVAVETDGNTVSAITYYEQGETPGLGGE 178

          .***..   * ****..*.*****..*** ***. **..*********.**** **..*.
Db    169 IENPNWASLFKGKKLFDEQHQPAIRIVKGQAPQD-EHSIDGLSGATLTGNGVQGTFNYWF 227
Qy    179 VENPSRRDQFIGKKLYNEDHQPAIKVVKGGAPQGSEHGVDGLSGATLTSNGVQHTFDFWL 238

          .  ****.* *.. *
Db    228 SKDGFGPYLEKLHSG 242
Qy    239 GDKGFGPFLAKVRDG 253


RESULT    9
>MJU67561_5
(U67561|gid:1591827 ) Methanococcus jannaschii from bases 1135955 t

  DB  4;  Score     137;  Match 20.5%;  QryMatch 11.7%;  Pred. No. 8.36e+01;
  Matches    53;  Conservative   73;  Mismatches 116;  Indels  17;  Gaps
15;

          **  .*     *.*.  *  ...  ..    **.*  . .  ...   .*   .**   .
Db    426 SIEDALKFGQKLPLIVLIDNGSTDEDIPAISKAKA-YGIEVIVIDHHFPGEVVDGKVEVD 484
Qy      7 SIKKTLGVVIGLSLVCSIIVSTAAVGLRDKQKANAVLDKQSKIVE--VAGIDANGKKVPE 64

           . .  ..* **.   .*.* *  .*   *  . * *  *   *   * . . ... *
Db    485 DYVDAHVNPYLVG-GDSNLTAGVLGTEIARMINPDVEDEIKHIPGIAVVGDHAKGEEAEQ 543
Qy     65 LFAE-YIEPRLVDLETGNFTEGNASTYDQREASKDAERSIALTPEEDVADIRRRANTAVV 123

          *.    * .. .   . ***  .   *   .*.  * ..  . . . .*   . *. ..
Db    544 YVKIALDRLNELS-KKYGKGRTYDREYLEKIALCMDFEAFY-LRFMDGKGIVDDILATNI 601
Qy    124 YLVKDQDEVQKVILPMHGKG-LWSMMY-AFVAVETDGNTVSAITYYE-QGETPG-LGGEV 179

           . .*....*.  **..  .   . .*.  *    . .. *.   **  .   * * *
Db    602 KEFGRHEELIDI-LYEQAMKMVERQMKAVIPALKTEFLENGIILNTLDVEKYAHKFTFPA 660
Qy    180 ENPSRRDQFIGKKLYNEDHQPAIKVVKGGAPQGSEHGVD-GLSGATLTSNGVQHTFDFWL 238

           .*  **.  .. . . **
Db    661 PGKTTGFAHDYIVQ-KYGE 678
Qy    239 GDK--GFGP-FLAKVRDGE 254
```

NqrD

Title: >NqrD
Description: No description found
Perfect Score: 999
Sequence: 1 MSSAQNVKKSILAPVLDNNP.....IGFLIWVIRILKPEQVEAKE 210

Scoring table: PAM 250
Gap 7

Searched: 540814 seqs, 168260508 residues

ALIGNMENTS

RESULT 1
>VANQRBOL_5(Z37111|gid:663273)
V;alginolyticus bolA, nqrA, nqrB, nqrC, nqrD and

DB 6; Score 999; Match 100.0%; QryMatch 100.0%; Pred. No. 2.51e-42;
Matches 210; Conservative 0; Mismatches 0; Indels 0; Gaps 0;

```
          ************************************************************
Db       1 MSSAQNVKKSILAPVLDNNPIALQVLGVCSALAVTTKLETAFVMTLAVTFVTALSNFSVS 60
Qy       1 MSSAQNVKKSILAPVLDNNPIALQVLGVCSALAVTTKLETAFVMTLAVTFVTALSNFSVS 60

          ************************************************************
Db      61 LIRNHIPNSVRIIVQMAIIASLVIVVDQVLKAYLYDISKQLSVFVGLIITNCIVMGRAEA 120
Qy      61 LIRNHIPNSVRIIVQMAIIASLVIVVDQVLKAYLYDISKQLSVFVGLIITNCIVMGRAEA 120

          ************************************************************
Db     121 FAMKSAPVPSLIDGIGNGLGYGFVLITVGFFRELFGSGKLFGLEVLPLVSNGGWYQPNGL 180
Qy     121 FAMKSAPVPSLIDGIGNGLGYGFVLITVGFFRELFGSGKLFGLEVLPLVSNGGWYQPNGL 180

          ******************************
Db     181 MLLAPSAFFLIGFLIWVIRILKPEQVEAKE 210
Qy     181 MLLAPSAFFLIGFLIWVIRILKPEQVEAKE 210
```

RESULT 4
>HIU32702_7(U32702|gid:1573125)
Haemophilus influenzae from bases 176044 to 18

DB 3; Score 787; Match 74.9%; QryMatch 78.8%; Pred. No. 1.04e-30;
Matches 155; Conservative 30; Mismatches 22; Indels 0; Gaps 0;

```
          **.  . *  .***.  *******.**.****************..***.**.***. **
Db       1 MSGKTSYKDLLLAPIAKNNPIALQILGICSALAVTTKLETAFVMAIAVTLVTGLSNLFVS 60
Qy       1 MSSAQNVKKSILAPVLDNNPIALQVLGVCSALAVTTKLETAFVMTLAVTFVTALSNFSVS 60

          **** ****.*****.************.**** *..************************
Db      61 LIRNYIPNSIRIIVQLAIIASLVIVVDQILKAYAYGLSKQLSVFVGLIITNCIVMGRAEA 120
Qy      61 LIRNHIPNSVRIIVQMAIIASLVIVVDQVLKAYLYDISKQLSVFVGLIITNCIVMGRAEA 120

          *****.** *..********** .** *.*****.*******. ..  . ******.***
Db     121 FAMKSPPVESFVDGIGNGLGYGSMLIIVAFFRELIGSGKLFGMTIFETIQNGGWYQANGL 180
Qy     121 FAMKSAPVPSLIDGIGNGLGYGFVLITVGFFRELFGSGKLFGLEVLPLVSNGGWYQPNGL 180
```

```
           ********.***.** .*  **** *
Db    181 FLLAPSAFFIIGFVIWGLRTWKPEQQE 207
Qy    181 MLLAPSAFFLIGFLIWVIRILKPEQVE 207



RESULT    8
>D90806_11(D90806|gid:1742690)
E;coli genomic DNA, Kohara clone #315(36;6-36;9

  DB  6;  Score     364;  Match 36.0%;  QryMatch 36.4%;  Pred. No. 2.45e-08;
  Matches    68;  Conservative   60;  Mismatches  58;  Indels   3;  Gaps
2;

           ..*  *.  .  **.  .*.**.*. ****.    *. . ** *.* .*.*...* .*.
Db      3 EIKDVIVQGLWKNNSALVQLLGLCPLLAVTSTATNALGLGLATTLVLTLTNLTISTLRHW 62
Qy      6 NVKKSILAPVLDNNPIALQVLGVCSALAVTTKLETAFVMTLAVTFVTALSNFSVSLIRNH 65

            *  .** . . ****.*  *. ...** ... . *..*. **.*****.******* *
Db     63 TPAEIRIPIYVMIIASVVSAVQMLINAYAFGLYQSLGIFIPLIVTNCIVVGRAEAFAAKK 122
Qy     66 IPNSVRIIVQMAIIASLVIVVDQVLKAYLYDISKQLSVFVGLIITNCIVMGRAEAFAMKS 125

           .*  * .**.. *.*    .. .* .**..*.* **.    .*.  *.* .   . ..
Db    123 GPALSALDGFSIGMGATCAMFVLGSLREIIGNGTLFD-GADALL--GSWAKVLRVEIFHT 179
Qy    126 APVPSLIDGIGNGLGYGFVLITVGFFRELFGSGKLFGLEVLPLVSNGGWYQPNGLMLLAP 185

            . **.. *
Db    180 DSPFLLAML 188
Qy    186 SAFFLIGFL 194



RESULT   13
>RCRNFABCD_6(Y11913|gid:1905813)
R;capsulatus rnfA, rnfB, rnfC, rnfD, rnfG, rnf

  DB  6;  Score     360;  Match 38.8%;  QryMatch 36.0%;  Pred. No. 3.89e-08;
  Matches    80;  Conservative   59;  Mismatches  55;  Indels  12;  Gaps
8;

           *.* .. *.*..*..**.*     .. * ** * *  ***  .* .*. *.  .**   .
Db     15 DKNIVTGQMLALCPTLAITGTATNGLGMGLATTVVLILSNVVISALRKTIAPEIRIPAFI 74
Qy     17 DNNPIALQVLGVCSALAVTTKLETAFVMTLAVTFVTALSNFSVSLIRNHIPNSVRIIVQM 76

            ***..* ***  *.*.* *. * *..*..**.*** ..******* . . ..* .**.
Db     75 LIIAAIVTVVDLALNAWLHDLHKVLGLFIALIVTNCAILGRAEAFASRFGVLASALDGLM 134
Qy     77 AIIASLVIVVDQVLKAYLYDISKQLSVFVGLIITNCIVMGRAEAFAMKSAPVPSLIDGIG 136

           *.*. . *. ** .**..*** **.   * * .. ..   *  *.  * * *.*.*..*
Db    135 MGIGFTLALVVVGAIREILGSGTLFAQASLLLGPHFAFMELQIFPDYPGFLIMILPPGGF 194
Qy    137 NGLGYGFVLITVGFFRELFGSGKLFGLEVLPLVSNGGW--YQ--PN--G-L-MLLAPSAF 188

           ...*  * * ..*   **  . * *.
Db    195 LVVGGLFALKRIIDARKPTIEQEIKQ 220
Qy    189 FLIG--F-LIWVIRILKPE-QVEAKE 210


NqrE

MPsrch_pp -run  -query /usr2/e_mpsrch/m-todo/970816014833-11306.seq -output
/usr2/e_mpsrch/m-todo/970816014833-11306.lis -pams 250 -gap 0 -summary 20 -
align 20 -ANNO NO -mode E -rank SC
-dbase genpept:all  -dbase nrprotein:all  -dbase swiss-prot:all
```

```
Title:          >NqrE
Description:    No description found
Perfect Score:  963
Sequence:       1 MEHYISLLVKSISSKHALSF.........TFITVGLMALGFMSFSGVQL 193

Scoring table:  PAM 250
                Gap 7

Searched:       540814 seqs, 168260508 residues
```

ALIGNMENTS

```
RESULT    1
>VIBNQR36_3(D49364|gid:893415)
Vibrio alginolyticus nqr operon (nqr3,4,5,6 gene

  DB  1;  Score     910;  Match 100.0%;  QryMatch 100.0%;  Pred. No. 2.59e-
33;
  Matches   189;  Conservative    1;  Mismatches   0;  Indels   5;  Gaps
2;

          ************************************************************
Db        1 MEHYISLLVKAVFIENMALSFFLGMCTFLAVSKKVKTSFGLGVAVVVVLTIAVPVNNLVY 60
Qy        1 MEHYISLLVKAVFIENMALSFFLGMCTFLAVSKKVKTSFGLGVAVVVVLTIAVPVNNLVY 59

          ************************************************************
Db       61 NLVLRENALVEGVDLSFLNFITFIGVIAALVQILEMVLDRFFPPLYNALGIFLPLITVNC 120
Qy       60 NLVLRENALVEGVDLSFLNFITFIGVIAALVQILEMVLDRFFPPLYNALGIFLPLITVNC 115

          ************************************************************
Db      121 AIFGGVSFMVQRDYNFAESIVYGFGSGVGWMLAIVALAGIREKMKYSDVPPGLRGLGITF 180
Qy      116 AIFGGVSFMVQRDYNFAESIVYGFGSGVGWMLAIVALAGIREKMKYSDVPPGLRGLGITF 175

          ******************
Db      181 ITVGLMALGFMSFSGVQL 198
Qy      176 ITVGLMALGFMSFSGVQL 193



RESULT    3
>HIU32702_8(U32702|gid:1573126)
Haemophilus influenzae from bases 176044 to 189

  DB  6;  Score     826;  Match 79.8%;  QryMatch 85.8%;  Pred. No. 3.55e-29;
  Matches   158;  Conservative   23;  Mismatches  12;  Indels   5;  Gaps
2;

          *******.*****************************  .****.**  ** ******.*.*
Db        1 MEHYISLFVKAVFIENMALSFFLGMCTFLAVSKKVSPAFGLGIAVTFVLGIAVPVNQLIY 60
Qy        1 MEHYISLLVKAVFIENMALSFFLGMCTFLAVSKKVKTSFGLGVAVVVVLTIAVPVNNLVY 59

            **.****.******************.**********.* *.************.***
Db       61 ANVLKENALIEGVDLSFLNFITFIGVIAGLVQILEMVLDKFMPSLYNALGIFLPLIAVNC 120
Qy       60 NLVLRENALVEGVDLSFLNFITFIGVIAALVQILEMVLDRFFPPLYNALGIFLPLITVNC 115

          ****************.**********.***********. *****.*.*.**.******
Db      121 AIFGGVSFMVQRDYNFPESIVYGFGSGLGWMLAIVALAGLTEKMKYADIPAGLKGLGITF 180
Qy      116 AIFGGVSFMVQRDYNFAESIVYGFGSGVGWMLAIVALAGIREKMKYSDVPPGLRGLGITF 175

          *.*************.**
Db      181 ISVGLMALGFMSFSGIQL 198
Qy      176 ITVGLMALGFMSFSGVQL 193
```

```
RESULT   11
>HIU32788_1
(U32788|gid:1221834 ) Haemophilus influenzae modB, modC, nth genes

  DB  2;  Score     431;  Match 40.5%;  QryMatch 44.8%;  Pred. No. 3.37e-10;
  Matches    79;  Conservative   57;  Mismatches  51;  Indels   8;  Gaps
7;

          * *** *..  .. .*  *  ***.* *..****. *. *.*.* . ***.*     **
Db      1 MTHYILLIIGTALINNFVLVKFLGLCPFMGVSKKIETAVGMGLATMFVLTVASLCAYLVD 60
Qy      1 MEHYISLLVKAVFIENMALSFFLGMCTFLAVSKKVKTSFGLGVAVVVVLTIAVPVNNLVY 59

          . .*   .*     *  * **  *.*.  . .. ...  * **  ********* ***..
Db     61 HYILI--PLNATF-LRTLVFILVIAVVVQFTEMAINKTSPTLYRLLGIFLPLITTNCAVL 117
Qy     60 NLVLRENALVEGVDLSFLNFITFIGVIAALVQI-LDRFFPPLYNALGIFLPLITVNCAIF 118

          * *... *.   *..  *.*****...*. * .* .*..**..  .*.*. .** .*..*
Db    118 G-VALLNVNLAHNLTGXSVVYGFGASLGFSLVLVLFAALRERLVAADIPATFRGSSIALI 176
Qy    119 GGVSFM-VQRDYNFAE-SIVYGFGSGVGWMLAIVALAGIREKMKYSDVPPGLRGLGITFI 176

          * ***.*.**.*.*.
Db    177 TAGLMSLAFMGFTGL 191
Qy    177 TVGLMALGFMSFSGV 191


RESULT   12
>ECAE000258_7(AE000258|gid:1787914)
Escherichia coli from bases 1697303 to 1710

  DB  6;  Score     422;  Match 41.1%;  QryMatch 43.8%;  Pred. No. 8.81e-10;
  Matches    81;  Conservative   55;  Mismatches  53;  Indels   8;  Gaps
7;

          * .*. *.* ..  .*  *  ***.* *..****. *. *.*.*   *.*.*     *.
Db      1 MTDYLLLFVGTVLVNNFVLVKFLGLCPFMGVSKKLETAMGMGLATTFVMTLASICAWLID 60
Qy      1 MEHYISLLVKAVFIENMALSFFLGMCTFLAVSKKVKTSFGLGVAVVVVLTIAVPVNNLVY 59

            .*    *.    *  * **  *.*.  . ... *  .* **  ********* ***..
Db     61 TWILIPLNLI--Y-LRTLAFILVIAVVVQFTEMVVRKTSPVLYRLLGIFLPLITTNCAVL 117
Qy     60 NLVLRENALVEGVDLSFLNFITFIGVIAALVQILDRFFPP-LYNALGIFLPLITVNCAIF 118

          * *... .. . ** .* .***...**. * .* .*.***..  .***. .** .*..**
Db    118 G-VALLNINLGHNFLQSALYGFSAAVGFSLVMVLFAAIRERLAVADVPAPFRGNAIALIT 176
Qy    119 GGVSFM-VQRDYNFAESIVYGFGSGVGWMLAIVALAGIREKMKYSDVPPGLRGLGITFIT 177

           ***.*.**.*** *.*
Db    177 AGLMSLAFMGFSGLVKL 193
Qy    178 VGLMALGFMSFSG-VQL 193


RESULT   13
>RCAFDXC_2(D13625|gid:216929)
R;capsulatus genes for potential iron-sulfur prot

  DB  6;  Score     393;  Match 36.6%;  QryMatch 40.8%;  Pred. No. 1.91e-08;
  Matches    71;  Conservative   63;  Mismatches  53;  Indels   7;  Gaps
7;

          *....  **  .. ..  *  ***.* *..**.*  ...*.*.*   *.*.* .   **
Db      1 MQDFLLVLLSTALVNNVVLVKFLGLCPFMGVSRKTDAAIGMGLATTFVITVASAACWLVE 60
Qy      1 MEHYI-SLLVKSISSKHALSFFLGMCTFLAVSKKVKTSFGLGVAVVVVLTIAVPVNNLVY 59
```

```
           *.* * .*     * .*. *  *. *  ... .. .  * * .****.***** ***..
Db      61 ALIL-E-PLDLKF-LRILSMILVIAAIVQFIETVMRKVTPDLHKALGIYLPLITTNCAVL 117
Qy      60 NLVLRENALVEGVDLSFLNFITFIGVIAALVQ-ILDRFFPPLYNALGIFLPLITVNCAIF 118

           * ...* .* . ..* * . ***..**. * .* .**.**..    **... *  *.*..
Db     118 G-LPLMYIQGHLSLAMSTLSGFGASVGFTLVLVIFAGMRERLAQLSVPAAFAGTPIAFVS 176
Qy     119 GGVSFM-VQRDYNFAESIVYGFGSGVGWMLAIVALAGIREKMKYSDVPPGLRGLGITFIT 177

           **..*.**.*.*.
Db     177 AGLLGLAFMGFAGL 190
Qy     178 VGLMALGFMSFSGV 191


RESULT   14
>RCAFDXC_2(D13625|gid:216929)
R;capsulatus genes for potential iron-sulfur pro

  DB  2;  Score     393;  Match 36.6%;  QryMatch 40.8%;  Pred. No. 1.91e-08;
  Matches    71;  Conservative   63;  Mismatches  53;  Indels   7;  Gaps
7;

           *....  *.  .  .*  *  ***.* *..**.*  ...*.*.*   *.*.* .   **
Db       1 MQDFLLVLLSTALVNNVVLVKFLGLCPFMGVSRKTDAAIGMGLATTFVITVASAACWLVE 60
Qy       1 MEHYISLLVKAVFIENMALSFFLGMCTFLAVSKKVKTSFGLGVAVVVVLTIAVPVNNLVY 59

           *.* * .*     * .*. *  *. *  ... .. .  * * .****.***** ***..
Db      61 ALIL-E-PLDLKF-LRILSMILVIAAIVQFIETVMRKVTPDLHKALGIYLPLITTNCAVL 117
Qy      60 NLVLRENALVEGVDLSFLNFITFIGVIAALVQ-ILDRFFPPLYNALGIFLPLITVNCAIF 118

           * ...* .* . ..* * . ***..**. * .* .**.**..    **... *  *.*..
Db     118 G-LPLMYIQGHLSLAMSTLSGFGASVGFTLVLVIFAGMRERLAQLSVPAAFAGTPIAFVS 176
Qy     119 GGVSFM-VQRDYNFAESIVYGFGSGVGWMLAIVALAGIREKMKYSDVPPGLRGLGITFIT 177

           **..*.**.*.*.
Db     177 AGLLGLAFMGFAGL 190
Qy     178 VGLMALGFMSFSGV 191


RESULT   15
>RCRNFG_5(X72888|gid:435527)
R;capsulatus genes rnfA - rnfF, fdxC, fdxN, Orf14

  DB  6;  Score     393;  Match 36.6%;  QryMatch 40.8%;  Pred. No. 1.91e-08;
  Matches    71;  Conservative   63;  Mismatches  53;  Indels   7;  Gaps
7;

           *....  *.  .. .*  *  ***.* *..**.*  ...*.*.*   *.*.* .   **
Db       1 MQDFLLVLLSTALVNNVVLVKFLGLCPFMGVSRKTDAAIGMGLATTFVITVASAACWLVE 60
Qy       1 MEHYISLLVKAVFIENMALSFFLGMCTFLAVSKKVKTSFGLGVAVVVVLTIAVPVNNLVY 59


           *.* * .*     * .*. *  *. *  ... .. .  * * .****.***** ***..
Db      61 ALIL-E-PLDLKF-LRILSMILVIAAIVQFIETVMRKVTPDLHKALGIYLPLITTNCAVL 117
Qy      60 NLVLRENALVEGVDLSFLNFITFIGVIAALVQ-ILDRFFPPLYNALGIFLPLITVNCAIF 118

           * ...* .* . ..* * . ***..**. * .* .**.**..    **... *  *.*..
Db     118 G-LPLMYIQGHLSLAMSTLSGFGASVGFTLVLVIFAGMRERLAQLSVPAAFAGTPIAFVS 176
Qy     119 GGVSFM-VQRDYNFAESIVYGFGSGVGWMLAIVALAGIREKMKYSDVPPGLRGLGITFIT 177

           **..*.**.*.*.
Db     177 AGLLGLAFMGFAGL 190
Qy     178 VGLMALGFMSFSGV 191
```

NqrF (N-terminal)

Title: >NqrF
Description: No description found
Perfect Score: 1476
Sequence: 1 MDIILGVVMFTLIVLALVLV.....EHGIIMLNVRIATPPPNNPD 238

Scoring table: PAM 180
Gap 9

Searched: 540814 seqs, 168260508 residues

ALIGNMENTS

RESULT 1
>VIBNQR36_4(D49364|gid:893416)
Vibrio alginolyticus nqr operon (nqr3,4,5,6 gene

DB 2; Score 1476; Match 100.0%; QryMatch 100.0%; Pred. No. 2.44e-220;
Matches 238; Conservative 0; Mismatches 0; Indels 0; Gaps 0;

```
          ************************************************************
Db       1 MDIILGVVMFTLIVLALVLVILFAKSKLVPTGDITISVNDDPSLAIVTQPGGKLLSALAG 60
Qy       1 MDIILGVVMFTLIVLALVLVILFAKSKLVPTGDITISVNDDPSLAIVTQPGGKLLSALAG 60

          ************************************************************
Db      61 AGVFVSSACGGGGSCGQCRVKVKSGGGDILPTELDHITKGEAREGERLACQVAMKTDMDI 120
Qy      61 AGVFVSSACGGGGSCGQCRVKVKSGGGDILPTELDHITKGEAREGERLACQVAMKTDMDI 120

          ************************************************************
Db     121 ELPEEIFGVKKWECTVISNDNKATFIKELKLQIPDGESVPFRAGGYIQIEAPAHHVKYAD 180
Qy     121 ELPEEIFGVKKWECTVISNDNKATFIKELKLQIPDGESVPFRAGGYIQIEAPAHHVKYAD 180

          ************************************************************
Db     181 YDIPEEYREDWEKFNLFRYESKVNEETIRAYSMANYPEEHGIIMLNVRIATPPPNNPD 238
Qy     181 YDIPEEYREDWEKFNLFRYESKVNEETIRAYSMANYPEEHGIIMLNVRIATPPPNNPD 238
```

RESULT 3
>HIU32702_9(U32702|gid:1573127)
Haemophilus influenzae from bases 176044 to 189

DB 6; Score 1167; Match 75.0%; QryMatch 79.1%; Pred. No. 5.88e-168;
Matches 177; Conservative 28; Mismatches 31; Indels 0; Gaps 0;

```
          . **.  **.*** ** .********* .***** .****  **   .*****.***. *
Db       7 LALGIAAFTVIVLVLVAIILFAKSKLVDSGDITIDINDDPEKAITLPAGGKLLGALASKG 66
Qy       3 IILGVVMFTLIVLALVLVILFAKSKLVPTGDITISVNDDPSLAIVTQPGGKLLSALAGAG 62

          .*************** ****.***.****** **.* **.** ****** .* .*..**
Db      67 IFVSSACGGGGSCGQCIVKVKNGGGEILPTELSHINKREAKEGYRLACQVNVKGNMEVEL 126
Qy      63 VFVSSACGGGGSCGQCRVKVKSGGGDILPTELDHITKGEAREGERLACQVAMKTDMDIEL 122

          ***************************** **.** ************* .* *.* *.*
Db     127 PEEIFGVKKWECTVISNDNKATFIKELKLAIPEGEEVPFRAGGYIQIEAEPHVVNYKDFD 186
```

```
Qy    123 PEEIFGVKKWECTVISNDNKATFIKELKLQIPDGESVPFRAGGYIQIEAPAHHVKYADYD 182

          *****.***.*..* ** ***.*  *******.**** **************  **
Db    187 IPEEYHEDWDKYDLWRYVSKVDEHIIRAYSMASYPEEKGIIMLNVRIATPPPRQPD 242
Qy    183 IPEEYREDWEKFNLFRYESKVNEETIRAYSMANYPEEHGIIMLNVRIATPPPNNPD 238


RESULT    4
>D64052(D64052)
phenolhydroxylase component homolog - Haemophilus influenzae (s

  DB  2;  Score    1167;  Match 75.0%;  QryMatch 79.1%;  Pred. No. 5.88e-
168;
  Matches   177;  Conservative   28;  Mismatches  31;  Indels   0;  Gaps
0;

          . **.  **.*** ** .********* .***** .****  **   .*****.***. *
Db      7 LALGIAAFTVIVLVLVAIILFAKSKLVDSGDITIDINDDPEKAITLPAGGKLLGALASKG 66
Qy      3 IILGVVMFTLIVLALVLVILFAKSKLVPTGDITISVNDDPSLAIVTQPGGKLLSALAGAG 62

          .*************** ****.***.****** **.* **.** ****** .* .*..**
Db     67 IFVSSACGGGGSCGQCIVKVKNGGGEILPTELSHINKREAKEGYRLACQVNVKGNMEVEL 126
Qy     63 VFVSSACGGGGSCGQCRVKVKSGGGDILPTELDHITKGEAREGERLACQVAMKTDMDIEL 122

          **************************** **.** ************ .* *.* *.*
Db    127 PEEIFGVKKWECTVISNDNKATFIKELKLAIPEGEEVPFRAGGYIQIEAEPHVVNYKDFD 186
Qy    123 PEEIFGVKKWECTVISNDNKATFIKELKLQIPDGESVPFRAGGYIQIEAPAHHVKYADYD 182

          *****.***.*..* ** ***.*  *******.**** **************  **
Db    187 IPEEYHEDWDKYDLWRYVSKVDEHIIRAYSMASYPEEKGIIMLNVRIATPPPRQPD 242
Qy    183 IPEEYREDWEKFNLFRYESKVNEETIRAYSMANYPEEHGIIMLNVRIATPPPNNPD 238


RESULT    5
>TFU73041_4(U73041|gid:1657805)
Thiobacillus ferrooxidans plasmid pTF5, partial

  DB  4;  Score     173;  Match 25.7%;  QryMatch 11.7%;  Pred. No. 4.11e-08;
  Matches    45;  Conservative   50;  Mismatches  65;  Indels  15;  Gaps
13;

          ****   *   ...*   .  ****   ......* *  * .** *   * .*   .
Db      5 DITIHTRDKQQVSFVCSEAEDLLSAADRGSILLPSQCRKG-TCGACVATVTAGTYHLGEV 63
Qy     33 DITISVNDDPSLAIVTQPGGKLLSALAGAGVFVSSACGGGGSCGQCRVKVKSGGGDILPT 92

           .. .  *..** *. * *.   ..*. .* * . . * *  .  .*  *.     **
Db     64 SMEALPEKAQAR-GDVLLCRTYPRADLILEAPYDYNYIRFERIPEREAEVMDVTMVATGT 122
Qy     93 ELDHIT-KGEAREGERLACQVAMKTDMDIELP-E-E-I-FG-VKKWECTVISNDNKATFI 146

          . * *.. **  * .  * ** ...*. *.   . ..  ....   .*.  ...*
Db    123 RRLLLRLQPDEQGGAAEFEAGQFMEIQVPGSDARRPN-SLANN--TNWNGDLEFF 174
Qy    147 KELKLQI-PD--GESVPFRAGGYIQIEAPAHHVKYADYDIPEEYREDWE-KFNLF 197


RESULT    7
>D63341_5(D63341|gid:939837)
Pseudomonas putida TOL plasmid pWWO xyl upper oper

  DB  6;  Score     169;  Match 29.3%;  QryMatch 11.4%;  Pred. No. 1.38e-07;
  Matches    51;  Conservative   44;  Mismatches  63;  Indels  16;  Gaps
15;

          .* * * * **  . *.**  . .. .    *  .* ***  .  * .  *  * *** *
```

```
Db      4 FFKKISGLFVPPPESTVSVRGQ-GFQFKVPRGQTILESALHQGIAF-PHDCKVG-SCGTC 60
Qy     22 LFAK-SKL-VPTGDITISVNDDPSLAIVTQPGGKLL-SALAGAGVFVSSACGGGGSCGQC 78

           . *. **  . * .    ..    . * **.**   * *..*** . ..*  .   *  .
Db     61 KYKLISGRVNELTSSAMGLSGDLYQSGYRLGCQCIPKEDLEIEL-DTVLGQALVPIETSA 119
Qy     79 RVKVKSGGGDILPTELDHITKGEAREGERLACQVAMKTDMDIELPEEIFG--VKKWE-CT 135

           .**.... .  * *. . .** . ..* .* * ..* *    *. *. .  * .
Db    120 LISKQKRLAHDIVEMEV-VPDKQ-IAFYPGQYADVECAECSAVRSYS-FSAPPQ 170
Qy    136 VISNDNKATF-IKELKLQIPDGESVPFRAGGYIQIE-APAHHVK-YADYDIPEE 186


RESULT    8
>XYLA_PSEPU
(P21394) XYLENE MONOOXYGENASE ELECTRON TRANSFER COMPONENT (CONTAINS

  DB  5;  Score     169;  Match 29.3%;  QryMatch 11.4%;  Pred. No. 1.38e-07;
  Matches    51;  Conservative   44;  Mismatches  63;  Indels  16;  Gaps
15;

           .* * * * **  . *.**  . . .    *  .* ***  .  * .  *  * *** *
Db      4 FFKKISGLFVPPPESTVSVRGQ-GFQFKVPRGQTILESALHQGIAF-PHDCKVG-SCGTC 60
Qy     22 LFAK-SKL-VPTGDITISVNDDPSLAIVTQPGGKLL-SALAGAGVFVSSACGGGGSCGQC 78

           . *. **  . * .    ..    . * **.**   * *..*** . ..*  .   *  .
Db     61 KYKLISGRVNELTSSAMGLSGDLYQSGYRLGCQCIPKEDLEIEL-DTVLGQALVPIETSA 119
Qy     79 RVKVKSGGGDILPTELDHITKGEAREGERLACQVAMKTDMDIELPEEIFG--VKKWE-CT 135

           .**.... .  * *. . .** . ..* .* * ..* *    *. *. .  * .
Db    120 LISKQKRLAHDIVEMEV-VPDKQ-IAFYPGQYADVECAECSAVRSYS-FSAPPQ 170
Qy    136 VISNDNKATF-IKELKLQIPDGESVPFRAGGYIQIE-APAHHVK-YADYDIPEE 186


RESULT    9
>PSEXYLMA_2(M37480|gid:151651)
TOL plasmid of P;putida xylene monooxygenase (xy

  DB  6;  Score     169;  Match 29.3%;  QryMatch 11.4%;  Pred. No. 1.38e-07;
  Matches    51;  Conservative   44;  Mismatches  63;  Indels  16;  Gaps
15;

           .* * * * **  . *.**  . . .    *  .* ***  .  * .  *  * *** *
Db      4 FFKKISGLFVPPPESTVSVRGQ-GFQFKVPRGQTILESALHQGIAF-PHDCKVG-SCGTC 60
Qy     22 LFAK-SKL-VPTGDITISVNDDPSLAIVTQPGGKLL-SALAGAGVFVSSACGGGGSCGQC 78

           . *. **  . * .    ..    . * **.**   * *..*** . ..*  .   *  .
Db     61 KYKLISGRVNELTSSAMGLSGDLYQSGYRLGCQCIPKEDLEIEL-DTVLGQALVPIETSA 119
Qy     79 RVKVKSGGGDILPTELDHITKGEAREGERLACQVAMKTDMDIELPEEIFG--VKKWE-CT 135

           .**.... .  * *. . .** . ..* .* * ..* *    *. *. .  * .
Db    120 LISKQKRLAHDIVEMEV-VPDKQ-IAFYPGQYADVECAECSAVRSYS-FSAPPQ 170
Qy    136 VISNDNKATF-IKELKLQIPDGESVPFRAGGYIQIE-APAHHVK-YADYDIPEE 186


RESULT   10
>B37316(B37316)
xylene monooxygenase (EC 1.-.-.-) chain A - Pseudomonas putida

  DB  4;  Score     169;  Match 29.3%;  QryMatch 11.4%;  Pred. No. 1.38e-07;
  Matches    51;  Conservative   44;  Mismatches  63;  Indels  16;  Gaps
15;

           .* * * * **  . *.**  . . .    *  .* ***  .  * .  *  * *** *
Db      4 FFKKISGLFVPPPESTVSVRGQ-GFQFKVPRGQTILESALHQGIAF-PHDCKVG-SCGTC 60
```

```
Qy      22 LFAK-SKL-VPTGDITISVNDDPSLAIVTQPGGKLL-SALAGAGVFVSSACGGGGSCGQC 78

           . *. **  . * .    ..    . * **.**   * *..*** . ..*  .   *  .
Db      61 KYKLISGRVNELTSSAMGLSGDLYQSGYRLGCQCIPKEDLEIEL-DTVLGQALVPIETSA 119
Qy      79 RVKVKSGGGDILPTELDHITKGEAREGERLACQVAMKTDMDIELPEEIFG--VKKWE-CT 135

           .**.... .  * *. . .** . ..* .* * ..* *    *. *. .  * .
Db     120 LISKQKRLAHDIVEMEV-VPDKQ-IAFYPGQYADVECAECSAVRSYS-FSAPPQ 170
Qy     136 VISNDNKATF-IKELKLQIPDGESVPFRAGGYIQIE-APAHHVK-YADYDIPEE 186


RESULT   11
>PSETBMAF_6(L40033|gid:1008901)
Pseudomonas sp; toluene/benzene-2-monooxygenase

  DB  6;  Score     166;  Match 32.6%;  QryMatch 11.2%;  Pred. No. 3.41e-07;
  Matches    44;  Conservative   29;  Mismatches  50;  Indels  12;  Gaps
11;

           *.. *  ** *   .**... *** *  ** *.* * **  *  ... * .   . . **
Db      16 VAE-GQTLLDAALRSGVYIPHACGHG-LCGTCKVQVTSGEVDHGAANPLRRSWISSGEEG 73
Qy      47 VTQPGGKLLSALAGAGVFVSSACGGGGSCGQCRVKVKSGGGDILPTE-LDHITKGEAREG 105

             ***   *.     . *.. *.    *    * **   *. .  ** *.* . * ..
Db      74 KTLACCATALSDVCIEADVDDEPDARASFPCGLWWATVTRIDTLTPTIKGLRLKL-D-QP 131
Qy     106 ERLAC-QVAM-KT--DMDIE-LPEE-I-FGVKKWECTVISNDNKATFIKELKLQIPDGES 158

           . *.** *. .* *.
Db     132 IDFQAGQYVMVEIPG 146
Qy     159 VPFRAGGYIQIEAPA 173


RESULT   12
>PSETBMAF_6
(L40033|gid:1008901 ) Pseudomonas sp; toluene/benzene-2-monooxygena

  DB  1;  Score     166;  Match 32.6%;  QryMatch 11.2%;  Pred. No. 3.41e-07;
  Matches    44;  Conservative   29;  Mismatches  50;  Indels  12;  Gaps
11;

           *.. *  ** *   .**... *** *  ** *.* * **  *  ... * .   . . **
Db      16 VAE-GQTLLDAALRSGVYIPHACGHG-LCGTCKVQVTSGEVDHGAANPLRRSWISSGEEG 73
Qy      47 VTQPGGKLLSALAGAGVFVSSACGGGGSCGQCRVKVKSGGGDILPTE-LDHITKGEAREG 105

             ***   *.     . *.. *.    *    * **   *. .  ** *.* . * ..
Db      74 KTLACCATALSDVCIEADVDDEPDARASFPCGLWWATVTRIDTLTPTIKGLRLKL-D-QP 131
Qy     106 ERLAC-QVAM-KT--DMDIE-LPEE-I-FGVKKWECTVISNDNKATFIKELKLQIPDGES 158

           . *.** *. .* *.
Db     132 IDFQAGQYVMVEIPG 146
Qy     159 VPFRAGGYIQIEAPA 173


RESULT   13
>ACPHENOL_6(Z36909|gid:535285)
A;calcoaceticus genes for phenolhydroxylase com

  DB  2;  Score     163;  Match 28.6%;  QryMatch 11.0%;  Pred. No. 8.37e-07;
  Matches    42;  Conservative   33;  Mismatches  60;  Indels  12;  Gaps
9;

           ..  *. .*. .*.  .    .* *    ** .. *** * .** *.* *  *    *.
Db       1 MSYQVTIEPAGTIIQVEEDQTILDAALRQGVWLPFACGHG-TCGTCKVQVTDGFYDVGEA 59
Qy      34 ITISVNDDPSLAIV-TQPGGKLLSALAGAGVFVSSACGGGGSCGQCRVKVKSG--G-GDI 89
```

```
           *  *  *  . * .       *  .  *  . *..  *...*  *    .  **    . .
Db      60 SPFALMDIEREENKVLAC-CCKPESDMVIEADVDEDEDFLGYLVQDYQAKVIEITDLSPT 118
Qy      90 LPTELDHITKGEAREGERLAC--QVAMKTDMDIELPEEIFG--VKKWECTVISNDNKATF 145

           ** ..**. *  .. *.** ** *. *
Db     119 IKGVRLQL-D-RPMQFQAGQYINIQLP 143
Qy     146 IKELKLQIPDGESVPFRAGGYIQIEAP 172


RESULT   14
>ACPHENOL_6(Z36909|gid:535285)
A;calcoaceticus genes for phenolhydroxylase comp

  DB  6;  Score     163;  Match 28.6%;  QryMatch 11.0%;  Pred. No. 8.37e-07;
  Matches    42;  Conservative   33;  Mismatches  60;  Indels  12;  Gaps
9;

           ..  *. .*. .*.  .    .* *    ** .. *** * .** *.* *  *    *.
Db      1 MSYQVTIEPAGTIIQVEEDQTILDAALRQGVWLPFACGHG-TCGTCKVQVTDGFYDVGEA 59
Qy     34 ITISVNDDPSLAIV-TQPGGKLLSALAGAGVFVSSACGGGGSCGQCRVKVKSG--G-GDI 89

           *  *  *  . * .       *  .  *  . *..  *...*  *    .  **    . .
Db     60 SPFALMDIEREENKVLAC-CCKPESDMVIEADVDEDEDFLGYLVQDYQAKVIEITDLSPT 118
Qy     90 LPTELDHITKGEAREGERLAC--QVAMKTDMDIELPEEIFG--VKKWECTVISNDNKATF 145

           ** ..**. *  .. *.** ** *. *
Db    119 IKGVRLQL-D-RPMQFQAGQYINIQLP 143
Qy    146 IKELKLQIPDGESVPFRAGGYIQIEAP 172


NqrF (C-terminal)

Title:           >NqrF
Description:     No description found
Perfect Score:   2633
Sequence:        1 MDIILGVVMFTLIVLALVLV.........GMLKDLGVEDENILLDDFGG 407

Scoring table:   PAM 180
                 Gap 9

Searched:        540814 seqs, 168260508 residues

                              ALIGNMENTS

RESULT    1
>VIBNQR36_4(D49364|gid:893416)
Vibrio alginolyticus nqr operon (nqr3,4,5,6 gene

  DB  2;  Score    2633;  Match 100.0%;  QryMatch 100.0%;  Pred. No.
0.00e+00;
  Matches   407;  Conservative    0;  Mismatches   0;  Indels   0;  Gaps
0;

           ************************************************************
Db      1 MDIILGVVMFTLIVLALVLVILFAKSKLVPTGDITISVNDDPSLAIVTQPGGKLLSALAG 60
Qy      1 MDIILGVVMFTLIVLALVLVILFAKSKLVPTGDITISVNDDPSLAIVTQPGGKLLSALAG 60

           ************************************************************
Db     61 AGVFVSSACGGGGSCGQCRVKVKSGGGDILPTELDHITKGEAREGERLACQVAMKTDMDI 120
Qy     61 AGVFVSSACGGGGSCGQCRVKVKSGGGDILPTELDHITKGEAREGERLACQVAMKTDMDI 120

           ************************************************************
```

```
Db    121 ELPEEIFGVKKWECTVISNDNKATFIKELKLQIPDGESVPFRAGGYIQIEAPAHHVKYAD 180
Qy    121 ELPEEIFGVKKWECTVISNDNKATFIKELKLQIPDGESVPFRAGGYIQIEAPAHHVKYAD 180

          ************************************************************
Db    181 YDIPEEYREDWEKFNLFRYESKVNEETIRAYSMANYPEEHGIIMLNVRIATPPPNNPDVP 240
Qy    181 YDIPEEYREDWEKFNLFRYESKVNEETIRAYSMANYPEEHGIIMLNVRIATPPPNNPDVP 240

          ************************************************************
Db    241 PGIMSSYIWSLKEGDKCTISGPFGEFFAKDTDAEMVFVGGGAGMAPMRSHIFDQLKRLHS 300
Qy    241 PGIMSSYIWSLKEGDKCTISGPFGEFFAKDTDAEMVFVGGGAGMAPMRSHIFDQLKRLHS 300

          ************************************************************
Db    301 KRKMSFWYGARSKREMFYVEDFDMLQAENDNFVWHCALSDPLPEDNWDGYTGFIHNVLYE 360
Qy    301 KRKMSFWYGARSKREMFYVEDFDMLQAENDNFVWHCALSDPLPEDNWDGYTGFIHNVLYE 360

          ************************************************
Db    361 NYLRDHEAPEDCEYYMCGPPMMNAAVIGMLKDLGVEDENILLDDFGG 407
Qy    361 NYLRDHEAPEDCEYYMCGPPMMNAAVIGMLKDLGVEDENILLDDFGG 407



RESULT    3
>HIU32702_9(U32702|gid:1573127)
Haemophilus influenzae from bases 176044 to 189

  DB  6;  Score    2202;  Match 81.2%;  QryMatch 83.6%;  Pred. No. 0.00e+00;
  Matches   329;  Conservative   35;  Mismatches  41;  Indels   0;  Gaps
0;

          . **.  **.*** ** .********* .***** .****  **   .*****.***. *
Db      7 LALGIAAFTVIVLVLVAIILFAKSKLVDSGDITIDINDDPEKAITLPAGGKLLGALASKG 66
Qy      3 IILGVVMFTLIVLALVLVILFAKSKLVPTGDITISVNDDPSLAIVTQPGGKLLSALAGAG 62

          .*************** ****.***.****** **.* **.** ****** .* .*..**
Db     67 IFVSSACGGGGSCGQCIVKVKNGGGEILPTELSHINKREAKEGYRLACQVNVKGNMEVEL 126
Qy     63 VFVSSACGGGGSCGQCRVKVKSGGGDILPTELDHITKGEAREGERLACQVAMKTDMDIEL 122

          ***************************** **.** ************* .* *.* *.*
Db    127 PEEIFGVKKWECTVISNDNKATFIKELKLAIPEGEEVPFRAGGYIQIEAEPHVVNYKDFD 186
Qy    123 PEEIFGVKKWECTVISNDNKATFIKELKLQIPDGESVPFRAGGYIQIEAPAHHVKYADYD 182

          *****.***.*..* ** ***.*  *******.**** **************  ** ***
Db    187 IPEEYHEDWDKYDLWRYVSKVDEHIIRAYSMASYPEEKGIIMLNVRIATPPPRQPDAPPG 246
Qy    183 IPEEYREDWEKFNLFRYESKVNEETIRAYSMANYPEEHGIIMLNVRIATPPPNNPDVPPG 242

           ********* *** ************.*******.************************
Db    247 QMSSYIWSLKAGDKVTISGPFGEFFAKETDAEMVFIGGGAGMAPMRSHIFDQLKRLHSKR 306
Qy    243 IMSSYIWSLKEGDKCTISGPFGEFFAKDTDAEMVFVGGGAGMAPMRSHIFDQLKRLHSKR 302

          *************.** **** ***** ***** ****.****** **************
Db    307 KMSFWYGARSKREIFYQEDFDQLQAENPNFVWHVALSDALPEDNWTGYTGFIHNVLYENY 366
Qy    303 KMSFWYGARSKREMFYVEDFDMLQAENDNFVWHCALSDPLPEDNWDGYTGFIHNVLYENY 362

          *..***************.****** ********************
Db    367 LKNHEAPEDCEYYMCGPPVMNAAVIKMLKDLGVEDENILLDDFGG 411
Qy    363 LRDHEAPEDCEYYMCGPPMMNAAVIGMLKDLGVEDENILLDDFGG 407



RESULT    4
>D64052(D64052)
phenolhydroxylase component homolog - Haemophilus influenzae (s

  DB  2;  Score    2202;  Match 81.2%;  QryMatch 83.6%;  Pred. No. 0.00e+00;
```

```
  Matches   329;  Conservative   35;  Mismatches  41;  Indels   0;  Gaps
0;

          . **.  **.*** ** .********* .***** .****  **   .*****.***. *
Db       7 LALGIAAFTVIVLVLVAIILFAKSKLVDSGDITIDINDDPEKAITLPAGGKLLGALASKG 66
Qy       3 IILGVVMFTLIVLALVLVILFAKSKLVPTGDITISVNDDPSLAIVTQPGGKLLSALAGAG 62

          .*************** ****.***.****** **.* **.** ****** .* .*..**
Db      67 IFVSSACGGGGSCGQCIVKVKNGGGEILPTELSHINKREAKEGYRLACQVNVKGNMEVEL 126
Qy      63 VFVSSACGGGGSCGQCRVKVKSGGGDILPTELDHITKGEAREGERLACQVAMKTDMDIEL 122

          ***************************** **.** ************ .* *.* *.*
Db     127 PEEIFGVKKWECTVISNDNKATFIKELKLAIPEGEEVPFRAGGYIQIEAEPHVVNYKDFD 186
Qy     123 PEEIFGVKKWECTVISNDNKATFIKELKLQIPDGESVPFRAGGYIQIEAPAHHVKYADYD 182

          *****.***.*..* ** ***.*  *******.**** **************  ** ***
Db     187 IPEEYHEDWDKYDLWRYVSKVDEHIIRAYSMASYPEEKGIIMLNVRIATPPPRQPDAPPG 246
Qy     183 IPEEYREDWEKFNLFRYESKVNEETIRAYSMANYPEEHGIIMLNVRIATPPPNNPDVPPG 242

           ********* *** ************.*******.************************
Db     247 QMSSYIWSLKAGDKVTISGPFGEFFAKETDAEMVFIGGGAGMAPMRSHIFDQLKRLHSKR 306
Qy     243 IMSSYIWSLKEGDKCTISGPFGEFFAKDTDAEMVFVGGGAGMAPMRSHIFDQLKRLHSKR 302

          *************.** **** ***** ***** **** .****** **************
Db     307 KMSFWYGARSKREIFYQEDFDQLQAENPNFVWHVALSDALPEDNWTGYTGFIHNVLYENY 366
Qy     303 KMSFWYGARSKREMFYVEDFDMLQAENDNFVWHCALSDPLPEDNWDGYTGFIHNVLYENY 362

          *..***************.****** ******************
Db     367 LKNHEAPEDCEYYMCGPPVMNAAVIKMLKDLGVEDENILLDDFGG 411
Qy     363 LRDHEAPEDCEYYMCGPPMMNAAVIGMLKDLGVEDENILLDDFGG 407


RESULT    5
>PPPHH_6(X79063|gid:483483)
P;putida genes for phenolhydroxylase and ferredoxi

  DB  4;  Score     340;  Match 32.0%;  QryMatch 12.9%;  Pred. No. 7.29e-32;
  Matches    54;  Conservative   52;  Mismatches  57;  Indels   6;  Gaps
6;

          *  *  .*.* . ** **   .***.*.** .*..* ...*..**.*... .* *** .
Db     170 VEGGAATSFIHRQLKVGDAVELSGPYGQFFVRDSQAGDLIFIAGGSGLSSPQSMIFDLFE 229
Qy     239 VPPGIMSSYI-WSLKEGDKCTISGPFGEFFAKDTDA-EMVFVGGGAGMAPMRSHIFDQLK 296

          *  . * ...  ***.. *..  * *. * * . **    **...  . .*.*. **.*.
Db     230 RGDT-RQITLFQGARNRAELYNRELFEELAARHSNFSYVPALNQAHDDPEWQGFKGFVHD 288
Qy     297 RLHSKRKMSFWYGARSKREMFYVEDFDMLQAENDNFVWHCALSDPLPEDNWDGYTGFIHN 356

              ..   . .     * .**** *  * *  *..  . . .*... *
Db     289 AAKAHF-DGRFSGHK-AY-LCGPPPMIDAAITTLMQGRLFERDIFMERF 334
Qy     357 VLYENYLRDHEAPEDCEYYMCGPPMMNAAVIGMLKDLGVEDENILLDDF 405


RESULT    6
>PPPHH_6(X79063|gid:483483)
P;putida genes for phenolhydroxylase and ferredoxin

  DB  6;  Score     340;  Match 32.0%;  QryMatch 12.9%;  Pred. No. 7.29e-32;
  Matches    54;  Conservative   52;  Mismatches  57;  Indels   6;  Gaps
6;

          *  *  .*.* . ** **   .***.*.** .*..* ...*..**.*... .* *** .
Db     170 VEGGAATSFIHRQLKVGDAVELSGPYGQFFVRDSQAGDLIFIAGGSGLSSPQSMIFDLFE 229
Qy     239 VPPGIMSSYI-WSLKEGDKCTISGPFGEFFAKDTDA-EMVFVGGGAGMAPMRSHIFDQLK 296
```

```
          *  . * ...  ***.. *..  * *. * * . **    **...  . .*.*. **.*.
Db    230 RGDT-RQITLFQGARNRAELYNRELFEELAARHSNFSYVPALNQAHDDPEWQGFKGFVHD 288
Qy    297 RLHSKRKMSFWYGARSKREMFYVEDFDMLQAENDNFVWHCALSDPLPEDNWDGYTGFIHN 356

              ..   . .     * .**** *  * *  *..  . . .*... *
Db    289 AAKAHF-DGRFSGHK-AY-LCGPPPMIDAAITTLMQGRLFERDIFMERF 334
Qy    357 VLYENYLRDHEAPEDCEYYMCGPPMMNAAVIGMLKDLGVEDENILLDDF 405


RESULT    7
>ACPHENOL_6(Z36909|gid:535285)
A;calcoaceticus genes for phenolhydroxylase com

  DB  2;  Score     337;  Match 32.4%;  QryMatch 12.8%;  Pred. No. 2.12e-31;
  Matches    55;  Conservative   47;  Mismatches  60;  Indels   8;  Gaps
7;

          *  *  . *.   *  *.  ..***.*.** . .* . ..*..**.*.....* *.* *
Db    170 VQGGAATRYVHDELSVGEEMALSGPYGQFFVRKSDQQNVIFIAGGSGLSSLQSMILDLLE 229
Qy    239 VPPGIMSSYIWS-LKEGDKCTISGPFGEFFAKDTDAE-MVFVGGGAGMAPMRSHIFDQLK 296

            *.  . . . . ***   *..  * *. *  *  **    **. * *** * *.**..*
Db    230 --HGDTRIIYLFQGARDVAELYNREKFEQLVKEYPNFRYIPALNAPKPEDQWTGFTGYVH 287
Qy    297 RLHSKRKMSFWY-GARSKREMFYVEDFDMLQAENDNFVWHCALSDPLPEDNWDGYTGFIH 355

          . .  **. ..  .     *.**** *  * *. *..  . . .*  . *
Db    288 EAV-ANYF-ENKCSGH-KAYLCGPPPMIDAAISTLMQSRLFEKDIHTERF 334
Qy    356 NVLYENYLRDHEAPEDCEYYMCGPPMMNAAVIGMLKDLGVEDENILLDDF 405


RESULT    8
>ACPHENOL_6(Z36909|gid:535285)
A;calcoaceticus genes for phenolhydroxylase comp

  DB  6;  Score     337;  Match 32.4%;  QryMatch 12.8%;  Pred. No. 2.12e-31;
  Matches    55;  Conservative   47;  Mismatches  60;  Indels   8;  Gaps
7;

          *  *  . *.   *  *.  ..***.*.** . .* . ..*..**.*.....* *.* *
Db    170 VQGGAATRYVHDELSVGEEMALSGPYGQFFVRKSDQQNVIFIAGGSGLSSLQSMILDLLE 229
Qy    239 VPPGIMSSYIWS-LKEGDKCTISGPFGEFFAKDTDAE-MVFVGGGAGMAPMRSHIFDQLK 296

            *.  . . . . ***   *..  * *. *  *  **    **. * *** * *.**..*
Db    230 --HGDTRIIYLFQGARDVAELYNREKFEQLVKEYPNFRYIPALNAPKPEDQWTGFTGYVH 287
Qy    297 RLHSKRKMSFWY-GARSKREMFYVEDFDMLQAENDNFVWHCALSDPLPEDNWDGYTGFIH 355

          . .  **. ..  .     *.**** *  * *. *..  . . .*  . *
Db    288 EAV-ANYF-ENKCSGH-KAYLCGPPPMIDAAISTLMQSRLFEKDIHTERF 334
Qy    356 NVLYENYLRDHEAPEDCEYYMCGPPMMNAAVIGMLKDLGVEDENILLDDF 405


RESULT    9
>DMPP_PSEPU
(P19734) PHENOL HYDROXYLASE P5 PROTEIN (EC 1.14.13.7) (PHENOL 2-MON

  DB  1;  Score     333;  Match 31.4%;  QryMatch 12.6%;  Pred. No. 8.77e-31;
  Matches    53;  Conservative   54;  Mismatches  56;  Indels   6;  Gaps
6;

          *  *  ...*  ' ** **   .***.*.** .*..* ...*..**.*... .* *.* *
Db    169 VEGGAATGFIHKQLKVGDAVELSGPYGQFFVRDSQAGDLIFIAGGSGLSSPQSMILDLLE 228
Qy    239 VPPGIMSSYIWS-LKEGDKCTISGPFGEFFAKDTDA-EMVFVGGGAGMAPMRSHIFDQLK 296
```

```
          *  ..* ...  ***.. *..  * *. * * . **    **...  . .*.*. **.*.
Db     229 RGDTRR-ITLFQGARNRAELYNCELFEELAARHPNFSYVPALNQANDDPEWQGFKGFVHD 287
Qy     297 RLHSKRKMSFWYGARSKREMFYVEDFDMLQAENDNFVWHCALSDPLPEDNWDGYTGFIHN 356

              ..   . . .   * .**** *  * *  *..  . . .*... *
Db     288 AAKAHF-DGRFGGQK-AY-LCGPPPMIDAAITTLMQGRLFERDIFMERF 333
Qy     357 VLYENYLRDHEAPEDCEYYMCGPPMMNAAVIGMLKDLGVEDENILLDDF 405


RESULT   10
>PSEPHHYD_6(M60276|gid:151455)
Pseudomonas putida phenol hydroxylase (dmpKLMNOP

  DB  6;  Score     333;  Match 31.4%;  QryMatch 12.6%;  Pred. No. 8.77e-31;
  Matches    53;  Conservative   54;  Mismatches  56;  Indels   6;  Gaps
6;

          *  *  ...*   ** **   .***.*.** .*..* ...*..**.*... .* *.* *
Db     170 VEGGAATGFIHKQLKVGDAVELSGPYGQFFVRDSQAGDLIFIAGGSGLSSPQSMILDLLE 229
Qy     239 VPPGIMSSYIWS-LKEGDKCTISGPFGEFFAKDTDA-EMVFVGGGAGMAPMRSHIFDQLK 296

          *  ..* ...  ***.. *..  * *. * * . **    **...  . .*.*. **.*.
Db     230 RGDTRR-ITLFQGARNRAELYNCELFEELAARHPNFSYVPALNQANDDPEWQGFKGFVHD 288
Qy     297 RLHSKRKMSFWYGARSKREMFYVEDFDMLQAENDNFVWHCALSDPLPEDNWDGYTGFIHN 356

              ..   . . .   * .**** *  * *  *..  . . .*... *
Db     289 AAKAHF-DGRFGGQK-AY-LCGPPPMIDAAITTLMQGRLFERDIFMERF 334
Qy     357 VLYENYLRDHEAPEDCEYYMCGPPMMNAAVIGMLKDLGVEDENILLDDF 405


RESULT   11
>F37831(F37831)
phenol 2-monooxygenase (EC 1.14.13.7) chain P5 - Pseudomonas sp

  DB  1;  Score     333;  Match 31.4%;  QryMatch 12.6%;  Pred. No. 8.77e-31;
  Matches    53;  Conservative   54;  Mismatches  56;  Indels   6;  Gaps
6;

          *  *  ...*   ** **   .***.*.** .*..* ...*..**.*... .* *.* *
Db     170 VEGGAATGFIHKQLKVGDAVELSGPYGQFFVRDSQAGDLIFIAGGSGLSSPQSMILDLLE 229
Qy     239 VPPGIMSSYIWS-LKEGDKCTISGPFGEFFAKDTDA-EMVFVGGGAGMAPMRSHIFDQLK 296

          *  ..* ...  ***.. *..  * *. * * . **    **...  . .*.*. **.*.
Db     230 RGDTRR-ITLFQGARNRAELYNCELFEELAARHPNFSYVPALNQANDDPEWQGFKGFVHD 288
Qy     297 RLHSKRKMSFWYGARSKREMFYVEDFDMLQAENDNFVWHCALSDPLPEDNWDGYTGFIHN 356

              ..   . . .   * .**** *  * *  *..  . . .*... *
Db     289 AAKAHF-DGRFGGQK-AY-LCGPPPMIDAAITTLMQGRLFERDIFMERF 334
Qy     357 VLYENYLRDHEAPEDCEYYMCGPPMMNAAVIGMLKDLGVEDENILLDDF 405


RESULT   12
>DMPP_PSEPU
(P19734) PHENOL HYDROXYLASE P5 PROTEIN (EC 1.14.13.7) (PHENOL 2-MON

  DB  5;  Score     333;  Match 31.4%;  QryMatch 12.6%;  Pred. No. 8.77e-31;
  Matches    53;  Conservative   54;  Mismatches  56;  Indels   6;  Gaps
6;

          *  *  ...*   ** **   .***.*.** .*..* ...*..**.*... .* *.* *
Db     169 VEGGAATGFIHKQLKVGDAVELSGPYGQFFVRDSQAGDLIFIAGGSGLSSPQSMILDLLE 228
Qy     239 VPPGIMSSYIWS-LKEGDKCTISGPFGEFFAKDTDA-EMVFVGGGAGMAPMRSHIFDQLK 296

          *  ..* ...  ***.. *..  * *. * * . **    **...  . .*.*. **.*.
```

```
Db    229 RGDTRR-ITLFQGARNRAELYNCELFEELAARHPNFSYVPALNQANDDPEWQGFKGFVHD 287
Qy    297 RLHSKRKMSFWYGARSKREMFYVEDFDMLQAENDNFVWHCALSDPLPEDNWDGYTGFIHN 356

              ..   . . .   * .**** *  * *  *..  . . .*... *
Db    288 AAKAHF-DGRFGGQK-AY-LCGPPPMIDAAITTLMQGRLFERDIFMERF 333
Qy    357 VLYENYLRDHEAPEDCEYYMCGPPMMNAAVIGMLKDLGVEDENILLDDF 405


RESULT   13
>PSEPHEAA_6(D28864|gid:468471)
Pseudomonas putida phe[A1, A2, A3, A4, A5, A6] g

  DB  6;  Score     331;  Match 30.8%;  QryMatch 12.6%;  Pred. No. 1.78e-30;
  Matches    52;  Conservative   55;  Mismatches  56;  Indels   6;  Gaps
6;

          *  *  ...*   ** **   .***.*.** .*..* ...*..**.*... .* *.. *
Db    170 VEGGAATGFIHKQLKVGDAVELSGPYGQFFVRDSQAGDLIFIAGGSGLSSPQSMILNLLE 229
Qy    239 VPPGIMSSYIWS-LKEGDKCTISGPFGEFFAKDTDA-EMVFVGGGAGMAPMRSHIFDQLK 296

          *  ..* ...  ***.. *..  * *. * * . **    **...  . .*.*. **.*.
Db    230 RGDTRR-ITLFQGARNRAELYNCELFEELAARHPNFSYVPALNQANDDPEWQGFKGFVHD 288
Qy    297 RLHSKRKMSFWYGARSKREMFYVEDFDMLQAENDNFVWHCALSDPLPEDNWDGYTGFIHN 356

              ..   . . .   * .**** *  * *  *..  . . .*... *
Db    289 AAKAHF-DGRFGGQK-AY-LCGPPPMIDAAITTLMQGRLFERDIFMERF 334
Qy    357 VLYENYLRDHEAPEDCEYYMCGPPMMNAAVIGMLKDLGVEDENILLDDF 405


RESULT   14
>PSEPHEAA_6
(D28864|gid:468471 ) Pseudomonas putida phe[A1, A2, A3, A4, A5, A6]

  DB  3;  Score     331;  Match 30.8%;  QryMatch 12.6%;  Pred. No. 1.78e-30;
  Matches    52;  Conservative   55;  Mismatches  56;  Indels   6;  Gaps
6;

          *  *  ...*   ** **   .***.*.** .*..* ...*..**.*... .* *.. *
Db    170 VEGGAATGFIHKQLKVGDAVELSGPYGQFFVRDSQAGDLIFIAGGSGLSSPQSMILNLLE 229
Qy    239 VPPGIMSSYIWS-LKEGDKCTISGPFGEFFAKDTDA-EMVFVGGGAGMAPMRSHIFDQLK 296

          *  ..* ...  ***.. *..  * *. * * . **    **...  . .*.*. **.*.
Db    230 RGDTRR-ITLFQGARNRAELYNCELFEELAARHPNFSYVPALNQANDDPEWQGFKGFVHD 288
Qy    297 RLHSKRKMSFWYGARSKREMFYVEDFDMLQAENDNFVWHCALSDPLPEDNWDGYTGFIHN 356

              ..   . . .   * .**** *  * *  *..  . . .*... *
Db    289 AAKAHF-DGRFGGQK-AY-LCGPPPMIDAAITTLMQGRLFERDIFMERF 334
Qy    357 VLYENYLRDHEAPEDCEYYMCGPPMMNAAVIGMLKDLGVEDENILLDDF 405


RESULT   15
>PPPHEHYD_6(X80765|gid:527552)
P;putida genes for phenolhydroxylase; Subunit of

  DB  6;  Score     329;  Match 30.2%;  QryMatch 12.5%;  Pred. No. 3.62e-30;
  Matches    51;  Conservative   54;  Mismatches  58;  Indels   6;  Gaps
6;

          *  *  ...* . ** **   .***.*.** . ..* ...*..**.*... .* .** *
Db    170 VEGGAATGFIHRQLKVGDAVELSGPYGQFFVRGSQAGDLIFIAGGSGLSSPQSMVFDLLA 229
Qy    239 VPPGIMSSYI-WSLKEGDKCTISGPFGEFFAKDTDA-EMVFVGGGAGMAPMRSHIFDQLK 296

          .  . * ...  ***.. *..  * *. * * . **    **...  . .*.*. **.*.
Db    230 QGDT-RQITLFQGARNRAELYNRELFEELAARHSNFSYVPALNQAHDDPEWQGFKGFVHD 288
```

```
Qy     297 RLHSKRKMSFWYGARSKREMFYVEDFDMLQAENDNFVWHCALSDPLPEDNWDGYTGFIHN 356

                ..    . .      * .**** *  * *  *..  . . .*... *
Db     289 AAKAHF-DGRFSGHK-AY-LCGPPPMIDAAITTLMQGRLFERDIFMERF 334
Qy     357 VLYENYLRDHEAPEDCEYYMCGPPMMNAAVIGMLKDLGVEDENILLDDF 405


RESULT   16
>PPPHEHYD_6(X80765|gid:527552)
P;putida genes for phenolhydroxylase; Subunit of

  DB  2;  Score     329;  Match 30.2%;  QryMatch 12.5%;  Pred. No. 3.62e-30;
  Matches    51;  Conservative   54;  Mismatches  58;  Indels   6;  Gaps
6;

            *  *  ...* . ** **   .***.*.** . ..* ...*..**.*... .* .** *
Db     170 VEGGAATGFIHRQLKVGDAVELSGPYGQFFVRGSQAGDLIFIAGGSGLSSPQSMVFDLLA 229
Qy     239 VPPGIMSSYI-WSLKEGDKCTISGPFGEFFAKDTDA-EMVFVGGGAGMAPMRSHIFDQLK 296

            .  . * ...  ***.. *..  * *. * * . **    **...  . .*.*. **.*.
Db     230 QGDT-RQITLFQGARNRAELYNRELFEELAARHSNFSYVPALNQAHDDPEWQGFKGFVHD 288
Qy     297 RLHSKRKMSFWYGARSKREMFYVEDFDMLQAENDNFVWHCALSDPLPEDNWDGYTGFIHN 356

                ..    . .      * .**** *  * *  *..  . . .*... *
Db     289 AAKAHF-DGRFSGHK-AY-LCGPPPMIDAAITTLMQGRLFERDIFMERF 334
Qy     357 VLYENYLRDHEAPEDCEYYMCGPPMMNAAVIGMLKDLGVEDENILLDDF 405


RESULT   17
>XYLA_PSEPU
(P21394) XYLENE MONOOXYGENASE ELECTRON TRANSFER COMPONENT (CONTAINS

  DB  5;  Score     287;  Match 28.2%;  QryMatch 10.9%;  Pred. No. 8.81e-24;
  Matches    48;  Conservative   52;  Mismatches  60;  Indels  10;  Gaps
9;

            ** *. *. . .  . *   *. .*.*.*   ...* ** *.**.*.**..  ... . .
Db     182 VPGGVFSGWLFGGDRTGATLTLRAPYGQFGLHESNATMVCVAGGTGLAPIKC-VLQSMTQ 240
Qy     239 VPPGIMSSYIWSL-KEGDKCTISGPFGEFFAKDTDAEMVFVGGGAGMAPMRSHIFDQLKR 297

             .  * . . .***  *... ..... ** .    *     **.  .  .* *  * . .
Db     241 AQRERDVLLFFGARQQRDLYCLDEIEALQLDWGGRFELIPVLSEESSTSSWKGKRGMVTE 300
Qy     298 LHSKRKMSFWYGARSKREMFYVEDFDMLQAE-NDNFVWHCALSDPLPEDNWDGYTGFIHN 356

             . .**  .  * .  * .**** *..**   ... ***  * .. * *
Db     301 -YFKEYLTGQ--PYE-GY-LCGPPPMVDAAETELVR-LGVARELVFADRF 344
Qy     357 VLYENYLRDHEAPEDCEYYMCGPP-MMNAAVIGMLKDLGVEDENILLDDF 405


RESULT   18
>D63341_5(D63341|gid:939837)
Pseudomonas putida TOL plasmid pWWO xyl upper oper

  DB  6;  Score     287;  Match 28.2%;  QryMatch 10.9%;  Pred. No. 8.81e-24;
  Matches    48;  Conservative   52;  Mismatches  60;  Indels  10;  Gaps
9;

            ** *. *. . .  . *   *. .*.*.*   ...* ** *.**.*.**..  ... . .
Db     182 VPGGVFSGWLFGGDRTGATLTLRAPYGQFGLHESNATMVCVAGGTGLAPIKC-VLQSMTQ 240
Qy     239 VPPGIMSSYIWSL-KEGDKCTISGPFGEFFAKDTDAEMVFVGGGAGMAPMRSHIFDQLKR 297

             .  * . . .***  *... ..... ** .    *     **.  .  .* *  * . .
Db     241 AQRERDVLLFFGARQQRDLYCLDEIEALQLDWGGRFELIPVLSEESSTSSWKGKRGMVTE 300
Qy     298 LHSKRKMSFWYGARSKREMFYVEDFDMLQAE-NDNFVWHCALSDPLPEDNWDGYTGFIHN 356
```

```
            . .**  .  * .  * .**** *..**   ... ***  * .. * *
Db    301 -YFKEYLTGQ--PYE-GY-LCGPPPMVDAAETELVR-LGVARELVFADRF 344
Qy    357 VLYENYLRDHEAPEDCEYYMCGPP-MMNAAVIGMLKDLGVEDENILLDDF 405


RESULT   19
>PSEXYLMA_2(M37480|gid:151651)
TOL plasmid of P;putida xylene monooxygenase (xy

  DB  6;  Score     287;  Match 28.2%;  QryMatch 10.9%;  Pred. No. 8.81e-24;
  Matches    48;  Conservative   52;  Mismatches  60;  Indels  10;  Gaps
9;

          ** *. *. . .  . *   *. .*.*.*   ...* ** *.**.*.**..  ... . .
Db    182 VPGGVFSGWLFGGDRTGATLTLRAPYGQFGLHESNATMVCVAGGTGLAPIKC-VLQSMTQ 240
Qy    239 VPPGIMSSYIWSL-KEGDKCTISGPFGEFFAKDTDAEMVFVGGGAGMAPMRSHIFDQLKR 297

            .  * . . .***  *... ..... ** .    *     **.  .  .* *  * . .
Db    241 AQRERDVLLFFGARQQRDLYCLDEIEALQLDWGGRFELIPVLSEESSTSSWKGKRGMVTE 300
Qy    298 LHSKRKMSFWYGARSKREMFYVEDFDMLQAE-NDNFVWHCALSDPLPEDNWDGYTGFIHN 356

            . .**  .  * .  * .**** *..**   ... ***  * .. * *
Db    301 -YFKEYLTGQ--PYE-GY-LCGPPPMVDAAETELVR-LGVARELVFADRF 344
Qy    357 VLYENYLRDHEAPEDCEYYMCGPP-MMNAAVIGMLKDLGVEDENILLDDF 405


RESULT   20
>B37316(B37316)
xylene monooxygenase (EC 1.-.-.-) chain A - Pseudomonas putida

  DB  4;  Score     287;  Match 28.2%;  QryMatch 10.9%;  Pred. No. 8.81e-24;
  Matches    48;  Conservative   52;  Mismatches  60;  Indels  10;  Gaps
9;

          ** *. *. . .  . *   *. .*.*.*   ...* ** *.**.*.**..  ... . .
Db    182 VPGGVFSGWLFGGDRTGATLTLRAPYGQFGLHESNATMVCVAGGTGLAPIKC-VLQSMTQ 240
Qy    239 VPPGIMSSYIWSL-KEGDKCTISGPFGEFFAKDTDAEMVFVGGGAGMAPMRSHIFDQLKR 297

            .  * . . .***  *... ..... ** .    *     **.  .  .* *  * . .
Db    241 AQRERDVLLFFGARQQRDLYCLDEIEALQLDWGGRFELIPVLSEESSTSSWKGKRGMVTE 300
Qy    298 LHSKRKMSFWYGARSKREMFYVEDFDMLQAE-NDNFVWHCALSDPLPEDNWDGYTGFIHN 356

            . .**  .  * .  * .**** *..**   ... ***  * .. * *
Db    301 -YFKEYLTGQ--PYE-GY-LCGPPPMVDAAETELVR-LGVARELVFADRF 344
Qy    357 VLYENYLRDHEAPEDCEYYMCGPP-MMNAAVIGMLKDLGVEDENILLDDF 405
```

FEBS Letters 356 (1994) 333–338

FEBS 14888

Cloning and sequencing of four structural genes for the Na^+-translocating NADH–ubiquinone oxidoreductase of *Vibrio alginolyticus*

P. Beattie[a], K. Tan[a], R.M. Bourne[b], D. Leach[a], P.R. Rich[b], F.B. Ward[a,*]

[a]*Institute for Cell and Molecular Biology, Darwin Building, Edinburgh University, Mayfield Rd, Edinburgh EH9 3JR, UK*
[b]*Glynn Research Institute, Bodmin, PL30 4AU, UK*

Received 26 October 1994

Abstract Oligonucleotide probes based on the N-terminal amino acid sequences of the NqrA and NqrC subunits were used to clone genes for the Na^+-dependent NADH–ubiquinone oxidoreductase complex from *Vibrio alginolyticus*. Four consecutive ORFs were identified encoding subunit proteins of 48.6, 46.8, 27.7 and 22.6 kDa, respectively (NqrA–D). A further ORF, showing 71% homology to the BolA protein of *Escherichia coli*, was located upstream. From sequence comparisons, we conclude that the Na^+-dependent NADH–ubiquinone oxidoreductase complex of *V. alginolyticus* is clearly distinct from the corresponding H^+-dependent enzymes of both prokaryotes and eukaryotes.

Key words: Cloning; Nucleotide sequence; NADH–ubiquinone oxidoreductase; *Vibrio alginolyticus*

1. Introduction

NADH–ubiquinone oxidoreductase (complex I) transfers electrons from NADH to ubiquinone and links this to proton translocation across the mitochondrial inner membrane. Complex I from eukaryotes has been extensively studied in *Bos taurus* and *Neurospora crassa*; the *B. taurus* complex I is thought to comprise 41 subunits and can be biochemically split into three fractions: FP (flavoprotein), IP (iron-sulphur protein) and HP (hydrophobic protein-ND subunits) [1]. The FP fraction contains a catalytic 51 kDa subunit containing NADH- and FMN-binding sites, a 24 kDa [2Fe-2S] subunit and a 10 kDa subunit. Seven of the genes are mitochondrially encoded and are highly hydrophobic; one subunit, ND1, contains a ubiquinone-binding site while another, ND2, is reactive towards both rotenone and DCCD [1]. Recently, gene clusters coding for proton-translocating NADH–ubiquinone oxidoreductases have been identified in two prokaryotes: *Paracoccus denitrificans* and *Escherichia coli* [2,3].

By contrast, the marine bacterium *Vibrio alginolyticus* has been shown to produce an electrochemical Na^+ gradient in aerobic respiration as the result of a sodium-translocating NADH–ubiquinone oxidoreductase, which is induced at alkaline pH [4–7]. The resulting sodium motive force is used to drive ATP synthesis, flagellar rotation and solute transport [1,8,9]. This alternative to H^+ coupling in membrane reactions enables bacteria to maintain a cytoplasmic pH near to neutrality in an alkaline environment. The Na^+-dependent NADH–ubiquinone oxidoreductase complex is distinct from a Na^+-independent NADH–ubiquinone oxidoreductase also found in *V. alginolyticus*, in that Na^+-dependent NADH–ubiquinone oxidoreductase is sensitive to inhibition by silver ions and by 2-*n*-heptyl-4-hydroxyquinoline *N*-oxide (HQNO), can generate a membrane potential, reduces quinone using a one-electron pathway (rather than a two-electron pathway), and can utilize the NADH analogue deaminoNADH[10–13]. Early biochemical studies indicated that the purified Na^+-dependent NADH–ubiquinone oxidoreductase complex is composed of three subunits: α, β and γ, with apparent M_r of 52, 46 and 32 kDa, respectively [14]. The FAD-binding β-subunit demonstrates NADH dehydrogenase activity, accepting electrons from NADH and reducing hydrophilic quinones, such as menadione, by a one-electron transfer reaction to produce semiquinones. This reaction is independent of Na^+. However, the reduction of hydrophobic quinones, such as ubiquinone, is Na^+-dependent and is catalyzed by the FMN-containing α-subunit in the presence of the β-subunit [10,14,15]. The γ subunit was proposed to increase the affinity of the β-subunit for quinones and to assist in the electron transfer reaction from β to α [16]. As part of a programme to study the structure and function of the sodium pump complex in *V. alginolyticus*, we have cloned and sequenced four genes of the Na^+-dependent NADH-ubiquinone oxidoreductase complex and the results are presented in this communication.

2. Materials and methods

2.1. Protein purification and N-terminal sequencing

Cells of *V. alginolyticus* were grown at 30°C in a medium of 5 g/l peptone, 5 g/l yeast extract, 39 g/l NaCl and 5 g/l dipotassium hydrogen orthophosphate. The initial pH of the medium was adjusted to 8.5 with Tris base. The culture was aerated with 95% O_2/5% CO_2 and pH was maintained above 8.2 with NaOH. Cells were harvested in late-log phase and washed in 20 mM Tris-HCl, 1 M NaCl, pH 8.0. Cells were lysed by osmotic shock in 40 mM Tris-HCl, 5 mM EDTA at pH 8.0, treated with RNase and DNase, pelleted by centrifugation at $18{,}000 \times g_{av}$ and stored frozen in 20 mM Tris-HCl, 10 mM NaCl, 10% (v/v) glycerol, pH 8.0.

Membranes were prewashed with 0.1% Synperonic PE/F68 detergent and the Na^+-dependent NADH–ubiquinone oxidoreductase solubilized with 1% (w/v) lauryl maltoside in 20 mM Tris-HCl, 10 mM NaCl, 5% (v/v) glycerol, pH 8.0. Insoluble material was removed by centrifugation at $70{,}000 \times g_{av}$ for 60 min. The supernatant was applied to a column of DEAE Sepharose CL6B and eluted in 0.5% (w/v) lauryl maltoside, 300 mM NaCl, 20 mM Tris-HCl, pH 8.0, and then further purified by preparative gel electrophoresis (BioRad 491 Prep Cell) using a 4% (w/v) acrylamide gel containing 1% (w/v) agarose in a gel buffer

*Corresponding author. Fax: (44) (31) 668 3870.
E-mail: bward@srv0.bio.ed.ac.uk

Abbreviations: ORF, open reading frame; PAGE, polyacrylamide gel electrophoresis; complex I, H^+-translocating NADH–ubiquinone oxidoreductase complex.

The sequence has the EMBL nucleotide sequence database accession number Z37111.

SSDI 0014-5793(94)01275-X

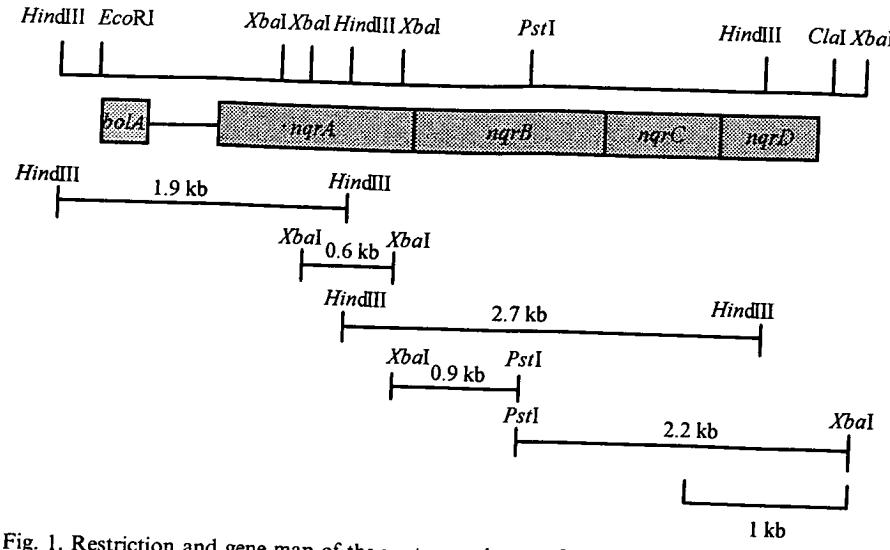

Fig. 1. Restriction and gene map of the upstream cluster of *nqr* genes in *Vibrio alginolyticus*.

of 0.1% (w/v) lauryl maltoside, 1 M Tris-HCl, pH 8.8. The elution buffer was 0.1% (w/v) lauryl maltoside, 20 mM Tris-HCl, 10 mM NaCl, 5% (v/v) glycerol, pH 8.0. Individual polypeptides were separated on 10% SDS-PAGE gels using appropriate molecular weight markers and electroblotted onto PVDF membranes using the method of Matsudaira [17]. Proteins were stained with Amido black and the excised bands analyzed for N-terminal sequence on an Applied Biosystems Analyser (WELMET). Activity of NADH dehydrogenase was detected on native gels using deaminoNADH and Nitrotetrazolium blue.

2.2. Construction and screening of a genomic DNA library

Genomic DNA was purified from *V. alginolyticus* NCIMB 11038 by standard methods, restricted with *Eco*RI and used to construct a library in the λ vector NM1149 [18]. Oligonucleotide probes were made by OSWEL (University of Edinburgh). These were probe 1, 5′-GATG-AT(CT)AC(ACGT)AT(CT)AA(AG)AA(AG)GG-3′ (degeneracy 64, based on MITIKKG of the α-subunit); probe 2, 5′-CA(AG)AA (AG)GA(AG)GA(AG)AC(AGCT)AA-3′ (degeneracy 32, based on QKEETK of the γ1-subunit); probe 3, 5′-CC(AGT)CA(AG)GC-(AGT)GA(AG)CA(AG)GT-3′ (degeneracy 72, based on PQAEQV of the γ1-subunit); probe 4, 5′-AA(CT)AA(CT)GA(CT)TC(AGT)AT (ACT)GG-3′ (degeneracy 72, based on NNDSIG of the γ2-subunit); and probe 5, 5′-AA(CT)AA(CT)GA(CT)AG(CT)AT(ACT)GG-3′ (degeneracy 48, based on NNDSIG of the γ2-subunit). These were end-labelled with ^{32}P and used for plaque hybridization at low stringency (2 × SSC, 22°C). Positively hybridizing plaques were picked, purified twice and re-probed at higher stringency (0.1 × SSC, 30°C).

2.3. Subcloning and sequencing

DNA was prepared from positively hybridizing clones, cut with the appropriate restriction enzyme and the fragments sized by agarose gel-electrophoresis. The DNA was blotted onto nitrocellulose filters, and Southern hybridization with the ^{32}P-labelled probes was used to identify the 5′ end of the corresponding *nqr* gene. Nucleotide sequence analysis was carried out on the double-stranded templates using a T7 polymerase method (Pharmacia). For GC-rich regions, a method using *Taq* polymerase and deazaGTP (Promega) was preferred. Both strands were sequenced using either vector primers (Universal and Reverse) or synthesized oligonucleotide primers (OSWEL). Sequences were analyzed using both the University of Wisconsin Genetics Computer Group programs and BLITZ (EMBL, Heidelberg) [19].

3. Results

3.1. N-terminal sequencing of the α- and γ-subunits

The Na^+-dependent NADH–ubiquinone oxidoreductase complex from *V. alginolyticus* was partially purified as described above. Zymogram staining of enzyme activity on non-denaturing PAGE gels indicated a M_r of 254 kDa for the complex. The subunits were separated on SDS-PAGE gels. From the partially purified preparations of NADH–ubiquinone reductase, we were able to identify four subunits: α (55 kDa), β (50 kDa), γ1 (33 kDa) and γ2 (30 kDa). These were blotted onto PVDF membranes and the N-terminal sequences determined as MITIKKGLDL for the α-subunit, QKEETKTEA-APQAEQVQ for the γ1-subunit, and ASNNDSIKKTLGVV-IGL-LV for the γ2-subunit. No N-terminal sequence for the β subunit could be obtained because of blocking at the N-terminus.

3.2. Identification and sequencing of nqrA *and* nqrC

From the N-terminal amino acid sequences, oligonucleotide probes were designed to probe the λ library. Several clones hybridizing to probe 1 (*nqrA*, α-subunit) were isolated and purified. From one positive clone, a 10.7 kb *Eco*RI insert was mapped and shown to give five *Hin*dIII fragments of approximate sizes 2.9, 2.7, 1.9, 1.65 and 1.0 kb. A partial restriction map of the cloned DNA is shown in Fig. 1. The 1.9 kb *Hin*dIII fragment hybridized with probe 1 and was subcloned into the sequencing vector pTZ19R (Pharmacia). DNA sequencing showed that the first 254 bp of DNA were of λ origin, representing the large region between *Hin*dIII and *Eco*RI in this vector and thereby locating the 1.9 kb fragment as being on the left end of the original 10.7 kb *Eco*RI fragment. Within the 1.9 kb *Hin*dIII fragment, three ORFs were detected. The first encodes a polypeptide of 102 amino acid residues, which showed

Fig. 2. The nucleotide and deduced protein sequences of the *nqr* and *bolA* genes. Double underlined protein sequence indicates sequence used to design oligonucleotide probes. Singly and doubly underlined protein sequence denotes that determined by amino acid sequencing. Double underlined nucleotide sequence denotes putative Shine–Dalgarno sequences. The region of nucleotide sequence with opposing arrows above the sequence represents a region of dyad symmetry adjacent to a poly(dT) region (single underline) that could act as a transcription terminator for the *bolA* gene. →

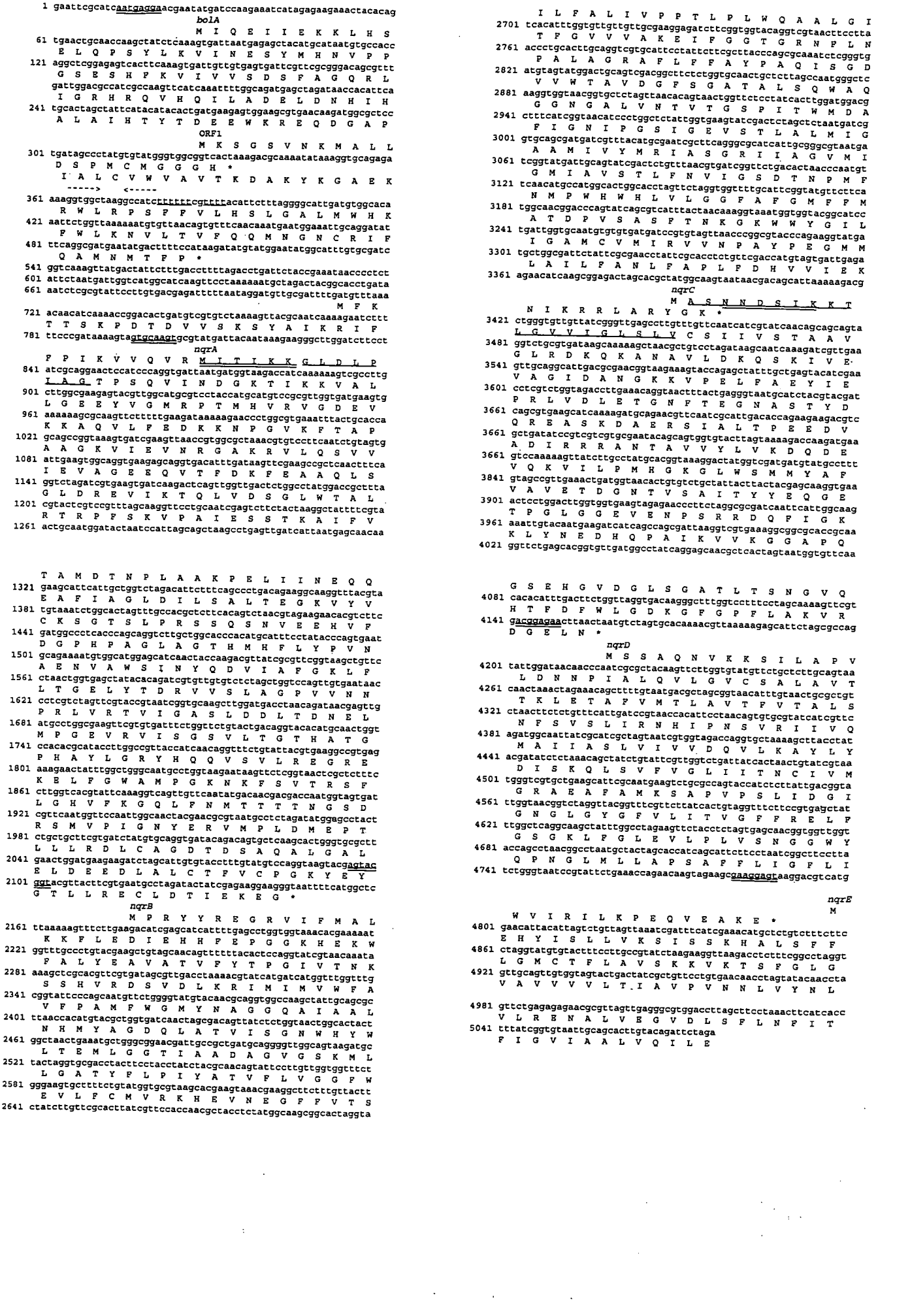
bolA
ORF1
nqrA
nqrC
nqrB
nqrD
nqrE

71% similarity and 55% identity with the *bolA* gene of *E. coli* [20]. The second ORF encodes a putative polypeptide of 80 amino acid residues. No strong homologies could be found to other proteins in the SWISSPROT database, but a 24% identity over 33 residues with chain 5 of the putative chloroplast NADH–plastoquinone oxidoreductase from *Oryza sativa* was observed [21]. The third ORF contained the sequence MITIKKG determined from the α-subunit and extended to the end of the 1.9 kb *Hin*dIII fragment. Further sequencing of the adjacent 2.7 kb *Hin*dIII fragment, the overlapping 0.6 kb *Xba*I and the 0.9 kb *Xba*I–*Pst*I fragments (Fig. 1) gave the sequence of the C-terminal portion (Fig. 2). Sequence comparison using the MOTIFS program detected no evidence of the presence of the highly conserved GAG(A/R)Y motif found in the FMN-containing subunit of complex I [1–3].

Hybridization experiments with probe 5 to detect the gene for the γ2-subunit showed that this gene was located on a 3.1 kb *Xba*I fragment subcloned from the original 10.7 kb *Eco*RI clone. This fragment contained a unique *Pst*I site that divided the fragment into a 2.2 kb and an 0.9 kb fragment (Fig. 1). Probe 5 reacted with the 2.2 kb fragment. Thus, the *nqrC* gene was shown to map to the same region of the chromosome as the *nqrA* gene and comprised an ORF of 768 bp in the same orientation as the *nqrA* gene and 1.2 kb downstream from the end of the *nqrA* gene. The N-terminal amino acid from sequencing agreed exactly with that obtained by protein analysis.

3.3. *Sequencing of* nqrB *and* nqrD

Two further ORFs, corresponding to *nqrB* and *nqrD*, were found on further sequencing of the region between *nqrA* and *nqrC* and the region immediately downstream of *nqrC*. *NqrB* is located immediately downstream of *nqrA* and extends 1278 bp from the 0.9 kb *Xba*I–*Pst*I fragment into the 2.2 kb *Pst*I–*Xba*I fragment. Downstream of *nqrC*, an ORF of 630 bp was found and this was termed *nqrD*. We have also found an ORF, designated *nqrE*, adjacent to *nqrD*, which has not been completely sequenced. Hydropathy plots of NqrB and NqrD indicate that they are integral membrane proteins that possess a number of putative membrane-spanning helices (data not shown).

Sequence comparisons of the proteins encoded by the *nqrA–D* genes was carried out using the BLITZ programme, over a range of PAM [22] values (40–350), to determine homology with other proteins in the SWISSPROT database over short and long regions. For NqrB and NqrD, a low homology to hydrophobic subunits of complex I from both eukaryotes and prokaryotes was apparent at high PAM values (250–350). However, these homologies were not to a single subunit of Complex I but to a number of different hydrophobic subunits. For example NqrB showed homology to chain 4 (equivalent to ND4) of *Paramecium tetraurelia*, chains 1 (equivalent to ND1) and 5 (equivalent to ND5) of *Oenothera bertiana* and NqrD to chain 4 of *Synechocystis* spp., subunits 13 and 14 (equivalent to bovine ND4 and ND2, respectively) of *P. denitrificans*, and chain 5 of both *Anopheles gambiae* and *Drosophila yakuba*. At PAM 250 the matches for NqrB and NqrD were 8 and 14% respectively; the corresponding values at PAM 350 were 15 and 21%. By contrast the same comparisons between the corresponding subunits of complex I from various species gave values in the range 20–>90%. Comparison of the predicted number, the number of results expected by chance to have a score greater or equal to the given score for the specific comparison, showed very low values for the corresponding hydrophobic subunits from different species (i.e. statistically meaningful) and also showed the previously described relationships between chain 5, chain 4 and chain 2 of complex I from different species [23]. The predicted numbers for comparisons between NqrD and hydrophobic subunits of complex I were high and of the same order as the predicted numbers for comparisons between chains 4 and 6, or between chains 4 and 1 of different species. In addition NqrB and NqrD also showed low homology to ion transporters over a range of PAM values (40–350). NqrD showed homology to Na^+-channel proteins over individual transmembrane segments (e.g. CIN2 of *Rattus norvegicus*). The Na^+-channel proteins have repeated units consisting of three transmembrane helices (S1–S3) followed by a positively charged segment (S4), thought to be the voltage sensor, and two further transmembrane helices [24,25]. By contrast NqrA and NqrC showed no obvious homology to proteins in the database. The deduced properties of the four completely sequenced subunits are shown in Table 1.

4. Discussion

Independent evidence shows that the structural genes for the α- (*nqrA*) and γ2- (*nqrC*) subunits are located close together on the chromosome of *V. alginolyticus*. The amino acid residues corresponding to the nucleotide sequences of the oligonucleotide probes for both *nqrA* and *nqrC* were found at the N-termini of the predicted amino sequences, and the amino acid sequence determined from nucleotide sequencing agreed well with that obtained by protein sequencing for 19 residues of NqrC and 10

Table 1
Summary of properties of polypeptides encoded by the *nqrA–D* genes of *V. alginolyticus*

Subunit	NqrA	NqrB	NqrC	NqrD
M_r	48,622	46,809	27,672	22,602
No. residues	446	426	257	210
pI	5.58	9.12	4.91	9.28
N-Terminus	MITIKKGLDL-	MPRYYREGV-	MASNNDSIKK-	MSSAQNVKKS-
Predicted no. of membrane-spanning helices	0	6–12	1 (N-terminal)	4–6
Comments		Very hydrophobic Weak homologies with complex I subunits and sodium channel proteins	Hydrophobic N-terminal region	Very hydrophobic Weak homologies with complex I subunits and sodium transporters

esidues for NqrA (Fig. 1), confirming that the sequences of hese two genes do correspond to the α- and γ2-subunits of the artially purified Na^+-dependent NADH–ubiquinone reductase. The serine codon of AGC found for residue 7 of *nqrC* is onsistent with the observation that probe 5, but not probe 4, ybridized to the N-terminal region of the *nqrC* gene. The redicted M_r values of 48.6 kDa for the α-subunit and 27.6 kDa or the γ2-subunit are in reasonable agreement with the experimental values of 55 and 30 kDa determined from SDS-PAGE els, as it is well documented that membrane proteins give oorer correlation than soluble proteins. Although no FMN-inding site was detected by sequence analysis, this does not reclude the α-subunit having FMN as a prosthetic group. earching the databases indicates that even for the highly conerved fumarate reductases, the FAD consensus sequence SH[ST]x(2)-A-x-GG is only found in a limited number of roteins. To date, a sequence coding for the catalytic subunit f the enzyme and containing NADH- and flavin-binding sites as not been identified and this gene may be located further ownstream. Searching for binding sites using the program IOTIFS did not reveal any NADH-, [Fe-S]-, or FAD-binding tes in the four genes. For *E. coli*, *P. denitrificans* and *B. taurus* ere is strong conservation of these binding sites in the c.51 Da catalytic subunit [2,3].

Comparison of the amino acid sequences for proteins NqrA– indicated that they are not closely related to the functionally rresponding complex I of either prokaryotes or eukaryotes. deed the observation that the low homologies between NqrD d subunits ND1, ND2, ND4 and ND5 of complex I from rious species are very similar support the postulate that the a^+-dependent NADH–ubiquinone oxidoreductase are either related or diverged early in evolution from complex I. It is rtinent to note that both ND2, ND4 and ND5 subunits have en postulated to evolve from a common ancestor by gene plication [26]. A further distinction between the Na^+-dependt NADH–ubiquinone oxidoreductase and complex I lies in e operon structure. For *E. coli* and *P. denitrificans* the gene der is identical. For *E. coli* the subunit sizes in kDa and the ne order are (*B. taurus* equivalents in brackets): 16 (ND3), (20 IP), 22 (23 IP), 46 (49 IP), 19 (24 FP), 50 (51 FP), 75 (IP) lowed by the mainly very hydrophobic proteins 36 (ND1), (23), 20 (ND6), 11 (ND4L), 66 (ND5), 51 (ND4) and 52 D2) [2]. The genes for the peripheral membrane proteins are jacent (*nuoC–G*). For *V. alginolyticus* the subunit sizes in kDa , in order: 49, 47 (HP), 28 and 23 (HP), which bears little rrespondence to the arrangement for *E. coli*. The divergence ween the Na^+-dependent NADH–ubiquinone oxidoreduce of *V. alginolyticus* and complex I of *E. coli* is in contrast the case for other genes, eg. *bolA* and *unc* genes of *V. alginolyticus* and *E. coli*, which are much more closely related [27]. e extent and nature of the AT-rich promoter control region *nqrA* is as yet uncertain. Downstream of *bolA* is a region dyad symmetry followed by a T-rich region (Fig. 2) that is racteristic of a rho-independent transcriptional regulator . It is preceded by an A-rich sequence upstream of the -rich motif that is complementary to the T-rich tail. Such ich sequences are thought to increase the efficiency of termiion [29]. The location of the *bolA* terminator region within F1 makes it likely that this putative gene product is not duced as a translational product. Evidence from N-terminal uencing strongly indicates that the NqrA subunit begins MITIKK etc., rather than MFKTTS, but further experiments to determine the transcriptional and translational starts are in progress.

In summary we have cloned and sequenced four genes for the Na^+-dependent NADH–ubiquinone oxidoreductase of *Vibrio alginolyticus*. Our data is consistent with the hypotheses that Na^+-dependent NADH–ubiquinone oxidoreductase is distinct from the H^+-translocating complex I, that the *nqr* genes form part of an operon, that the complex is larger than the three subunits isolated previously, and that at least two proteins (NqrB and NqrD) may form ion channels. Further experiments are in progress to determine the function of these subunits and the regulation of *nqr* gene expression.

Acknowledgements: Financial support from Glynn Research Foundation is gratefully acknowledged. We thank Professor R. Ambler and Dr. D. Finnegan in Edinburgh for advice and support and Dr. B. Meunier at Glynn for advice.

References

[1] Walker, J.E. (1992) Quart. Rev. Biophys. 25, 253–324.
[2] Weidner, U., Geier, G., Ptock, A., Friedrich, T., Leif, H. and Weiss, H. (1993) J. Mol. Biol. 233, 109–122.
[3] Xu, X., Matsuno-Yagi, A. and Yagi, T. (1993) Biochemistry 32, 968–981.
[4] Skulachev, V.P. (1988) Membrane Bioenergetics, pp. 293–326, Springer-Verlag, Berlin.
[5] Tokuda, H. and Unemoto, T. (1981) Biochem. Biophys. Res. Commun. 102, 265–271.
[6] Tokuda, H. and Unemoto, T. (1982) J. Biol. Chem. 257, 10007–10014.
[7] Unemoto, T., Tokuda, H. and Hayashi, M. (1990) in: Bacterial Energetics (Krulwiche, T.A., Ed.) pp. 35–54, Academic Press, San Diego.
[8] Avetisyan, A.V., Bogachev, A.V., Murtasina, R.A. and Skulachev, V.P. (1993) FEBS Lett. 317, 267–270.
[9] Dimroth, P. (1987) Microbiol. Rev. 51, 320–340.
[10] Unemoto, T. and Hayashi, M. (1989) J. Bioenerg. Biomembr. 21, 649–662.
[11] Hayashi, M., Miyoshi, T., Sato, M. and Unemoto, T. (1992) Biochim. Biophys. Acta 1099, 145–151.
[12] Unemoto, T., Miyoshi, T. and Hayashi, M. (1992) FEBS Lett. 306, 51–53.
[13] Unemoto, T., Ogura, T. and Hayashi, M. (1993) Biochim. Biophys. Acta 1183, 201–205.
[14] Hayashi, M. and Unemoto, T. (1986) FEBS Lett. 202, 327–330.
[15] Hayashi, M. and Unemoto, T. (1987b) Biochim. Biophys. Acta 890, 47–54.
[16] Hayashi, M. and Unemoto, T. (1987a) Biochim. Biophys. Acta 767, 470–478.
[??] Tokuda, H. and Kogure, K. (1989) J. Gen. Microbiol. 135, 703–709.
[17] Matsudaira, P.T. (1989) A Practical Guide to Protein and Peptide Purification for Microsequencing, Academic Press.
[18] Murray, N.E. (1983) in: Lambda II (Hendrix, R.W., Roberts, J.W., Stahl, F.W., Weisberg, R.A., Eds.) pp. 395–432, Cold Spring Harbor Laboratory.
[19] Devereux, J., Haeberli, P. and Smithies, O. (1984) Nucleic Acids Res. 12, 387–395.
[20] Aldea, M., Garrido, T., Hernandez-Chico, C., Vicente, M. and Kushner, S.R. (1989) EMBO J. 8, 3923–3931.
[21] Hiratsuka, J., Shimada, H., Whittier, R., Ishibashi, T., Sakamoto, M., Mori, M., Kondo, C., Honji, Y., Sun, C.-R., Meng, B.-Y., Li, Y.-Q., Kanno, A., Nishizawa, Y., Hirai, A., Shinozaki, K. and Sugiura, M. (1989) Mol. Gen. Genet. 217, 185–194.
[22] Schwarz, R.M. and Dayhoff, M.O. (1978) in: Atlas of Protein Structure and Function (Dayhoff, M.O., Ed.) pp. 353–358, National Biomedical Research Foundation.

[23] Fearnley, I.M. and Walker, J.E. (1992) Biochim. Biophys. Acta 1140, 105–134.
[24] Noda, M., Okeda, T., Kayano, T., Suzuki, H., Takeshima, H., Kurasaki, M., Takahashi, H. and Numa, S. (1986) Nature 320, 188–192.
[25] Catterall, W.A. (1988) Annu. Rev. Biochem. 55, 953–985.
[26] Kikuno, R. and Miyata, T. (1985) FEBS Lett. 189, 85–88.
[27] Krumholz, L.R., Esser, U. and Simoni, R.D. (1989) Nucleic Acids Res. 16, 7993–7994.
[28] d'Aubenton Carafa, Y., Brody, E. and Thermes, C. (1990) J. Mol. Biol. 216, 835–858.
[29] Wright, J.J., Kumar, A. and Hayward, R.S. (1992) EMBO J. 11, 1957–1964.

Expression and analysis of the gene for the catalytic β subunit of the sodium-translocating NADH-ubiquinone oxidoreductase of *Vibrio alginolyticus*.

KAREN TAN, PAMELA BEATTIE, DAVID R.F.LEACH, PETER R. RICH*, ANDREW F.W. COULSON and F.BRUCE WARD.

Institute for Cell and Molecular Biology, Edinburgh University, Edinburgh, EH9 3JR, Scotland
*Glynn Research Institute, Bodmin,Cornwall, PL30 4AU.

The NADH-ubiquinone oxidoreductase complex of *Vibrio alginolyticus*, the first complex in the aerobic respiratory chain of this bacterium, is a primary electrogenic pump that appears to be specifically induced under conditions of alkaline pH. Unlike the corresponding NADH-ubiquinone oxidoreductases found in most bacteria and eukaryotic mitochondria, the translocated ions are Na^+ rather than H^+. Previously we cloned and sequenced the first 4 genes (*nqrA-nqrD*) coding for subunits of the *Vibrio alginolyticus* NADH-ubiquinone oxidoreductase complex [1] and demonstrated that this complex is both structurally and evolutionarily distinct from the H^+-translocating NADH-ubiquinone oxidoreductases. These genes were located within the first 5 kb of a 10.1 kb *Eco*RI fragment.
We have now sequenced the remainder of this fragment and in agreement with the recent report of Hayashi *et al.*, [2] showed that there are two further open reading frames , *nqrE* and *nqrF* prior to a transcription stop signal, a polydT tail and a further 293 bp of non-coding DNA. The identity of the open reading frames downstream of this region has not been clearly established. The second open reading frame shows homology with Na^+/H^+ antiporters but is distinct from the previously sequenced Na^+/H^+ antiporter of *V. alginolyticus* [3]. The amino acid sequence of NqrF is shown in Fig. 1.

```
1   MDIILGVVMF TLIVLALVLV ILFAKSKLVP
31  TGDITISVND DPSLAIVTQP GGKLLSALAG
                  (A)
61  AGVFVSSACG GGGSCGQCRV KVKSGGGDIL
91  PTELDHITKG EAREGERLAC QVAMKTDMDI
121 ELPEEIFGVK KWECTVISND NKATFIKELK
151 LQIPDGESVP FRAGGYIQIE APAHHVKYAD
                                  (B)
181 YDIPEEYRED WEKFNLFRYE SKVNEETIRA
    (B)
211 YSMANYPEEH GIIMLNVRIA TPPPNNPDVP
        (B)
241 PGIMSSYIWS LKEGDKCTIS GPFGEFFAKD
                  (C)
271 TDAEMVFVGG  GAGMAPMRSH IFDQLKRLHS
301 KRKMSFWYGA RSKREMFYVE DFDMLQAEND
331 NFVWHCALSD PLPEDNWDGY TGFIHNVLYE
                  (C)
361 NYLRDHEAPE DCEYYMCGPP MMNAAVIGML
                (C)
391 KDLGVEDENI LLDDFGG*
```

Fig. 1. Deduced amino acid sequence of NqrF . The double underlined /bold regions are those proposed to be involved in binding a [2Fe-2S] centre (A), FAD (B) and NADH (C).

Both sequence analysis and expression studies indicate that the *nqrF* gene encodes the β-subunit of the NADH-ubiquinone oxidoreductase, which is the site for NADH oxidation. Subcloning of the *nqrF* gene into the expression vector pET16b on a 2.3 kb *Kpn*I-*Sal*I fragment resulted in production of a 46 kDa protein .on IPTG induction. This protein showed NADH dehydrogenase activity on native PAGE gels with tetrazolium blue. Purification of this expressed protein to homogeneity confirmed that it had similar properties to the FAD-containing subunit of NADH-ubiquinone oxidoreductase previously purified from *V. alginolyticus* [4,5] with respect to utilisation of dNADH as a substrate , inhibition by $Ag^+$and Na^+-independence.

Sequence analysis of the *nqrF* gene using the computer program MPsrch and a range of PAM values (40-350) indicated that the *N*-terminal region was similar to a number of ferredoxins while the C-terminal region showed homology with several NAD(P)H-binding flavoproteins including spinach ferredoxin-$NADP^+$ reductase (FNR) , phthalate dioxygenase (PDR) and xylene monooxygenase (electron transfer component). The high homologies (e.g. a predicted no. of 5.42e-28 at PAM 180 for XylA of xylene monooxygenase) indicate NqrF is very likely to be a NADH-FAD reductase containing an iron-sulphur centre. By comparison with the known crystal structure of FNR we identified F265 as the border between the flavin domain (c.171-265) and the NAD^+-binding domain (266-407). Analysis of the three domains: the ferredoxin domain, the flavin domain and the NAD^+-binding domain was carried out independently using MPsrch. The ferredoxin domain was most similar to xylene monooxygenase (1.74e-09), CDP-6-deoxy-3,4 glucoseen reductase (1.73e-07), methane monooxygenase component C(7.84e-06), phenol hydroxylase (1.70e-04) and a large number of ferredoxins including plant-type ferredoxins (7.58e-04). In all cases there was high identity in the cysteine-rich region of the ferredoxin motif (Fig 1.) although the spacing was C-x_5-C-x_2-C as in putidaredoxin rather than the C-x_4-C-x_2-C motif of plant-type ferredoxins [6]. The flavin domain showed least homology with other proteins in the database but was similar to a number of NAD^+-dependent nitrate reductases, NADH-cytochrome b5 reductases as well as lipoxygenase and benzoate 1,2 dioxygenase (a ferredoxin:ferredoxin-NAD^+-reductase). From this analysis two motifs important in FAD binding, RAYS and GIMSSY were identified [7,8]. The NAD^+-binding domain showed high similarities with over 40 NAD^+-dependent enzymes including phenol hydroxylase, xylene monooxygenase, methane monooxygenase, benzoate 1,2 dioxygenase and a plant ferredoxin-NAD^+ reductase with predicted numbers of 9.88e-28, 1.40e-21, 1.09e-13 and 7.65e-08.The motifs GGGAGMAP and YMCGPP were clearly recognised by a number of analyses while the motif LDDF was determined by comparison with FNR and PDR [7,8].

These results demonstrate unequivocally that the β subunit of *V. alginolyticus* NADH-ubiquinone oxidoreductase has a three domain structure: ferredoxin domain, flavin domain and NAD^+- binding domain. This arrangement is also found in pthalate dioxygenase reductase for which a crystal structure is known but in this case the ferredoxin domain is *C*-terminal. This domain structure is similar to the ferredoxin:ferredoxin-NAD^+-reductase components of benzoate 1,2 dioxygenase and xylene monooxygenase. Our results will enable us to construct a model of the predicted three dimensional structure of the β subunit based on sequence alignment , secondary structure and the known X-ray crystal structures of highly homologous proteins.

Abbreviations used: FNR, spinach ferredoxin-$NADP^+$ reductase; PDR, phthalate dioxygenase

1. Beattie, P., Tan, K., Bourne, R.M., Leach, D. Rich, P.R. and Ward, F.B. (1994) FEBS Lett. **356**, 333-338
2. Hayashi, M., Hirai,K. and Unemoto, T. (1995) FEBS Lett. **363**, 75-77
3. Nakamura, T;Komano, Y;Itaya, E;Tsukamoto, K;Tsuchiya, T;Unemoto, T (1994) Biochim.Biophys.Acta **1190**, 465-468
4. Hayashi, M. and Unemoto, T. (1984) Biochim.Biophys.Acta **767**, 47-478
5. Asano, M., Hayashi,M., Unemoto, T and Tokuda, H. (1985). Agric. Biol. Chem. **49**, 2813-2817
6. Cammack, R (1992). Advances in Inorganic Chemistry **38**, 281-322
7. Correll, C.C., Batie, C.J., Ballou, D.P., and Ludwig, M.L. (1992) Science **258** 1604-1610
8. Bruns, C.M. and Karplus, P.A. (1994) In Flavins And Flavoproteins, Yagi, G. *et al.*, Editors,Walter de Gruyter, Berlin. pp.443-446